UNIVERSIDADE DA BEIRA INTERIOR
Engenharia

Planning of Power Distribution Systems with High Penetration of Renewable Energy Sources Using Stochastic Optimization

Sérgio da Fonseca Santos

Tese para obtenção do Grau de Doutor em
Engenharia Electrotécnica e de Computadores
(3º ciclo de estudos)

Orientador: Prof. Doutor João Paulo da Silva Catalão
Co-orientador: Prof. Doutor Carlos Manuel Pereira Cabrita
Co-orientador: Doutor Desta Zahlay Fitiwi

Covilhã, julho de 2017

UNIVERSITY OF BEIRA INTERIOR
Engineering

Planning of Power Distribution Systems with High Penetration of Renewable Energy Sources Using Stochastic Optimization

Sérgio da Fonseca Santos

Thesis submitted in fulfillment of the requirements for the degree of
Doctor of Philosophy in

Electrical and Computer Engineering

(3rd cycle of studies)

Supervisor: Prof. Dr. João Paulo da Silva Catalão
(University of Porto)
Co-supervisors: Prof. Dr. Carlos Manuel Pereira Cabrita
(University of Beira Interior)
Dr. Desta Zahlay Fitiwi
(Comillas Pontifical University)

Covilhã, July 2017

This work was supported by FEDER funds through COMPETE 2020 and by Portuguese funds through FCT, under Projects FCOMP-01-0124-FEDER-020282 (Ref. PTDC/EEA-EEL/118519/2010), POCI-01-0145-FEDER-016434, POCI-01-0145-FEDER-006961, UID/EEA/50014/2013, UID/CEC/50021/2013, and UID/EMS/00151/2013. Also, the research leading to these results has received funding from the EU Seventh Framework Programme FP7/2007-2013 under grant agreement no. 309048. Moreover, Sérgio F. Santos gratefully acknowledges UBI / Santander Totta for the doctoral incentive grant in the Engineering Faculty.

Acknowledgments

Firstly, I would like to express my sincere gratitude to my Ph.D. advisors Prof. João Paulo da Silva Catalão and Prof. Carlos Manuel Pereira Cabrita for the continuous support of my Ph.D. study and related research, for their patience, motivation and immense knowledge. Their guidance helped me at all times during the research and writing of this thesis.

Besides my advisors, I would like to address a special thanks to Dr. Desta Zahlay Fitiwi, my co-advisor and friend, for his trust, support and especially for his insightful comments throughout my studies.

I thank all the co-authors of my works and especially to my closest collaborators, Dr. Miadreza Shafie-khah, Dr. Bizuayehu Abebe Worke, Dr. Nikolaos Paterakis and Dr. Ozan Erdinç. I thank my fellow colleagues in the “Sustainable Energy Systems Lab” for the stimulating discussions and for all their help in the past years.

I also want to thank Eng. Filipe Mendonça, from EDA, S.A. - Eletricidade dos Açores, for his demonstrated availability, for the real data used in the case studies in this thesis, and especially for patiently addressing my urgent requests, always responding so promptly.

I would like to thank the European Project FP7 SiNGULAR (*Smart and Sustainable Electricity Grids under Large-Scale Renewable Integration*) and the Santander Research Grant from the Engineering Faculty of UBI, which provided me with economic means to fulfill this Ph.D. Thesis.

Last but not least, I would like to thank my family, especially my parents, and all my friends who have been beside me in the last two years.

Resumo

Atualmente há um esforço global para integrar mais recursos energéticos distribuídos nas redes elétricas, impulsionado por fatores técnico-económicos e ambientais, particularmente ao nível da rede de distribuição. Estes recursos incluem tipicamente tecnologias facilitadoras das redes elétricas inteligentes, tais como geração distribuída, sistemas de armazenamento de energia, e gestão ativa da procura.

A integração de fontes de geração distribuída (energias renováveis, principalmente) está a aumentar progressivamente em muitas redes de distribuição, e é provável que esta tendência continue nos próximos anos devido ao avanço de soluções emergentes, esperando-se assim que as limitações técnicas existentes sejam ultrapassadas e que facilitem a integração progressiva das fontes de geração distribuída. Espera-se também que os acordos feitos pelos países para limitar as emissões de gases de efeito de estufa e para mitigar as alterações climáticas acelerem a integração de fontes de energia renováveis.

No entanto, a natureza intermitente e volátil da maioria das fontes de energia renováveis (em particular, eólica e solar) faz com que a sua integração nas redes de distribuição seja uma tarefa complexa. Isto porque tais recursos introduzem variabilidade operacional e incerteza no sistema. Assim, é essencial o desenvolvimento de novas metodologias e ferramentas computacionais inovadoras para beneficiar uma integração óptima da geração distribuída renovável e minimizar os possíveis efeitos colaterais.

Nesta tese são desenvolvidas novas metodologias e ferramentas computacionais inovadoras que consideram a variabilidade operacional e a incerteza associadas à geração a partir de fontes de energia renováveis, juntamente com a integração de tecnologias facilitadoras das redes elétricas inteligentes. As metodologias e ferramentas computacionais desenvolvidas são testadas em casos de estudo reais, bem como em casos de estudo clássicos, demonstrando a sua proficiência computacional comparativamente ao atual estado-da-arte. Devido à inerente incerteza e variabilidade das fontes de energia renováveis, nesta tese utiliza-se programação estocástica. Ainda, para assegurar a convergência para soluções ótimas, o problema é formulado utilizando programação linear inteira-mista.

Palavras Chave

Fontes de energia renováveis; Geração distribuída; Planeamento de investimentos; Programação linear inteira-mista estocástica; Redes elétricas inteligentes; Reforço da rede; Sistemas de armazenamento de energia; Variabilidade e incerteza.

Abstract

Driven by techno-economic and environmental factors, there is a global drive to integrate more distributed energy resources in power systems, particularly at the distribution level. These typically include smart-grid enabling technologies, such as distributed generation (DG), energy storage systems and demand-side management.

Especially, the scale of DG sources (mainly renewables) integrated in many distribution networks is steadily increasing. This trend is more likely to continue in the years to come due to the advent of emerging solutions, which are expected to alleviate existing technical limitations and facilitate smooth integration of DGs. The favorable agreements of countries to limit greenhouse gas (GHG) emissions and mitigate climate change are also expected to accelerate the integration of renewable energy sources (RESs).

However, the intermittent and volatile nature of most of these RESs (particularly, wind and solar) makes their integration in distribution networks a more challenging task. This is because such resources introduce significant operational variability and uncertainty to the system. Hence, the development of novel methodologies and innovative computational tools is crucial to realize an optimal and cost-efficient integration of such DGs, minimizing also their side effects.

Novel methodologies and innovative computational tools are developed in this thesis that take into account the operational variability and uncertainty associated with the RES power generation, along with the integration of smart-grid enabling technologies. The developed methodologies and computational tools are tested in real-life power systems, as well as in standard test systems, demonstrating their computational proficiency when compared with the current state-of-the-art. Due to the inherent uncertainty and variability of RESs, stochastic programming is used in this thesis. Moreover, to ensure convergence and to use efficient off-the-shelf solvers, the problems addressed in this thesis are formulated using a mixed integer linear programming (MILP) approach.

Keywords

Distributed Generation (DG); Energy Storage Systems (ESSs); Investment planning; Network reinforcement; Renewable Energy Sources (RES); Smart grids; Stochastic mixed integer linear programming; Variability and uncertainty.

Contents

List of Figures

List of Tables

List of Symbols

The main notations used in Chapters 3, 4 and 5 are listed below. Other symbols are defined where they first appear.

Chapter3

Sets and Indices

k/Ω^k	Index/Set of DG alternatives of the same type
$m,n/\Omega^n$	Indices/Set of nodes
p/Ω^p	Index/Set of DG types
$s/\Omega^s, w/\Omega^w$	Indices/Sets of scenarios and snapshots, respectively
ss/Ω^{ss}	Index/Set of substations
t/Ω^t	Index/Set of planning stages (*t* = *1*, *2*… *T*)
E	Index for existing DGs
N	Index for new DGs
SS	Substation
T	Planning horizon

Parameters

b_{nm}	Susceptance of line $n-m$ (p.u.)
$d_{n,s,w,t}$	Electricity demand at each node (MW)
$ER_{p,k}^N, ER_{p,k}^E$	Emission rate of a new or existing generator (tons of CO_2/MWh)
f_{nm}^{max}	Flow limit of line $n-m$ (MW)
g_{nm}	Conductance of line $n-m$ (p.u.)
i	Interest rate
$IC_{p,k}^N$	Installation cost of DG (€)
$InvLim_t$	Available annual budget for investment (€)
$MC_{p,k}^N$, $MC_{p,k}^E$	Maintenance cost of new and existing DGs (€), respectively
M_{nm}	Big-M parameter corresponding to line $n-m$
N_n	Number of nodes
N_{SS}	Number of substations
$OC_{p,k}^N$, $OC_{p,k}^E$	Operation cost of new and existing DGs (€/MWh), respectively
$V_{nominal}$	Nominal voltage of the system (V)
$\eta_{p,k}$	Lifetime of DGs (years)
$\lambda_{s,w,t}^{EMI}$	Emission price (€/tons)
$\lambda_{s,w,t}$	Average cost of electricity (€/MWh)
π_w	Weight associated to representative snapshot *w* (hours)
ρ_s	Probability of scenario *s*
$\sigma_{ss,s,w,t}$	Price of purchased electricity (€/MWh)

$\upsilon_{s,w,t}$	Penalty for unserved energy (€/MWh)
φ	DG penetration limit factor (%)

Variables and Functions

$f_{nm,s,w,t}$	Power flow through feeder $n-m$
$g^{E}_{p,k,n,s,w,t}, g^{N}_{p,k,n,s,w,t}$	Power generated by existing and new DG
$g^{SS}_{ss,s,w,t}$	Power purchased from upstream (grid)
$u^{E}_{p,k,n,t}$	Utilization indicator variable (1 if an existing generator is utilized; 0 otherwise)
$x^{N}_{p,k,n,t}$	Binary investment variable for DG
z_{nm}	Binary variable associated to line $n-m$ (1 if the line is connected; 0 otherwise)
EC^{E}_{t}, EC^{N}_{t}	Expected cost of energy generated by existing and new DGs (€)
EC^{SS}_{t}	Expected cost of purchased energy (€)
EMC^{E}_{t}, EMC^{N}_{t}	Expected cost of emissions for existing and new DGs (€)
$ENSC_{t}$	Expected cost of unserved energy (€)
$InvC^{N}_{t}$	Amortized NPV investment cost of DG (€)
$MntC^{N}_{t}$, $MntC^{E}_{t}$	Annual maintenance cost of new and existing DGs, respectively (€)
$\delta_{n,s,w,t}$	Unserved power (MW)
$\Delta V_{n,s,w,t}$	Voltage deviation at each node (kV)
$\theta_{nm,s,w,t}$	Voltage angle difference between nodes $n-m$ (radians)

Chapter 4

Sets and Indices

k/Ω^{k}	Index/Set for DG alternatives of the same type
l/Ω^{l}	Index/set for generation cost linearization
n/Ω^{n}	Index/set of nodes
p/Ω^{p}	Index/set for DG types
s/Ω^{s}	Index/set for scenarios
ss/Ω^{ss}	Index/set for substations
t/Ω^{t}	Index/set for planning stages (*t* = 1, 2… *T*)
w/Ω^{w}	Index/set for snapshots
N1	DG investment pool in the first period
N2	DG investment pool in the second period
Ω^{c}	Set of all network corridors
τ/Ω^{P1}; ζ/Ω^{P2}	Indices/Sets of planning stages in periods *P1* and *P2*, respectively

Parameters

b_{nm}	Susceptance of line $n-m$ (S)

$d_{n,s,w,t}$	Electricity demand at each node (MW)
f_{nm}^{max}	Flow limit of line $n-m$ (MW)
g_{nm}	Conductance of line $n-m$ (S)
i	Discount rate (%)
$ER_{p,k}^{N}, ER_{p,k}^{E}$	Emission rate of new or existing generator (tons/MWh)
ER_{ss}^{SS}	Emission rate at substation ss
$D_{s,w,t}$	Total demand in the system for each scenario, snapshot and year (MW)
$Gmax_{p,k,s,w}^{DG}$	Maximum generation limits of existing or new DGs (MW), where $DG \in \{E, N\}$
$Gmin_{p,k,s,w}^{DG}$	Minimum generation limits of existing or new DG (MW), where $DG \in \{E, N\}$
$IC_{p,k}^{N}$	Investment cost of DG (€)
$InvLim_t$	Maximum available budget for investment (€)
L	Number of piecewise linear segments
M_{nm}	Big-M parameter corresponding to line $n-m$
N_n	Number of nodes
N_{SS}	Number of substations
$MC_{p,k}^{N}, MC_{p,k}^{E}$	Annual maintenance cost of new or existing DGs (€)
T	Length of the planning horizon
$T1$	Length of the first investment period
$T2$	Length of the second investment period
$V_{nominal}$	Nominal voltage of the system (kV)
$\alpha, \beta, \gamma, \xi$	Relevance factors of the cost terms
$\eta_{p,k}$	Life-time of DG (years)
$\mu_{s,w,t}^{EMI}$	Emission price (€/tons)
π_w	Weight associated to snapshot w (in hours)
ρ_s	Probability of scenario s
$\sigma_{ss,s,w,t}$	Price of purchased electricity (€/MWh)
φ	DG penetration limit (%)
$\upsilon_{s,w,t}$	Penalty for unserved energy (€/MWh)
$\kappa_{s,w,t}$	Cost of losses (€/MWh)

Variables and Functions

$f_{nm,s,w,t}$	Power flow through feeder $n-m$
$g_{ss,s,w,t}^{SS}$	Power purchased from upstream (grid)
$g_{p,k,n,s,w,t}^{E}, g_{p,k,n,s,w,t}^{N}$	Power generated by existing or new generator
EC_t^{SS}	Expected NPV cost of purchased energy (€)
EC_t^{N}, EC_t^{E}	Expected NPV cost of energy production using new and existing DGs (€)
EMC_t^{E}, EMC_t^{N}	Expected NPV emission cost of existing or new DGs (€)

$ENSC_t$	Expected NPV cost of unserved power (€)
$InvC_t^N$	NPV investment cost of DGs (€)
$Loss_t$	Expected cost of network losses (€)
$MntC_t^N$, $MntC_t^E$	Expected NPV annual maintenance cost of new and existing DGs, respectively (€)
$OC_{p,k,s,nw,t}^N$, $OC_{p,k,s,n,w,t}^E$	Cost of production using new or existing DGs (€/MWh)
$u1_{p,k,n,\tau}^E$	Binary variable for indicating the utilization of an existing generator in the 1st period
$u2_{p,k,n,s,\zeta}^E$	Binary variable for indicating the utilization of an existing generator in the 2nd period
$x_{p,k,n,t}^{N1}$	"Here and now" investment variable of DG (in the 1st period), 0 if not installed; otherwise, non-zero
$xx_{p,k,n,s,t}^{N1}$	"Wait and see" (Recourse) investment variable of DG (in the 2nd period), 0 if not installed; otherwise, non-zero
$y_{p,k,n,s,t}^{N2}$	Investment variable of DG in the 2nd period, 0 if not installed; otherwise, non-zero
z_{nm}	Binary utilization variable associated to line $n-m$
$\delta_{n,s,w,t}$	Unserved power (MW)
$\lambda_{p,k,n,s,w,t,l}^E$	SOS2 variable in generation cost curve linearization of existing DGs
$\lambda_{p,k,n,s,w,t,l}^{N1}$	SOS2 variable for piecewise linearization of generation cost curve of new DGs in the first pool
$\lambda_{p,k,n,s,w,\zeta,l}^{N2}$	SOS2 variable for piecewise linearization of generation cost curve of new DGs in the second pool
$\Delta V_{n,s,w,t}$	Voltage deviation at each node (kV)
$\theta_{nm,s,w,t}$	Voltage angle difference between nodes $n-m$ (radians)

Chapter 5

Sets/Indices

g/Ω^g / Ω^{DG}	Index/set of generators/DGs
k/Ω^k	Index/set of branches
s/Ω^s	Index/set of scenarios
t/Ω^t	Index/set of time stages
w/Ω^w	Index/set of snapshots
$\varsigma/\Omega^\varsigma$	Index/set of substations

Parameters

$ER_g^E, ER_g^N, ER_\varsigma^{SS}$	Emission rates of existing and new DGs, and energy purchased, respectively (tCO_2e/MWh)

$IC_{g,i}, IC_k, \ IC_{tr}, IC_{es,i}$	Investment cost of DG, line, transformer and energy storage, respectively (M€)
$LT_{es}, LT_g, LT_k, LT_{tr}$	Lifetimes of energy storage, DG, distribution line, and transformer system, respectively (years)
MC_{es}^E, MC_{es}^N	Maintenance cost of existing / new storage per year (M€)
MC_g^E, MC_g^N	Maintenance costs of existing and new DGs (M€/yr)
MC_k^N, MC_k^E	Maintenance cost of new and existing line (M€/yr)
MC_{tr}^N, MC_{tr}^E	Maintenance cost of new/existing transformer per year (M€)
$OC_{g,i,s,w,t}^E, OC_{g,i,s,w,t}^N$	Operation cost of unit energy production by existing and new DGs (€/MWh)
$\eta_{ch,es}, \eta_{dch,es}$	Charging/discharging efficiency
$\lambda_{s,w,t}^{CO_2e}$	Price of emissions (€/tons of CO_2 equivalent)
$\lambda_{s,w,t}^{es}$	Variable cost of energy storage (€/MWh)
$\lambda_{s,w,t}^{\varsigma}$	Price of electricity purchased (€/MWh)
μ_{es}	Scaling factor
ρ_s, π_w	Probability of scenario *s* and weight (in hours) of snapshot group *w*
$\upsilon_{s,w,t}$	Penalty for unserved power (€/MW)

Variables

$D_{s,w,t}^i$	Active power demand at node *i* (MW)
$E_{es,i,s,w,t}$	Reservoir level of ESS (MWh)
$I_{es,i,s,w,t}^{ch}, I_{es,i,s,w,t}^{dch}$	Charging/discharging indicator variables
$P_{es,i,s,w,t}^{ch}, P_{es,i,s,w,t}^{dch}$	Charged/discharged power (MW)
$P_{g,i,s,w,t}^E, P_{g,i,s,w,t}^N$	Active power produced by existing and new DGs (MW)
$P_{k,s,w,t}$	Power flow through branch *k* (MW)
$P_{\varsigma,s,w,t}^{SS}$	Active power imported from grid (MW)
$u_{g,i,t}, u_{k,t}$	Utilization variables of existing DG and lines
$x_{g,i,t}, \ x_{es,i,t}, \ x_{k,t}, \ x_{tr,ss,t}$	Investment variables for DG, storage systems, transformer and distribution lines, respectively
$\delta_{i,s,w,t}$	Unserved power at node *i* (MW)
$\varphi_{k,s,w,t}$	Losses associated to each feeder (MW)

Functions

EC_t^{DG}	Expected cost of energy from DGs (M€)
EC_t^{ES}	Expected cost of energy from energy storage (M€)
EC_t^{SS}	Expected cost of energy purchased from upstream (M€)
$EmiC_t^{DG}$	Expected emission cost of DG power production (M€)

$EmiC_t^N, EmiC_t^E$	Expected emission cost of power production using new and existing DGs, respectively (M€)
$EmiC_t^{SS}$	Expected emission cost of purchased power (M€)
$ENSC_t$	Expected cost of unserved power (M€)
$InvC_t^{DNS}$, $MntC_t^{DNS}$	NPV investment/maintenance cost of DNS components (M€)

Chapter 6

Sets/Indices

c/Ω^c	Index/set of capacitor banks
es/Ω^{es}	Index/set of energy storages
i/Ω^i	Index/set of buses
g/Ω^g / Ω^{DG}	Index/set of DGs
k/Ω^k	Index/set of branches
s/Ω^s	Index/set of scenarios
t/Ω^t	Index/set of time stages
w/Ω^w	Index/set of snapshots
$\varsigma/\Omega^\varsigma$	Index/set of substations

Parameters

C_{ij}	Cost of branch *i-j* (€)
$E_{es,i}^{min}, E_{es,i}^{max}$	Energy storage limits (MWh)
$ER_g^N, ER_g^E, ER_\varsigma^{SS}$	Emission rates of new and existing DGs, and energy purchased at sub-stations, respectively (tons of CO_2 equivalent—tCO_2e/MWh)
g_k, b_k, S_k^{max}	Conductance, susceptance and flow limit of branch *k* (Ω, Ω, MVA)
$IC_{g,i}$, IC_k, $IC_{es,i}, IC_{c,i}$	Investment cost of DG, line, energy storage system and capacitor banks, respectively (€)
L	Total number of linear segments (€)
$LT_g, LT_k, LT_{es,}LT_c$	Lifetimes of DG, line, energy storage system and capacitor banks, respectively (years)
MC_c, MC_{es}	Maintenance cost of capacitor bank and energy storage system per year (€)
MC_g^N, MC_g^E	Maintenance costs of new and existing DGs per year (€)
MC_k^N, MC_k^E	Maintenance costs of new and existing branch *k* per year (€)
MP_k, MQ_k	Big-M parameters associated to active and reactive power flows through branch *k*, respectively (€)
N_i, N_ς	Number of buses and substations, respectively
$OC_{g,i,s,w,t}^N, OC_{g,i,s,w,t}^E$	Operation cost of unit energy production by new and existing DGs (€/MWh)
$P_{es,i}^{ch,max}, P_{es,i}^{dch,max}$	Charging and discharging power limits of a storage system (MW)

$P_{sol,h}$	Hourly solar PV output (MW)
P_r	Rated power of a DG unit (MW)
$P_{wnd,h}$	Hourly wind power output (MW)
Q_c^0	Rating of minimum capacitor bank
R_c	A certain radiation point (often taken to be 150 W/m^2)
R_h	Hourly solar radiation (W/m^2)
r_k, x_k	Resistance and reactance of branch k, respectively
R_{std}	Solar radiation in standard condition (usually set to 1000 W/m^2)
v_{ci}	Cut-in wind speed (m/s)
v_{co}	Cut-out wind speed (m/s)
v_h	Observed/sampled hourly wind speed (m/s)
V_{nom}	Nominal voltage (kV)
v_r	Rated wind speed (m/s)
Z_{ij}	Impedance of branch i-j (Ω)
α_l, β_l	Slopes of linear segments
$\eta_{es}^{ch}, \eta_{es}^{dch}$	Charging and discharging efficiencies of a storage system (%)
$\lambda_{s,w,t}^{CO_2e}$	Price of emissions (€/tCO_2e)
$\lambda_{es,i,s,w,t}^{dch}$	Cost of energy discharged from storage system (€/MWh)
$\lambda_{s,w,t}^{\varsigma}$	Price of electricity purchased from upstream (€/MWh)
ρ_s, π_w	Probability of scenario s and weight (in hours) of snapshot group w
$\upsilon_{s,w,t}$	Penalty for unserved power (€/MWh)

Variables

$D_{s,w,t}^i$, $Q_{s,w,t}^i$	Active and reactive power demand at node i (MW, MVAr)
$E_{es,i,s,w,t}$	Stored energy (MWh)
$I_{es,i,s,w,t}^{ch}, I_{es,i,s,w,t}^{dch}$	Charge-discharge indicator variables
$P_{g,i,s,w,t}^N, P_{g,i,s,w,t}^E$	Active power produced by new and existing DGs (MW)
$P_{\varsigma,s,w,t}^{SS}$, $Q_{\varsigma,s,w,t}^{SS}$	Active and reactive power imported from grid (MW)
P_k, Q_k, θ_k	Active and reactive power flows, and voltage angle difference of link k, respectively (MW, MVAr, radians)
$p_{k,s,w,t,l}, q_{k,s,w,t,l}$	Step variables used in linearization of quadratic flows (MW, MVAr)
PL_k, QL_k	Active and reactive power losses, respectively (MW, MVAr)
$PL_{\varsigma,s,w,t}, QL_{\varsigma,s,w,t}$	Active and reactive losses at substation ς (MW, MVAr)
$P_{es,i,s,w,t}^{ch}, P_{es,i,s,w,t}^{dch}$	Power charged to and discharged from storage system (MW)
$Q_{i,s,w,t}^c$	Reactive power injected by capacitor bank at node i (MVAr)
$Q_{g,i,s,w,t}^N, Q_{g,i,s,w,t}^E$	Reactive power consumed/produced by new and existing DGs (MVAr)
$u_{g,i,t}$, $u_{k,t}$	Utilization (status) variables of DG and line (1 if it is connected; 0, otherwise)

V_i, V_j	Voltage magnitudes at nodes *i* and *j* (kV)
$x_{g,i,t}, x_{es,i,t}, x_{c,i,t}, x_{k,t}$	Investment variables for DG, energy storage system, capacitor banks and distribution lines
$\delta_{i,s,w,t}$	Unserved power at node *i* (MW)
θ_i, θ_j	Voltage angles at nodes *i* and *j* (radians)

Functions

EC_t^{SS}	Expected cost of energy purchased from upstream (€)
$ENSC_t$	Expected cost of unserved power (€)
$EmiC_t^{DG}$	Expected emission cost of power production using DG (€)
$EmiC_t^N, EmiC_t^E$	Expected emission cost of power production using new and existing DGs, respectively (€)
$EmiC_t^{SS}$	Expected emission cost of purchased power (€)
$InvC_t^{CAP}, MntC_t^{Cap}$	NPV investment/maintenance cost of capacitor banks (€)
$InvC_t^{DG}, MntC_t^{DG}, EC_t^{DG}$	NPV investment/maintenance/expected energy cost of DGs, respectively (€)
$InvC_t^{ES}, MntC_t^{ES}, EC_t^{ES}$	NPV investment/ maintenance/ expected energy cost of an energy storage system, respectively (€)
$InvC_t^{LN}, MntC_t^{LN}$	NPV investment/ maintenance cost of a distribution line (€)

Relevant Acronyms

AC	Alternating Current
BRICS	Brazil, Russia, India, China, South Africa
CIU	Cost of Ignoring Uncertainty
CO_2	Carbon Dioxide
COE	Cost of Energy
CSP	Concentrated Solar Power
DC	Direct Current
DERs	Distributed Energy Resources
DG	Distributed Generation
DGIP	Distributed Generation Investment Planning
DNSs	Distribution Network Systems
DSO	Distribution System Operator
ECIU	Expected Cost of Ignoring Uncertainty
EU	European Union
EVPI	Expected value of perfect information
GAMS	General Algebraic Modelling System
GHG	Greenhouse Gas
IEA	International Energy Agency
IREN	International Renewable Energy Agency
LCOE	Levelized Costs of Electricity
MILP	Mixed Integer Linear Programming
NOx	Nitrogen Oxide
NPV	Net Present Value
OMR	Operation, Maintenance and Reliability
OM&ENS	Operation, Maintenance and Energy Not Served
PDFs	Probability Distribution Functions
PV	Solar Photovoltaic Power
RESs	Renewable Energy Sources
S-MILP	Stochastic Mixed Integer Linear Programming
SOS2	Special Ordered Sets of type 2
SOx	Sulphur Oxide
TEMC	Total Emissions Cost
TIC	Total Investment Cost
TLC	Total Losses Cost
TOMRC	Total Operation, Maintenance and Reliability Cost
TOMUEC	Total Operation, Maintenance and Unserved Energy Cost
TSOs	Transmission System Operators
UN	United Nations

US	United States
WD	Wind

Chapter 1

Introduction

1.1 Background

Electrical energy is one of the most important factors in today's modern societies, specifically the relationship with a complex energy system that eases transportation, allows the manufacture of consumer products and facilitates the dissemination of information and knowledge through the media. The energy in modern societies provides comfort, well-being, security and leisure to the society.

The vast majority of the energy consumed today in the societies comes from non-sustainable energy sources, also called conventional energy sources. Conventional energy sources constitute fossil fuels such as coal, natural gas and refined petroleum products and nuclear power. Only a small part of the energy produced in the world comes from renewables, often called unconventional energy sources.

Renewable energy sources (RESs) include solar, hydro, wind, biomass, geothermal power or tidal energy. The fact that most of the energy used nowadays comes from conventional sources raises several concerns, especially in relation to energy dependence, security, affordability and sustainability. Such concerns are leading to the current perspective of large-scale RES integration, which is one of the most important trends in the electrical systems around the world.

RESs have enormous potential because, in principle, they can meet several times the world's energy demand [1]. They can provide sustainable energy services because of the vast availability of such resources, wide-spread across the globe. Thus, it is now widely recognized that the integration of RESs brings a lot of benefits to all electric system stakeholders from economic, environmental, social and/or technical perspectives.

RES integration can increase the electricity markets diversification, contributing to the realization of a long-term sustainable energy strategy, and the much needed reduction of GHG emissions locally and globally by reducing the carbon footprint of power generation using conventional means.

Generally, there is a global consensus on climate change mitigation and limiting GHG emissions that along with energy dependence, security and other structural issues are forcing states to create new market policies and introduce new energy policies (policies related to RES, in particular) that support the development and utilization of RESs.

The integration of RESs in electrical systems (particularly, at distribution levels) is expected to accelerate as a result of the agreements of several countries [2] to limit the emissions and mitigate climate change. The level of distributed generation (DG) introduced in distribution systems follows an upward trend, and it is generally acknowledged that DGs will contribute immensely to the effort of resolving most of the aforementioned concerns both globally and locally, including the realization of RES integration goals set forth by different entities [3].

The availability of several mature DG technologies and their decreasing trend of costs, along with the complicated nature of building new transmission lines, the increasing demand for greater reliability of supply, among others, has encouraged significant investment in DGs (particularly in the renewable type, such as wind and solar).

As already mentioned, the integration of RESs in power systems has been growing since 2005 in a gradual and sustainable manner [4]. So far, the renewable energy investment targets, including climate change policies and improved cost-competitiveness, have been sufficient to allow the steady growth of global electricity production share of RESs at the expense of polluting power sources. A very high renewable investment was recorded in 2011 buoyed by the different initiatives such as "green stimulus" in Germany and Italians' solar roofs [3]. However, in 2015, RES investment showed a 5% increase compared to 2014 as shown in Figure 1.1. It can be seen in Figure 1.1 that the total investment in 2015 was six times the value recorded in 2004. For the first time in 2015, the amount of investment increased and overall RES generation capacity added in developing countries exceeded that of the developed economies [1]. The developing countries that contributed most to such a significant increase were China, India and Brazil, whose combined investment surged by 19% compared to 2014. In particular, China contributed most (approximately 17%) to this achievement, by aggressively investing in renewables. In India and Brazil, the net increases in RES investment in 2015 with reference to 2014 are over 22% and 10%, respectively.

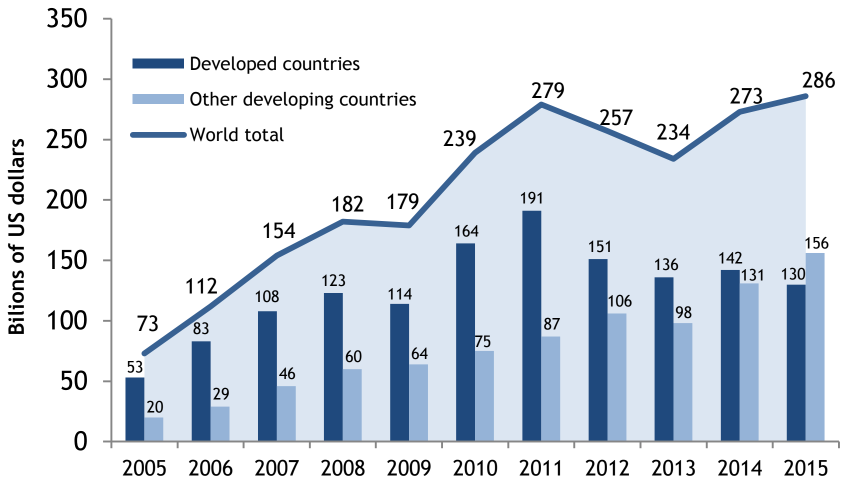

Figure 1.1 - Global overview of new investments in renewable energy [1].

The developing countries that contributed most to such a significant increase were China, India and Brazil, whose combined investment surged by 19% compared to 2014. In particular, China contributed most (approximately 17%) to this achievement, by aggressively investing in renewables. In India and Brazil, the net increases in RES investment in 2015 with reference to 2014 are over 22% and 10%, respectively. Other countries that also made significant investments in 2015 were South Africa (329% compared to 2014) as well as Mexico and Chile whose investments in 2015 increased by 105% and 151% compared to 2014, respectively. All together, they are the top 10 countries that have invested more in renewable energy in 2015 along with Morocco, Uruguay, the Philippines, Pakistan and Honduras. Investments can be clearly seen in Figure 1.2, which shows the renewable investment trajectories by country and/or region. In comparison, RES investments in Europe fell by 21%, despite the wind energy financing record of 17 billion US dollars, an increase of 11%. In the United States, investments increased by 19%, two thirds of which were in solar energy.

Among the several renewable energy types, the one that saw significant growth was the large-scale hydro. However, excluding this one, it can be seen that from all renewable energy sources, wind and solar were the ones that attracted the highest investments in 2015 (constituting 62 and 56 GW of new installed capacity, respectively), well above the 2014 values. In Figure 1.3, one can see the new investments in renewable energy by sector, and it appears that, for the first time, investment in solar energy was higher than that of any other renewable type (excluding large-scale hydro).

In 2015, although there was a new record, the generation capacity (Figure 1.4) added is far from what would be desired to address the current global challenges, mentioned earlier. The United Nations conference in Paris on climate change, known as COP21, generated an unprecedented agreement among 195 countries to achieve zero emissions in the second half of the century [2]. Thus, the large-scale integration of renewable energy sources (especially, in distribution systems) will require significant investments in infrastructures.

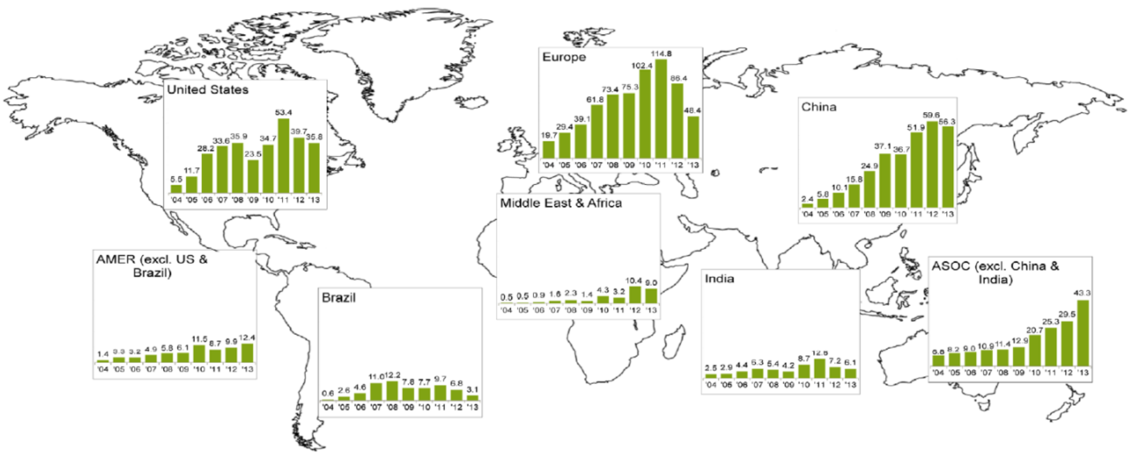

Figure 1.2 – Global overview of investments in renewables by region [1].

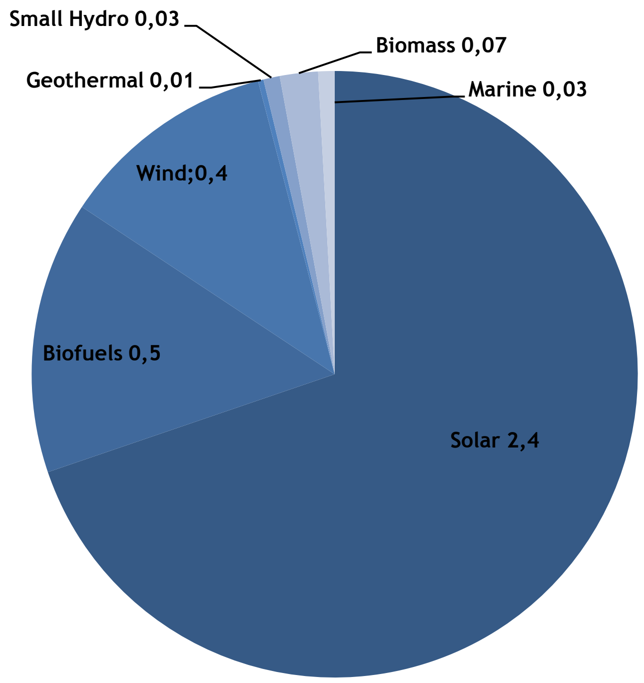

Figure 1.3 - New investments in renewable energy by sector (in billions of US dollars) [5].

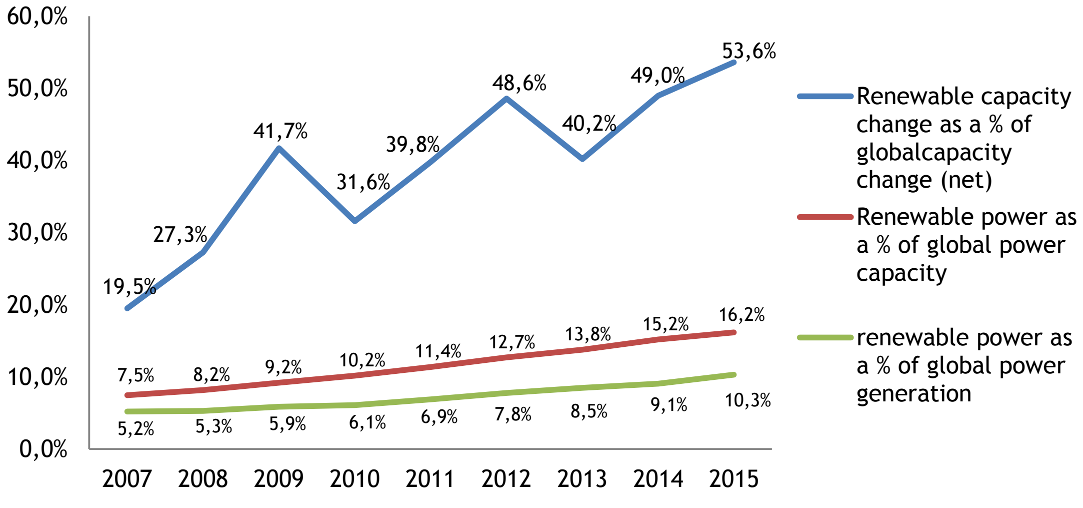

Figure 1.4 - Renewable power generation capacity as a share of global power [1].

However, large-scale integration of RES-based DGs often poses a number of technical challenges in the system from the stability, reliability and power quality perspectives. This is because integrating RESs introduces significant operational variability and uncertainty to the distribution system, making operation, planning and control rather complicated.

Hence, such a high-level integration effort is likely to be supported by certain smart-grid technologies and concepts that have the capability to enhance the flexibility of the entire distribution systems. Energy Storage Systems (ESSs) can play a vital role in integrating variable energy sources. In addition, a dynamic Reconfiguration of Distribution Systems (RDS) can be very important because it can considerably enhance the flexibility of the system and voltage profiles, thereby increasing chances of accommodating large-scale RES power.

1.2 Research Motivation and Problem Definition

As demonstrated in the background, RESs make a crucial part of the solution for environmental sustainability; hence, they will play an important role in power systems. The integration of RESs should, in principle, reduce the risk of fuel price volatility and geopolitical pressures and ensure that these do not pose a significant impact on the overall public welfare. However, large-scale penetration of RESs will necessarily involve a process of adapting and changing the existing infrastructure because of their intrinsic characteristics, such as intermittency and variability.

The growing need for intermittent RESs, in conjunction with the electrical mix changes in the long-term, will probably affect the distribution and transmission systems. In this context, a change in power generation options, resulting from a high contribution of RESs, may require network grid updates. Regulatory agencies are heavily committed to increasing RES integration, not only due to environmental but also technical and economic reasons, as explained in the previous section.

The main challenge with most RESs is their inherent variability and uncertainty, making operation, control and planning very complicated. DG penetration increases the variation of voltage and current in the network. Hence, increasing DG penetration may have a negative or a positive impact depending on various factors such as the size of the system and the loads type, requiring comprehensive modeling and simulations to assess its impact. If not properly planned, this may lead to an uncertain increase in the feeders' power flows, resulting in network congestion and increased losses in the network. It is in this context that the first two problems, addressed in this thesis, appear.

The integration of smart-grid enabling technologies has the capability to alleviate the negative consequences of large-scale integration of DGs. In other words, in order to facilitate (speed up) the much-needed transformation of conventional (passive) Distribution Network Systems (DNSs) and support large-scale RES integration, different smart-grid enabling technologies such as reactive power sources, advanced switching and storage devices are expected to be massively deployed in the short-term.

The integration of Energy Storage Systems (ESSs) along with RESs has become one of the most viable solutions to facilitate the increased penetration of DG resources. Energy storage systems “level” the mismatch between renewable power generation and demand. This is because these devices store energy during periods of low electricity demand (price) or high RES power production, and then release it during periods of peak demand and low RES production. Therefore, in addition to their technical support to the system, ESSs bring substantial benefits for end-users and DG owners through reliability and power quality improvement as well as cost reduction. Besides, ESSs are being developed and applied in power grids to cope with a number of issues such as smoothing the energy output from RESs and improving the stability of the electrical system. ESSs also increase savings during peak hours and minimize the impact of intermittent generation sources, leading to a more efficient management of the integrated system. Despite the high capital costs of many ESS technologies, their deployment in distribution systems is in the upward trend. Cost-cutting and the strong need of integrating RES-based DGs is expected to push the demand for the simultaneous deployment of ESSs in distribution network systems. In other words, distributed ESSs will increase dramatically in the years to come. Hence, proper planning of such systems is crucial for a healthy operation of the system as a whole.

Electrical distribution systems are interconnected by switches but predominantly operated radially. These switches are often used for emergency purposes such as to evade load curtailment during fault cases. However, the system can be reconfigured to find the best topology that minimizes power losses in the system and improve operational performance. This in turn improves the flexibility in the system, which may help to accommodate (absorb) more variable power. Investigating the capability of network switching and/or expansion along with ESS deployment in RES integration level is another problem addressed in this thesis. Generally, this thesis develops strategies, methods and tools that are very crucial to guide such a complex decision-making process, i.e. maximizing the penetration level of RESs in DNSs without jeopardizing the power quality, system stability and integrity.

1.3 Research Questions, Objectives and Contributions of the Thesis

This thesis presents a comprehensive analysis of DG investment planning decisions (renewables in particular). New analysis tools and methods are developed in this thesis that take into account the operational variability and uncertainty associated with the RES power generation along with the integration of smart-grid enabling technologies. The ultimate aim of all this is to enable existing systems to accommodate large-scale variable energy sources (wind and solar type DGs in particular) while maintaining the power quality and system stability at the required/standard levels at a minimum possible cost.

In particular, the following research questions are addressed:

- *What is the current status of RES penetration across the world (with a special focus at distribution levels)? What are the main impeding factors for RES integration? How can the potential benefits of RESs be reaped without significant negative consequences?*
- *What are the parameters of uncertainty and/or variability that most influence the decision-making process in terms of investment solutions in DGs (especially, renewables)?*
- *How should different sources of uncertainty be modeled in the complex decision-making problem concerning DG investment planning?*
- *From a quantitative and qualitative point of view, what are the impacts of network switching and/or reinforcement, as well as deployment of ESSs on the level of renewable power integrated in the system?*
- *How can the penetration of renewable energy sources in the power distribution system be maximized with currently available technologies?*
    - *What is the effect of reactive power support capability on the RES-based DG integration level?*
    - *What are the implications of integrating smart-grid enabling technologies in the distribution systems with respect to maximizing RES integration, reducing energy losses, costs and improving voltage profiles?*

The main objectives of this thesis are:

- To carry out a state-of-the-art review on the current status of RES penetration across the world (with a particular focus at distribution levels), their economic aspects, current integration challenges and future prospects, and other related issues.
- To develop appropriate optimization models and methods for planning distribution systems under uncertainty and large-scale penetration of variable energy sources.
- To perform a comprehensive analysis with the aim of identifying the stochastic parameters that most influence the decision-making process in terms of investment solutions in DGs (especially, renewables).
- To develop methods for handling the most significant sources of uncertainty in the complex decision-making problem concerning DG investment planning.

- To investigate the impacts of network switching and/or reinforcement, as well as deployment of ESSs on the level of renewable power integrated in the system.
- To develop mechanisms for maximizing the penetration level of variable energy sources in the power distribution systems with the help of currently available technologies.
- To optimally deploy smart-grid enabling technologies in the distribution systems, and investigate the implications in terms of RES-based integration level and overall system performance.

The contributions of this thesis (all already published in prestigious venues) are summarized as follows:

- An overview on RESs and the underlying issues related to the RES theme such as climate change and its mitigation, RES characteristics and technological aspects, the most important economic aspects as well as the challenges and opportunities of integrating RESs in power systems. This contribution is published in the form of a **Book Chapter in *ELSEVIER*** [6].
- The development of an improved multi-stage and multi-scenario DG investment planning mathematical formulation that investigates the effect of uncertainty and operational variability on DG investment solutions. This contribution is published in the ***IEEE Transactions on Sustainable Energy*** [7].
- The development of a two-period planning framework that combines both robust short-term and strategic medium to long-term decisions in dynamic and stochastic DG investment problems. This contribution is published in the ***IEEE Transactions on Sustainable Energy*** [8].
- The development of a multi-stage and stochastic model, which considers simultaneous integration of ESSs and RES-based DGs as well as network reconfiguration/reinforcement. This contribution is published in ***Applied Energy - ELSEVIER*** [9].
- The presentation of a novel approach which simultaneously considers the optimal sizing, time and placement integration of smart-grid enabling technologies to support a large-scale RES-based DG integration. A comprehensive analysis of considering RES based DGs with and without reactive power support capabilities is also included. This contribution is published in the ***IEEE Transactions on Sustainable Energy***, ***Part I*** [10] and ***Part II*** [11].

1.4 Methodology

The mathematical models developed in this thesis are based on well-established methods, namely, mixed-integer linear programming (MILP), multi-objective optimization and two-period stochastic programming. In order to achieve the main research objective, beyond simulation models, this thesis develops methods and solution strategies to analyze the expansion planning of DNSs under uncertainty, and a dramatically changing power generation scheme over time.

The proposed optimization models and the solutions strategies are implemented in GAMS© and solved in most cases using the CPLEX™ algorithm, mostly by invoking default parameters. The clustering methodology is implemented in the MATLAB© programming environment, and Visual Basic™ with Excel© used as an interface for this purpose.

1.5 Notation

The present thesis uses the notation commonly used in the scientific literature, harmonizing the common aspects in all sections, wherever possible. However, whenever necessary, in each section, a suitable notation may be used. The mathematical formulas will be identified with reference to the subsection in which they appear and not in a sequential manner throughout the thesis, restarting them whenever a new section or subsection is created. Moreover, figures and tables will be identified with reference to the section in which they are inserted and not in a sequential manner throughout the thesis.

Mathematical formulas are identified by parentheses (x.x.x) and called “Equation (x.x.x)” and references are identified by square brackets [xx]. The acronyms used in this thesis are structured under synthesis of names and technical information coming from both the Portuguese or English languages, as accepted in the technical and scientific community.

1.6 Organization of the Thesis

The thesis comprises seven chapters which are organized as follows:

Chapter 1 is the introductory chapter of the thesis. First, the background of the thesis is presented. Then, the research motivations and the problem definition are provided. Subsequently, the research questions and contributions of this thesis are presented. Then, the methodology used throughout the thesis is introduced, followed by the adopted notations. Finally, the chapter concludes by outlining the structure of the thesis.

In Chapter 2, a comprehensive overview of RES is presented. First, RESs are framed in the climate change perspective, followed by a renewable energy trend. Then, the green energy production options are presented and the individual characterization in recent years of each one is made jointly with the respective technologies. Subsequently, the most important economic aspects on RESs to be considered when investing in this type of technology are presented. Finally, the benefits and RES integration barriers as well the present/future perspectives are discussed.

In Chapter 3, a DG investment planning model is formulated as a novel multi-stage and multi-scenario optimization problem, in order to perform a comprehensive sensitivity analysis and identify the uncertain parameters which significantly influence the decision-making in distributed generation investments and quantify their degree of influence. A real–world distribution network system is used to carry out the analysis.

Taking the findings of the analysis in Chapter 3 as input, a detailed model is developed to guide the complex decisions-making process of DG investment planning in distribution system in the face of uncertainty. This is presented in Chapter 4. The problem is formulated from a coordinated system planning viewpoint, in which the net present value of costs rated to losses, emission, operation and maintenance, as well as the cost of unserved energy are simultaneously minimized. The formulation is anchored on a two-period planning horizon, each having multiple stages. The operational variability and uncertainty introduced by intermittent generation sources, electricity demand, emission prices, demand growth and others are accounted for via probabilistic and stochastic methods, respectively. Metrics such as cost of ignoring uncertainty and value of perfect information are used to clearly demonstrate the benefits of the proposed stochastic model.

Chapter 5 presents a novel mechanism to quantify the impacts of network switching and/or reinforcement as well as deployment of ESSs on the level of renewable power integrated in the system. To carry out this analysis, a dynamic and multi-objective stochastic mixed integer linear programming (S-MILP) model is developed, which jointly takes the optimal deployment of RES-based DGs and ESSs into account in coordination with distribution network reinforcement and/or reconfiguration.

A new multi-stage and stochastic mathematical model, developed to support the decision-making process of planning distribution network systems (DNSs) for integrating large-scale “clean” energy sources is presented in Chapter 6. Another aim of this chapter is to examine the theoretical aspects and mathematical formulation in a comprehensive manner. The proposed model is formulated from the system operator’s viewpoint, and determines the optimal sizing, timing and placement of distributed energy technologies (particularly, renewables) in coordination with some enabling technologies. Moreover, heuristic strategies for reducing the combinatorial solution search space in relation to the optimal placement of DGs, ESSs and reactive power sources are investigated.

Chapter 7 presents the main conclusions of this work. Guidelines for future works in these fields of research are provided. Moreover, this chapter reports the scientific contributions that resulted from this research work and that have been published in journals with high impact factor (first quartile), as book chapters or in conference proceedings of high standard (IEEE).

Chapter 2

Renewable Energy Systems: An Overview

This chapter aspires to provide an overview of RESs and the underlying issues related to the RESs theme such as climate change and its mitigation. The types of RESs are also briefly discussed focusing on their characteristics and technological aspects. This is followed by the most important economic aspects as well as the challenges and opportunities of integrating RESs in power systems. All this leads to an efficient exploitation of their wide-range benefits while sufficiently minimizing their negative impacts. Finally, the chapter is summarized with some concluding remarks.

2.1 Introduction

All societies need energy services to satisfy their needs (such as cooking, lighting, heating, communications, etc.) and to support productive services. In order to secure sustainable development, the delivery of energy services needs to be safe and cause low environmental impacts [12]–[14].

Social sustainability and economic development require security and easy access to energy resources, which are indispensable to promote sustainable energy and essential services. This means applying different strategies at different levels to revamp economic development. To be environmentally benign, energy services should provoke low environmental impacts, including greenhouse gas (GHG) emissions.

According to the study in [3], fossil fuels are still the main primary energy sources. A major revolution is required in how energy is produced and used in order to preserve a sustainable economy capable of providing the required public services (both in developed and developing countries), and laying effective support mechanisms to climate change mitigation and adaptation efforts [15].

A major concern in both developed and developing countries, including emerging economies, is that without having abundant and accessible energy sources, it is not possible to maintain the current paradigm in the medium and long term, from an economic point of view. In accordance with the International Energy Agency (IEA) reference scenario, the primary global energy consumption will grow between 40% and 50% until 2030, at an annual average rate of 1.6%. Without a major paradigm shift in energy policies throughout the world, fossil fuels are still expected to cover about 83% of the increase in demand [3].

The reasons for this strong growth are essentially two: the continuous increase in world population and the economic convergence between developed and developing countries, especially with emerging economies such as India and China that are leading the economic recovery from the recent global economic crisis, and becoming the major consumers of non-renewable energy sources. This change must be answered with structural measures, such as by putting a real monetary value to energy. Some of the promising solutions are accelerating renewable energy integration, promoting energy efficiency and supporting transport systems modernization. This can be achieved by promoting more transparent markets to flourish and creating an enabling environment for competition in all sectors of the economy and energy production [16].

The sustainability of energy systems is now an important factor for socio-economic development. Sustainability depends on three major components (as schematically demonstrated in Figure 2.1): i) the security of access to energy, ii) the accessibility of services and iii) environmental compatibility. Changing the energy scenario presents itself as a huge challenge whose solution ultimately depends on the political will of governing bodies to make the necessary investments on a global scale. In the medium and long term horizon, investment decisions will affect the cost and the environmental impacts of infrastructures. Most likely, the energy supply will be the main factor of possible models for future development at global, regional and national levels.

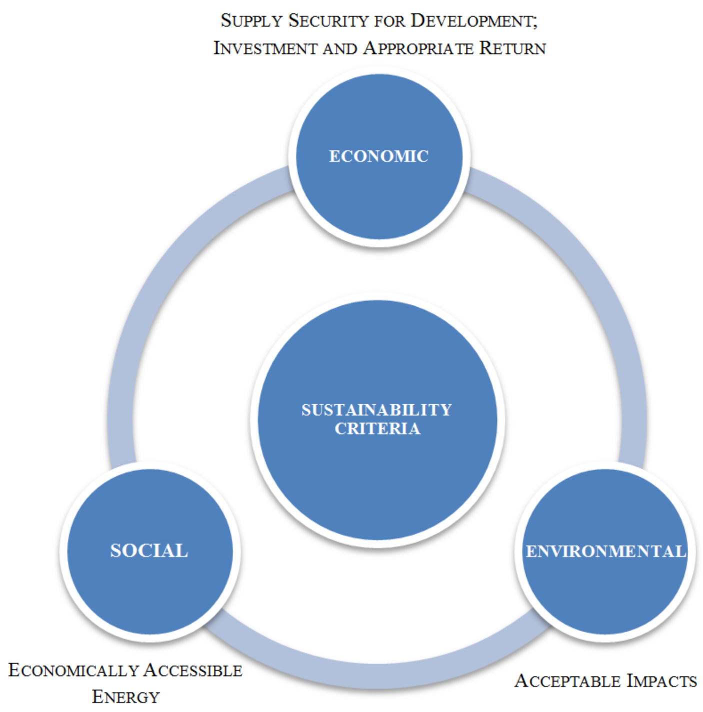

Figure 2.1 - Sustainability in the electricity sector [17].

2.2 Clime Change

GHG emissions associated with energy services are the major causes of climate change. The report in [3] indicates that “most of the observed increase in global average temperature since the mid-20th century is very likely due to the observed increase in anthropogenic greenhouse gas concentrations”.

The carbon dioxide (CO_2) concentrations have grown continuously to about 390 ppm of CO_2 in 2010, a 39% increase since pre-industrial levels [18]. The global average temperature increased by 0.76 ºC (from 0.57 °C to 0.95 °C) between 1850 and 1899. And, between 2001 and 2015, the warming trend has increased significantly. Note that forest abatement, fires, and the release of non-CO_2 gases from industry, trade and agriculture also contribute to global warming [18]. Moreover, all indicators show that there will be a significant increase in demand for primary energy during the twenty-first century [18].

The emission rates are also expected to substantially exceed the natural removal rates, causing a continuous increase in GHG concentrations in the atmosphere, and consequently the rise in average global temperature. The Cancun agreement [19] appeals to reduce GHG emissions and limit the global average temperature rise below 2°C, taking the pre-industrial value as a reference. It has recently been agreed on to a target level of 1.5°C in the average temperature rise.

Historically, developed countries are the main contributors to global GHG emissions, and continue to have the highest total history of per capita emissions [20]. In recent years, GHG emissions in most developing countries have been increasing, currently covering more than half of the total emissions. For instance, the total annual emissions in China surpassed that of the USA in recent years [20].

However, the latest climate conference, COP-21 (UN climate conference) in Paris [21], brings hope for the fight against climate change where, for the first time, representatives of almost every country in the world convened together in an effort to reduce emissions and counter the effects of global warming.

The Paris Agreement, which will take effect after 2020, underscores the fact that the participation of all nations – not just rich countries – is crucial to combat climate change. On the whole, 195 member countries of the UN Climate Convention and the European Union have ratified the document [21].

The long-term goal of the agreement is to keep global warming "well below 2°C." This is the point in which scientists argue that the planet is doomed to a future of no return, leading to devastating effects such as rising sea levels, extreme weather events (droughts, storms and floods), and lack of water and food.

2.3 Renewable Energy Trend

An increase in an overall world trend in the awareness of climate change and the need for mitigation efforts is bringing forth huge increase in the deployment of renewable energy in comparison to fossil fuel energy sources. The landmark that signals the dawning of this renewable age goes hand in hand with the degree of advancement in technologies and a higher degree of RES penetration, which is being achieved around the world. Furthermore, there are several driving factors for these remarkable growths among which are favorable government support policy and increasing competitiveness in costs. After several decades of efforts in research and continuous development in RES, the yearly growth in the capacity of these plants is becoming greater than the total investment capacity added in power plants based on coal, natural gas and oil all combined together [22]. Nowadays, RESs have reached a significant level of share in energy supply options, becoming one of the prominent global alternative power supply sources. This trend will continue increasing at faster rates as long as the world's desire for industrial scale clean energy sources is on the higher side [3].

The latest global trends in renewable energy investment status reports indicate that, renewables represented a 58.5% of net additions to global power capacity in 2014, with significant growth in all regions, which represents an estimated 27.7% of the world's power generating capacity, enough to supply an estimated 22.8% of global electricity. Wind, solar and biomass power generations reached an estimated 9.1% of the world's electricity in 2014, up from 8.5% in 2013. According to renewables status report [23], the overall cost-cutting achieved to date helped to ensure such a strong momentum in 2014, reaching an investment boom up to 29% in solar, and 11% in wind technologies, and geothermal managing to raise 23%. Further cuts in the cost of generation for both solar and wind look to be on the cards in 2015 [23]. The report on global renewable energy 2015 [23] also indicates the continued growth of RES participation in parallel proportion with the energy consumption and the falling oil prices. In addition, issues related to the untapped RES potentials indicate that it still requires a growing effort in pursuing innovative approaches to increase its participation in order to guarantee a clean energy future. Concerning the regional expansion of RES utilization, such growth scheme is not limited to the industrialized regions, but also an increasing number of developing countries are even becoming important manufacturers and installers of this fashionable energy source.

Another essential growth trend currently being observed, which is worth mentioning here, is the diversity of applications of the renewable sources. The use of renewables is no more limited to the power generation only, but its use is expanding in heat related and transpiration applications. In this regard, several supporting technologies like heat supply and storage systems are helping flourish the deployment of these important energy resources across many countries. Also, a significant contribution to the world transport sector is being promoted with an increased share in the use of Ethanol and Biodiesel in combination with fossil fuels.

In relation to the job creation opportunities, renewable energy employment continues expanding, which according to IRENA [24], in 2014 an estimated 7.7 million people are working directly or indirectly in this sector. Also, concerning government policies, the number of countries, states and provinces which adopted renewable policies and targets tripled since 2004. Regarding investment mechanisms, innovative approaches have been introduced like in the case of Asian investment banks, representing a new investment vehicles for renewable energy projects such as green bonds, yield companies, and crowd funding which have attached new classes of capital providers and are helping to reduce the cost of capital for financing renewable energy projects [23]. As a result, the investment flow in renewables has outpaced fossil fuels for five consecutive years in all regions.

According to the global status report [23], currently, there is no systematic linkage between the so called renewable energy twin pillars: the renewable energy sources and energy efficiency, in technical as well as policy wise.

2.4 Green Energy Production Options

A major change in the energy sector between 2014 and 2015 has been the rapid fall of oil prices, as well as natural gas and coal but not so drastically. After an extensive period of stable high oil price, it has been falling from more than $ 100 until the middle of 2014 to a level below 50 dollars at the beginning of 2015 [24]. In 2016, further fall is observed, and as it stands now the price of oil oscillates around 50 dollars /barrel.

Renewable technologies are becoming increasingly competitive in a number of countries but government support is still needed to enhance the development of these schemes in many other countries. The capacity increase of base renewable generation is estimated to be 128 GW in 2014 (Table 2.1), out of which 37% is related to wind, nearly a third to solar energy and more than one quarter to hydropower [20] (see in Figure. 2.2). The growth in installed wind power capacity has been developed mainly onshore, but offshore wind development has also shown substantial. China continues to have the largest wind power market with a 20 GW installed capacity. Germany stands second by installing more than 5 GW of wind power, while the wind capacity added in the US was at a very low level in 2013 and 2014, standing at almost 5 GW [25]. The solar photovoltaic (PV) was greatly expanded in Asia, especially in China and Japan. In Japan, the expansion is supported by generous feed-in tariffs. The low price of oil proves to be a challenge for other forms of renewable energy, including biofuels for transport and renewable based heating system, as the latter directly competes with natural gas based heating (whose price is still, in many cases, linked to the oil price). Although biofuels face challenges stemming from lower oil prices, some other developments served to improve their prospects.

Table 2.1 - Renewable Electric Power Capacity (Top Regions/Countries in 2013) [20]

TECHNOLOGY	WORLD	EU-28	BRICS	CHINA	UNITED STATES	GERMANY	SPAIN	ITALY	INDIA
					(GW)				
Wind Power	318	117	115	91	61	34	23	8.6	20
Solar Energy PV	139	80	21	19.9	12.1	36	5.6	17.6	2.2
Solar Energy CSP	3.4	2.3	0.1	~0	0.9	~0	2.3	~0	0.1
Geothermal	12	1	0.1	~0	3.4	~0	0	0.9	0
Hydropower	1,000	124	437	260	78	5.6	17.1	18.3	44
Bioenergy	88	35	24	6.2	15.8	8.1	1	4	4.4
Ocean Power	0.5	0.2	~0	~0	~0	0	~0	0	0
Total Renewable Power Capacity	560	235	162	118	93	78	32	31	27

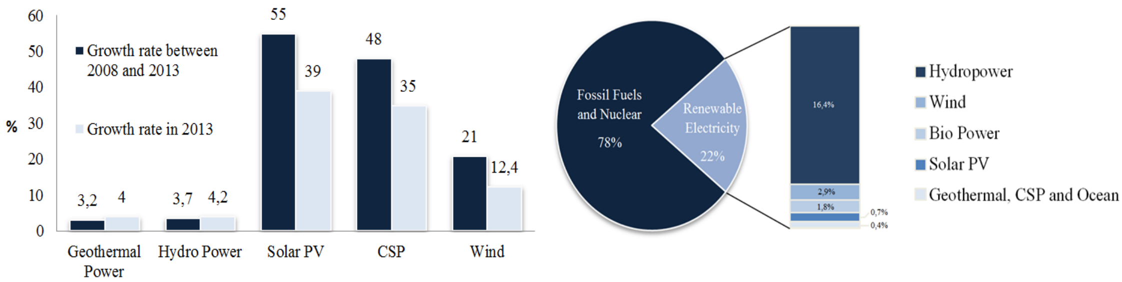

a) b)

Figure 2.2 - a) Average Annual Growth Rates of Renewables (2008 – 2013); b) Global Electricity Production (2013) [20].

For instance, to overcome the current dark prospects of biofuels in Brazil, the government increased the ethanol rate of mixture from 25% to 27% and from 5% in biodiesel to 7%, and increased gasoline taxes, while Argentina and Indonesia have increased their biofuels mandates [20]. A long period of low oil prices could result in neglecting the promotion of energy efficiency and instead returning to wasteful consumption. However, there is no evidence to date that this has occurred [22].

2.4.1 Wind Energy

Wind power has been used for thousands of years in a variety of applications. Wind energy can be transformed into mechanical energy or electricity. But wind power remained in the background in detriment of other fuels for various technical, social and economic reasons. It was the oil crisis in the 1970s, which led to a renewed interest in wind power technology especially for electricity generation connected to the grid, to pump water and to provide power in remote areas.

The technical potential of wind power to serve the energy needs is immense. Although wind resource varies around the globe, there is enough potential in most regions to support high levels of wind power generation. Wind resources are not a barrier to the global expansion of this technology in the coming decades. New wind power technologies have contributed to significant advances in wind power penetration. In a general perspective, the global wind power capacity has been increasing [26], smoothly from 2000 to 2006, and in a more accentuated way from 2007 to 2013 as shown in Figure 2.3. More than 51 GW of wind power were added to the power systems, representing a 44% increase compared to 2013, making an overall contribution of approximately 370 GW to the energy production mix, as shown in Table 2.2. The top 10 countries accounted for 84% of the installed capacity in the world at the end of 2013, but there are dynamic and emerging markets in most regions [20].

Table 2.2 - Wind Power Global Capacity and Additions [20]

COUNTRY	TOTAL END 2012 (GW)	ADDED 2013 (GW)	TOTAL END 2013 (GW)
China	60.8/75.3	14.1/16.1	75.5/91.4
United States	60.0	1.1	61.1
Germany	31.3	3.2/3.6	34.3/34.7
Spain	22.8	0.2	23
India	18.4	1.7	20.2
United Kingdom	8.6	1.9	10.5
Italy	8.1	0.4	8.6
France	7.6	0.6	8.3
Canada	6.3	1.6	7.8
Denmark	4.2	0.7	4.8
Rest of World	41	7	48
World Total	283	35	318

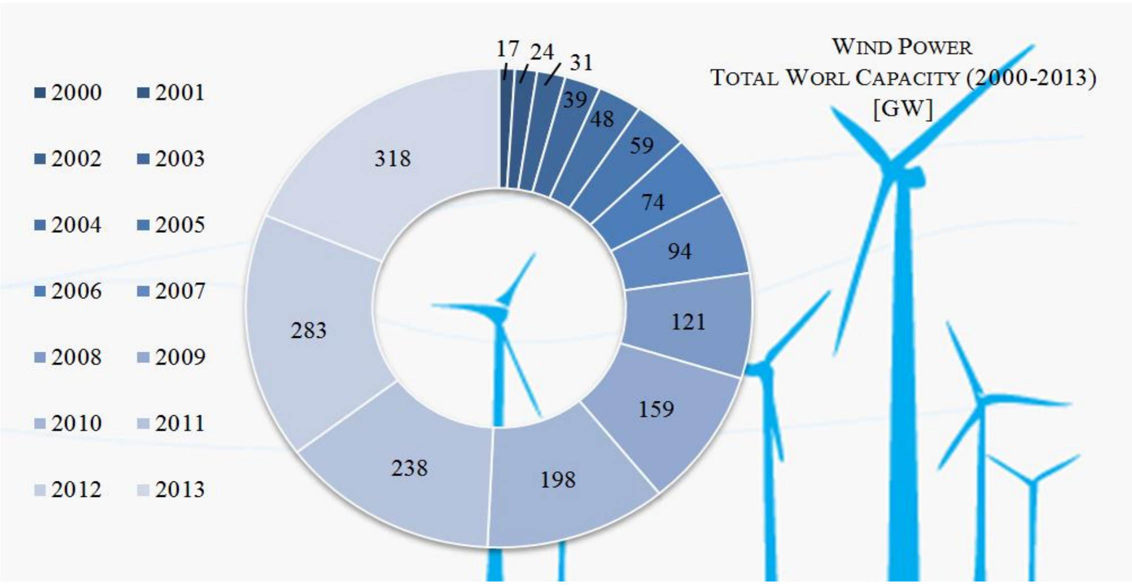

Figure 2.3 - Wind power total world capacity (2000-2013) [26] .

In continental terms, Asia is the one that have successively grown in recent years and holds half of the new capacity added, followed by the European Union in Europe (23% in 2014, compared with about 32% in 2013) and North America, which has grown by 13% in 2014, an 8% less compared with 2013. From Table 2.2, it can be seen that only China accommodates 45% of the new wind added globally, followed by Germany, United States and India. Other countries in the top 10 are Canada, UK, Sweden, France and Denmark. Growth in some of the major markets was driven by uncertainty about future policy changes.

The significant wind power growth is due to the continuous technological advances and relative maturity, supporting mechanisms and incentive packages, favorable policy, continuously falling capital costs among others. Table 2.3 shows the main wind power generation technologies, their technical characteristics and associated costs. The three main turbine types are classified by their sizes and deployment site (onshore or offshore). For each technology, two types of capital costs are shown in US dollars per kW and the typical costs of energy production in US cents per kWh.

2.4.2 Solar Energy

2.4.2.1. Solar PV

Solar energy is the main and largely inexhaustible source of energy for most countries [15]. In recent years, the deployment of PV has been breaking records year after year. After nearly a stagnated period, it has steadily grown to be one of the leading technologies in terms of installed capacity. More than 39 GW has been added in 2013, bringing the total installed capacity to over 139 GW in this technology by 2013.

Table 2.3 - Wind Power Generation Technologies [20]

TECHNOLOGY	TYPICAL CHARACTERISTICS	CAPITAL COSTS (USD/kW)
Wind Onshore	Turbine size: 1.5-3.5 MW Capacity factor: 25-40%	925-1,470 (China and India) 1,500-1,950 (elsewhere)
Wind Offshore	Turbine size: 1.5-7.5 MW Capacity factor: 35-45%	4,500-5,500 (Global) 2,250-6,250 (OCDE)
Wind Onshore Small-scale	Turbine size: up to 100 kW Average: 0.85 kW (Global) 0.5 kW (China) 1.4 kW (United States) 4.7 kW (United Kingdom)	2,300-10,000(United States) 1,900 (China) 5,870 (United Kingdom)

There has been a geographical shift of the biggest installers, led by China, Japan and the United States, and Asia is becoming the largest solar PV market worldwide instead of Europe. China have witnessed higher growth than Europe, and other promising markets such as the US and others have experienced an extremely slow growth [16].

In 2013, nine countries added more than 1.0 GW of solar PV to their networks, and new facilities continue to appear as can be seen in Table 2.4. At the end of 2013, at least 10 GW of total capacity was added in five countries instead of two in 2012. The leaders of solar energy per capita were Germany, Italy, Greece, Czech Republic and Australia [20]. Asia added 22.7 GW at the end of 2013, bringing the total amount of solar PV in operation to almost 42 GW. China had almost a one third share of the global installed capacity.

Apart from Asia, about 16.7 GW were added around the world, mainly in the EU (about 10.4 GW) and North America (5.4 GW) in which the United States led became the third largest market in 2013.

The Solar PV technologies can be divided into two main types depending on where they are placed, rooftop or ground-mounted. Each has a set of characteristics. However, it can be said that there are three transverse characteristics of both types of technologies: the peak capacity, the capacity factor and the conversion efficiency (as depicted in Table 2.5).

These technologies are also distinguished based on where/how they are being deployed: residential, commercial and industrial consumer in particular with respect to peak capacity. Note that the receptivity of each type of technology varies greatly from one geographical area to another mainly due to the differences in energy cost of each of these areas, and often the incentives/compensation for the adherence to these technologies [15].

2.4.2.2. Solar CSP

The concentrated solar power (CSP) is a market that is so far small but it is growing mainly thanks to the increased efficiency levels in places with direct sunlight and low humidity. This technology continues to spread to new markets with significant projects already completed in late 2013 in Australia, Italy and the United States and progress in Chile, Namibia, Portugal, Saudi Arabia, among others [20].

The biggest market is China with 50 MW. More than 165 MW were added in systems operating in over 20 countries led by China and the United States, as can be seen in Table 2.6.

Table 2.4 - Solar PV Global Capacity and Additions [20]

COUNTRY	TOTAL END 2012 (GW)	ADDED 2013 (GW)	TOTAL END 2013 (GW)
Germany	32.6	3.3	35.9
China	7.0	12.9	19.9
Italy	16.4	1.5	17.6
Japan	6.6	6.9	13.6
United States	7.2	4.8	12.1
Spain	5.4	0.2	5.6
France	4.0	0.6	4.6
United Kingdom	1.8	1.5	3.3
Australia	2.4	0.8	3.3
Belgium	2.7	0.2	3.0
Rest of World	13.8	6.5	20.2
World Total	100	39	139

Table 2.5 - Solar Energy Technologies [20]

TECHNOLOGY	TYPICAL CHARACTERISTICS	CAPITAL COSTS (USD/kW)
Solar PV (rooftop)	**Peak capacity:** 3-5 kW (residential); 100 kW (commercial); 500 kW (industrial) **Capacity factor:** 10-25% (fixed tilt)	**Residential costs:** 2,200 (Germany); 3,500-7,00 (U.S.A.) 4,260 (Japan); 2,150 (China) 3,380 (Australia); 2,400-3,000 (Italy) **Commercial costs:** 3,800 (United States); 2,900-3,800 (Japan)
Solar PV (ground-mounted; Utility-scale)	**Peak capacity:** 2.5-250 MW **Capacity factor:** 10-25% (fixed tilt) **Conversion efficiency:** 10-30%	1,200 -1,950 (typical global); As much as 3,800 including Japan. Averages: 2,000 (United States); 1,710 (China); 1,450 (Germany); 1,510 (India)

*LCOE- Levelized Cost of Energy

Table 2.6 - Concentrating Solar Thermal Power (CSP) [20]

COUNTRY	TOTAL END 2012 (MW)	ADDED 2013 (MW)	TOTAL END 2013 (MW)
Spain	1,950	350	2,300
United States	507	375	882
United Arab Emirates	0	100	100
India	0	50	50
Algeria	25	0	25
Egypt	20	0	20
Morocco	20	0	20
Australia	12	0	12
China	0	10	10
Thailand	5	0	5
World Total	2,540	885	3,425

The solar thermal power market continues to grow after the record in 2012. In 2013, the overall capacity grew by 36%, more than 3.4 GW, with Spain and the United States being the major markets [15].

A summary of the main CSP technologies can be found in Table 2.7, which shows the main characteristics as well as the cost of these technologies by country or area. In the typical characteristics, the main types of CSP, the size of the plants and the capacity factor are shown.

2.4.3 Geothermal Energy

Geothermal energy can be used efficiently in the development of networks whether they are connected or not, and is especially useful in rural electrification schemes and direct applications such as district heating, cooking, bathing and industrial processes, etc. [17]. Geothermal resources provide energy in electrical form and heating/ direct cooling. Global electricity generation from geothermal sources is estimated to be just under half of the total geothermal production of 76 TWh, with the remaining 91 TWh accounting for direct use [17].

From Table 2.8, it can be seen that, in 2013, the estimated generation capacity added was at least 530 MW, bringing the total global capacity to 12 GW, with an estimated annual generation of 76 TWh [20].

The countries that added more production capacity in 2013 were New Zealand, Turkey, the United States, Kenya, Mexico, Philippines, Germany, Italy and Australia. By the end of 2013, the countries with the largest installed generation capacity were the United States with 3.4 GW, the Philippines with 1.9 GW, Indonesia with 1.3 GW, Mexico with 1.0 GW, Italy with 0.9 GW, New Zealand with 0.9 GW, Iceland with 0.7 GW and Japan with 0.5 GW.

Table 2.7 - Solar CSP Energy Technologies [20]

TECHNOLOGY	TYPICAL CHARACTERISTICS	CAPITAL COSTS (USD/kW)
Concentrating solar thermal power (CSP)	Types: parabolic, trough, tower, dis Plant size: 50-250 MW (trough); 20-250 MW (tower); 10-100 MW (Fresnel) Capacity factor: 20-40% (so storage); 35-75% (with storage)	Trough, no storage: 4,000-7,300 (OCDE) 3,100-4,050 (not OCDE) Trough, 6 hours storage: 7,100-9,800 Tower: 5,600 (United States without storage) 9,000 (United States with storage)

*LCOE- Levelized Cost of Energy

This resource can be classified into two categories [27]:

- High temperature (T> 150°C): This resource is usually associated with areas of volcanic activity, seismic or magma. At these temperatures, it is possible to use the geothermal resource for power generation purpose;
- Low temperature (T <100°C) generally results from the meteoric rise of water circulation in faults and fractures as well as resident water inside porous rocks at deep underground.

The geothermal energy conversion process involves energy transfer by convection, transforming the heat produced and contained inside the earth into a useful energy in the form of electricity or other forms. The energy can also be extracted using the water injection technology from the surface in hot rock formations. Table 2.9 summarizes some general characteristics of geothermal technologies.

Table 2.8 - Geothermal Power Global Capacity and Additions [20]

	NET ADDED 2013	TOTAL END 2013
Top Countries by Total Capacity	(MW)	(MW)
United States	507	375
Philippines	0	100
Indonesia	0	50
Mexico	25	0
New Zealand	20	0
Top Countries by New Additions	MW	MW
New Zealand	196	0.9
Turkey	112	0.3
United States	84	3.4
Kenya	36	0.2
Philippines	20	1.9
Mexico	10	1.0
World Total	465	12

Table 2.9 - Geothermal Power Technology [20]

TECHNOLOGY	TYPICAL CHARACTERISTICS	CAPITAL COSTS (USD/kW)
Geothermal Power	Plant size: 1-100 MW Capacity factor: 60-90%	Condensing flash: 1,900-3800 Binary: 2,250 - 2,200

2.4.4 Hydro Energy

The production of hydroelectricity is mainly through hydroelectric plants, which are associated with large or medium capacity dams, forming a reservoir of water by interrupting the flow of water. Also, this energy has been exploited by applying the so-called small hydro plants, which consist of the construction of small reservoirs or dams that divert part of rivers for an unleveled location (where the turbines are installed), thereby producing electricity. The production of hydroelectricity is the most efficient and one of the least polluting processes. Many of the effects are reversible, and nature with the human contribution, ultimately find a new balance.

The capacity of global hydropower production in 2013 increased by 4% (approximately 40 GW), which varies every year according to the metrological conditions of the places where they are located, was estimated at 3,750 TWh in 2013.

The countries with the highest production capacity are China (260 GW/ 905 TWh), Brazil (85.7 GW/ 415 TWh), the US (78.4 GW/ 269 TWh), Canada (76.2 GW/ 388 TWh), Russia (46.7 GW/ 174.7 TWh), India and Norway, which together have 62% of global installed capacity [3].

It is estimated that a pumped storage capacity in the order of 2 GW was added in 2013, bringing the global hydropower to 135-140 GW. The country that installed more hydropower capacity in 2013 was China. Other countries with significant installed hydropower capacity were Turkey, Brazil, Vietnam, India and Russia as can be seen in Table 2.10.

Table 2.10 - Hydro Power Global Capacity and Additions [20]

	NET ADDED 2013	TOTAL END 2013
Top Countries by Total Capacity	(GW)	(GW)
China	28.7	260
Brazil	1.5	86
United States	0.2	78
Canada	0.5	76
Russia	0.7	47
India	0.8	44
Top Countries by New Additions	GW	GW
China	28.7	260
Turkey	2.9	22
Brazil	1.5	86
Vietnam	1.3	14
India	0.8	44
Russia	0.7	47
World Total	40	1,000

Hydropower is the most developed technology among the renewables, reaching levels of optimality when coupled with the wind. The summary of the main technological characteristics can be found in Table 2.11, including the typical technology cost for each type. It can be emphasized that, among the presented technologies, it is the one that has the lowest typical cost.

2.4.5 Bioenergy

Bioenergy is the designation for the energy obtained from biomass. There are three forms of fundamental energy: heat energy, mechanical energy and electricity, all of which can be obtained from biomass sources.

The systems that produce mechanical energy as combustion engines or turbines of direct and indirect combustion are coupled to electrical generators, which convert mechanical energy into electrical energy. The conversion of mechanical energy to electrical energy generates heat approximately two-third to one-third of the generated electricity, which demonstrates the increased economic efficiency of cogeneration (simultaneous production of heat and electricity) in stationary applications. The biogas from landfills, recycling of agricultural wastes and other organic wastes can be used in stationary power plants for energy production [28].

Bioenergy has shown steady growth rates in the last years and it is expected to keep on this path in the future. In EU, the consumption of biomass energy is projected to increase by at least 33 Mtoe by 2020, as shown in Figure 2.4. The electricity generation in the EU from solid biomass in 2014 was approximately 81.6 TWh. The five top producers were the US followed by Germany, Finland, United Kingdom, Sweden and Poland having a total production in Europe of 63% [29].

Table 2.11 – Hydro Power Technologies [20]

TECHNOLOGY	TYPICAL CHARACTERISTICS	CAPITAL COSTS (USD/kW)
Hydropower (grid-based)	Plant size: 1 MW -18,000 MW Plant type: reservoir, run-of-river Capacity factor: 30-60%	Projects > 300 MW: 1,000-2,250 Projects 20-300 MW: 750-2,500 Projects < 20 MW: 750-4,000
Hydropower (off-grid/rural)	Plant size:0.1-1,000 kW Plant type: run-of-river, hydrokinetic, diurnal storage	1,175-6,000

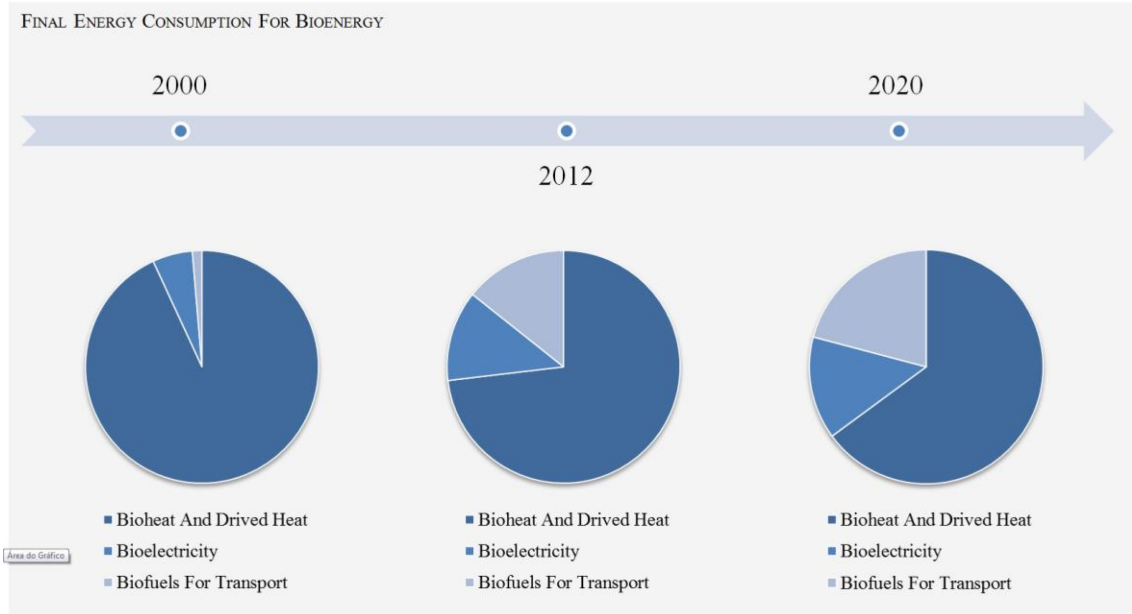

Figure 2.4 - Final energy consumption for Bioenergy in EU [30].

The estimated growth of bioenergy market in 2014 was 5 GW, bringing the total capacity worldwide to approximately 93 GW. Country wise, the bio-generation leaders are the United States with 69.1 TWh, Germany with 49.1 TWh, China with 41.6 TWh, Brazil with 32.9 TWh and Japan with 30.2 TWh.

2.4.6 Ocean Energy

Ocean power refers to any energy harnessed from the ocean waves, tidal range (up and down), tidal currents, ocean currents, temperature gradients and salinity gradients [31]. The development of this emerging sector can contribute to the achievement set targets for renewable energy integration, reduction of GHGs and their harmful effects, and simultaneously boost economic growth through innovation and new job creation [32].

At the end of 2013, the capacity of the ocean energy was about 530 MW, most of this coming from the tidal power category [3]. Majority of ocean power projects currently in operation generate power from ocean tides. Among these is the Sihwa plant in Korea, completed in 2011 with a capacity of 254 MW, the central Rance in France with a capacity of 240 MW, the central Annapolis Nova Scotia, Canada with a capacity of 3.9 MW and Jiangxia in China with the capacity of 3.9 MW. Other projects are smaller, and many of them are pre-commercial demonstration projects with a remarkable concentration of wave and tidal development facilities (in the order of 11 MW) in the UK [20]. Some of the tidal technology characteristics are summarized in Table 2.12.

Table 2.12 - Ocean Power Technologies [20]

TECHNOLOGY	TYPICAL CHARACTERISTICS	CAPITAL COSTS (USD/kW)
Ocean Power (tidal range)	Plant size: <1 to >250 MW Capacity factor: 23-29%	5.290-5,870

2.5 Economic Aspect of Renewable Energy Systems

Installation cost, net annual energy production and value of energy are the three main economic factors to make a decision about employing renewable energy systems. The value of energy is equal to the electricity price or tariff for renewable energy systems located on the supply side; while it can be equal to the retail price for demand side renewable resources (the systems that use energy on site). The reason for using retail price in studies of renewable energy systems on the demand side is that, the purchased energy from the grid by the consumer is displaced by the on-site generation. In order to investigate economic feasibility of renewable resources, they have to enter in a competition with other available energy resources and technologies. Fossil fuel prices have had considerable variations over the past ten years, and there is an uncertainty about these prices in future. Considering carbon emission is also another factor that has affected the fossil fuel cost [33]. In order to concentrate on the fuel cost and its uncertainty in more details, it should be noted that a cost between 0.5 and $1.0/gallon is added to the gasoline cost in the US that is related to the military expenditures just to ensure the oil flow from the Middle East [4].

In order to improve the penetration level of renewable energy resources in the power system, the installation costs should be returned during a rational period. This would be obtained by producing sufficient power at an appropriate price. In the cases that renewable energy systems are installed in places where there is no connection to the power system network, the price of electricity would be high, because it would be obtained by a cost competition with other available energy careers. On this basis, the electricity price of renewable energy systems is associated with the range of prices of the energy careers. There are many factors that induce uncertainty in the future cost of energy careers. These factors are mostly related to the level of dependency on imported energy careers, policies on emission reduction, as well as policies on developing renewable energy resources [34].

The price of all energy careers is strongly associated with the price of oil that has been difficult to forecast due to many factors such as political aspects [35]. Fluctuations of oil price in the past few years prove this claim that prediction of energy prices has become more complex. For example, in some reports, the peak time of oil price was forecasted to occur in 2007, while other reports forecasted it to happen in 2015 and even 2040 [36]. Note that, since the oil price is also related to the demand growth, a wide range of its fluctuations must be considered for each time and geographic area [37].

It should be noted that, energy economics is highly dependent on incentive- and penalty-driven policies. On this basis, it is very difficult to impose life cycle costs without considering the impacts of emission and government supports that motivate investors for investing in renewable energy systems [38]. According to the aforementioned description, the regulatory supports for renewable energy systems have been driving the world market.

2.5.1 Driving Factors

Many factors affect investments in renewable energies systems. Incentives are a key element in choosing the renewable systems, since both type and size of renewable energy systems are determined by investors based on the differences between market incentives. Another affecting factor is the cost of land that has an important impact on type and number of renewable energy systems. In order to have the optimal rate of return, renewable energy systems should have the highest amount of availability to ensure they can produce an appropriate level of energy. On this basis, they should have the capability to be operated as much time as possible. To this end, the reliability of the network and consequently the unavailability to transfer generated power due to network failures should be estimated.

It should be noted that, if the renewable energy system generates when the demand peak occurs, the income of the system is augmented due to the increase in energy price. Owners of on-site renewable resources can also benefit more when the generated energy by the systems is required by the on-site demand. For example, the wind power generator produces electricity at nights when the space heating systems are highly required during winter.

Renewable energy systems are able to generate power to supply the on-site demand, or to inject to the grid. The amount of energy that is consumed by on-site demand is replaced with the supplied energy by the grid. On this basis, if the amount of generation is less than the on-site demand, using renewable energy systems can reduce the net load. On the contrary, if the on-site consumption is less than the generated energy, the surplus is injected into the grid at a price/tariff based on an agreement with the utility.

Externalities are also an important factor for making a decision about renewable energy resources. This is due to the fact that in life-cycle cost analysis emission and carbon dioxide costs should be considered [39], [40]. There is a wide range of rates of externalities that depends on the rules and regulations in various countries. Since power producers do not like paying the cost of externalities, in the US there are litigations by all sides to decrease the externality rates based on the reason that there is no reliable evidence to prove carbon dioxide emission is harmful to society. In European countries, there are various costs for carbon dioxide emission that provide a better base for renewable energy resources by making them more cost competitive [40].

2.5.2 Life-Cycle Costs

The life-cycle cost is a method that analyzes the total cost of the system by considering the expenditures during the system life and salvage value [25]. By using a life-cycle cost analysis different investment options can be compared. Moreover, the most economic design for the system can be achieved. There are some other options that the renewable energy systems must compete with such as small-scale diesel generators and electrical energy storage systems. In this case, the effective factors are the initial cost, the electricity price, and the required infrastructures [41], [42]. It is noteworthy that, the life-cycle cost is also useful to compare different plans even if the renewable energy system is the only choice. Furthermore, this analysis is employed to determine if a hybrid renewable-based system can be the most economic plan. The life-cycle cost analysis enables to investigate impacts of employing several components with various reliability and lifetimes.

Discount rate indicates how much increase or decrease in finance happens over the time. Note that, using the inaccurate amount of discount rate for calculating life-cycle cost can cause to unrealistic solutions. Although most of the renewable energy systems are economical, in order to select the best plan between all available options, the life-cycle cost analysis is the best method [41], [42]. The financial assessment can be carried out over an annual base to calculate economic indices such as payback period and cash flow.

It should be mentioned that, annualized cost of energy considered for renewable energy systems should be compared with that for other resources. In other words, the annualized cost of energy should not be directly compared with the current cost of energy, since it is not sensible. The mentioned costs of energy create an appropriate base to compare different plans considering alternative resources and to select the best resource of energy.

There are some calculating tools to analyze renewable energy projects and assess the life-cycle cost, and even emission considerations [43]. These calculations prove that the current renewable energy systems are economical.

2.5.3 Economic Trend of Renewable Energy Systems

Renewable energy systems are strongly promoted by policy makers, because they are a key element for economic development. The renewable systems are able to compete with current thermal power plants [35]. They can also improve the economy by job creation, since more than 100 jobs for installing a wind power plant and more than 10 jobs for its operation are required for each 100 MW project [4]. There are some attempts to reduce the property tax of wind power plants in order to better motivate the investor to invest in the renewable system and consequently the economic development [44].

Wind power generation is one of the most economic renewable energy systems, since its cost of energy (COE) is about $70/MWh that can compete with thermal units. Trend studies have shown that before 2003, COE of wind power plants was higher than fuel fossil units; however, in the period of 2003 to 2009, it approximately equaled to the thermal units [4]. In 2009, the COE of wind farms dropped to the levels lower than conventional power.

The studies on various resources indicate that annualized COE of wind power plants can even compete with the one of combined cycle gas turbines, although the fuel price of these thermal units is low [45]. In some countries, such as the US, conventional power plants benefit from that the fuel costs are not taxed, whereas the renewable energy systems do not have the cost of fuel at all. On this basis, the main issue of renewable resources is the high investment cost, which causes people to prefer paying for the fuels. It should be noted that, in the case of on-site renewable energy systems, the small-scale wind power generation cannot compete with the retail prices [46].

In the case of supply side, another barrier to integration of renewable energy systems is the capacity of transmission network that may cause the power curtailment in order to ensure the system security [47]. Since most of the renewable energies such as wind, solar and geothermal resources are far from the load centers, they can impose an extra cost on the transmission system [48].

Although the future of energy is uncertain and ambiguous, and every prediction can be risky, as oil price forecast has been a challenge, the trend of renewable energies is almost evident [37]. On this basis it can be expected that in future distributed renewable energy systems will have more penetration and even some new distributed electricity markets will help these new resources [46].

In addition, with developments of the high-voltage transmission network, large farms of renewable energy systems will be installed much far from the load centers [47]. In near future, renewable energy resources can better compete with other energy alternatives just due to the carbon cost. Even other air emission costs such as NO_X and SO_X will motivate people to invest in systems without fuel and emission costs. This can cause that renewable energies, particularly wind power, become the most economic resource of producing electricity [41], [42].

It should be noted that one part of the installation cost of renewable energy systems has been supplied by the income resulted from carbon trading. The future of energy without renewable energy system developments would be an unsolvable problem due to the growth of environmental concerns. In order to avoid this problem and to provide a sustainable energy, policy makers should put more weight on the renewable energy as well as conservation and energy efficiency.

2.6 Benefits and Barriers of RESs

2.6.1 RES Integration Opportunities

Most of the electric energy consumed come from non-renewable energy sources (mainly, fossil fuels). This has led to a series of questions from energy dependence concerns to climate change issues, which are some of the major drivers of RES integrations in many power systems across the world. It is now widely recognized that integrating RESs in power systems brings about a lot of economic, environmental, societal and technical benefits to all stakeholders. These are some of the reasons behind the rapid growth of RES integrations in many power systems across the world, as indicated in a 2015 report by the International Energy Agency (IEA). The report further shows that, in 2013, an approximately 19.1% of global electric energy consumption came from RESs, most of which was from hydropower [3].

Among the wide-range benefits of RESs is their significant contribution to the GHGs which are leading to not only climate change and its dire consequences but also series environmental and health problems. Most RES technologies (wind and solar PV, for instance) have very low carbon footprints, making them very suitable to mitigate climate change and reduce its consequences. Hence, integrating RESs in power systems partly replaces polluting (conventional) power generation sources, resulting in a “cleaner” energy mix i.e. one with lower emission levels.

RES integration also has an undisputable positive impact on the social and economic development of nations. It is widely understood that the three socio-economic indicators, per capita income, per capita energy use and economic growth, are highly correlated with each other. Economic growth can be considered, for instance, as the main driver for energy consumption. Therefore, RESs can spur economic growth and create job opportunities. Because of their distributed nature, RES integration can also be integrated into a national policy (especially, in developing countries) to foster rural development. Currently, the RES business currently employs an estimated 7.7 million people throughout the world [3]. RESs also play a crucial role in energy access. Currently, more than 1.2 billion people do not have access to electricity globally (85% of which are in rural areas where RESs are abundant) [3]. Exploiting the potential of RESs should be at the forefront to address this societal problem.

Energy security concern is also one of the main drivers of RES integration. Current electric energy production scheme is dominated by conventional generation sources, which use fossil fuels whose prices are subject to significant volatilities. In addition to these volatilities, geopolitical availability of fossil fuels is also becoming a concern for many countries. The combination of all these can have significant impacts on the energy supply security. Because of this, generation of electricity locally using RESs can significantly contribute to the energy security of nations. As a result, this can reduce the heavy dependence on fossil fuels for power generation.

In addition to the benefits briefly explained above, RESs can bring technical benefits such as improved system stability and voltage profiles, reduced losses and electricity prices, etc. The combination of conventional generation capacity with the renewable generation capacity will be able to address the continuous increase in demand, in opposition to the scenario of conventional generation capacity only, which according to forecasts would not be able to meet the demand, Figure 2.5.

2.6.2 RES Integration Challenges and Barriers

Despite the robust growth of integration RES in many power systems, there are still certain challenges and barriers that impede the smooth integration of RESs. These challenges and barriers can be broadly classified into two categories: technical and non-technical. The non-technical category includes challenges and barriers related to capital costs, market and economic issues, information and public awareness, socio-cultural matters, the conflict between stakeholders, regulation and policy.

The variable cost of energy production by RESs is very small (close to zero); however, they are generally capital intensive. Even if the capital costs are declining for most RES technologies, their levelized costs of electricity (LCOE) are yet to be competitive with that of conventional energy sources. This can make investing in RESs less attractive for potential investors. However, this is likely to change as RES costs continue to fall while that of conventional energy sources become more expensive amid resource depletion and policies to internalize external costs such as environmental pollution costs.

Market and economic barriers exist when there is a lack of clearly designed economic and financial instruments to support RES integration efforts. For instance, whenever there is market failure associated with internalizing the cost of environmental pollution, it is very difficult to expect a lot of investments coming in from RES developers.

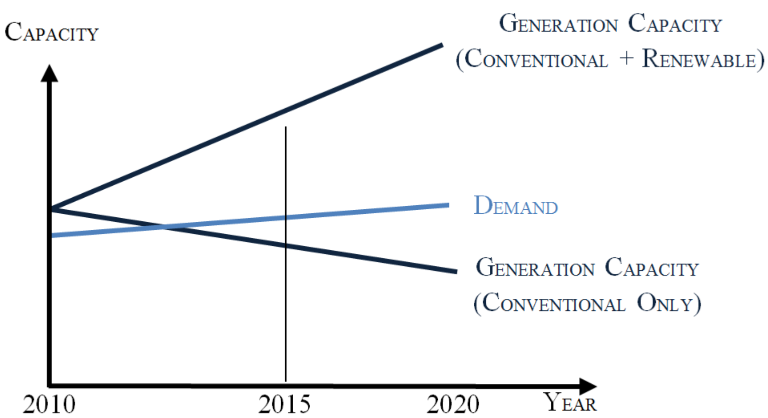

Figure 2.5 - Development and future trend of generation capacity, demand and wholesale electricity market price in Central Europe from 2010 [49].

Information gap and lack of public awareness on RESs and their benefits can also significantly hinder RES integration. Moreover, socio-cultural issues such as conflicting land use requirements can sometimes lead to contentious issues regarding RES development, directly affecting the level of penetration. The conflict between stakeholders is another barrier, more specifically the lack of communication, as shown in Figure 2.6. The challenges and barriers related to the regulatory and policy issues emanate from the structure of energy industries and existing technical regulations, the level of support for technology transfer and R&D, etc.

Technical limitations (barriers), on the other hand, are related to the nature of the resources and the power systems. Some of the most common RESs depend on primary energy sources such as wind speed, solar radiation and wave, which are subject to high level variability and unpredictability (the latter also known as uncertainty), resulting in considerable grid integration challenges [51]. This is because the uncontrollable variability and uncertainty of such sources introduce a lot of technical problems in the system, making the real-time operation of the system very challenging. The intermittent nature of power production from these resources also dramatically affects the reliability of energy supply. Moreover, such sources are found geographically dispersed across a vast area, and their availability is site-specific. Unlike conventional power sources, these energy sources cannot be transported to areas close to demand centers. This means harnessing these resources requires the higher need for network investments than conventional ones.

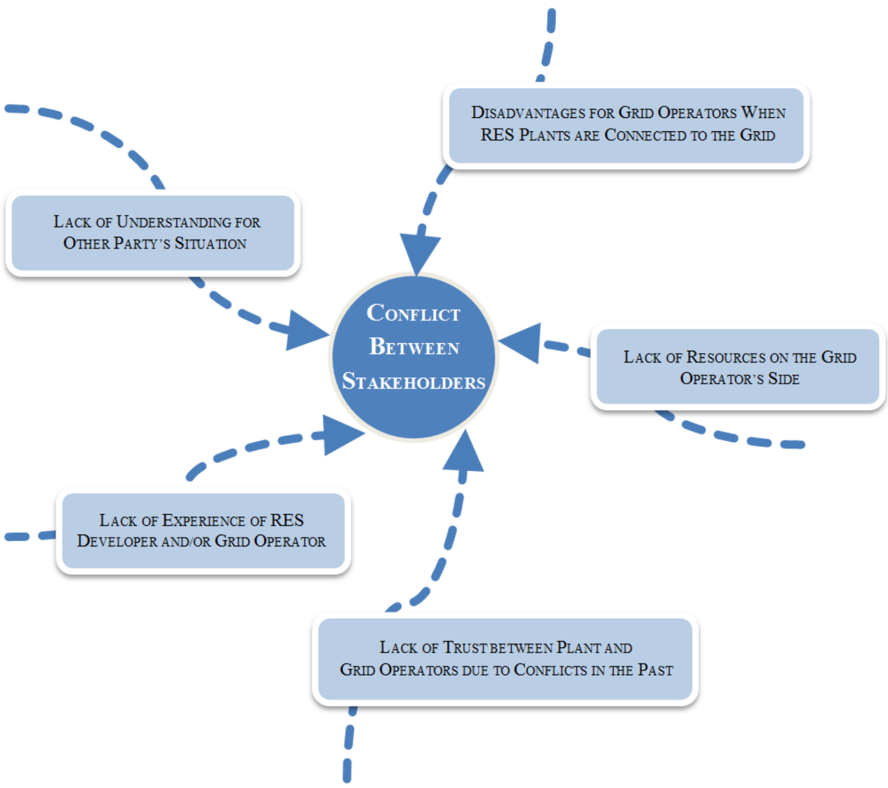

Figure 2.6 - Main reasons in the EU 27 for issue “Lack of communication” [50].

In addition, RESs based on the aforementioned primary energy sources are characterized by low capacity factors (i.e. low energy production per MW installed) compared to conventional power sources. In other words, the spatial energy intensity of RESs based on these sources is very low. This means that, for the same amount MW installed, the size of land required for such RESs is several times higher than that of the conventional one, which can sometimes be problematic during integration efforts because this creates fierce competition with other land use claims or requirements [52].

2.6.3 Alleviating the Challenges and Barriers

Most of the challenges and barriers explained before have proven solutions that happen to be overlooked in many systems [53]. In general, these are summarized as follows:

- Market and economic barriers are often fixed by streamlining appropriate market and economic signals related to carbon taxes, emission trading schemes, finances, and incentive mechanisms as well as enhancing public support for R&D, and creating a conducive environment for RES development. All this can have a considerable positive impact on the level of RES integration.
- Setting energy standards, continuous information campaigns and technical training about RESs and their benefits can enhance public knowledge and awareness, which can in the end have supportive roles in RES development.
- Creating an enabling environment for R&D, improving technical regulations, scaling up international support for technology transfer, liberalizing energy industries, providing incentive packages to RES developers, designing appropriate policies of RESs and conventional energy sources, minimize the regulatory and policy barriers to developing RESs.
- Coordinating investments of RESs based on variable generation resources such as wind and solar power with large-scale energy storage systems, demand side management participation and grid expansion can significantly increase the level of RES integration.
- Enhancing operation and the flexibility of conventional power generation sources can also be very useful to scale up RES integration.
- Designing an efficient wholesale market such as dynamic retail pricing and developing coordinated operation and planning tools (such as joint network and generation investment planning models) can have a positive role in RES integration.
- For full utilization of RESs, the coordination between distribution system operators (DSOs) and transmission system operators (TSOs) is also vital.
- It is also important to improve prediction tools, monitoring and control protocols that can help efficient utilization of the RESs.

- Ensuring regional interconnections via regional cooperation and increasing the level of participation of all stakeholders (including RES generators) in voltage control, provision of reserves, reactive power support, etc. are significantly helpful for the stated purpose.

- Using smart-grid technologies and concepts are also expected to facilitate smooth integrations of large-scale RESs because these are equipped with advanced control and management tools to counterbalance the intermittent nature of most RES energy productions.

2.7 Current Trend and Future Prospects

During the past decades, the level of global RES integration has been steadily growing. This has been against a number of odds such as the recent global financial crisis, the dramatically falling fuel prices and the slowdown of increasing global electricity consumption that have been thought to decelerate or stall this trend [23]. In general, there is a general consensus globally that RESs will cover a significant amount of electricity consumption in the years to come. The high uncertainty of RESs can be partially solved by the introduction of a bigger operational flexibility, as shows in Figure 2.7, through coordinated participation of various stakeholders.

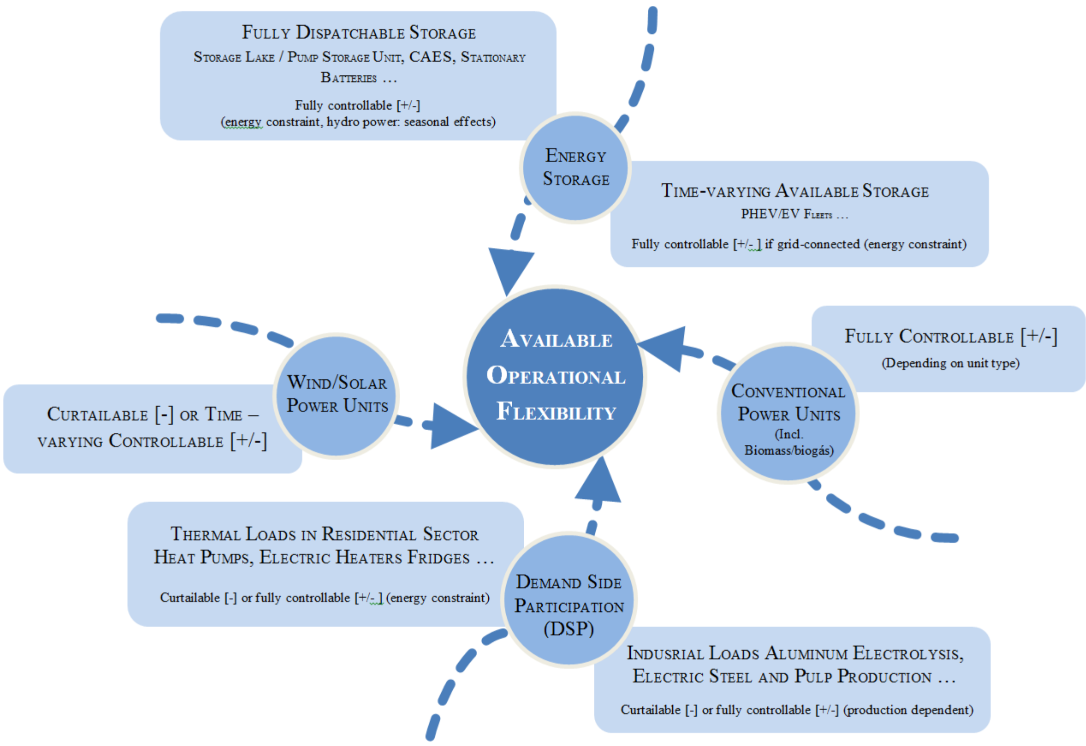

Figure 2.7 - Sources of Operational flexibility in power systems, adapted from [54].

The recent developments in the 2015 Paris climate conference (COP-21), overall trends in international policy on RESs, energy dependence concerns, the falling capital costs of several matured RES technologies, and other techno-economic factors are all favorably expected to further accelerate the level RES integrated into power systems.

2.8 Chapter Conclusions

The potential of RESs is huge because in principle they can meet several times the world's demand. RESs such as wind, biomass, hydro, biomass and geothermal can provide sustainable energy services based on available resources in all parts of the world. The transition to renewable energy based power systems tends to increase, while their costs continuously decline as gas and oil prices continue to oscillate. In the last half century, the demand for wind and solar systems has been continuously increasing, experiencing a reduction in capital costs and generated electricity costs. There have been continuous performance improvement and R&D undergoing in the sector in the past decades. As a result, the prices of renewable energy and fossil fuels, as well as social and environmental costs are to diverge in opposite directions. Economic and political mechanisms must support the wide spread of sustainable markets for the rapid development of RES. At this point, it is clear that the present and future growth will occur mainly in renewable energy and in some natural gas-based systems, and not common sources like coal or oil. The progress of RESs can increase diversity in the electricity markets, contributing to obtain long-term sustainable energy, helping reduce local and global GHG emissions and promote attractive trade options to meet specific energy needs, particularly in developing countries and rural areas, helping to create new opportunities.

Chapter 3

Impact of Operational Variability and Uncertainty on Distributed Generation Investment Planning: A Comprehensive Sensitivity Analysis

This chapter presents a DG investment planning model formulated as a novel multi-stage and multi-scenario optimization problem, in order to perform a comprehensive sensitivity analysis and identify the uncertain parameters which significantly influence the decision-making in distributed generation investments and quantify their degree of influence.

3.1 Introduction

Driven by techno-economic and environmental factors, nowadays, there is a global drive to integrate more distributed energy resources (DERs) in power systems, particularly at the distribution level. These typically include DG, storage technologies, and demand side management [55]. Especially, the scale of DG sources (mainly, renewables such as wind and solar) integrated in many distribution networks is steadily increasing. This trend is more likely to continue in the years to come due to the advent of emerging solutions such as active management of distribution networks [56], [57], which are expected to alleviate existing technical limitations, and facilitate smooth integration of DGs. The favorable agreement of countries in the recent climate change conference in Paris (COP21) is also expected to accelerate the integration of RESs. As a result, the level of electricity demand covered by energy coming from RESs is expected to dramatically increase, and such energy sources will play a significant role in distribution systems.

As a result, the issue of DG investment planning (DGIP) is becoming critical. This is especially more relevant in the case of insular network systems because new regulations are put in place to reduce the heavy dependence of such systems on fossil fuels for energy production. Tapping available energy resources (wind, solar, hydro, etc.) is inevitable to meet not only the increasing demand for electricity, but also environmental constraints and renewable energy source (RES) integration targets set forth either globally or locally through Government initiatives.

However, the intermittent nature of most of these RESs (particularly, wind and solar) makes their integration in distribution networks a more challenging task. This is because such resources introduce significant operational variability and uncertainty to the system. Hence, the development of efficient methods and tools is mandatory to realize an optimal or a cost-efficient integration of such DGs and minimize their side effects.

In addition, the increasing level of DG integration in distribution systems is already leading to substantial changes in the traditional role of distribution systems, which has predominantly been to carry power unidirectionally from substations to consumers in a radial scheme. In other words, distribution network systems are slowly evolving from passive to active networks [56]. This paradigm shift will make sure that they are adequately equipped with the necessary, flexible and intelligent tools which have the capability to minimize the underlining challenges of integrating DERs in such network systems, and, hence, pave the way to high level integration of DERs, RES-based DGs in particular. The advent of modern-day technological advances (such as smart grid technologies with state-of-the-art control and protection mechanisms) combined with conventional power system management systems (such as active and reactive power management tools) will make active networks effectively materialize [58].

Generally, the broad-range transformations in distribution networks are largely expected to effectively address current limitations of integrating DERs. As a result, the highly needed benefits of DERs, extensively discussed in [55] and [59], will be optimally exploited. In this regard, previous works on investment planning of DGs in distribution systems such as [60], [61] highlight the multi-faceted benefits of DGIP. In particular, the work in [61] demonstrate that “investment in DG is an attractive distribution planning option for adding flexibility to an expansion plan, mainly by deferring network reinforcements”. Other wide-range benefits of DGs have been extensively discussed in [62]-[66] . As mentioned earlier, the integration of DG in distribution systems comes with certain challenges [67]-[69]. For example, if DGs are not properly planned and operated, they can pose considerable technical problems such as reduced voltage quality and stability. However, these are expected to be adequately mitigated in active distribution networks [61].

From a modeling perspective, DGIP has been carried out in previous works jointly with distribution network expansion planning [70]-[76] or independently [60], [61], [77], [78]. Either way, the decision variables encompass the type of DG, its capacity and location as well as the time of investment when a dynamic planning scheme is adopted as in [60], [70], [71], [74]-[78]. In the context of micro-grid or autonomous/insular systems, the prospects of DG planning, scheduling and operation have been gaining attention. Authors in [79] present a community-based long-term planning tool for RESs in insular systems with an ultimate objective of maximizing social welfare perceived by the community. The work in [80] proposes a methodology for siting and sizing of DGs from a micro-grid context, and the resulting problem is solved using the prospects of particle swarm optimization and genetic algorithm methods.

Due to the inherent uncertainty and variability, stochastic programming has been used in operation and planning of distribution systems [81]-[85]. Authors in [81] propose a stochastic model for a bidding strategy in the day-ahead market of microgrids in the presence of energy storage systems, RES-based and conventional DGs.

A stochastic energy management of microgrids, consisting of conventional and RES-based DGs as well as price-sensitive loads, is proposed in [82]. Similarly, the work in [83] presents a stochastic operation model to coordinate vehicle-to-grid services with energy trading in the presence of conventional and wind type DGs. Reference [84] develops a stochastic DGIP model based on a mixed integer linear programming (MILP) framework. Uncertainties related to energy price, electricity demand, wind and solar PV power outputs are accounted by forming and dividing the corresponding duration curves.

A DG allocation problem in radial distribution networks is solved using genetic algorithm in [86]. Here, uncertainty due to forecasting errors in load and generation is modeled using a fuzzy approach. A dynamic expansion planning of distribution systems with DGs is proposed in [87], and a relatively new meta-heuristic algorithm is employed to solve the resulting problem. Uncertainty and operational variability are not accounted for in this work. The use of non-exact methods such as the meta-heuristic solution methods used in [80], [86], [87] do neither guarantee global optimality nor a measure to the global optimal solution. Since DG includes intermittent energy sources, the planning model should adequately take into account the uncertainty and variability introduced as a result, including that of electricity demand. In this respect, variability in load [60], [61], [70], [71], [74]–[77], [86] and [88], electricity prices [60], [61], [70], [71], [77], wind power output [71], [77], [79], [86], solar power output [77], [79], [86], fuel prices [77], demand growth [60], [61], and DG failures [72] are among several sources of uncertainties which have been given some attention in distribution planning works in the literature. The compound effect of all these relevant uncertainty and variability issues requires designing new methods and tools in order to have an optimal or a cost-efficient integration of DGs. To guide the development of such methods and tools, it is necessary to investigate first the impact of variability and/or uncertainty of different model parameters on DG investment decisions, which is the main objective of this chapter.

In this chapter, a comprehensive sensitivity analysis is carried out to meet the aforementioned objective is presented. The ultimate goal is to identify those parameters which influence the decision-making process and quantify their degree of influence. To perform the analyses, a DGIP model, formulated as a multi-stage and multi-scenario optimization problem, is used. In addition, to ensure tractability and make use of exact solution methods, the entire problem is formulated as a mixed integer linear programming (MILP) optimization. The resulting DGIP problem minimizes the net present value of investment, operation and maintenance, unserved energy and emission costs taking into account a number of technical and economic constraints. Note that the problem here is formulated from the distribution system operator's (DSO) point of view and with a particular focus on insular networks. In such networks, where there does not often exist a functional market, in addition to managing the network system, the DSO may own and operate some utility-based DGs, and/or oversee DG investments to keep reliability, stability and power quality in the system at the required levels.

The remainder of this chapter is organized as follows: Section 3.2 presents the terminologies; and, the approaches for management of uncertainty and operational variability including their definitions are also briefly described in this section. Subsequently, in Section 3.3, the mathematical formulation and description of the DGIP model are presented. Section 3.4 discusses the results of case studies. Finally, relevant conclusions are drawn in Section 3.5.

3.2 Uncertainty and Variability in DGIP

3.2.1 Terminology

The terminologies uncertainty and variability are often incorrectly used interchangeably in the literature despite the fact that they are different [89]. Variability, as defined in [90] refers to the natural variation in time of a specific uncertain parameter, whereas uncertainty refers to "the degree of precision with which the parameter is measured" or predicted. We follow these terminologies in the thesis when referring to operational variability and uncertainty, which are introduced by model parameters. For example, wind power output is characterized by both phenomena; its hourly variation corresponds to the variability while its partial unpredictability (i.e. the error introduced in predicting the wind power output) is related to uncertainty.

The schematic illustration in Figure 3.1 clearly distinguishes both terminologies. As demonstrated in this figure, the hourly differences in wind power outputs are due to the natural variability of primary energy source (wind speed); whereas, the likelihood of having different power outputs at a given hour is a result of uncertainty (partial unpredictability) in the wind speed. Other terminologies used in this thesis are snapshot and scenario. A snapshot refers to an hourly operational situation. Alternatively, it can be understood as a demand—generation pattern at a given hour. A scenario, on the other hand, denotes the evolution of an uncertain parameter over a given time horizon (often yearly). For example, the hourly variations of wind power production and electricity consumption collectively form a group of snapshots; whereas, the annual demand growth (which is subject to uncertainty) and RES power output uncertainty are represented by a number of possible storylines (scenarios) [89].

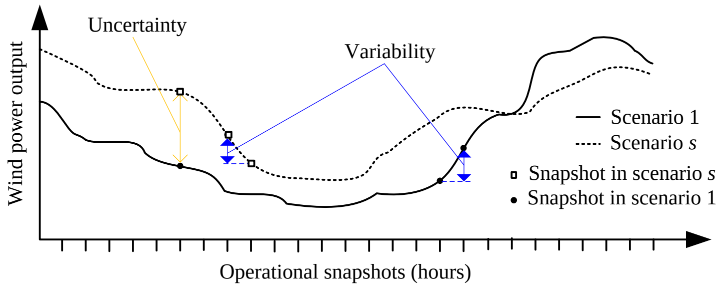

Figure 3.1 - Illustration of variability and uncertainty in wind power output.

3.2.2 Sources of Uncertainty and Variability in DGIP

The various sources of uncertainties in DGIP are related to the variability and randomness of operational situations. There are some other uncertainties mostly related to the long-term price, rules, regulations and policies, etc. They can be generally categorized as random and nonrandom uncertainties [91]. The random ones are also known as high-frequency uncertainties because they correspond to situations that occur repeatedly, and hence, possess historical data. In general, they can be characterized by probability distribution functions (PDFs), estimated by fitting the historical data. Such uncertainties have a profound impact on the operation of power distribution systems. Demand variability is one example in this category. On the other hand, nonrandom uncertainties do not occur repeatedly or they are characterized by low frequency situations; so, they can hardly be statistically represented. A good example here is budget available for investment [89].

A well-developed DGIP tool should therefore encompass a methodology which effectively and efficiently takes into account both types of uncertainties. Exhaustive modeling of all sources of uncertainty and variability may not only be computationally unaffordable but also inefficient. Identifying the most relevant sources of uncertainty and variability for the target problem is a crucial step that should not be overlooked. For example, consider two uncertain parameters: wind power output and emission price. Even if both are subject to uncertainty and variability, the degree of variation or uncertainty of one is totally different from the other. Apparently, the variability and uncertainty of wind power output are a lot higher than that of emission price. Hence, one would expect the former to have a higher influence on the planning outcome compared to the latter.

In this chapter, the variability due to intermittent DG power outputs (mainly wind and solar) and demand are captured by considering a sufficiently large number of hourly operational states, also known here as “snapshots”. The hourly data may be historical or generated from individual or joint PDFs of uncertain parameters. To ensure problem tractability, the hourly snapshots are then reduced by means of k-means clustering, which leads to a substantially lower number of representative snapshots compared to the original set of data. This means each of the selected snapshots, representing a group of similar operational situations, is assigned a weight π_w proportional to the number of operational situations in its group. For instance, the wind power output profile in Figure 3.1 has two profiles for the sample hours. Each day throughout the planning horizon has such profiles of its own. This means that for a horizon of three years long the number of snapshots per scenario is equal to 3x8760. Such number of operational snapshots in each year and scenario are clustered into a predefined number of snapshot groups. In addition to the characterization of the RES power output uncertainty via scenarios (as in Figure 3.1), the uncertainty regarding the evolution of the system (emission price, demand growth, etc.) is also represented by a number of scenarios (or storylines) unfolding as time passes by. Combinations of all these scenarios then form the final set of scenarios (as in Figure 3.2) that are used in the analysis.

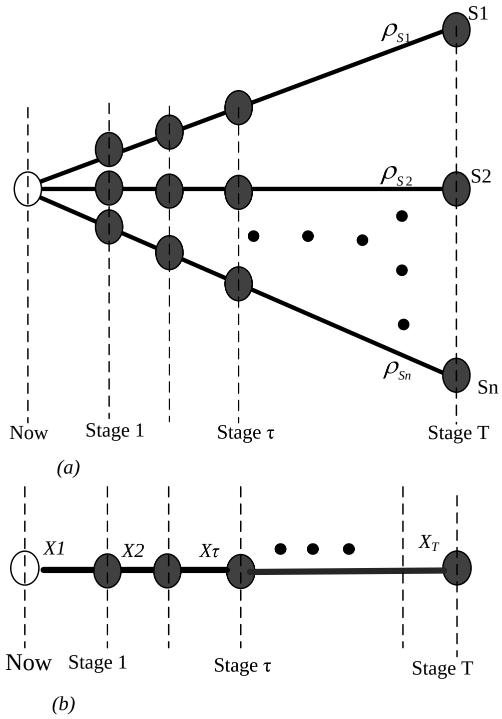

Figure 3.2 - A schematic representation of (a) possible future scenarios' trajectories with multiple scenario spots along the planning horizon, (b) a decision structure at each stage [89].

The schematic representation in Figure 3.2 illustrates the multi-stage and multi-scenario DGIP modeling framework and the expansion solution structure (i.e. Xi's). At each stage of the planning horizon, we obtain a single and robust expansion strategy which is good enough for all scenarios [89], [92]. Note that while operational variables depend on each scenario and snapshot, the investment decision variables only depend on the time stage index. This means that the investment solution obtained should satisfy all conditions in every scenario, making the solution robust against any realization of the considered scenarios. It should be noted here that the robustness of the solution is directly related with the level of details of uncertainty and variability characterization. Generally, the higher the numbers of snapshots and scenarios considered are, the more robust the solution is. However, there is always a threshold beyond which adding more snapshots and scenarios does not significantly change the solution but increases unnecessary computational burden. If the scenarios considered in the planning are carefully selected to be representative enough of all possible uncertainty realizations, then, the robustness and reliability of the solution can be more guaranteed.

In this chapter, the evolution of carbon dioxide (CO_2) price and electricity demand growth are captured through a predefined number of scenarios, each with a certain degree of realization ρ_s. For the sake of simplicity, all scenarios are assumed to be equally probable. The effects of other sources of uncertainty such as fuel prices, and tariffs of energy generated by various DGs (both conventional and renewable power generation units) are then analyzed via sensitivity analysis.

3.3 Mathematical Model

3.3.1 Brief Description of the problem

This chapter focuses on investigating how sensitive DG investment decisions are with respect to variations of selected uncertain parameters. This is relevant for identifying the parameters with the highest influence on DG investment so as to design a DGIP model by adequately factoring the variability and the uncertainty of the most relevant parameters. Eventually, this helps to ensure an optimal integration of DG in network systems.

A DGIP problem is naturally dynamic because the solution has to explicitly provide the necessary information regarding when DG investments are needed. Regarding the planning horizon and decision stages, accounting for the dynamic nature of the problem, a more realistic approach would be to formulate the problem with multiple decision stages (i.e. multi-year decision framework) while accounting for all possible future scenarios. However, to ensure tractability, the numbers of stages and scenarios are usually limited.

In this chapter, the DGIP problem is formulated as a multi-stage and multi-scenario optimization model within a given planning window (horizon). This modeling framework assumes that there are n probable future storylines (or scenarios) each associated with a probability of realization ρ_s that stochastically represents relevant sources of uncertainties.

3.3.2 Objective Function

The resulting DGIP model, a MILP optimization problem, minimizes the sum of net present value (NPV) of four cost terms as in (3.1). Here, the binary investment and utilization variables as well as the operational variables such as generated power, flows, etc. constitute the set of decision variables of the optimization.

The first term in (3.1), TIC, represents the total NPV of the investment costs of DG, constituting conventional and various renewable energy sources, under the assumption of a perpetual planning horizon [93]. In other words, "the investment cost is amortized in annual installments throughout the lifetime of the installed DG", as is done in [71]. The second term $TOMRC$ corresponds to the total sum of NPV: (i) operation, maintenance and reliability (OMR) costs throughout the planning stages, and (ii) the OMR costs incurred after the last planning stage. Note that the costs in (ii) rely on the OMR costs of the last planning stage and a perpetual planning horizon is assumed when spreading these costs after the last planning stage. To further clarify this, consider the illustrative example in Figure 3.3. It is understood that investments are made in a specific year within the planning horizon (the second year in this case) and the investment costs are amortized throughout its lifetime. However, the OMR costs are incurred every year within and after the planning horizon. To balance these cost terms, a perpetual planning horizon, i.e. an endless payment of fixed payments is assumed.

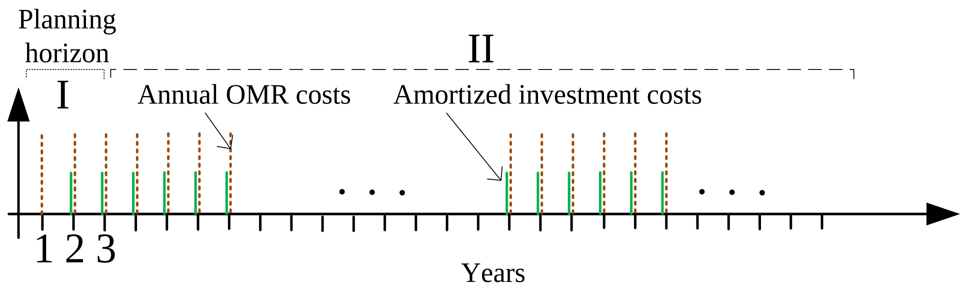

Figure 3.3- Illustration of cost components within and outside the planning horizon [89].

Based on the finance theory [93], the present value of perpetuity, which is the sum of the net worth of infinite annual fixed payments, is determined by dividing the fixed payment at a given period by the interest rate i. Based on this, the OMR costs include the associated annual costs within (part I) and outside the planning horizon (part II). The latter (part II) are determined by the perpetuity of the costs in the last planning stage updated by net present value factor in this case $(1+i)^{-3}$. Note that after the lifetime of the DG elapses, investments will be made in the same DG with the same cost according to the assumption of a perpetual planning horizon.

The third term $TEMC$ in (3.1) corresponds to the total sum of NPV emission costs in the system throughout the planning stages and those incurred after the last planning stage under the same assumptions as in the case of OMR costs. Similarly, the last term TLC in (3.1) accounts for the total NPV cost of losses.

$$Minimize\ TC = TIC + TOMRC + TEMC + TLC \tag{3.1}$$

where $$TIC = \underbrace{\sum_{t\epsilon\Omega^t} (1+i)^{-t} InvC_t^N / i}_{NPV\ of\ investment\ cost}$$

$$TOMRC = \underbrace{\sum_{t\epsilon\Omega^t} (1+i)^{-t} \left(MntC_t^N + MntC_t^E + EC_t^N + EC_t^E + EC_t^{SS} + ENSC_t\right)}_{NPV\ of\ operation,\ maintenance\ and\ reliability\ costs}$$

$$+ \underbrace{(1+i)^{-T}\left(MntC_T^N + MntC_T^E + EC_T^N + EC_T^E + EC_t^{SS} + ENSC_T\right)/i}_{Operation,\ maintenance\ and\ reliability\ costs\ incurred\ after\ stage\ T}$$

$$TEMC = \underbrace{\sum_{t\epsilon\Omega^t}(1+i)^{-t}\ (EMC_t^N + EMC_t^E)}_{NPV\ of emission\ costs} + \underbrace{(1+i)^{-T}(EMC_T^N + EMC_T^E)/i}_{Emission\ costs\ incurred\ after\ stage\ T}$$

and

$$TLC = \underbrace{\sum_{t\epsilon\Omega^t}(1+i)^{-t}\ Loss_t}_{NPV\ of losses\ cost} + \underbrace{(1+i)^{-T}Loss_T/i}_{Losses\ cost\ incurred\ after\ stage\ T}$$

The individual cost terms in (3.1) are computed as follows. The NPV of the total costs is given by the sum of the amortized investment costs of DG, constituting conventional and various renewable energy sources (3.1.1), expected maintenance and operation cost of new (3.1.2, 3.1.4) and existing (3.1.3, 1.5) DGs, as well as the expected cost of unserved energy which is captured by penalizing any unserved power as in (3.1.6). In addition, the expected cost of emission and energy purchased from the grid (if any) are also included in the objective function (see equations 3.1.7 through 3.1.9). The cost of network losses in the system, computed as in (3.1.10), is also included in the objective function. Note that to keep the problem linear, the quadratic flow function in (3.1.10) is linearized using a first-order approximation (i.e. piecewise linearization) as in [17].

In order this chapter to be self-contained, the linearized model is provided in Appendix A. Here, five piecewise linear segments are considered throughout analysis, which is in line with the findings in [94].

$$InvC_t^N = \sum_{n\in\Omega^n}\sum_{k\epsilon\Omega^k}\sum_{p\epsilon\Omega^p}\frac{i(1+i)^{\eta_{p,k}}}{(1+i)^{\eta_{p,k}}-1} IC_{p,k}^N(x_{p,k,n,t}^N - x_{p,k,n,t-1}^N) \qquad (3.1.1)$$

$$MntC_t^N = \sum_{n\in\Omega^n}\sum_{k\epsilon\Omega^k}\sum_{p\epsilon\Omega^p} MC_{p,k}^N\, x_{p,k,n,t}^N \qquad (3.1.2)$$

$$MntC_t^E = \sum_{n\in\Omega^n}\sum_{k\epsilon\Omega^k}\sum_{p\epsilon\Omega^p} MC_{p,k}^E\, u_{p,k,n,t}^E \qquad (3.1.3)$$

$$EC_t^N = \sum_{s\epsilon\Omega^s}\rho_s\sum_{w\epsilon\Omega^w}\pi_w\sum_{n\in\Omega^n}\sum_{k\epsilon\Omega^k}\sum_{p\epsilon\Omega^p} OC_{p,k}^N\, g_{p,k,n,s,w,t}^N \qquad (3.1.4)$$

$$EC_t^E = \sum_{s\epsilon\Omega^s}\rho_s\sum_{w\epsilon\Omega^w}\pi_w\sum_{n\in\Omega^n}\sum_{k\epsilon\Omega^k}\sum_{p\epsilon\Omega^p} OC_{p,k}^E\, g_{p,k,n,s,w,t}^E \qquad (3.1.5)$$

$$ENSC_t = \sum_{n\epsilon\Omega^n} \sum_{s\epsilon\Omega^s} \rho_s \sum_{w\epsilon\Omega^w} \pi_w \upsilon_{s,w,t} \delta_{n,s,w,t} \tag{3.1.6}$$

$$EMC_t^N = \sum_{s\epsilon\Omega^s} \rho_s \sum_{w\epsilon\Omega^w} \pi_w \sum_{n\epsilon\Omega^n} \sum_{k\epsilon\Omega^k} \sum_{p\epsilon\Omega^p} \lambda_{s,w,t}^{EMI} \, ER_{p,k}^N \, g_{p,k,n,s,w,t}^N \tag{3.1.7}$$

$$EMC_t^E = \sum_{s\epsilon\Omega^s} \rho_s \sum_{w\epsilon\Omega^w} \pi_w \sum_{n\epsilon\Omega^n} \sum_{k\epsilon\Omega^k} \sum_{p\epsilon\Omega^p} \lambda_{s,w,t}^{EMI} \, ER_{p,k}^E \, g_{p,k,n,s,w,t}^E \tag{3.1.8}$$

$$EC_t^{SS} = \sum_{s\epsilon\Omega^s} \rho_s \sum_{w\epsilon\Omega^w} \pi_w \sum_{ss\in\Omega^{ss}} \lambda_{ss,s,w,t} g_{ss,s,w,t}^{SS} \tag{3.1.9}$$

$$Loss_t = \sum_{s\epsilon\Omega^s} \rho_s \sum_{w\epsilon\Omega^w} \pi_w \sum_{n,m\in\Omega^n} \lambda_{s,w,t} \frac{g_{nm}}{(V_{nominal} * b_{nm})^2} \left(f_{nm,s,w,t}\right)^2 \tag{3.1.10}$$

Notice that equation (3.1.1) is weighted by the capital recovery factor $\frac{i(1+i)^{\eta_{p,k}}}{(1+i)^{\eta_{p,k}}-1}$. Besides, $x_{p,k,n,0}^N$is defined to be zero, and the formulation in (3.1.1) ensures that the investment cost of each DG is considered only once in the summation. For example, suppose an investment in a particular DG is made in the fourth year of a five-year planning horizon. This means the DG will be available during the fourth and the fifth years because of the logical constraint in (3.8). Hence, the binary variables associated to this DG in those years will be 1 while the rest will be zero i.e. $x_{p,k,n,t}^N = \{0,0,0,1,1\}$. In this particular case, only the difference $(x_{p,k,n,4}^N - x_{p,k,n,3}^N)$ equals 1 while the remaining ones are all zero, i.e. $(x_{p,k,n,t}^N - x_{p,k,n,t-1}^N) = 0, \forall t \neq 4$, and hence the investment cost is considered only once. Equations (3.1.2) and (3.1.3) stand for the annual maintenance costs of candidate and existing DGs, respectively. These cost components are multiplied by the corresponding binary variables to determine whether each DG is being utilized or not. Note that the binary investment variable is also used for this purpose because there is no economic explanation or justification as to why it cannot be utilized immediately after an investment is made on a given asset. For the case example given above, the DG will incur maintenance costs in the last two years. For existing generators, binary variables are used to indicate their respective utilizations. The operation costs given by (3.1.4) and (3.1.5) for candidate and existing DGs, respectively, depend on the amount of power generated for each scenario, snapshot, stage and DG type. Therefore, these costs represent the expected costs of operation. Similarly, the penalty term for the unserved power, given by (3.1.6), is dependent on the scenarios, snapshots and time stages. Equation (3.1.6) therefore gives the expected cost of unserved energy. The expected emission costs of candidate and existing generators are given by (3.1.7) and (3.1.8), respectively.

3.3.3 Constraints

3.3.3.1 *Load Balance Constraints*

The load balance at each node is given by equation (3.2).

$$\sum_{k\epsilon\Omega^k}\sum_{p\epsilon\Omega^p}(g^E_{n,p,k,s,w,t}+g^N_{n,p,k,s,w,t})+\sum_{ss\in\Omega^{ss}}g^{SS}_{ss,s,w,t}+\delta_{n,s,w,t}-\sum_{n,m\in\Omega^n}f_{nm,s,w,t} + \sum_{n,m\in\Omega^n}f_{mn,s,w,t}\geq d_{n,s,w,t} \quad ;\forall s\in n \tag{3.2}$$

3.3.3.2 *Investment Limits*

In real problems, there always exist financial constraints; therefore, the maximum allowable budget for investment in DGs for a given year is limited by (3.3).

$$\sum_{n\in\Omega^n}\sum_{k\epsilon\Omega^k}\sum_{p\epsilon\Omega^p}IC^N_{p,k}(x^N_{p,k,n,t}-x^N_{p,k,n,t-1})\leq InvLim_t \tag{3.3}$$

3.3.3.3 *Generation Capacity Limits*

The minimum and maximum capacity limits of existing and candidate generators are represented by (3.4) and (3.5), respectively. Note that the binary variables also appear here and multiply these bounds. This is to make sure that the power generation variable is zero when the generator remains either unutilized or unselected for investment. In the case of intermittent power source, the lower generation limits $G^E_{p,k,s,w,min}$ and $G^N_{p,k,s,w,min}$is often set to 0 while the corresponding upper limits are set equal to the actual power output of the DG corresponding to the level of primary energy source (wind speed and solar radiation, for instance). Hence, the upper bound in this case depends on the operational state (i.e. the snapshot) and the scenario.

$$u^E_{n,p,k,t}G^E_{p,k,s,w,min}\leq g^E_{p,k,n,s,w,t}\leq u^E_{n,p,k,t}G^E_{p,k,s,w,max} \tag{3.4}$$

$$x^N_{n,p,k,t}G^N_{p,k,s,w,min}\leq g^N_{p,k,n,s,w,t}\leq x^N_{n,p,k,t}G^N_{p,k,s,w,max} \tag{3.5}$$

3.3.3.4 *Unserved Power Limit*

The upper and lower limits of the unserved power are given by (3.6). Normally, the maximum unserved power one can have at a certain node is the demand at that node. However, the upper bound may be superfluous because, under normal circumstances, when a sufficiently large penalty factor is used in the objective function, the unserved power variable will tend to be very close to zero by optimality.

$$0 \le \delta_{n,s,w,t} \le d_{n,s,w,t} \tag{3.6}$$

3.3.3.5 *DG Penetration Level Limit*

Mainly due to technical reasons, there can be a maximum penetration level of DG integration (or, equivalently saying, the maximum percentage of demand covered by DG power). This is ensured by adding the constraints in (3.7).

$$\sum_{n\in\Omega^n}\sum_{p\epsilon\Omega^p}\sum_{k\epsilon\Omega^k}(g^E_{p,k,n,s,w,t} + g^N_{p,k,n,s,w,t}) \le \varphi d_{n,s,w,t} \tag{3.7}$$

3.3.3.6 *Logical Constraints*

Logically, an investment made at time stage t cannot be reversed or divested in the subsequent time stages; hence, the asset should be available for utilization immediately after the investment is made. Such constraints can be realized using (3.8).

$$x^N_{p,k,n,t} \ge x^N_{p,k,n,t-1} \tag{3.8}$$

3.3.3.7 *Network Model Constraints*

As mentioned earlier, integrating DGs could in some cases result in technical problems in the system such as congestion, voltage rise and stability issues. Therefore, if these issues are deemed critical, it may be desirable to include network constraints so that power flows and node voltages remain within their respective permissible ranges. To this end, a linearized network model, first proposed in [95] in the context of transmission expansion planning and further extended to distribution network system planning in [96], is used here. In distribution systems, since active power flow dominates the apparent power flow, reactive power flow can be neglected. Hence, without loss of generality, only the active power flow through a given line, given by (3.9), can be considered. Equation (3.10) ensures that the flow through the distribution lines do not exceed their corresponding thermal capacities.

$$M_{nm}(z_{nm}-1) \leq f_{nm,s,w,t} - \{V_{nominal}(\Delta V_{n,s,w,t} - \Delta V_{m,s,w,t})g_{nm} - V_{nominal}^2 b_{nm}\theta_{nm,s,w,t}\} \leq M_{nm}(1-z_{nm}) \tag{3.9}$$

$$-f_{nm}^{max} z_{nm} \leq f_{nm,s,w,t} \leq z_{nm} f_{nm}^{max} \tag{3.10}$$

Note that the voltage at each node is assumed to be equal to $V_{nom} + \Delta V_{n,s,w,t}$ where $\Delta V_{n,s,w,t}$ stands for the voltage deviation at each node which is bounded as $-\varepsilon * V_{nominal} \leq \Delta V_{n,s,w,t} \leq \varepsilon * V_{nominal}$. For the analysis throughout this chapter, the tolerance factor ε is set to 0.05, and the voltage magnitude and angle at all substations are set to $1.05V_{nominal}$ and 0, respectively.

3.3.3.8 *Radiality Constraints*

The traditional radiality constraint in (3.11) [97], along with the load balance equation, gives the necessary condition for a distribution network to be radial and connected. The analysis in this chapter considers a radial network, and does not include grid expansion or switching. Therefore, equation (3.11) is sufficient to keep the radiality of the network and ensure that all nodes are connected.

$$\sum_{n,m \in \Omega^n} z_{nm} = N_n - N_{SS} \tag{3.11}$$

3.4 Case Studies

3.4.1 System Data

The system considered in the study is a real-life insular distribution network in São Miguel Island, Azores, Portugal. In this system, currently, there is no electricity market, and there is no energy imported (purchased) from the transmission grid. The system has a peak demand of 70.2 MW, and information about existing generators is shown in Table 3.1. The investment limit in each year is set to 120 M€. The average cost of electricity $\lambda_{s,w,t}$ used for estimating cost of losses is assumed to be the average of all marginal costs of power production of DGs. In this system, various DG types with capacities ranging from 1 to 30 MW are considered as candidates for investment (see in Table 3.2). These fall into small-to medium-scale DG categories according to the capacity-based classification of DGs in [98]. The installation and maintenance costs of each DG are either directly obtained from [98] and [99] or estimated using the so-called six-tenths rule [100], which e stablishes a relationship between cost and quantity (in this case, installed capacity).

Table 3.1 – Data for existing generators

	Generator type, p	Alternative, k	Installed capacity (MW)	$OC_{p,k}$ (€/MWh)	$IC_{p,k}$ (M€)	$MC_{p,k}$ (M€)	$ER_{p,k}$ (tons /MWh)
1	Hydro	Hydro	4.07	7.0	NA	0.38	0.0121
2	Geothermal	GEOT	24.0	5.0	NA	1.20	0.0165
3	HFO-T*	HFO	98.0	145.4	NA	0.01	0.5600
4	Wind	WD 0	10.0	17.0	NA	0.80	0.0276

** Heavy fuel oil turbine*

Table 3.2 – Data for candidate generators

	Generator type, p	Alternative, k	Installed capacity (MW)	$OC_{p,k}$ (€/MWh)	$IC_{p,k}$ (M€)	$MC_{p,k}$ (M€)	$ER_{p,k}$ (tons/MWh)
1	Solar	PV 1	1.0	40	3.00	0.06	0.0584
2	Solar	PV 2	1.5	40	3.83	0.08	0.0584
3	Solar	PV 3	2.0	40	4.55	0.09	0.0584
4	Solar	PV 4	2.5	40	5.20	0.10	0.0584
5	Solar	PV 5	3.0	40	5.80	0.12	0.0584
6	Solar	PV 6	4.0	40	6.89	0.14	0.0584
7	Solar	PV 7	6.0	40	8.79	0.17	0.0584
8	Solar	PV 8	10	40	11.94	0.24	0.0584
9	Wind	WD 1	1.0	17	2.64	0.05	0.0276
10	Wind	WD 2	2.0	17	4.00	0.08	0.0276
11	Wind	WD 3	5.0	17	6.93	0.14	0.0276
12	Wind	WD 4	10	17	10.51	0.21	0.0276
13	CGT**	CGT 1	30	145.4	27.00	0.01	0.5600
14	Biomass	BM 1	20	20	80.00	3.00	0.0276

*** Combustion gas turbine*

This method reflects the economy of scale that exists in DGIP, i.e. the higher the installed capacities of DGs of the same type, the lower the costs per installed kW get. The hourly series (historical data) of wind speed and solar radiation at various locations of the island are obtained from publicly available databases [101], [102], respectively.

The correlation among the hourly wind speed and solar radiation series is approximately -0.13. The geographical coordinates where these data are taken from include (37.790,-25.385), (37.778,-25.489), (37.866,-25.816), (37.797,-25.170), (37.717,-25.505), (37.823,-25.487), (37.772,-25.375) and (37.782,-25.661). Then, the wind (WD) and solar photovoltaic (PV) power production series used in the simulations are determined by plugging the wind speed and the radiation data in the corresponding power curve expressions.

The DGIP problem is coded in GAMS 24.0 and solved using CPLEX 12.0. All simulations are carried out in HP Z820 Workstation with E5-2687W processor, clocking at 3.1 GHz.

3.4.2 Scenario Definition

Defining scenarios is in itself a complex problem, which requires exhaustive research and sufficient knowledge of the evolution of the system under consideration. Because of this, the number and the nature of scenarios are mostly predefined, and, to do this, planners often rely on expert knowledge. In this work, three scenarios (storylines) are defined in connection to the possible evolutions of two relevant uncertain parameters over the planning horizon, namely, electricity demand growth and emission price. Table 3.3 shows the three evolutions of demand growth, denoted as Low, Moderate and High, having an equal degree of realization. Similarly, the emission price is represented by three equally probable storylines (scenarios), as depicted in Table 3.3. Out of these individual scenarios, assuming the two uncertain parameters are independent, we can get nine different combinations, which form the new set of scenarios used in the simulations. With this as a base-case, sensitivity analyses are carried out to study the impact of several system parameters other than these, which involve some degree of uncertainty, on DG investment decisions. These parameters include interest rate, DG penetration limit, solar PV and wind power output uncertainty, generator availability, electricity tariffs and fuel prices.

3.4.3 Impact of Network Inclusion/Exclusion on DGIP Solution

To assess the impacts on the DGIP solution, the formulated problem is solved with and without network. The former considers the entire network system but the latter assumes that the electricity demand is aggregated and connected to a hypothetical node and all generators are assumed to be connected to this node. One of the main differences lies in the network losses which are only accounted for when considering the network. However, since distribution networks span over a small geographical area, the feeders and distribution lines are usually short. Therefore, in properly designed distribution networks, power losses are negligible and, hence, they are not expected to significantly change DG investment planning solution. This argument has been experimentally verified by running simulations with and without a network on two insular networks (the distribution networks of São Miguel Island described before and La Graciosa Island presented in [103]). In both cases, the DGIP results with and without network are very similar, only differing in one DG investment. Moreover, the differences in total investment cost throughout a three-year planning horizon are 2.2 and 3.5%, respectively.

Table 3.3 - Demand growth and CO_2 price scenarios

	Demand growth scenarios			CO_2 price scenarios (€/ton of CO_2)		
Stages	Low	Moderate	High	Low	Moderate	High
T0	0%	0%	0%	5	5	5
T1	2%	5%	10%	7	12	20
T2	5%	10%	20%	10	18	30
T3	7%	15%	30%	13	25	45

Generally, excluding the network slightly results in overinvestment. This is because neglecting the network would naturally mean neglecting the voltage constraints. As a result, this would lead to an increase in the size of DG integrated to the system that would otherwise be impossible when considering the network due to voltage rise issues.

In the systems studied, the increase in DG investments as a result of not considering the network is negligible. Moreover, the cost of losses in both test cases is too small (accounting for less than 0.02 % of the total system cost) to have an impact on the solution. Based on these results, the sensitivity analysis here is carried out without considering the network. This is not expected to affect the analysis work since the main aim of the work here is to identify the parameters that significantly influence DGIP solutions.

It should be clearly understood that the work in this chapter is not to make investment decisions; it should rather be understood as an important step that provides relevant input to the development of robust planning tools. The exclusion of network (i.e. collapsing the whole system into one node) reduces the computation burden and helps one to increase the level of details of other relevant issues such as uncertainty and variability of uncertain parameters. It should however be noted that the aforementioned findings may largely depend on the size and the type the system being considered.

3.4.4 Results and Discussion

The analysis results with regards to the sensitivity of investment decisions on DGs with variations of selected system parameters are presented and discussed as follows.

3.4.4.1 *Demand Growth and CO_2 Price*

The total investment cost for every combination of demand growth and emission price scenarios are shown in Table 3.4, along with the corresponding overall system costs as in Table 3.5. We can see in these tables that DG investments are more sensitive to emission price uncertainty than to demand growth. The DG investment decisions corresponding to each scenario and time stage are given in Table B.1 of Appendix B.

Table 3.4 - Impact of demand growth and CO_2 price uncertainty on DG investments

	TIC (M€)	CO_2 price scenarios		
		Low	Moderate	High
Demand growth scenarios	Low	38.462	46.220	54.540
	Moderate	38.462	46.996	64.245
	High	38.462	53.078	64.757

3.4.4.2 Interest Rate

The evolution of interest rate remains uncertain, and hence it is subject to change at any time in the future. To see its effect on DG investment decisions, it is changed by holding other parameters at their base case values. Generally, investments in DG fall as the interest rate increases. This is illustrated in Figure 3.4, where one can clearly observe the decreasing trends of investment in DG (renewables, in particular). Their share in the total energy produced also follows a similar trend. This is in line with financial theory which states that higher interest rates deter investments because this raises the expected rate of return of an investment, which does not incentivize investments. As an example, an interest rate of 2% results in investments in all candidate DGs of wind and solar types except PV1 and PV2 (see in Table 3.2); whereas, for an interest rate of 12%, the investments made only include PV7, PV8 and all wind type DGs. The huge difference here highlights how sensitive the investment decisions can be with respect to the interest rate.

3.4.4.3 DG Penetration Level Factor

This factor is another relevant parameter that affects the investment decisions of DGs. Intuitively, one may ponder that the higher the value of this factor, the higher the incentive for integrating more renewables, and therefore, the higher the DG investments

Table 3.5 - Variation of objective function value with demand growth and CO_2 price scenarios

	TC (M€)	CO_2 price scenarios: Low	Moderate	High
Demand growth scenarios	Low	246.111	283.029	338.211
	Moderate	289.224	336.038	406.261
	High	375.187	442.091	543.606

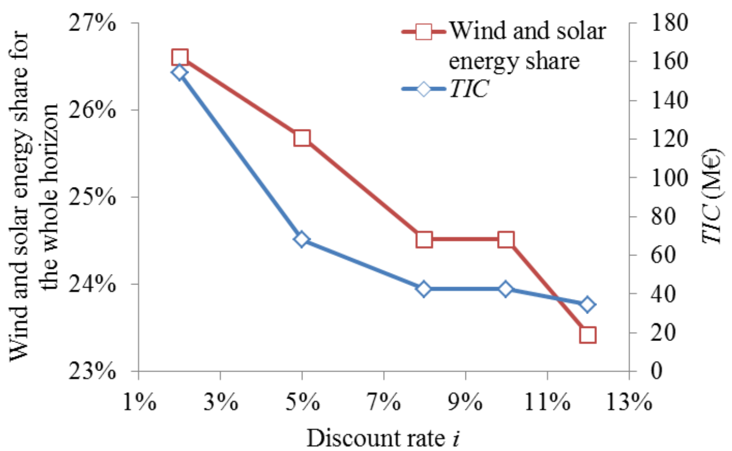

Figure 3.4 - Impact of interest rate on DG investments and energy production from wind and solar sources.

But this holds only up to a certain threshold, beyond which there seems to be few or no new investments made. Figure 3.5 clearly reflects this phenomenon. In the case study presented in this chapter, the threshold value of the penetration level seems to be 40%. Below this level, investments made in DG steadily increase with the penetration level from almost no investments at 10% to seven investments at 40%. However, this is not the case for higher penetration levels. Even if the penetration level is set beyond 40%, no new investments are justified.

As can be seen in Figure 3.5, the impact of DG penetration level on emissions and expected system costs is also significant. As expected, the increase in DG investments is offset by a higher decrease in operation and emission costs, leading to decreasing trends of the expected system cost and the emissions with increasing penetration level. Beyond 40%, the rate of changes in both curves is however insignificant. This may be the maximum technical penetration limit of variable energy sources in the absence of energy storage and appropriate reactive power compensation mechanisms put in place to counter the negative effects of integrating variable generation such as voltage and grid stability issues. To maintain a healthy operation of the system, high production levels of RES-based DGs need to be curtailed. The curtailment rate and level increase with the size of variable power capacity installed in the system. Hence, in this situation, further investment on such resources (beyond 40%) may not be justified because doing so does not lead to further reduction in system costs.

Alternatively, Figure 3.6 shows the variation of DG investments with respect to the DG penetration level factor. The results in this figure also strengthen the fact that DG investments show some variations with an increasing level of this factor. The level of emissions gets lower as the DG penetration factor is increased up to a certain level (around 40%), beyond which the change is insignificant. This is indicative of the effect of increasing investments in DGs up to this level, which is in line with the previous statement.

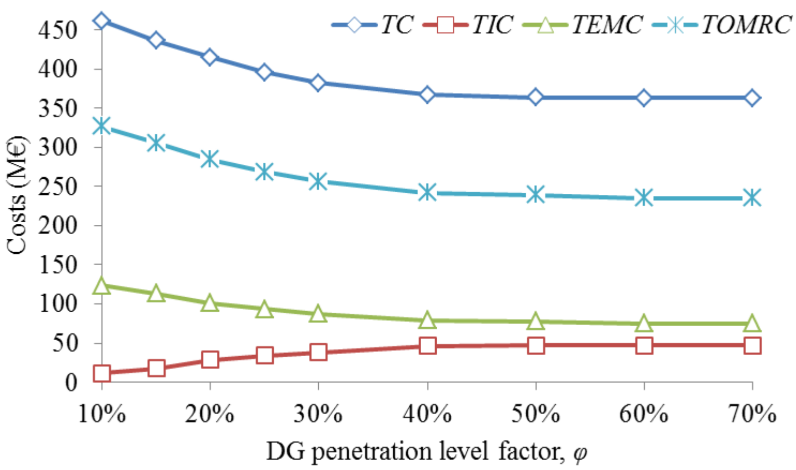

Figure 3.5 - Variations of emissions, investment and expected system costs with DG penetration level factor.

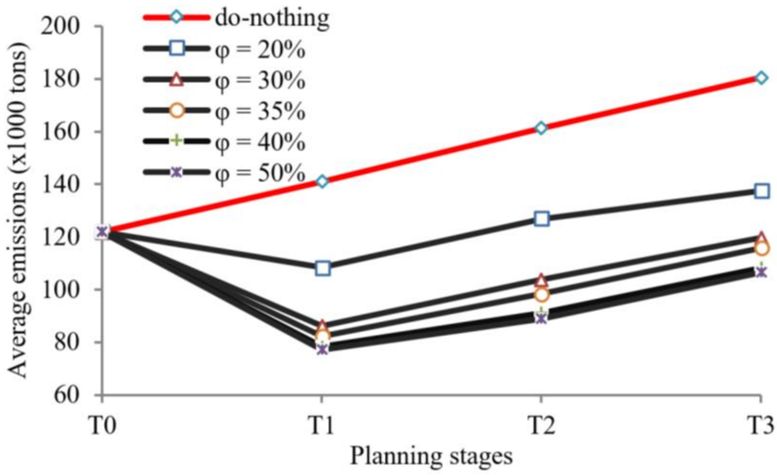

Figure 3.6 - Variation of DG investments with penetration level and their effect on total CO2 emissions.

3.4.4.4 Fuel Prices and Electricity Tariffs

The impact of fuel prices and electricity tariffs of renewable generators are also analyzed by varying the levels of these parameters. The results of this sensitivity analysis are summarized in Table 3.6. As it can be seen in this table, DG investment decisions are very sensitive to fuel prices. For example, when the fuel price is considered to be 30% lower than that of the base case, it becomes less attractive to invest on DG (especially solar photovoltaics). But a fuel price 30% higher results in more investments in PV.

In addition to fuel prices, electricity tariffs also play a significant role in the decision-making process, particularly in the context of DG investment planning. In general terms, the price of electricity generated from wind or solar DG highly depends on the initial level of capital invested on these DG technologies. Once the investments are made, operation costs are normally very low. Nowadays, the capital costs of the main components pertaining to these technologies are continuously falling, with a learning rate of more than 20% per annum. This trend will most likely be sustained [99], resulting in a dramatically lower final cost of electricity (tariff) generated from such resources.

The effects of variations in PV energy tariffs on DG investments are especially investigated in this chapter. As shown in Table 3.6, when solar PV generators are considered to be as competitive as wind power generators, i.e. with a tariff of €20/MWh, more investments in PV are made compared to the base case. On the other hand, if the electricity tariff of energy coming from PV turns out to be twice that of the base case (€80/MWh), the number of investments made in solar PV declines. However, this is not likely to happen given the current learning rate of solar PV technology. It is also worth mentioning that the planning solution in the case of +100% tariff for PV energy is exactly the same as the solution in the -30% fuel price case, which shows the importance of energy tariff arrangement by the regulatory body.

The crowding of investment decisions in the first stage in Table 3.6 may be due to two reasons. The first reason could be because of the absence of investment constraints related to financial and logistic matters. The second reason could be because of the relatively higher net present value of operation, maintenance and emission costs in the first stage when compared with that of any other stage. This, along with the first reason, may justify more investments to be made in the first stage rather than in any one of the subsequent stages.

3.4.4.5 Wind and Solar Power Output Uncertainty

To analyze the effect of uncertainty in wind and solar power outputs, two scenarios are created for each. One scenario is taken to be above the average hourly profile (roughly 30% higher than that of the base case), and the other one is taken below the average profile (approximately 30% lower than that of the base case) in each case. The results of the analysis are summarized in Table 3.7. One can observe that when the B-wind scenario is considered, the number of investments on wind type DGs becomes lower than these of the base case (see in Table 3.6). This is because of the lower yield of wind resources. In contrast, more investments are made on wind type DGs when the A-wind scenario is considered. The sensitivity of investments in solar PVs with respect to the uncertainty of PV outputs is even higher, as can be seen in this table. Note that the reasons mentioned before in the case of Table 3.6 could explain the crowding of investments in the first stage in Table 3.7.

Table 3.6 - Impact of price and DG tariffs on DG investment decisions

		Changes in fuel price			Changes in PV energy tariff	
	Stages	+0%	-30%	+30%	-50%	+100%
Investment in wind and solar DGs	T1	PV8, WD1, WD2, WD3, WD4	WD1, WD2, WD3, WD4	PV7, PV8, WD1, WD2, WD3, WD4	PV7, PV8, WD1, WD2, WD3, WD4	WD1, WD2, WD3, WD4
	T2	PV7	PV8	PV6	-	PV8
	T3	-	-	PV5	PV6	-
TC (M€)		364	312	412	358	372
Total expected emissions (x 1000 tons of CO_2)		268.8	296.4	256.5	263.1	296.4

Table 3.7 - Impact of wind and solar PV output uncertainty on DG investment decisions

Scenarios		Time stages				
		T1	T2	T3	*TIC* (M€)	*TC* (M€)
Wind Scenarios	Below average (B)	PV8,WD2, WD3,WD4	PV7	-	44.81	412
	Above average (A)	PV8, WD1,WD2, WD3,WD4	-	-	38.46	339
Solar Scenarios	Below average (B)	PV8, WD1,WD2, WD3,WD4	-	-	38.46	373
	Above average (A)	PV8, WD1,WD2, WD3,WD4	PV7	PV6	47.00	360

3.4.4.6 Demand and RES Power Output Uncertainty

As stated earlier, the natural variation with time that exists in some of the system parameters such as demand and renewable energy source (RES) outputs leads to a large number of operational situations, adding extra complexity to the DGIP problem. Because of this, a significantly reduced number of snapshots are usually considered in such problems. For example, demand variability is commonly represented by a load duration curve, which is then aggregated into three to five load blocks.

Unfortunately, this may compromise the quality of solution obtained. In light of this, we investigate how the reduction of operational situations, via clustering, affects the DG investment solution. To do this, we make use of k-means clustering algorithm, a popular clustering analysis method in data mining, to obtain different number of data clusters (aggregates). The representative snapshot in each cluster is assumed to be the mean of the snapshots grouped together. For different number of clusters, the investments made, along with total cost and average simulation time, are summarized in Table 3.8.

According to the results in this table, there seems to be a tendency to overinvest when the snapshots are further reduced. This may be due to an overestimation of the operation costs, which triggers more investments. Basically, investments are justified if the net reduction in operation costs (which may include cost of energy production, emission and losses) is higher than or equal to the overall investment costs. Based on this, if the operation costs are artificially overstated for some reason such as clustering inaccuracy, the net reduction in operation costs may seemingly be high, leading to the justification of more investments. However, it should be noted that this may not always be the case, i.e. a lower number of clusters may not necessarily be associated with an overestimation of operation costs. Depending on how the representative snapshots in all clusters are taken, the operation costs may be overestimated or underestimated, resulting in overinvestment or underinvestment, respectively.

Table 3.8 – Impact of snapshot aggregation on DG investment decisions

Number of snapshots	*TIC* (M€)			*TC* (M€)	Average simulation time (seconds)
	Stage 1 (T1)	Stage 2 (T2)	Stage 3 (T3)		
Peak demand	47.849	6.691	5.118	-	-
100	38.462	8.533	6.082	359.45	2
300	38.462	8.533	6.082	360.66	4
324 * [71]	38.462	8.533	6.082	362.98	6
500	38.462	8.533	6.082	361.56	7
1000	38.462	8.533	6.082	362.37	21
2000	38.462	8.533	6.082	363.09	60
4000	38.462	8.533	0.000	363.55	210
6000	38.462	8.533	0.000	363.70	420
8760	38.462	8.533	0.000	363.80	720

* *Snapshots are reduced according to the method in the reference*

Another important observation from Table 3.8 is that clustering the hourly operational snapshots in a year shows little impact on the investment solution beyond a certain threshold (which lies somewhere in the range of 300 and 400). This reflects that as far as the initially large number snapshots are clustered into 300 or more and the representative snapshots are carefully selected, the investment outcomes may not be influenced by clustering operational situations but significantly facilitate the solution process.

3.4.4.7 Generator Availability

It is understood that a generator can only produce power when it is available. There are two main factors which affect generator's availability: unplanned (forced) and planned (scheduled) outages. Such outages may also condition DG investment solution. Especially, more investments can be expected if, by chance, generator outages partially or fully coincide with relatively high production times of DG candidates. For example, if outages essentially occur during sunny hours, more investments could be made on solar PV candidate generators to fill in the generation gap left behind as a result of the outages. However, the chance of this happening can be very low since both processes are independent. In the particular example presented earlier, the effects of forced outages of geothermal and hydro power units on the solution are analyzed. The availability series of these units are generated using a binomial distribution function, assuming generator outage rates of 15% and 10%, respectively. Note that these rates consider both types of outages. When generating the series, an average off-time of 4 hours is factored in for both generator types. Given this input information, the DGIP problem is solved and its solution includes PV8 and all wind DG candidates in the first stage, PV7 in the second stage, and PV6 in the third stage with a total investment cost of 53.08 M€. This solution differs from that of the base case by one investment (i.e. PV6). But, in general, more investments could be justified if the generator outages occur during/around the peak hours of renewable power productions.

3.5 Chapter Conclusions

This chapter has presented comprehensive experimental analyses to determine the sensitivity of DG investments with variations of several uncertain parameters. The aim of such analyses has been first to investigate the effect of variability and uncertainty in model parameters on the investment decisions of DGs, and second to identify the parameters that have the highest degree of influence on DG investments. The results of our analyses generally showed that both uncertainty and variability have a meaningful influence on DG investment decisions. In fact, the degree of influence varies from one parameter to another. Results from the case study show that generator outages have little or no impact on the RES-based DG investments; whereas, uncertainty in CO_2 and fuel prices, interest rate and RES power outputs significantly influence investment decisions especially in variable energy sources.

In particular, it has been found out that uncertainty in CO_2 and fuel prices as well as interest rate dramatically condition decisions compared to the uncertainty in demand growth and RES power outputs. A thorough investigation on the number of clusters of the hourly operational snapshots in a year shows that the clustering process results in little impact on the investment solution beyond a certain threshold (somewhere in the range of 300 and 400). This reflects that as far as the initially large number snapshots are clustered into 300 or more, and the representative snapshots are carefully selected, the results may not be influenced by clustering operational situations but significantly facilitate the solution process.

In general, the results reveal that ignoring or inadequately considering uncertainty and variability in model parameters has a quantifiable cost. Based the extensive analysis, a stochastic modeling of uncertainty related to emission and fuel prices, interest rate, RES power outputs and demand growth is very critical for obtaining robust investment decisions. The comprehensive analysis performed in this chapter can help planners to properly weigh the effect of ignoring or considering the uncertainty and/or variability of one or more model parameters. Accordingly, a realistic planning tool considering all relevant sources of uncertainty and/or variability and solution methodologies can be developed, which leads to high quality and robust investment solutions.

Chapter 4

Multi-Stage Stochastic DG Investment Planning with Recourse

Taking the findings of the analysis in Chapter 3 as input, a detailed model is developed in Chapter 4 to guide the complex decisions-making process of DG investment planning in the distribution system in the face of uncertainty. The problem is formulated from a coordinated system planning viewpoint and the operational variability and uncertainty introduced by intermittent generation sources, electricity demand, emission prices, demand growth and others are accounted for via probabilistic and stochastic methods, respectively.

4.1 Introduction

The advent of emerging solutions such as active management of distribution networks [57] or fully automated and intelligent networks – the so-called smart grids [104] - is expected to keep on facilitating smooth integration of DGs by alleviating existing technical limitations. Hence, DG is expected to play an important role in distribution systems, making the issue of DG investment planning (DGIP) highly important. This is because, throughout the world, new regulations are put in place to reduce the heavy dependence of such systems on fossil fuels for energy production. However, several DG sources are intermittent in nature, making the operation and planning of distribution networks very challenging. This is because such sources introduce significant operational variability and uncertainty to the system. The terms (operational) variability and uncertainty in this chapter should be understood according to the following definitions. Variability, as defined in [90], refers to the natural variation in time of a specific uncertain parameter; whereas, uncertainty refers to “the degree of precision with which the parameter is measured” or predicted. In addition to the aforementioned sources of uncertainty, there are several other parameters (such as fuel prices, demand growth, etc.) which are subject to high level uncertainty. The compounded effect of all these relevant issues certainly requires crafting new methods and tools in order to realize an optimal or a cost-efficient integration of DGs. Indeed, the robustness and reliability of the solutions obtained from DGIP models highly depends on the level of details of the methods and tools embedded in such models and their effectiveness in managing uncertainty and variability.

This chapter aims to introduce a novel multi-stage stochastic DGIP model with recourse under a high penetration level of stochastic generation resources in distribution systems. The model incorporates methods to manage uncertainty and operational variability introduced by the variable energy sources (such as wind and solar) as well as demand. This enhances the robustness of the decisions made.

The problem, formulated as a mixed integer linear programming (MILP) optimization, simultaneously minimizes the net present value of losses, emission, operation and maintenance as well as unserved energy costs, while fulfilling a number of technical and economic constraints. Note that the DGIP problem here is formulated from the system perspective (i.e. a coordinated planning approach).

This chapter is organized as follows: In section 4.2, the uncertainty and the operational variability facing a DGIP problem are briefly explained. Subsequently, section 4.3 presents the mathematical formulation and detailed description of the DGIP model. Section 4.4 discusses the results of the case studies. Finally, in Section 4.5, the relevant conclusions and implications based on the outcome are drawn.

4.2 Modeling Uncertainty and Variability in DGIP

The various sources of uncertainty and variability in a DGIP problem are related to the variability in time and the randomness of operational situations [105]. In addition, there are some other uncertainties mostly related to the long-term electricity, emission and fuel prices, rules, regulations and policies, etc.

A well-developed DGIP tool should therefore encompass a methodology which effectively and efficiently takes account of operational variability and uncertainty. Exhaustive modeling of all sources of uncertainty and variability may not only be computationally unaffordable but also inefficient. A systemic approach is required to handle these issues in an efficient and effective manner. In this thesis, the variability due to intermittent DG power outputs (mainly, wind and solar) and demand are captured by considering a sufficiently large number of operational states, also known as here “snapshots”. The hourly data may be historical or generated from individual or joint PDFs of uncertain parameters.

To ensure tractability, a standard clustering technique is used to reduce the number of snapshots. Here, each cluster represents a group of similar operational situations. A representative snapshot is then selected from each cluster based on certain criteria (for example, the medoid). Then, each of the selected snapshots, representing a group of similar operational situations, is assigned a weight π_w proportional to the number of operational situations in its group. In addition to variability, demand and RES outputs are subject to uncertainty due to partially unpredictable nature (especially variable energy sources such as wind and solar). In other words, the realizations of these parameters cannot be perfectly forecast. This relevant issue (i.e. uncertainty) is accounted for considering a sufficiently large number of scenarios for each individual uncertain parameter. In the case of wind power output uncertainty, for instance, each scenario represents a possible hourly wind power output profile throughout the planning horizon. Hence, one can generate multiple profiles of this type, each with a certain degree of realization.

However, for computational reasons, the number of scenarios needs to be limited. Similarly, a number of scenarios are also defined to characterize the solar power output uncertainty. In addition, the evolutions of emission price and demand growth can be each represented by many scenario trajectories, each showing the considered parameter's data realizations. Combinations of all these individual scenarios then form the final set of global scenarios that are used in the analysis. This is schematically illustrated in Figure 4.1. The global scenarios (*S1* through *Sn*) are formed by combining individual scenarios. Note that the profiles in this figure are shown only for the purpose of illustrating the concepts; the profiles used in the analysis are actually different from these. The actual ones, for instance, span over the entire planning horizon.

4.3 Mathematical Model

4.3.1 Overview and Modeling Assumptions

Although many studies have been carried out on DGIP, most of them focus on a small subset of the vast sources of variability and uncertainty when formulating the DGIP problem. As it can be observed in the literature presented in Chapter 3, dealing with the variability pertaining to electricity demand seems to be considered in many works in the literature (often by aggregating it into 3 to 5 demand levels) while the others are largely ignored or represented in an overly simplified manner. Moreover, analyses in previous works are mostly limited to one or two DG types; the possible investment options pertaining to the size and technology type of DGs are not sufficiently explored in most of them. Therefore, a comprehensive DGIP model, equipped with appropriate tools for managing the most relevant sources of variability and uncertainty as well as considering various DG types and sizes, is still needed to guide the complex decision making process of DGIP. This way, an optimal integration of DGs can be guaranteed.

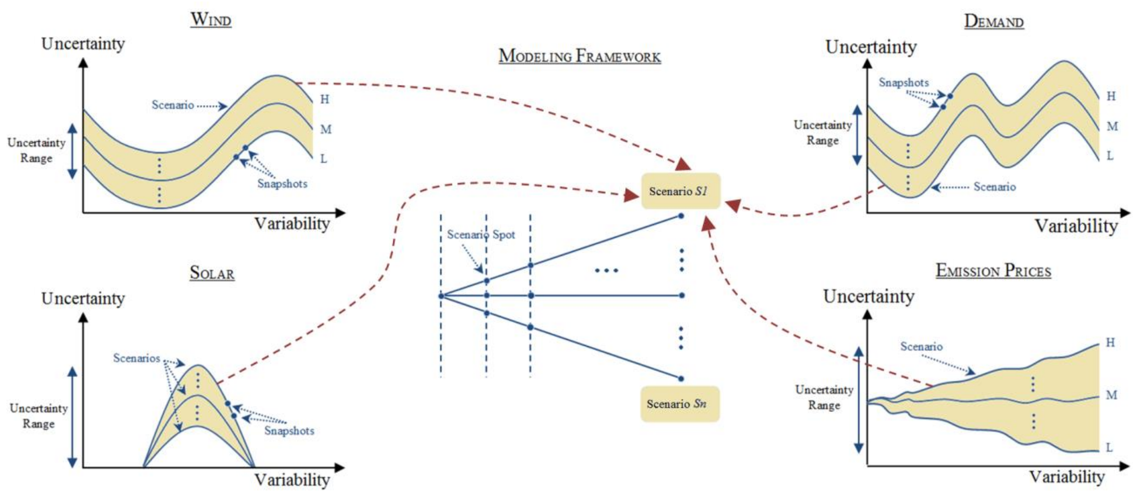

Figure 4.1 - A graphical illustration of scenario generation.

Furthermore, the issue of combining robust and flexible investment decisions has not been addressed so far. It is understood that most real-world problems often require two types of investment decisions to be made: robust decisions (short-term) and adaptive decisions (medium to long-term) both in the face of high level uncertainty. The former are sometimes called “here and now” decisions while the latter are referred to as “wait and see” decisions.

In the present work, to emulate such a decision-making process, a two-period planning framework is proposed. Each period has multiple planning stages. The first period is a short-term horizon in which robust decisions, good enough for all scenarios, are pursued. The second one spans over a medium to long-term horizon involving exploratory and/or flexible investment decisions that are scenario-dependent [89].

Note that the investment solution in the second period can also be understood as a set of investments required to make adjustments to the first-period decisions depending on the scenario unveiled in the second period. In other words, the proposed model combines both robust (short-term) and adaptive (medium to long-term) decisions, which is one of its salient features.

4.3.2 Brief Description of the Problem

As stated in the previous sections, the DGIP problem is formulated considering the dynamic nature of the problem i.e. featuring multiple planning stages. In addition, in order to combine “here and now” and “wait and see” investment decisions, a two-period stochastic optimization framework is proposed in this chapter.

This modeling framework assumes that there are n probable future storylines (or scenarios) each associated with a probability of realization ρ_s that stochastically represents relevant sources of uncertainties. Note that the terminologies snapshot and scenario, as defined in this chapter, correspond to an operational situation at a particular hour, and the evolution of an uncertain parameter over a given time horizon (often yearly), respectively.

The whole modeling scheme adopted in this chapter (i.e. the multi-stage and multi-scenario DGIP modeling framework and the expansion solution structure) is illustrated in Figure 4.2. This figure schematically represents possible future scenario trajectories with multiple scenario spots along the planning horizon. The figure also illustrates the decision structure, involving investment decisions independent of the scenarios and decisions, adapted to every scenario in every stage of the second period in a “what-if” fashion.

The decisions in the first period form a set of stochastic solutions which should be good enough for all scenarios. Those in the second period can be regarded as a set of adaptive solutions because the investment decisions made depend on the scenarios.

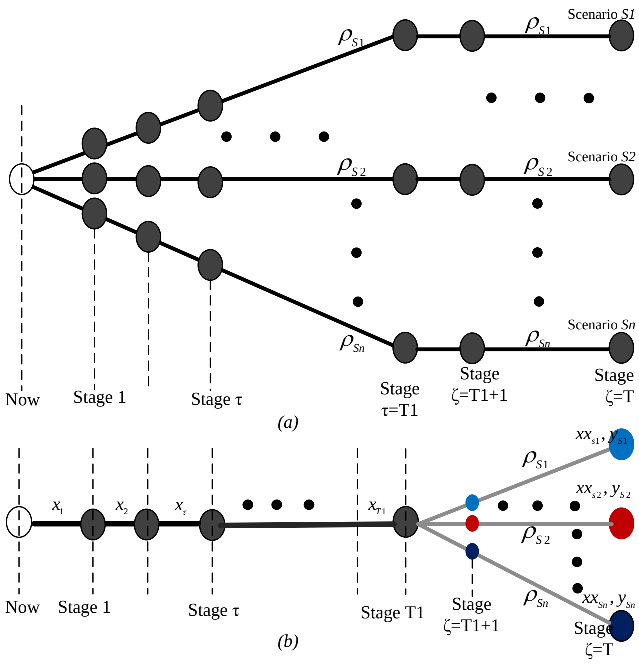

Figure 4.2 - A schematic representation of (a) possible future scenario trajectories and (b) a decision structure [92].

As shown in Figure 4.2, in the first planning period, a single robust investment decision, x_τ , is made at the τ^{th} stage (where $\tau = 1, 2, \ldots, T1$) which are common (or good enough) for all scenarios [92]. On the other hand, flexible or adaptive decisions $xx_{s,\zeta}$ and $y_{s,\zeta}$ (where $\zeta = T1 + 1, T1 + 2, \ldots, T$) are made at every stage of the second period [92]. Note that the decisions in the first period are more relevant than those made in the second period because they correspond to the "here and now" decisions, where the latter are implementable straightforwardly. However, the second-period decisions can also be very useful if seen from the flexibility/strategic planning perspective. In order to broaden the investment options, two DG investment pools are considered, one for each period. The context of an investment pool should be understood as a given set of DGs which is a candidate for investment. The lengths of the first and the second investment periods are given by T1 and T2, respectively.

Here, the recourse formulation makes it possible to postpone investments from the first period, x_τ, to the second period, $xx_{s,\zeta}$, if deemed economical. The algebraic formulation of the model developed here is presented and explained in detail in the following sub-sections.

4.3.3 Objective Function

The objective function is composed of seven cost terms, each weighted by the net present value (NPV) factor as in (4.1). Here, the investment and the utilization variables as well as the operational variables such as generated power, flows, etc. constitute the set of decision variables of the optimization.

$$\min_{\substack{InvVar,\\ OpVar}} TC = \alpha * TIC + \beta * TOMUEC + \gamma * TEMC + \xi * TLC \tag{4.1}$$

where $InvVar$ and $OpVar$ denote all investment and operational variables. Moreover, the subtotal costs related to investment (TIC), operation, maintenance and unnerved energy ($TOMUEC$), emissions ($TEMC$) and losses (TLC) in (4.1) are computed using the corresponding expressions in Table 4.1.

The first term in (4.1) represents the NPV of DG investment costs under the assumption of perpetual planning horizon [93]. In other words, "the investment cost is amortized in annual installments throughout the lifetime of the installed DG", as is done in [71].

The second term corresponds to the sum of NPV operation, maintenance and energy not served (OM&ENS) costs throughout the planning stages. The third one gathers the corresponding OM&ENS costs incurred after the last planning stage, which rely on the OM&ENS costs of the last planning stage. Note that a perpetual planning horizon is assumed when spreading these costs over the horizon following the last planning stage. The fourth term in (4.1) refers to the sum of NPV emission costs in the system throughout the planning stages.

Table 4.1 – Expression of cost components in the objective function.

Cost terms	Expression
TIC	$\underbrace{\sum_{t\epsilon\Omega^t} \frac{InvC_t^N}{i(1+i)^t}}_{NPV\ of\ investment\ cost}$
$TOMUEC$	$\underbrace{\sum_{t\epsilon\Omega^t} \frac{(MntC_t^N + MntC_t^E + EC_t^N + EC_t^E + EC_t^{SS} + ENSC_t)}{(1+i)^t}}_{NPV\ of\ operation,\ maintenance\ and\ PNS\ costs} + \underbrace{\frac{(MntC_T^N + MntC_T^E + EC_T^N + EC_T^E + EC_t^{SS} + ENSC_T)}{i(1+i)^T}}_{Operation,\ maintenance\ and\ PNS\ costs\ incurred\ after\ stage\ T}$
$TEMC$	$\underbrace{\sum_{t\epsilon\Omega^t} \frac{(EMC_t^N + EMC_t^E + EMC_t^{SS})}{(1+i)^t}}_{NPV\ of emission\ costs} + \underbrace{\frac{(EMC_T^N + EMC_{T.}^E + EMC_T^{SS})}{i(1+i)^T}}_{Costs\ incurred\ after\ stage\ T}$
TLC	$\underbrace{\sum_{t\epsilon\Omega^t} \frac{Loss_t}{(1+i)^t}}_{NPV\ of losses\ cost} + \underbrace{\frac{(1+i)^{-T} Loss_T}{i}}_{Losses\ cost\ incurred\ after\ stage\ T}$

And, the emission costs incurred after the last planning stage under the assumption of perpetual planning horizon are also given by the fifth term. Similarly, the last two cost terms in (4.1) compute the total NPV cost of losses throughout the planning horizon and those incurred after the last planning stage, respectively.

The sum of all these costs gives the total cost (TC) which is to be minimized. Note that the four relevance factors in (4.1) (i.e. α, β , γ and ξ) are all assumed to be equal throughout this chapter but depending on the relative importance of each cost component, different factors may be considered. In the event that different factor values were adopted, normalization may be required to avoid undesirable effect in terms of solution fidelity that may arise from unbalances in cost components.

Each of the cost "functions" in Table 4.1 is computed as follows. Equation (4.2) represents the total sum of amortized DG investment costs weighted by the capital recovery factor, $\frac{i(1+i)^{\eta_{p,k}}}{(1+i)^{\eta_{p,k}}-1}$. Note that $x^{N}_{p,k,n,0}$ is defined to be zero, and the formulation in (4.2) ensures that the investment cost of each DG is considered only once in the summation. For example, suppose an investment in a particular DG is made in the fourth year of a five-year planning horizon. This means the DG unit will be available during the fourth and the fifth years. Hence, the binary variable associated to this DG in those years will be 1 while the rest will be zero i.e. $x^{N1}_{p,k,n,t} = \{0,0,0,1,1\}$. In this particular case, only the difference $(x^{N1}_{p,k,n,4} - x^{N1}_{p,k,n,3})$ equals 1, implying that the investment cost is considered only once. It should be noted that the DG investment variables can also be integers (i.e. with possible integer values other than 0 and 1).

Equations (4.3) and (4.4) stand for the sum of annual maintenance costs of new and existing DGs, respectively. These cost components are multiplied by the corresponding binary variables to determine whether each DG is being utilized or not. Note that the binary investment variable is also used for this purpose because there is no economic explanation or justification as to why it cannot be utilized immediately after an investment is made on a given asset. For the case example given above, the DG unit will incur maintenance costs in the last two years. For existing generators, binary variables are used for indicating their respective utilizations.

$$
\begin{aligned}
InvC^{N}_{t} = & \sum_{n\in\Omega^{n}}\sum_{k\in\Omega^{k}}\sum_{p\in\Omega^{p}}\frac{i(1+i)^{\eta_{p,k}}}{(1+i)^{\eta_{p,k}}-1}IC^{N1}_{p,k}(x^{N1}_{p,k,n,\tau}-x^{N1}_{p,k,n,\tau-1}) \\
& +\sum_{s\in\Omega^{s}}\rho_{s}\sum_{n\in\Omega^{n}}\sum_{k\in\Omega^{k}}\sum_{p\in\Omega^{p}}\frac{i(1+i)^{\eta_{p,k}}}{(1+i)^{\eta_{p,k}}-1}IC^{N1}_{p,k}\left(xx^{N1}_{p,k,n,s,\zeta}-xx^{N1}_{p,k,n,s,\zeta-1}\right) \\
& +\sum_{s\in\Omega^{s}}\rho_{s}\sum_{n\in\Omega^{n}}\sum_{k\in\Omega^{k}}\sum_{p\in\Omega^{p}}\frac{i(1+i)^{\eta_{p,k}}}{(1+i)^{\eta_{p,k}}-1}IC^{N2}_{p,k}(y^{N2}_{p,k,n,s,\zeta}-y^{N2}_{p,k,n,s,\zeta-1})\ ;\ \forall\tau\in\Omega^{P1};\ \forall\zeta\in\Omega^{P2}
\end{aligned}
\tag{4.2}
$$

$$MntC_t^N = \sum_{n\in\Omega^n}\sum_{k\in\Omega^k}\sum_{p\in\Omega^p} MC_{p,k}^{N1}\, x_{p,k,n,t}^{N1}$$
$$+\sum_{s\in\Omega^s}\rho_s \sum_{n\in\Omega^n}\sum_{k\in\Omega^k}\sum_{p\in\Omega^p} MC_{p,k}^{N1}\, xx_{p,k,n,s,\zeta}^{N1} \tag{4.3}$$
$$+\sum_{s\in\Omega^s}\rho_s \sum_{n\in\Omega^n}\sum_{k\in\Omega^k}\sum_{p\in\Omega^p} MC_{p,k}^{N2}\, y_{p,k,n,s,\zeta}^{N2} \quad ;\forall t\in\Omega^t;\ \forall\zeta\in\Omega^{P2}$$

$$MntC_t^E = \sum_{n\in\Omega^n}\sum_{k\in\Omega^k}\sum_{p\in\Omega^p} MC_{p,k}^{E}\, u1_{p,k,n,\tau}^{E}$$
$$+\sum_{s\in\Omega^s}\rho_s \sum_{n\in\Omega^n}\sum_{k\in\Omega^k}\sum_{p\in\Omega^p} MC_{p,k}^{E}\, u2_{p,k,n,s,\zeta}^{E} \quad ;\forall\tau\in\Omega^{P1};\ \forall\zeta\in\Omega^{P2} \tag{4.4}$$

$$EC_t^N = \sum_{s\in\Omega^s}\rho_s \sum_{n\in\Omega^n}\sum_{w\in\Omega^w}\pi_w \sum_{k\in\Omega^k}\sum_{p\in\Omega^p} OC_{p,k,n,s,w,\tau}^{N1}$$
$$+\sum_{s\in\Omega^s}\rho_s \sum_{n\in\Omega^n}\sum_{w\in\Omega^w}\pi_w \sum_{k\in\Omega^k}\sum_{p\in\Omega^p} OC_{p,k,n,s,w,\zeta}^{N2} \quad ;\ \forall\tau\in\Omega^t;\ \forall\zeta\in\Omega^{P2} \tag{4.5}$$

$$EC_t^E = \sum_{s\in\Omega^s}\rho_s \sum_{n\in\Omega^n}\sum_{w\in\Omega^w}\pi_w \sum_{k\in\Omega^k}\sum_{p\in\Omega^p} OC_{p,k,s,w,t}^{E} \quad ;\ \forall t\in\Omega^t \tag{4.6}$$

$$ENSC_t = \sum_{s\in\Omega^s}\rho_s \sum_{n\in\Omega^n}\sum_{w\in\Omega^w}\pi_w \upsilon_{s,w,t}\delta_{n,s,w,t} \quad ;\ \forall t\in\Omega^t \tag{4.7}$$

$$EMC_t^N = \sum_{s\in\Omega^s}\rho_s \sum_{n\in\Omega^n}\sum_{w\in\Omega^w}\pi_w \sum_{k\in\Omega^k}\sum_{p\in\Omega^p} \mu_{s,w,t}^{EMI}\, ER_{p,k}^{N1}\, g_{p,k,n,s,w,t}^{N1}$$
$$+\sum_{s\in\Omega^s}\rho_s \sum_{n\in\Omega^n}\sum_{w\in\Omega^w}\pi_w \sum_{k\in\Omega^k}\sum_{p\in\Omega^p} \mu_{s,w,\zeta}^{EMI}\, ER_{p,k}^{N2}\, g_{p,k,n,s,w,\zeta}^{N2} \quad ;\forall t\in\Omega^t;\ \forall\zeta\in\Omega^{P2} \tag{4.8}$$

$$E\ MC_t^E = \sum_{s\in\Omega^s}\rho_s \sum_{n\in\Omega^n}\sum_{w\in\Omega^w}\pi_w \sum_{k\in\Omega^k}\sum_{p\in\Omega^p} \mu_{s,w,t}^{EMI}\, ER_{p,k}^{E}\, g_{p,k,n,s,w,t}^{E} \quad ;\forall t\in\Omega^t \tag{4.9}$$

$$EMC_t^{SS} = \sum_{s\in\Omega^s}\rho_s \sum_{w\in\Omega^w}\pi_w \sum_{ss\in\Omega^{SS}} \mu_{s,w,t}^{EMI} ER_{ss}^{SS}\, g_{ss,s,w,t}^{SS} \quad ;\ \forall t\in\Omega^t \tag{4.10}$$

$$EC_t^{SS} = \sum_{s\in\Omega^s} \rho_s \sum_{w\in\Omega^w} \pi_w \sum_{ss\in\Omega^{ss}} \sigma_{ss,s,w,t} g_{ss,s,w,t}^{SS} \ ; \ \forall t \in \Omega^t \tag{4.11}$$

$$Loss_t = \sum_{s\in\Omega^s} \rho_s \sum_{w\in\Omega^w} \pi_w \sum_{n,m\in\Omega^n} \kappa_{s,w,t} \frac{r_{nm}}{(V_{nominal})^2} \left(f_{nm,s,w,t}\right)^2 \ ; \ \forall t \in \Omega^t \tag{4.12}$$

The total operation costs given by (4.5) and (4.6) for candidate and existing DGs, respectively, depend on the amount of power generated for each scenario, snapshot and stage. Therefore, these costs represent the expected costs of operation. Similarly, the penalty term for the unserved power, given by (4.7), is dependent on the scenarios, snapshots and decision stages. Equation (4.7) therefore gives the expected cost of unserved energy in the system. The expected emission costs of power generated by new and existing generators, and that of power purchased from the grid are given by (4.8), (4.9) and (4.10), respectively. The expected cost of energy purchased from upstream (i.e. transmission grid), is also accounted for by (4.11). The expected cost of network losses in the system are computed as in (12). Note that, to keep the problem linear, the quadratic flow function in (4.12) is linearized using a first-order approximation employed in [17]. In order this chapter to be self-contained, the linearized model is provided in Appendix A. Here, five piecewise linear partitions are considered throughout the analysis, which is in line with the findings in [94].

4.3.4 Constraints

4.3.4.1 *Load Balance Constraints*

Equation (4.13) enforces the Kirchhoff's current law (i.e. the load balance) at each node.

$$\sum_{k\in\Omega^k} \sum_{p\in\Omega^p} (g_{p,k,n,s,w,t}^{E} + g_{p,k,n,s,w,t}^{N1}) + \sum_{k\in\Omega^k} \sum_{p\in\Omega^p} g_{p,k,n,s,w,\zeta}^{N2} + \sum_{ss\Omega^{ss}} g_{ss,s,w,t}^{SS} + \delta_{n,s,w,t} = d_{n,s,w,t} \ ;$$
$$\forall n \in \Omega^n; \ \forall t \in \Omega^t; \ \forall \zeta \in \Omega^{P2}; \ \forall s \in \Omega^s; \forall w \in \Omega^w \tag{4.13}$$

4.3.4.2 *Linear Constraints of Generation Cost*

The cost of a conventional power generation unit $\mathrm{C(P)}$ is a nonlinear function of the generated power P. Such nonlinear relationship is often approximated by a quadratic curve, i.e. $C(P) = A + B * P + C * P^2$; where A, B and C are the cost coefficients which mainly depend on the type of fuel used. In order to linearize this curve, we use an SOS2 (special order set of type 2) approach, which is extensively discussed in [94]. The constraints related to the linear cost models of existing and new DGs can be found in Appendix C.

4.3.4.3 *Investment Limits*

A budget constraint for investing in DGs is enforced by adding constraint (4.14) for the first period and (4.15) for the second one.

$$\sum_{n\in\Omega^n}\sum_{k\in\Omega^k}\sum_{p\in\Omega^p} IC^{N1}_{p,k}(x^{N1}_{p,k,n,\tau}-x^{N1}_{p,k,n,\tau-1}) \leq InvLim_{\tau}\ ; \forall\tau\in\Omega^{P1} \tag{4.14}$$

$$\sum_{n\in\Omega^n}\sum_{k\in\Omega^k}\sum_{p\in\Omega^p} IC^{N1}_{p,k}(y^{N2}_{p,k,n,s,\zeta}-y^{N2}_{p,k,n,s,\zeta-1}) + \sum_{n\in\Omega^n}\sum_{k\in\Omega^k}\sum_{p\in\Omega^p} IC^{N1}_{p,k}(xx^{N1}_{p,k,n,s,\zeta}-xx^{N1}_{p,k,n,s,\zeta-1}) \leq InvLim_{s,\zeta}\ ;\ \forall\zeta\in\Omega^{P2};\ \forall s\in\Omega^{s} \tag{4.15}$$

4.3.4.4 *Generation Capacity Limits*

The capacity limits of existing generators in the first and the second periods are given by (16) and (4.17), respectively. In the case of candidate generators, the corresponding constraints are (4.18)—(4.20). Note that the binary variable associated to a given generator multiplies the corresponding generation limits. This is to make sure that the power generation variable is zero when the generator remains either unutilized or unselected for investment.

$$u1^{E}_{p,k,n,\tau}Gmin^{E}_{p,k,s,w} \leq g^{E}_{p,k,n,s,w,\tau} \leq u1^{E}_{p,k,n,\tau}Gmax^{E}_{p,k,s,w}\ ; \quad \forall n\in\Omega^{n};\ \forall\tau\in\Omega^{P1};\ \forall s\in\Omega^{s};\ \forall w\in\Omega^{w};\ \forall k\in\Omega^{k}\ ; \forall p\in\Omega^{p} \tag{4.16}$$

$$u2^{E}_{p,k,n,\zeta}Gmin^{E}_{p,k,s,w} \leq g^{E}_{p,k,n,s,w,\zeta} \leq u2^{E}_{p,k,n,\zeta}Gmax^{E}_{p,k,s,w}\ ; \quad \forall n\in\Omega^{n};\ \forall\zeta\in\Omega^{P2};\ \forall s\in\Omega^{s};\ \forall w\in\Omega^{w};\ \forall k\in\Omega^{k};\ \forall p\in\Omega^{p} \tag{4.17}$$

$$x^{N1}_{p,k,n,t}Gmin^{N1}_{p,k,s,w} \leq g^{N1}_{p,k,n,s,w,t} \leq x^{N1}_{p,k,n,t}Gmax^{N1}_{p,k,s,w}\ ; \quad \forall n\in\Omega^{n};\ \forall t\in\Omega^{P1};\ \forall s\in\Omega^{s};\ \forall w\in\Omega^{w};\ \forall k\in\Omega^{k};\ \forall p\in\Omega^{p} \tag{4.18}$$

$$xx^{N1}_{p,k,n,s,\zeta}Gmin^{N1}_{p,k,s,w} \leq g^{N1}_{p,k,n,s,w,\zeta} \leq xx^{N1}_{p,k,n,s,\zeta}Gmax^{N1}_{p,k,s,w}\ ; \quad \forall n\in\Omega^{n};\ \forall\zeta\in\Omega^{P2};\ \forall s\in\Omega^{s};\ \forall w\in\Omega^{w};\ \forall k\in\Omega^{k};\ \forall p\in\Omega^{p} \tag{4.19}$$

$$y_{p,k,n,s,\zeta}^{N2} Gmin_{p,k,s,w}^{N2} \leq g_{p,k,n,s,w,\zeta}^{N2} \leq y_{p,k,n,s,\zeta}^{N2} Gmax_{p,k,s,w}^{N2} ;$$

$$\forall n \in \Omega^{n};\ \forall \zeta \in \Omega^{P2};\ \forall s \in \Omega^{s};\ \forall w \in \Omega^{w};\ \forall k \in \Omega^{k};\ \forall p \in \Omega^{p} \tag{4.20}$$

It should be noted that the above constraints are in generalized forms because the upper and the lower limits are scenario and snapshot dependent. These constraints need to otherwise be different for different types of DGs. For instance, for conventional DGs, both the upper and the lower power generation limits are often fixed; they do not usually vary with the yearly scenarios or hourly snapshots. However, this is different in the case of intermittent generators such as solar and wind types, whose upper bounds are determined by the availability of the primary energy sources (solar radiation and wind speed, in this case) while the lower bounds are often set to zero.

4.3.4.5 *Unserved Power Limit*

The unserved power at any given node cannot exceed the demand at that node, and this is enforced by:

$$0 \leq \delta_{n,s,w,t} \leq d_{n,s,w,t} ;$$

$$\forall n \in \Omega^{n};\ \forall t \in \Omega^{t};\ \forall s \in \Omega^{s};\ \forall w \in \Omega^{w} \tag{4.21}$$

4.3.4.6 *DG Penetration Limit*

It has been stated earlier that DG integration may in some cases negatively influence stability, power quality and security of distribution systems. In order to alleviate such technical problems, the penetration level of DG power is often limited. This is enforced by adding the constraints in (4.22). This constraint ensures that the total power generated by existing and new DGs at any operation time should be less than a certain percentage of the demand at the same time. Note that the second term in (4.22) is considered in the summation only when $t > T1$.

$$\sum_{n\in\Omega^{n}} \sum_{p\in\Omega^{p}} \sum_{k\in\Omega^{k}} (g_{p,k,n,s,w,t}^{E} + g_{p,k,n,s,w,t}^{N1}) + \sum_{n\in\Omega^{n}} \sum_{p\in\Omega^{p}} \sum_{k\in\Omega^{k}} g_{p,k,n,s,w,\zeta}^{N2} \leq \varphi D_{s,w,t}$$

$$;\forall t \in \Omega^{t};\ \forall \zeta \in \Omega^{P2};\ \forall s \in \Omega^{s};\ \forall w \in \Omega^{w};\ \forall k \in \Omega^{k};\ \forall p \in \Omega^{p} \tag{4.22}$$

4.3.4.7 *Logical Constraints*

The set of constraints in (4.23)—(4.28) ensure that an investment made at decision stage t cannot be reversed or divested in the subsequent stages; instead, the asset should be available for utilization immediately after the investment is made. The logical constraints in (4.23) guarantee that investment decisions made at a given stage in the first period are available in the immediate stages in the first stage.

$$x_{p,k,n,\tau}^{N1} \geq x_{p,k,n,\tau-1}^{N1} \;; \quad \forall n \in \Omega^{n};\; \forall \tau \in \Omega^{P1};\; \forall k \in \Omega^{k};\; \forall p \in \Omega^{p} \tag{4.23}$$

$$x_{p,k,n,\zeta}^{N1} = x_{p,k,n,T1}^{N1} \;; \quad \forall n \in \Omega^{n};\; \forall \zeta \in \Omega^{P2};\; \forall k \in \Omega^{k};\; \forall p \in \Omega^{p} \tag{4.24}$$

$$xx_{p,k,n,s,\zeta}^{N1} \geq xx_{p,k,n,s,\zeta-1}^{N1} \;; \quad \forall n \in \Omega^{n};\; \forall \zeta \in \Omega^{P2};\; \forall s \in \Omega^{s};\; \forall k \in \Omega^{k}; \forall p \in \Omega^{p} \tag{4.25}$$

$$xx_{p,k,n,s,T1}^{N1} = x_{p,k,n,T1}^{N1} \;; \quad \forall n \in \Omega^{n};\; \forall s \in \Omega^{s};\; \forall k \in \Omega^{k};\; \forall p \in \Omega^{p} \tag{4.26}$$

$$y_{p,k,n,s,\zeta}^{N2} \geq y_{p,k,n,s,\zeta-1}^{N2} \;; \quad \forall n \in \Omega^{n};\; \forall \zeta \in \Omega^{P2};\; \forall s \in \Omega^{s};\; \forall k \in \Omega^{k};\; \forall p \in \Omega^{p}; \forall n \in \Omega^{n} \tag{4.27}$$

$$y_{p,k,n,s,T1}^{N2} = 0 \;; \quad \forall n \in \Omega^{n};\; \forall s \in \Omega^{s};\; \forall k \in \Omega^{k};\; \forall p \in \Omega^{p} \tag{4.28}$$

4.3.4.8 *Network Model Constraints*

The active power flow through each line in the network is represented by a linearized AC network model, first proposed in [95] in the context of transmission expansion planning and further extended to distribution network system planning in [96].

Modeling both active and reactive power flows is the most elegant approach. The importance of reactive power in a system is unquestionable. However, unlike active power, it is widely accepted that reactive power “does not travel very far”; it can be produced (compensated) locally.

In other words, the reactive power requirement in a system can be met by reactive power sources placed very close to the locations where such power is “consumed”. Otherwise, reactive power flows in the network may increase, leading to an increase in losses which is not desirable. Generally, in well-compensated distribution network systems, such flows are normally expected to be very small. Because of this and computation reasons, they are neglected in the analysis throughout this chapter. Although the most orthodox way of modeling the system is to use a full-AC model or its variants that consider both active and reactive power flows, embedding such a model in a complex, long-term stochastic planning model (as in the present work) is not computationally affordable. Because of this, the “direct current” (DC) network model (which does not consider reactive power flow) is widely used in power system planning and operation problems. In some cases, long-term planning problems under uncertainty are developed without explicitly modeling the physical equations of networks, mainly due to computational reasons. In general, the use of a DC network model in such problems yields reasonably accurate planning solutions. In the present work, the modified DC model [95], [96] is employed where the active power flow model is given by (4.29). The constraint in (4.30) ensures that the flow through the distribution lines do not exceed their corresponding thermal limits.

$$\begin{gathered} M_{nm}(z_{nm}-1) \leq \\ f_{nm,s,w,t} - \left\{V_{nominal}\left(\Delta V_{n,s,w,t} - \Delta V_{m,s,w,t}\right)g_{nm} - V_{nominal}^{2} b_{nm}\theta_{nm,s,w,t}\right\} \\ \leq\; M_{nm}(1-z_{nm})\;; \\ \forall n,m \in \Omega^{n};\; \forall s \in \Omega^{s};\; \forall w \in \Omega^{w} \forall t \in \Omega^{t} \end{gathered} \tag{4.29}$$

Note that the voltage deviations at each node $\Delta V_{n,s,w,t}$ and $\Delta V_{m,s,w,t}$ are bounded as $-\varepsilon * V_{nominal} \leq \Delta V_{n,s,w,t} \leq \varepsilon * V_{nominal}$. For the analysis throughout this chapter, the tolerance factor ε is set to 0.05, and the voltage magnitude and angle at the substation are set to $1.05 V_{nominal}$ and 0, respectively.

$$\begin{gathered} -f_{nm}^{max} z_{nm} \leq f_{nm,s,w,t} \leq z_{nm} f_{nm}^{max}\;; \\ \forall n,m \in \Omega^{n};\; \forall s \in \Omega^{s};\; \forall w \in \Omega^{w} \forall t \in \Omega^{t} \end{gathered} \tag{4.30}$$

4.3.4.9 *Radiality Constraints*

Current distribution systems are predominantly operated in a radial structure. Moreover, island operation, which may be imminent with DG integration, is not often desired. In this regard, the traditional radiality constraint in (4.31) [97], along with the load balance equation, gives the necessary condition for a distribution network to be radial and connected.

However, this constraint alone is not sufficient to fulfill the aforementioned requirements (i.e. to keep radiality and all nodes connected) particularly in planning problems involving grid expansion, switching and integration of DGs or reactive power sources [106]. Additional constraints as in [97] needs to be incorporated to guarantee that all nodes in the system are connected. However, this is out of the scope of this thesis, and will be addressed in future works considering grid expansion and switching.

The work in this chapter considers a radial network. Therefore, for this case, Equation (4.31) is sufficient to keep the radiality of the network and ensure that all nodes are connected.

$$\sum_{n,m \in \Omega^n} z_{nm} = N_n - N_{SS} \ ; \quad \forall (n,m) \in \Omega^c \tag{4.31}$$

4.4 Case Studies

4.4.1 System Data and Assumptions

The system considered in the study is a real-life distribution network in São Miguel Island, Portugal. The system has a peak demand of 70.2 MW, and info about existing generators is shown in Table 4.2.

In this system, various DG types with capacities ranging from 1 to 30 MW are considered as candidates for investment (see Table 4.3). These fall into small to medium-scale DG categories according to the capacity-based classification of DGs in [98]. The installation and maintenance costs of each DG are either directly obtained from [98] and [99] or estimated using the so-called six-tenths rule [100], which establishes a relationship between cost and quantity (in this case, the installed capacity). This method reflects the economy of scale that exists in DGIP i.e. the higher the installed capacities of DGs of the same type are, the lower the costs per installed kW get.

Table 4.2 – Data for existing generators

No.	Generator type, p	Alternative, k	Installed capacity (MW)	$OC_{p,k}$ (€/MWh)	$IC_{p,k}$ (M€)	$MC_{p,k}$ (M€)	$ER_{p,k}$ (tons/MWh)
1	Hydro	Hydro	4.07	7.0	NA	0.38	0.0121
2	Geothermal	GEOT	24.0	5.0	NA	1.20	0.0165
3	HFO-T*	HFO	98.0	145.4	NA	0.01	0.5600
4	Wind	WD 0	10.0	17.0	NA	0.80	0.0276

** Heavy fuel oil turbine, NA = Not applicable*

Table 4.3 - Data for candidate generators

No.	DG type, *p*	DG alternative *k*	Installed capacity [MW]	$OC_{p,k}$ [€/MWh]	$IC_{p,k}$ [M€]	$MC_{p,k}$ [M€]	$ER_{p,k}$ [tons/ MWh]
1	Solar	PV 1	1.0	40	3.00	0.06	0.0584
2	Solar	PV 2	1.5	40	3.83	0.08	0.0584
3	Solar	PV 3	2.0	40	4.55	0.09	0.0584
4	Solar	PV 4	2.5	40	5.20	0.10	0.0584
5	Solar	PV 5	3.0	40	5.80	0.12	0.0584
6	Solar	PV 6	4.0	40	6.89	0.14	0.0584
7	Solar	PV 7	6.0	40	8.79	0.17	0.0584
8	Solar	PV 8	10	40	11.94	0.24	0.0584
9	Wind	WD 1	1.0	17	2.64	0.05	0.0276
10	Wind	WD 2	2.0	17	4.00	0.08	0.0276
11	Wind	WD 3	5.0	17	6.93	0.14	0.0276
12	Wind	WD 4	10	17	10.51	0.21	0.0276
13	CGT*	CGT 1	30	145.4	27.00	0.01	0.5600
14	BM**	BM 1	20	20	80.00	3.00	0.0900

* *Combustion gas turbine; ** Biomass*

The hourly series (historical data) of wind speed and solar radiation at various locations of the island are obtained from publicly available databases [101], [102], respectively. The geographical coordinates where these data are taken from include (37.790,-25.385), (37.778,-25.489), (37.866,-25.816), (37.797,-25.170), (37.717,-25.505), (37.823,-25.487), (37.772,-25.375) and (37.782,-25.661). Then, the wind (WD) and solar photovoltaic (PV) power production series, used in the simulations, are determined by plugging in the wind speed and radiation data in the corresponding power curve expressions. Note that two wind-speed regimes (offshore and onshore) are considered in the case study.

4.4.2 Scenario Definition

In this chapter, the uncertainty introduced by four most relevant uncertain parameters namely, electricity demand growth, emission price, wind and solar PV power output is taken into consideration. In other words, the evolutions of emission price, electricity demand growth as well as uncertainty due to intermittent energy sources (solar PV and wind, in particular) are captured through a predefined number of scenarios, each with a certain probability. The demand growth for a certain year can be somehow estimated via forecasting tools but this introduces some uncertainty due to the forecasting error. As illustrated in Figure 4.3, this leads to a confidence interval in which the demand profile is likely to lie. Similarly, the confidence intervals of wind and solar power outputs are formed, as shown in Figure 4.4. And, for the analysis in this work, three demand growth scenarios are considered corresponding to the middle, top and bottom curves which form the band in Figure 4.3. In a similar manner, the wind and solar power output scenarios are defined.

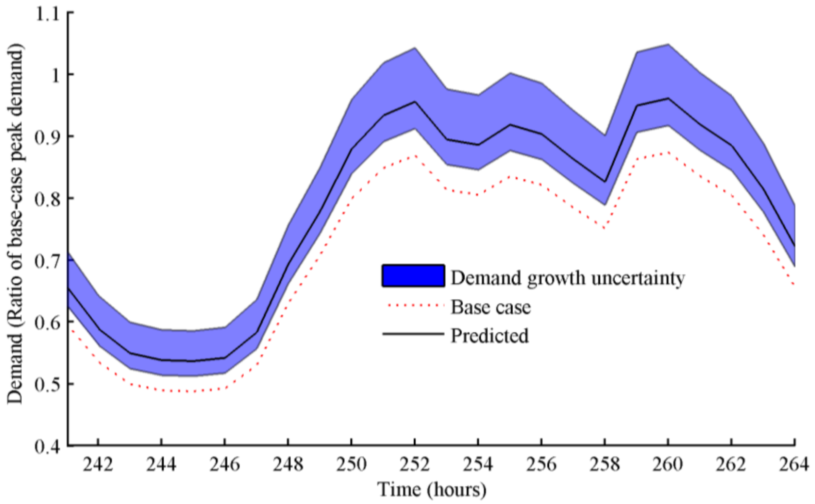

Figure 4.3 - A sample demand profile for day 11 in the second stage (i.e. τ = 2) of the first period, reflecting demand growth uncertainty.

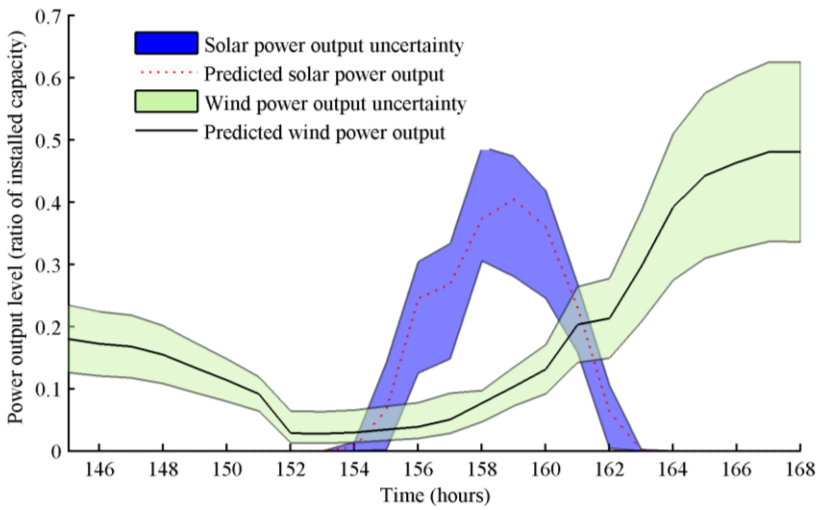

Figure 4.4 - Wind and solar PV power output uncertainty characterization example.

The following assumptions are made for the case study:

- Discount rate is set to 7% and kept the same throughout the planning horizon.
- DG penetration limit factor is assumed to be 40%.
- The lifetime of all DGs is considered to be 20 years.
- In order to take account of the variability introduced by electricity demand, solar PV and wind power sources, an initial set of 8760 snapshots (either historical data, obtained using forecasting tools or generated via Monte Carlo methods), corresponding to the hourly operational situations in a single year, is assumed to be available.
- An ordinary clustering methodology (*k-mea*ns algorithm) is employed to reduce these snapshots to 300 representative ones (see in the following subsection how this is decided).

- For the sake of simplicity, the same candidate DG pools are considered in the first and the second periods.
- Investment decisions in the first period can be postponed to the second period, if deemed economical.
- The planning horizon is considered to be 8 years, in which the length of the first period is three years.
- The cost coefficients (A, B and C) of the conventional generation units are assumed to be 0.74 €/h, 35 €/MWh and 550 €/h/(MW)^2. For the RES-based generation units, A and C are both zero while B is set equal to $OC_{p,k}$ in Table 4.3.
- The cost of unserved energy is assumed to be 3000 €/MWh.

In general, a total of 81 scenarios (storylines) are defined in connection to the possible evolutions of the aforementioned parameters over the planning horizon. Table 4.4 shows the three evolutions of demand growth, denoted as Low, Moderate and High, having equal degree of realization. To further illustrate this, hourly demand profiles of a sample day in the second stage, corresponding to the three demand growth scenarios, are shown in Fig. 4.3. Similarly, the emission price is represented by three equally probable storylines (scenarios), as shown in Table 4.4. Wind and solar PV power output uncertainties are also represented by three equiprobable scenarios as explained above. Given these individual scenarios, assuming all uncertain parameters are independent, 81 different combinations are obtained, which form the new set of scenarios used in the simulations.

4.4.3 Results and Discussion

The formulated DGIP problem is coded in GAMS 24.0, and solved using CPLEX 12.0. The optimality gap is set to zero in all cases. All simulations are carried out in an HP Z820 Workstation having E5-2687W processor with two cores, clocking at 3.1GHz speed.

Table 4.4 – Demand growth and emissions scenarios

Stage	Demand growth scenarios			Emission price scenarios (€/tons)		
	Low	Moderate	High	Low	Moderate	High
τ=0	0.0%	0%	0%	7	7	7
τ=1	2.0%	5%	10%	9	12	20
τ=2	5.0%	10%	20%	12	18	30
τ=3	7.0%	15%	30%	16	25	45
ζ=4	9.0%	20%	40%	20	30	50
ζ=5	11.0%	25%	50%	20	30	50
ζ=6	13.0%	30%	60%	20	30	50
ζ=7	14.5%	35%	70%	20	30	50
ζ=8	16.0%	40%	80%	20	30	50

4.4.3.1 *Deciding the number of representative clusters*

It has already been stated earlier that the large number of snapshots (operational situations) should be reduced to ensure problem tractability. This is accomplished by clustering the large initial set of snapshots. The minimum number of clusters, which sufficiently balances accuracy and computational burden, is often decided by trial and error. A famous rule of thumb in this case is the "Elbow" method, which is commonly used in clustering analysis. This method simply approximates the minimum number of clusters by plotting the objective value of the clustering algorithm for different number of clusters. Instead of using the objective value of the algorithm, the values of certain system variables, namely, investment and total costs, expected emissions and simulation time are used here. We analyze the impact of reducing the snapshots on these system variables.

The analysis results are summarized in Table 4.5. For the sake of clarity, Figure 4.5 also plots the computational time and investment cost against the number of clusters. It is evident to see that the higher the number of clusters is, the more accurately the aforementioned variables are optimized but the higher the computational requirement is.

Table 4.5 - Impact of snapshot reduction on system variables

Number of clusters	Total investment cost (M€)	Total cost (M€)	CPU time (h)	Expected emissions (tons)		
				Period 1	Period 2	Entire horizon
100	70.01	468.40	0.20	293142	877712	877712
200	69.93	469.67	0.58	294279	882015	882015
300	69.74	470.41	1.50	295122	885118	885118
400	69.58	470.79	3.87	295530	887225	887225
500	69.55	471.10	6.50	295935	888015	888015
1000	69.53	472.25	25.50	297215	892531	892531

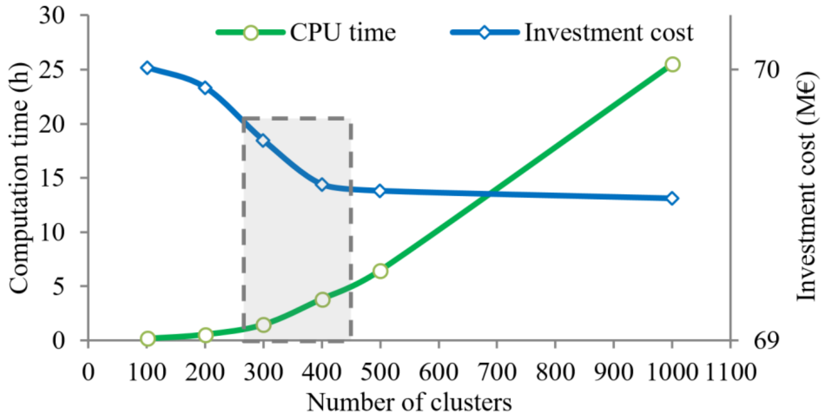

Figure 4.5 - Effect of snapshot reduction on the investment cost.

On the contrary, when the number of clusters is further reduced, the computational burden decreases, but this compromises the overall accuracy of the solution. Increasing the clusters further beyond a certain threshold does not lead to significant variations in the results apart from adding considerable computational burden. This threshold is related to the minimum number of clusters required to effectively balance accuracy and computational requirement. One can easily see in Table 4.5 and Figure 4.5 that the threshold lies somewhere between 250 and 400. Accordingly, the number of clusters is taken to be 300 for the rest of the analysis. Hence, the finally reduced number of snapshots that are used in the planning process is 300.

4.4.3.2 *DGIP results*

The DGIP problem is solved considering the investment variable of DG as binary {0, 1} and integer {0,1,2,…} investment variables. These two cases are optimized separately but assuming the same set of candidate DGs. Table 4.6 summarizes the investment outcome at each stage of the two planning periods for both cases. As it can be observed in this table, majority of the investments tend to be made in the beginning of each period (i.e. the first and the fourth stages, in particular). Two reasons may explain the crowding of investment decisions towards the beginning of each investment period. The first reason may be because of the net present value (NPV) of operation and emission costs, which is higher in the foremost decision stages of the planning horizon. For instance, the operation, maintenance and emission costs are relatively higher in the first stage when compared with that of any other stage throughout the planning horizon. Hence, it becomes more attractive to invest in the leading stages so that such costs are reduced in short-run as well as in medium/long-run. The second reason may be because of lack of investment constraints related to financial and logistical matters.

Table 4.6 – DG investments in each stage

		DG investment solution		NPV of investment cost (M€)	
Horizon	Stages	Binary	Integer	Binary	Integer
1st period	$\tau = 1$	PV7, PV8, WD1, WD2, WD3, WD4	5 WD4	35.644	56.093
	$\tau = 2$	-	-	0	0
	$\tau = 3$	-	1 WD4	0	9.272
2nd period	$\zeta = 4$	PV6, PV7, PV8, WD1, WD2, WD3, WD4	PV8, WD4	27.123†	15.215†
	$\zeta = 5$	PV5, PV6, PV7, PV8, WD1, WD2, WD3	PV8, WD4	3.675†	3.444†
	$\zeta = 6$	PV4, PV6, PV7, PV8, WD1, WD2	PV8, WD4	1.534†	2.173†
	$\zeta = 7$	PV4, PV5, PV6, PV7, PV8, WD1, WD2	PV8, WD4	1.009†	2.914†
	$\zeta = 8$	PV3, PV4, PV5, PV6, PV7, PV8, WD1, WD2	PV8, WD4	0.754†	2.210†
NPV of total cost (M€)				470.415	400.991†
Computational time (h)				1.5	21

† *Expected investment cost (weighted by the probabilities of scenarios)*

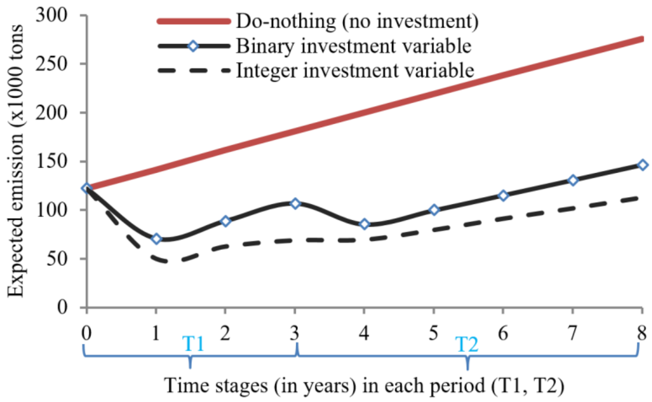

Figure 4.6 - Evolution of emissions over the planning stages.

In line with the investments made, the evolution of expected emissions over the entire planning horizon also follows a predictable trend. For instance, because of the huge investments in stage 1, the expected (average) emissions are significantly reduced, and a similar phenomenon can be observed in stage 4. Apart from these two stages, emissions tend to slightly increase. Such increase in emissions can be explained by the increasing trend of demand because, in the absence of more investments in RESs, conventional generators should generate more to meet the increasing demand. However, as illustrated in Figure 4.6, the average emissions curve remains far below that of the "do-nothing" scenario, where no investments are assumed to be made. Table 4.6 clearly shows the differences between the binary and the integer solutions. The overall impact of each solution on the expected emissions is also illustrated in Figure 4.6. One can infer from Table 4.6 that the model based on integer variables better exploits the benefits of economy of scale as there is a tendency of avoiding investment in DGs with low capacities. As shown in this table, the integer investment solution only encompasses multiples of WD4 in the first period, and WD4 and PV8 in the second period. Even if this means higher investment cost, the overall/total cost is found out to be about 15% lower than that of the model with binary ones. In addition, when using the integer-based model, the overall reduction in emissions is higher than when using the binary-based model, as illustrated in Figure 4.6. However, it is worth mentioning here that solving the general integer-based model is much harder (about 14 times according to the results in Table 4.6) than the binary-based one.

4.4.3.3 *The significance of the proposed models*

The importance of planning under uncertainty i.e. the significance of the proposed stochastic model can be shown by comparing decisions made under uncertainty and by ignoring uncertainty. Also, relevant metrics can be used to quantify the importance of uncertainty and demonstrate the practicality of the stochastic model. Here, we employ two metrics, expected value of perfect information (EVPI) and expected cost of ignoring uncertainty (ECIU), which are commonly used in stochastic programming applications for similar purposes.

As its name implies, EVPI gives an estimate of the maximum amount a planner would be willing to pay in return for perfect information or a prediction tool that allows the planner to have a perfect foresight about the future. In other words, EVPI quantifies the value of knowing the future with certainty. This parameter is given by the difference between the expected cost of stochastic solution and its fully deterministic counterpart. For the binary-based stochastic solution, the EVPI amounts to 2.39 M€. Putting this value in perspective of the total investment cost in the first period (see in Table 4.6), one can observe that it is not negligible. The ECIU, on the other hand, measures the cost of making naïve decisions i.e. the cost of assuming that a given scenario happens with certainty. This metric can be alternatively understood as the value of stochastic solution. For the binary-based stochastic model, the ECIU is calculated to be 3.43 M€, which is not also negligible. When comparing this value with the total NPV of investment costs in the first period (see in Table 4.6), one can easily see that it amounts to more than 9% of this cost. Moreover, note that this value corresponds to a weighted sum of the cost of ignoring uncertainty (CIU) across all scenarios.

Depending on which deterministic scenario is considered to obtain the naïve decisions, the CIU value varies tremendously as depicted in Figure 4.7. Here, for some scenarios, CIU is as high as 22 M€, which clearly shows that naïve/deterministic solutions (i.e. decisions made by ignoring uncertainty) can have significant costs. In other words, this indicates the quality of the stochastic solution, and hence, the practicality of the proposed stochastic model.

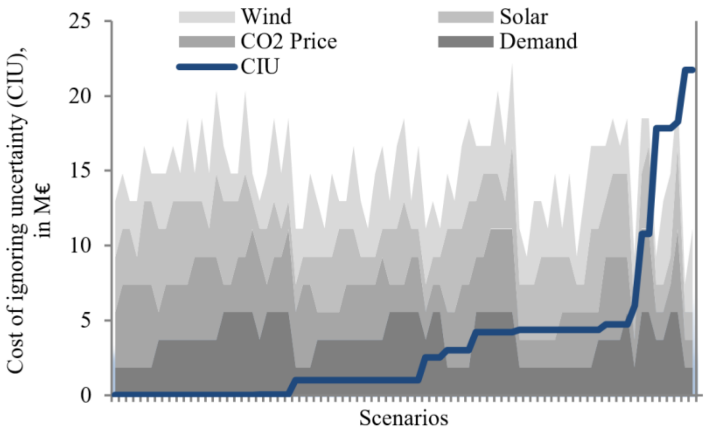

Figure 4.7 – Cost of ignoring uncertainty.

4.5 Chapter Conclusions

In this chapter was presented a novel multi-stage stochastic distributed generation investment planning model for making investment decisions under uncertainty. The problem was formulated from a coordinated system planning viewpoint, simultaneously minimizing the net present value of costs rated to losses, emission, operation and maintenance, as well as the cost of unserved energy.

The formulation was anchored on a two-period planning horizon, each having multiple stages. The first period was a short-term horizon in which robust decisions were pursued in the face of uncertainty; whereas, the second one spans over a medium to long-term horizon involving exploratory and/or flexible investment decisions. The operational variability and uncertainty introduced by intermittent generation sources, electricity demand, emission prices, demand growth and others were accounted for via probabilistic and stochastic methods, respectively. Metrics such as cost of ignoring uncertainty and value of perfect information were used to clearly demonstrate the benefits of the proposed stochastic model. A real-life distribution network system was used as a case study, and the results showed the effectiveness of the proposed model.

Chapter 5

Impacts of Optimal Energy Storage Deployment and Network Reconfiguration on Renewable Integration Level in Distribution System

This chapter is based on the previous chapter but gives a step ahead by adding network switching to the problem and a novel mechanism to quantify the impacts of network switching and/or reinforcement as well as deployment of ESSs on the level of renewable power integrated in the system. To carry out this analysis, a dynamic and multi-objective stochastic mixed integer linear programming (S-MILP) model is presented, which jointly takes the optimal deployment of RES-based DGs and ESSs into account in coordination with distribution network reinforcement and/or reconfiguration.

5.1 Introduction

To overcome or alleviate the negative consequences of RES integration in distribution systems, a number of smart-grid related technologies and concepts are available which can be rolled out in coordination with the variable energy sources. Among these technologies, energy storage systems (ESSs) have been poised to be viable solutions to increase the level of penetration of RES-based distributed generations while minimizing their side effects [107]. The use of ESS "levels" the gap between renewable generation and demand by storing energy in periods of low electricity demand or high production from renewable energy sources, and releasing the stored energy in periods of higher demand [108]. Such a practice brings about several technical and economic benefits especially in terms of cost reduction as well as reliability, power quality and stability improvements in the system. Distribution reconfiguration can also increase the flexibility of the system, possibly paving the way to an increased penetration level of variable energy sources.

The increased penetration of variable renewable DGs will have a positive and/or negative impact based on system conditions. Conventional electrical networks carry a unidirectional power flow. The introduction of DGs implies a bidirectional power flow and increased variability and uncertainty in the system. Such variability and uncertainty of RES power production can be partly counterbalanced by deploying ESSs. In other words, integrating ESSs in the network systems can counteract the unpredictable variation of the energy supplied by intermittent RESs. In addition, ESSs balance demand and power generation. Excess energy is stored during periods of high RES power production and low demand, and is released during periods of peak demand [108]. The placement and sizing optimization of ESSs is important to mitigate the unpredictable variation of the energy supplied by RESs. In [109], a detailed review is presented, including the individual ESS applications with respect to several storage options, settings, sizing methodologies and control.

Previous studies in the literature about DSR have traditionally focused on the minimization of system losses [110]. However, the DSR problem needs to address not only the classic objectives, i.e. minimizing losses, the voltage profile improvement and/or system reliability, but also two additional problems complementary to these issues: the massive RES integration and the paradigm of smart grid from the perspective of intelligent reconfiguration [111], [112], [113]. Because of all this, performing reconfiguration is becoming one of the most relevant topics in connection with the distribution network systems.

Given the background, this chapter develops a new joint optimization model that maximizes the RES integration in distribution network systems. The model simultaneously determines the optimal allocation, sizing and timing of DGs as well as ESSs. In addition, this chapter presents a comprehensive analysis on the impacts of distribution reconfiguration and joint deployment of ESSs on the RES-based integration level.

The remainder of this chapter is organized as follows: In Section 5.2, a description of the developed mathematical model is presented. Subsequently, Section 5.3 presents and discusses the obtained results. Finally, in Section 5.4, the relevant conclusions and implications based on the outcome are drawn.

5.2 Mathematical Model

5.2.1 Objective Function

The problem is formulated as a multi-objective stochastic MILP optimization with an overall cost minimization as in (5.1). The objective function in (5.1) is composed of NPV of five cost terms each weighted by a certain relevance factor $\gamma_j; \forall j \in \{1,2, \dots ,5\}$.

The first term in (1), TInvC, represents the total investment cost under the assumption of a perpetual planning horizon. In other words, “the investment cost is amortized in annual instalments throughout the lifetime of the installed component”.

Here, the total investment cost is the sum of investment costs of DGs, distribution network system (DNS) components (feeders and transformers) and ESSs, as in (5.2). This cost is computed as in (5.7)—(5.9).

The second term, TMC, in (5.1) denotes the total maintenance costs which is given by the sum of maintenance costs of new and existing DGs as well as that of DNS components and ESSs at each stage plus the corresponding costs incurred after the last time stage, as in (5.3). Note that the latter depend on the maintenance costs of the last stage according to a perpetual planning horizon. These maintenance costs are computed using equations (5.10)—(5.12).

The third term, TEC, in (5.1) refers to the total cost of energy in the system, which is the sum of the cost of power produced by new and existing DGs, supplied by ESSs and purchased from upstream at each stage as in (5.4). Equation (5.4) also includes the total energy costs incurred after the last time stage under the assumption of a perpetual planning horizon. Note that these costs depend on the energy costs of the last stage. The detailed mathematical expressions for computing the cost of DG power produced and ESS power supplied as well as that of purchased power are given in (5.13), (5.14) and (5.15), respectively. The fourth term TENSC represents the total cost of unserved power in the system, given as in (5.5). This is computed using equation (5.16). The last term, TEmiC, gathers the total emission costs in the system, given by the sum of emission costs for the existing and new DGs in equations (5.17)—(5.19) as well that of purchased power (5.20).

$$Minimize\ TC = \gamma_1 * TInvC + \gamma_2 * TMC + \gamma_3 * TEC + \gamma_4 * TENSC + \gamma_5 * TEmiC \tag{5.1}$$

As mentioned earlier, the objective function is composed of five terms, each associated with a certain relevance factor. These factors can have dual purposes. The first one is to provide the planner with the needed flexibility for the planner to include/exclude each cost term in/from the objective function. In this case, the associated relevance factor is set to 1 if the cost term is included; otherwise the factor is set to 0. Another purpose of these factors boils down to the relative weight in which the planner wants to apply on each cost term. To emphasize the importance of a given cost term, a relatively higher value can be assigned than any other term in the objective function.

$$TInvC = \underbrace{\sum_{t\epsilon\Omega^t} \frac{(1+r)^{-t}}{r}\left(InvC_t^{DG} + InvC_t^{LN} + InvC_t^{ES} + InvC_t^{CAP}\right)}_{NPV\ of\ investment\ cost} \tag{5.2}$$

$$\begin{aligned} TMC = & \underbrace{\sum_{t\epsilon\Omega^t} (1+r)^{-t}\ \left(MntC_t^{DG} + MntC_t^{LN} + MntC_t^{ES} + MntC_t^{Cap}\right)}_{NPV\ of\ maintenance\ costs} \\ & + \underbrace{\frac{(1+r)^{-T}}{r}\left(MntC_T^{DG} + MntC_T^{LN} + MntC_T^{ES} + MntC_T^{Cap}\right)}_{NPV\ maintenance\ costs\ incured\ after\ stage\ T} \end{aligned} \tag{5.3}$$

$$TEC = \underbrace{\sum_{t\epsilon\Omega^t} (1+r)^{-t}\ \left(EC_t^{DG} + EC_t^{ES} + EC_t^{SS}\right)}_{NPV\ of\ operation\ costs} + \underbrace{\frac{(1+r)^{-T}}{r}\left(EC_T^{DG} + EC_T^{ES} + EC_T^{SS}\right)}_{NPV\ operation\ costs\ incured\ after\ stage\ T} \tag{5.4}$$

$$ENSC = \underbrace{\sum_{t\epsilon\Omega^t}(1+r)^{-t}\ ENSC_t}_{NPV\ of\ \ reliability\ costs} + \underbrace{\frac{(1+r)^{-T}}{r} ENSC_T}_{NPV\ reliability\ costs\ incured\ after\ stage\ T} \tag{5.5}$$

$$TEmiC = \underbrace{\sum_{t\epsilon\Omega^t}(1+r)^{-t}\ (EmiC_t^{DG} + EmiC_t^{SS})}_{NPV\ emission\ costs} + \underbrace{\frac{(1+r)^{-T}}{r}(EmiC_T^{DG} + EmiC_T^{SS})}_{NPV\ emission\ costs\ incured\ after\ stage\ T} \tag{5.6}$$

Equation (5.2) translates the total investment costs within the planning horizon, where $\mathrm{InvC_t^{DG}}$ denotes the investment costs of DGs, $\mathrm{InvC_t^{DNS}}$ is the investment costs in the distribution network system and $\mathrm{InvC_t^{ES}}$ is the investment cost in ESS. Equation (5.3) represents the total maintenance costs of new and existing DGs, DNS components and ESSs at each stage. These costs are updated by the NPV factor associated to each year. Here, $\mathrm{MntC_t^{DG}}$ denotes the maintenance cost of DGs while $\mathrm{MntC_t^{DNS}}$ and $\mathrm{MntC_t^{ES}}$correspond to the maintenance costs of distribution network system and ESSs, respectively. Equation (5.4) shows the total cost of energy in the system, which is the sum of the cost of power produced by new and existing DGs, supplied by ESSs and purchased from upstream at each stage. TENSC in (5.5) represents the total cost of unserved power in the system. This is interpreted as the energy not supplied costs (ENSC). The total emission cost of power production using DGs ($\mathrm{EmiC_t^{DG}}$) and that of purchased power ($\mathrm{EmiC_t^{SS}}$) is given by (5.6).

Equations (5.7)—(5.9) represent the investment costs of DGs, feeders and energy storage system, respectively. Notice that all investment costs are weighted by the capital recovery factor, $\frac{\mathrm{r(1+r)^{LT}}}{\mathrm{(1+r)^{LT}-1}}$. The formulations in (5.7)—(5.10) ensure that the investment cost of each component added to the system is considered only once in the summation.

$$InvC_t^{DG} = \sum_{g\epsilon\Omega^g}\sum_{i\epsilon\Omega^i}\frac{r(1+r)^{LT_g}}{(1+r)^{LT_g}-1} IC_{g,i}(x_{g,i,t} - x_{g,i,t-1})\ ; where\ x_{g,i,0} = 0 \tag{5.7}$$

$$\begin{aligned} InvC_t^{DNS} = &\sum_{k\epsilon\Omega^\ell}\frac{r(1+r)^{LT_k}}{(1+r)^{LT_k}-1} IC_k(x_{k,t} - x_{k,t-1}) \\ &+ \sum_{ss\epsilon\Omega^{SS}}\sum_{tr\epsilon\Omega^{tr}}\frac{i(1+i)^{LT_{tr}}}{(1+i)^{LT_{tr}}-1} IC_{tr}\big(x_{tr,ss,t} - x_{tr,ss,t-1}\big)\ ; \end{aligned} \tag{5.8}$$

$$InvC_t^{ES} = \sum_{c\epsilon\Omega^c}\sum_{i\epsilon\Omega^i}\frac{r(1+r)^{LT_{es}}}{(1+r)^{LT_{es}}-1} IC_{es,i}(x_{es,i,t} - x_{es,i,t-1})\ ; where\ x_{es,i,0} = 0 \tag{5.9}$$

Equation (5.10) stands for the maintenance costs of new and existing DGs at each time stage. The maintenance cost of a new/existing feeder is included only when its corresponding investment/utilization variable is different from zero, as shown in (5.11). Equation (5.12) is related to the maintenance costs of energy storage at each stage.

$$MntC_t^{DG} = \sum_{g\epsilon\Omega^g}\sum_{i\epsilon\Omega^i} MC_g^N\, x_{g,i,t} + \sum_{g\epsilon\Omega^g}\sum_{i\epsilon\Omega^i} MC_g^E\, u_{g,i,t} \tag{5.10}$$

$$MntC_t^{DNS} = \sum_{k\epsilon\Omega^{e\ell}} MC_k^E\, u_{k,t} + \sum_{k\epsilon\Omega^{n\ell}} MC_k^N x_{k,t} + \sum_{tr\epsilon\Omega^{E\_tr}} MC_{tr}^E\, u_{tr,ss,t} + \sum_{tr\epsilon\Omega^{N\_tr}} MC_{tr}^N x_{tr,ss,t} \tag{5.11}$$

$$MntC_t^{ES} = \sum_{c\epsilon\Omega^c}\sum_{i\epsilon\Omega^i} MC_{es} x_{es,i,t} \tag{5.12}$$

The total cost of power produced by new and existing DGs is given by equation (5.13). Note that these costs depend on the amount of power generated in each scenario, snapshot and stage. Therefore, they represent the expected costs of operation. Similarly, equations (5.14) and (5.15) account for the expected costs of energy supplied by the energy storage system, and that purchased from upstream (i.e. transmission grid), respectively.

$$EC_t^{DG} = \sum_{s\epsilon\Omega^s}\rho_s \sum_{w\epsilon\Omega^w}\pi_w \sum_{g\epsilon\Omega^g}\sum_{i\epsilon\Omega^i}(OC_{g,i,s,w,t}^N P_{g,i,s,w,t}^N + OC_{g,i,s,w,t}^E\, P_{g,i,s,w,t}^E) \tag{5.13}$$

$$EC_t^{ES} = \sum_{s\epsilon\Omega^s}\rho_s \sum_{w\epsilon\Omega^w}\pi_w \sum_{es\in\Omega^{es}} \lambda_{s,w,t}^{es} P_{es,i,s,w,t}^{dch} \tag{5.14}$$

$$EC_t^{SS} = \sum_{s\epsilon\Omega^s}\rho_s \sum_{w\epsilon\Omega^w}\pi_w \sum_{\varsigma\in\Omega^\varsigma} \lambda_{s,w,t}^{\varsigma} P_{\varsigma,s,w,t}^{SS} \tag{5.15}$$

The penalty for the unserved power, given by (5.16), is also dependent on the scenarios, snapshots and time stages. Therefore, equation (5.16) gives the expected cost of unserved energy in the system.

$$ENSC_t = \sum_{s\epsilon\Omega^s}\rho_s \sum_{w\epsilon\Omega^w}\sum_{i\epsilon\Omega^i}\pi_w \upsilon_{s,w,t}\delta_{i,s,w,t} \tag{5.16}$$

The expected emission costs of power generated by new and existing DGs are given by (5.17)—(5.19), and that of energy purchased from the grid is calculated using (5.20). Note that, for the sake of simplicity, a linear emission cost function is assumed here. In reality, the emission cost function is highly nonlinear and nonconvex.

$$EmiC_t^{DG} = EmiC_t^N + EmiC_t^E \tag{5.17}$$

$$EmiC_t^N = \sum_{s\epsilon\Omega^s} \rho_s \sum_{w\epsilon\Omega^w} \pi_w \sum_{g\epsilon\Omega^g} \sum_{i\epsilon\Omega^i} \lambda_{s,w,t}^{CO_2e} ER_g^N P_{g,i,s,w,t}^N \tag{5.18}$$

$$EmiC_t^E = \sum_{s\epsilon\Omega^s} \rho_s \sum_{w\epsilon\Omega^w} \pi_w \sum_{g\epsilon\Omega^g} \sum_{i\epsilon\Omega^i} \lambda_{s,w,t}^{CO_2e} ER_g^E P_{g,i,s,w,t}^E \tag{5.19}$$

$$EmiC_t^{SS} = \sum_{s\epsilon\Omega^s} \rho_s \sum_{w\epsilon\Omega^w} \pi_w \sum_{\varsigma\epsilon\Omega^\varsigma} \sum_{i\epsilon\Omega^i} \lambda_{s,w,t}^{CO_2e} ER_\varsigma^{SS} P_{\varsigma,s,w,t}^{SS} \tag{5.20}$$

Note that ρ_s denotes the probability of each scenario while π_w is the weight associated with each representative snapshot. These parameters appear in equations (5.13)—(5.20). Setting values for these parameters is not generally straightforward. For the sake of simplicity, all scenarios are assumed to be equally probable. The steps being followed to determine the value of each representative snapshot are described as follows. First, a large number of snapshots are clustered into a predefined number of groups, substantially lower than the original number of snapshots. The number of groups needs to ideally strike the right balance between accuracy and numerical feasibility. Each group contains a set of snapshots with similar characteristics. Then, a representative snapshot (for instance, the medoid) is selected in each group. This snapshot is used in the analysis by assigning a weight π_w proportional to the number of snapshots grouped together.

5.2.2 Constraints

5.2.2.1 *Kirchhoff's Current Law (Active Power Balances)*

The active power balance at each node is enforced by equation (5.21):

$$\begin{aligned}\sum_{g\epsilon\Omega^{DG}} \left(P_{g,i,s,w,t}^E + P_{g,i,s,w,t}^N\right) + \sum_{es\epsilon\Omega^{es}} \left(P_{es,i,s,w,t}^{dch} - P_{es,i,s,w,t}^{ch}\right) + P_{\varsigma,s,w,t}^{SS} + \sum_{in,k\epsilon i} P_{k,s,w,t} - \sum_{out,k\epsilon i} P_{k,s,w,t} + \delta_{i,s,w,t} \\ = \sum_{in,k\epsilon i} 0.5\varphi_{k,s,w,t} + \sum_{out,k\epsilon i} 0.5\varphi_{k,s,w,t} + D_{s,w,t}^i \; ; \; \forall\varsigma, \forall\varsigma\epsilon i.\end{aligned} \tag{5.21}$$

Equation (5.21) denotes that the sum of all incoming flows should be equal to the sum of all outgoing flows at each node. The losses in every feeder are considered as “virtual loads” which are equally distributed between the nodes connecting the feeder. Note that losses are a quadratic function of flows (not shown here). Hence, they are linearized using a first order approximation, as in [114]. Five linear partitions are used throughout the analysis in this chapter, which is in line with the findings in [94].

5.2.2.2 *Energy Storage Model Constraints*

For the sake of simplicity, a generic ESS is employed here. This is modelled by the set of constraints in (5.22)—(5.28). Equations (5.22) and (5.23) represent the bounds of power capacity of the ESS while being charged and discharged, respectively. Inequality (5.24) prevents simultaneous charging and discharging operation of the ESS in a given operational time w. The amount of stored energy in the ESS reservoir at a given operational time w as a function of the energy stored until $w-1$ is given by (5.25). The maximum and minimum levels of storages in the operational time w are also considered through inequality (5.26). Equation (5.27) shows the initial level of stored energy in the ESS as a function of its maximum reservoir capacity. In a multi-stage planning approach, Equation (5.28) ensures that the initial level of energy in the ESS at a given year is equal to the final level of energy in the ESS in the preceding year. Moreover, the reservoir level at the end of the planning horizon should be equal to the initial level, which is enforced by the second constraint in (5.28). Such a constraint guarantees that the optimal solution returned by the solution algorithm is not because of the initial reservoir level. Here, η_{es}^{dch} is assumed to be η_{es}^{ch}.

$$0 \le P_{es,i,s,w,t}^{ch} \le I_{es,i,s,w,t}^{ch} x_{es,i,t} P_{es,i}^{ch,max} \tag{5.22}$$

$$0 \le P_{es,i,s,w,t}^{dch} \le I_{es,i,s,w,t}^{ch} x_{es,i,t} P_{es,i}^{ch,max} \tag{5.23}$$

$$I_{es,i,s,w,t}^{ch} + I_{es,i,s,w,t}^{dch} \le 1 \tag{5.24}$$

$$E_{es,i,s,w,t} = E_{es,i,s,w-1,t} + \eta_{ch,es} P_{es,i,s,w,t}^{ch} - P_{es,i,s,w,t}^{dch} / \eta_{dch,es} \tag{5.25}$$

$$E_{es,i}^{min} x_{es,i,t} \le E_{es,i,s,w,t} \le x_{es,i,t} E_{es,i}^{max} \tag{5.26}$$

$$E_{es,i,s,w_0,T1} = \mu_{es} x_{es,i,T1} E_{es,i}^{max} \tag{5.27}$$

$$E_{es,i,s,w_1,t+1} = E_{es,i,s,W,t};\ \ E_{es,i,s,W,T} = E_{es,i,s,w_0,T1} \tag{5.28}$$

Notice that inequalities (5.22) and (5.23) involve products of charging/discharging indicator variables and investment variable. In order to overcome these nonlinearities, new continuous positive variables $z^{ch}_{es,i,s,w,t}$, and $z^{dch}_{es,i,s,w,t}$, which replace the bilinear products in each constraint, are introduced such that the set of linear constraints in (5.29) and (5.30) hold. For instance, the product $I^{dch}_{es,i,s,w,t}x_{es,i,t}$ is replaced by the positive variable $z^{dch}_{es,i,s,w,t}$. Then, the bilinear product is decoupled by introducing the set of constraints in (5.29) [115]. Similarly, the product $I^{ch}_{es,i,s,w,t}x_{es,i,t}$is decoupled by including the set of constraints in (5.30).

$$z^{dch}_{es,i,s,w,t} \le x^{max}_{es} I^{dch}_{es,i,s,w,t}\ ;\ z^{dch}_{es,i,s,w,t} \le x_{es,i,t}\ ; z^{dch}_{es,i,s,w,t} \ge x_{es,i,t} - \left(1 - I^{dch}_{es,i,s,w,t}\right)x^{max}_{es} \tag{5.29}$$

$$z^{ch}_{es,i,s,w,t} \le x^{max}_{es} I^{ch}_{es,i,s,w,t}\ ;\ z^{ch}_{es,i,s,w,t} \le x_{es,i,t}\ ; z^{ch}_{es,i,s,w,t} \ge x_{es,i,t} - \left(1 - I^{ch}_{es,i,s,w,t}\right)x^{max}_{es} \tag{5.30}$$

5.2.2.3 *Active Power Limits of DGs*

The active power limits of existing generators are given by (5.31). Inequality (5.32) represents the corresponding constraints in the case of new generators. Note that the binary variables multiply both bounds to make sure that the power generation variable is zero when the generator remains either unutilized or unselected for investment.

$$P^{E,min}_{g,i,s,w,t}u_{g,i,t} \le P^{E}_{g,i,s,w,t} \le P^{E,max}_{g,i,s,w,t}u_{g,i,t} \tag{5.31}$$

$$P^{N,min}_{g,i,s,w,t}x_{g,i,t} \le P^{N}_{g,i,s,w,t} \le P^{N,max}_{g,i,s,w,t}x_{g,i,t} \tag{5.32}$$

It should be noted that these constraints are applicable only for conventional DGs. In the case of variable generation sources (such as wind and solar PV), the upper bound $P^{max}_{g,i,s,w,t}$ should be set equal to the minimum of the actual production level at a given hour, which is dependent on the level of primary energy source (wind speed and solar radiation), and the rated (installed) capacity of the generating unit. The lower bound $P^{max}_{g,i,s,w,t}$ in this case is simply set to zero.

5.2.2.4 *Active Power Limits of Power Purchased*

$$P^{E,min}_{g,i,s,w,t}u_{g,i,t} \le P^{E}_{g,i,s,w,t} \le P^{E,max}_{g,i,s,w,t}u_{g,i,t} \tag{5.33}$$

For technical reasons, the power that can be purchased from the transmission grid could have minimum and maximum limits, which is enforced by (5.33). However, it is understood that setting such limits is difficult. These constraints are included here for the sake of completeness. In this chapter, these limits are set to 1.5 times the minimum and maximum levels of the total load in the system.

5.2.2.5 *Logical Constraints*

The set of logical constraints in (5.34) ensure that an investment decision already made cannot be reversed. In addition to the constraints described above, the direct current (DC) based network model and radiality related constraints presented in [114] are used here.

$$x_{k,t} \geq x_{k,t-1};\ \ x_{g,i,t} \geq x_{g,i,t-1};\ \ x_{es,i,t} \geq x_{es,i,t-1} \tag{5.34}$$

5.2.2.6 *Radiality Constraints*

There are two conditions that must be fulfilled in order a distribution network system (DNS) to be radial. First, the solution must have $N_i - N_{SS}$ circuits. Second, the final topology should be connected. Equation (5.35) represents the first necessary condition for maintaining the radial topology of a DNS.

$$\sum_{k \in \Omega^{ij}} OR(x_{k,t}, u_{k,t}) = N_i - N_{SS} \quad ;\forall t \tag{5.35}$$

Note that the above equation assumes that a line investment is possible in all corridors. Hence, in a given corridor, we can have either an existing branch or a new one, or both connected in parallel, depending on the economic benefits of the final setup (solution) brings about to the system. The radiality constraint in (5.35) then has to accommodate this condition. One way to do this is using the Boolean logic operation given as in (5.35). Unfortunately, this introduces nonlinearity. We show how this logic can be linearized using an additional auxiliary variable $z_{k,t}$ and the binary variables associated to existing and new branches i.e. $u_{k,t}$ and $x_{k,t}$, respectively. Given$z_{k,t} := OR(x_{k,t}\ ,\ u_{k,t})$, this Boolean operation can be expressed using the following set of linear constraints:

$$z_{k,t} \leq x_{k,t} + u_{k,t};\ z_{k,t} \geq x_{k,t};\ z_{k,t} \geq u_{k,t}; 0 \leq z_{k,t} \leq 1 \quad ;\forall t \tag{5.36}$$

Then, the radiality constraints in (5.35) can be reformulated using the $z_{k,t}$ variables as:

$$\sum_{k\in\Omega^{ij}} z_{k,t} = N_i - N_{SS} \qquad ;\forall t \tag{5.37}$$

When all loads in the DNS are only powered up by power imported through a number of substations, the final solution obtained automatically satisfies the two aforementioned conditions; hence, no additional constraints are required i.e. (5.36) along with (5.37) are sufficient to guarantee radiality. However, it should be noted that, in the presence of DGs and reactive power sources, these constraints alone may not ensure the radiality of the distribution network, as pointed out in [106] and further discussed in [97].

5.3 Case Studies

5.3.1 System Data and Assumptions

The standard IEEE 119-bus distribution network, shown in Figure 5.1, is used here for carrying out the required analysis mentioned earlier. The system has a rated voltage of 11.0 kV, and a total demand of 22709.72 kW and 17041.068 kVAr. Network data and other related information about this test system can be found in [116] and the data are in the Appendix E. According to [117], the active power losses in this system is 1298.09 kW, and the minimum node voltage of the system is 0.8783 p.u., which occurs at bus 116.

Other data and assumptions made throughout this chapter are as follows. The planning horizon is 3 years long, which is divided into yearly decision stages, and a fixed interest rate of 7% is used. The expected lifetime of the generic ESS is assumed to be 15 years while that of DGs and feeders is 25 years. Two investment options with installed capacities of 0.5 and 1.0 MVA are considered for each wind and solar PV type DG units. The installation cost and emission related data of these DG units in [118] are used here. For the sake of simplicity, all maintenance cost of each DG is assumed to be 2% of the corresponding investment cost while that of any feeder is 450 €/km/year. The investment cost of each feeder is 38700 €/km. The current flow limits of each feeder are considered to be as follows. The current limit in each of the feeders {(1,2); (2,4); (1,66); (66,67)} is 1200 A while the set of feeders {(4,5); (5,6); (6,7); (4,29); (29,30); (30,31); (67,68); (67,81); (81,82); (1,105); (105,106); (106,107)} have each 800 A capacity limit. The current flow limits of the remaining feeders are considered to be 400 A. Moreover, it is assumed that all feeders can be switched on/off, if deemed necessary. In addition, it is assumed that the availability of wind and solar power sources is uniform throughout the system nodes. The operational variability and uncertainty introduced by wind and solar PV type DGs, demand and electricity price are accounted for via the clustering method proposed in [103].

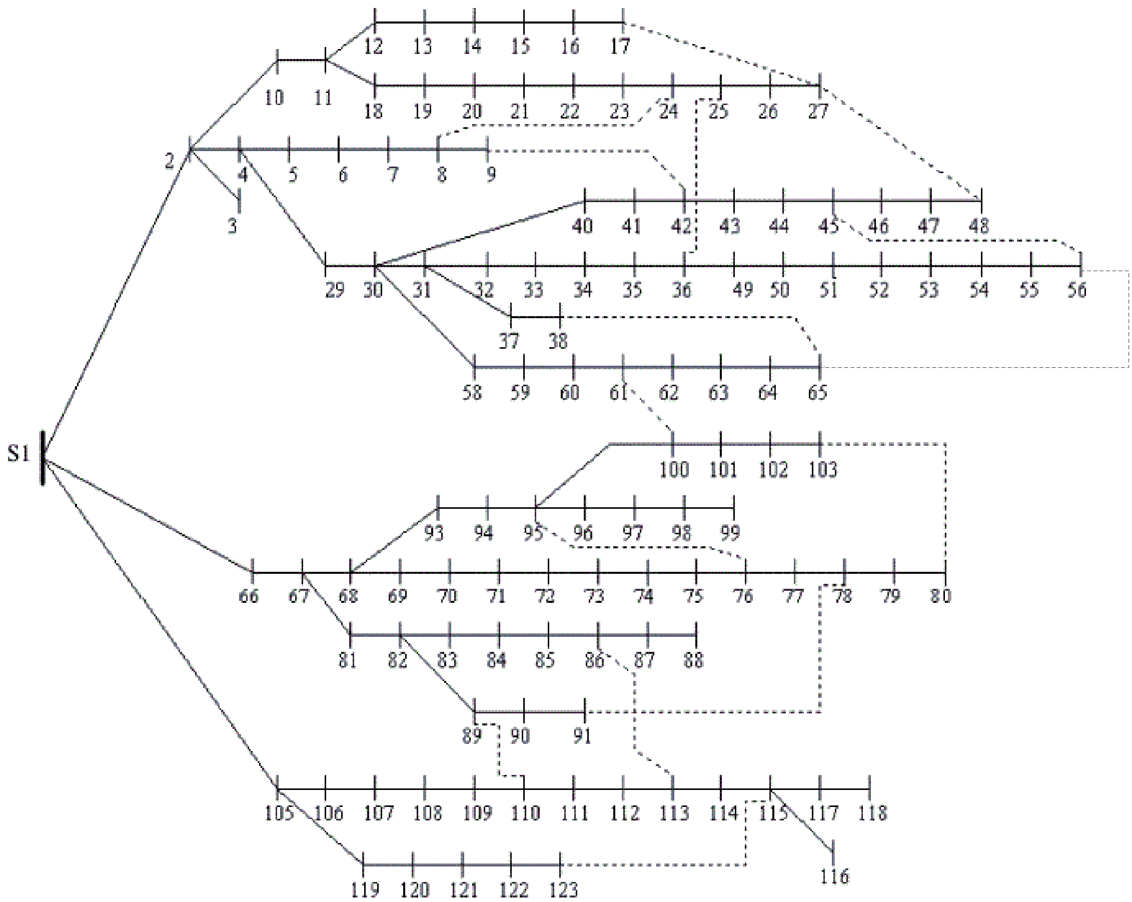

Figure 5.1 - Single line diagram of the test system in base case.

The maximum allowable bus voltage deviation in the system is set to 5%, and node 1 is considered as a reference with a voltage magnitude of 1.0. Taking the base case demand as a reference, annual demand growths of 0%, 5% and 10% are also considered in all simulations. Emission prices in the first, second and third time stages are set to 25, 45 and 60 €/tCO_2e, respectively, and the emission rate of power purchased from upstream is arbitrarily set to 0.4 tCO2e/MWh. The cost of unserved energy is 2000 €/MWh. A power factor of 0.9 is considered throughout the system, and is assumed to be the same throughout. The base power is set to 1 MVA. An ESS with a 1 MW power and a 5 MWh reservoir capacity is considered for investment.

5.3.2 Results and Discussion

Given the aforementioned data and assumptions, the developed optimization problem has been solved considering six different cases (designated as A though F). Case A represents the base case topology where no investments are made. This case can be alternatively understood as the "do-nothing" scenario. Case B is similar to the base case (i.e. with no investments) but considers the network reconfiguration problem. Case C corresponds to a scenario where only DG investments are made on the base case topology (i.e. without reconfiguration).

Case D is similar to Case C except that the former simultaneously considers optimal reconfiguration and DG investments. The last two cases (Cases E and F) correspond to scenarios where optimal investment planning in DGs is coordinated with that of ESSs. The difference is that Case E uses the base case topology (i.e. without reconfiguration) while Case F optimizes the network via reconfiguration. Table 5.1 clearly summarizes the different cases.

The values of the most relevant variables are analyzed (as depicted in Table 5.2) over the three years planning horizon. The results in Table 5.2 reveal the significant differences in overall NPV cost in the system, share of the combined energy supplied by RES and ESS, cost of total network losses and unserved power among the aforementioned cases. The results are also compared with the base case system where no investments are made and the network topology is held the same (i.e. the "do-nothing" scenario). Carrying out an optimal reconfiguration of the network alone, as in Case B, results in about 5.44 % reduction in the cost of losses, and a 15.9% reduction in the NPV overall system cost compared with that of Case A. In addition, network reconfiguration reduces a total of 1.18 p.u. average load curtailment in the third year to 0.57 p.u. in Case B that would otherwise occur at nodes 52, 53, 54, 55, 56 and 116 due to a number of factors such as technical constraints and high demand level.

Another more interesting observation from Table 5.2 is that Cases C and D lead to (approximately) 50% reduction in the overall system cost, and a 75% reduction in the amount of imported energy. Wind and solar power sources are complementary by nature. This natural phenomenon seems to be exploited when DG investments are not accompanied by investments in ESSs (i.e. Cases C and D). This is because, according to the DG investment solution in Table 5.2, the operational variability in the system seems to be handled by investing an appreciable amount in both complementary power sources (wind and solar). The level of demand covered by RESs in both cases amounts to nearly 75%. Moreover, as a result of investing in DGs, losses in the system are slashed down by about 82%. Generally, the corresponding reductions in Case D are slightly higher than those in Case C. This is due to the network reconfiguration which has been considered in Case D.

Table 5.1 - Distinguishing the different cases

		Investment	
Cases	Reconfiguration	DGs	ESSs
A	No	No	No
B	Yes	No	No
C	No	Yes	No
D	Yes	Yes	No
E	No	Yes	Yes
F	Yes	Yes	Yes

Table 5.2 - Results of relevant variables for different cases

Optimization variables		Cases*					
		A	B	C	D	E	F
Cost terms (k€)	Investment	0	0	92478	88489	100754	99368
	Maintenance	189	201	52604	50355	57295	56513
	Energy + Emission	424715	433188	121820	123232	48424	48973
	PNS	94441	2095	926	0	0	0
	Losses	12515	11834	2204	2161	1242	1098
Total cost (k€)		531860	447318	270033	264236	207715	205952
Energy share (%)	Wind	-	-	64	64	89	90
	Solar	-	-	10	11	0	0
	Imported	100	100	26	25	11	10
Installed size (p.u.)	Wind	-	-	36	33	40	40
	Solar	-	-	10	11	0	0
	ESS	-	-	-	-	18	17

*A: Base case; B: Reconfiguration only; C: DG investment on base case topology; D: DG investment plus reconfiguration; E: DG and ESS investment on base case topology; F: DG and ESS investment plus reconfiguration.

The results corresponding to Cases E and F show that the total cost and cost of losses are dramatically reduced by more than 60% and 90%, respectively. These figures are in line with the results reported in a similar work [113]. The reductions in active losses are 88.56% and 89.66%, respectively. Moreover, the amount of imported energy is 11% and 10% of the total energy demand in Cases E and F, respectively. All this reveals the substantial benefits of coordinating investments in DG with ESSs. Generally, ESSs significantly improve system flexibility, enabling large-scale accommodation of RES energy. Interestingly, the total amount of installed DGs (40 MVA) is lower in Cases E and F (with ESSs) than in Cases C and D (without ESSs). Even if this is the case, in the absence of a storage medium (as in Cases C and D), there may be frequent RES power spillages when the demand is lower than the total generated power. However, the installation of ESSs leads to an efficient utilization of RES power. This is evident from the amount of energy consumption covered by the combined energy from RESs and ESSs in Cases E and F is about 90%. Normally, a network switching capability also improves system flexibility, leading to a high level RES penetration. In this particular study, the effect of network switching on the level of RES power absorbed by the system is not significant as one can observe in Table 5.2. This may however be case-dependent. A more frequent switching capability could, for instance, have a significant impact.

The optimal location and size of installed DGs and ESSs corresponding to Cases C through F is summarized in Table 5.3. This is also conveniently plotted in Figure 5.2. As the formulated problem is based on a multi-year decision framework, the aggregate investment decisions made in each stage along the planning horizon is presented in Table 5.4.

Table 5.3 - Optimal sizes and locations of DGs and ESSs for different cases

	Wind *				Solar *, §		ESS *, †	
Nodes	Case C	Case D	Case E	Case F	Case C	Case D	Case E	Case F
14	1	1	1	1	0	0	0	0
19	1	0	1	0	0	0	0	0
20	1	0	2	1	0	0	1	1
21	0	1	0	1	0	0	0	0
24	0	1	1	1	0	0	0	0
25	1	0	0	0	0	0	0	0
29	0	0	0	0	0	0	2	1
32	1	1	1	2	0	0	0	0
33	1	1	1	1	0	0	1	1
34	0	0	1	0	0	0	0	0
35	1	0	0	1	1	1	0	0
37	1	1	1	1	0	0	0	0
38	1	1	1	1	0	0	0	1
42	0	1	2	1	0	0	0	0
43	1	0	0	1	0	0	1	1
44	1	1	2	1	1	1	0	0
52	2	2	2	2	1	2	2	1
53	1	1	1	1	0	0	0	0
56	3	1	1	1	0	0	1	1
61	1	1	1	1	0	0	1	1
66	0	0	0	0	0	0	1	1
69	1	1	1	1	0	0	0	0
73	1	1	1	1	1	1	1	1
74	1	1	1	1	0	0	0	0
77	1	1	1	2	1	1	1	1
79	1	1	1	1	0	0	0	0
82	0	0	1	1	0	0	0	0
83	1	1	1	1	0	0	1	1
84	0	0	0	0	1	1	0	0
85	1	1	1	1	0	0	0	0
89	1	1	1	1	0	0	1	1
96	1	1	1	1	0	0	0	0
100	0	1	0	1	1	1	1	1
101	1	1	2	1	0	0	0	0
106	1	1	1	1	0	0	0	0
107	0	0	0	0	0	0	1	1
108	1	1	1	1	0	0	0	0
109	0	0	0	1	0	0	0	0
112	1	1	1	1	1	1	1	1
113	0	0	0	0	0	0	0	0
114	1	1	1	1	0	1	0	0
115	0	0	0	0	1	0	0	0
116	2	2	3	2	1	1	1	1
117	1	1	1	1	0	0	0	0
119	0	1	1	1	0	0	0	0
121	1	0	0	0	0	0	0	0
Total (p.u.)	34	31	38	38	10	11	18	17

*A: Base case; B: Reconfiguration only; C: DG investment on base case topology; D: DG investment plus reconfiguration; E: DG and ESS investment on base case topology; F: DG and ESS investment plus reconfiguration. § No solar type investment decisions in cases E and F; † ESS investments are not considered in the cases other than E and F.

Table 5.4 - Total DGs and ESSs for different cases

	Case C		Case D		Case E			Case E		
Year	Wind	Solar	Wind	Solar	Wind	Solar	ESS	Wind	Solar	ESS
1	31	9	29	7	36	0	17	36	0	15
2	2	0	2	2	2	0	0	1	0	2
3	3	1	2	2	2	0	1	3	0	0
Total	**36**	**10**	**33**	**11**	**40**	**0**	**18**	**40**	**0**	**17**

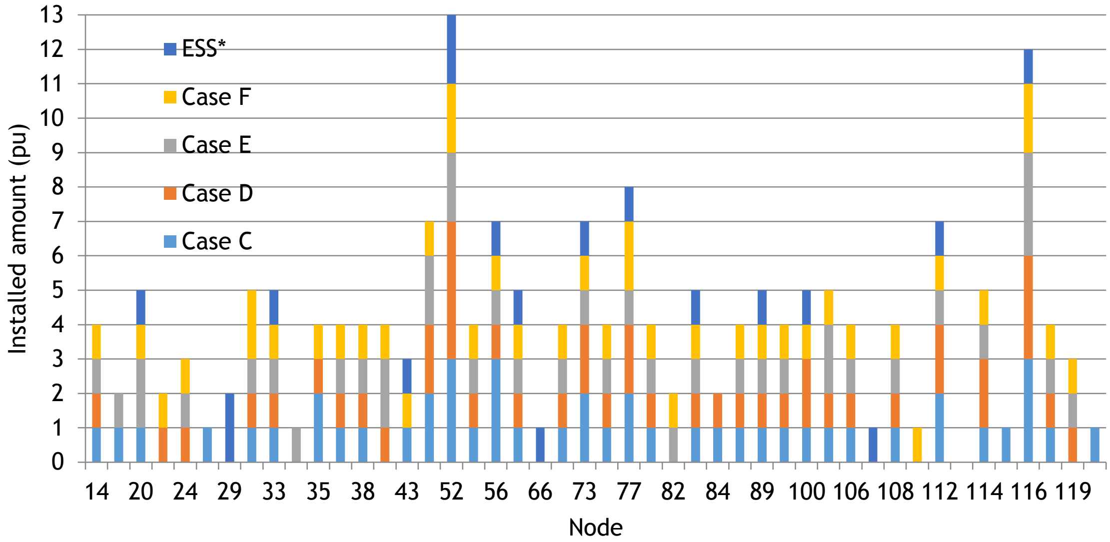

Figure 5.2 - Optimal placement and size of DGs and ESSs for different cases (* only in cases E and F).

As it can be seen in this table, majority of the investments are made in the first stage. This may be because of two reasons. The first one could be due to lack of appropriate financial and logistical constraints in the optimization model. The second and most plausible reason could be due to higher NPV factor of the first stage than any subsequent one. Note that the higher this factor is, the more relevant the associated costs in the objective function are, hence, leading to more investments in DGs and ESSs.

The average voltage profiles at each node and for each case are depicted in Figure 5.3. A cumulative distribution of the average voltage values, corresponding to different cases, is also conveniently represented in Figure 5.4. In both figures, it is interesting to see the substantial contributions of DG and ESS installations to voltage profile improvement. As shown in Figure 5.3, the coordinated integration of DGs and ESSs along with reconfiguration (i.e. Case F), especially leads to the best voltage profile which is almost flat throughout the system.

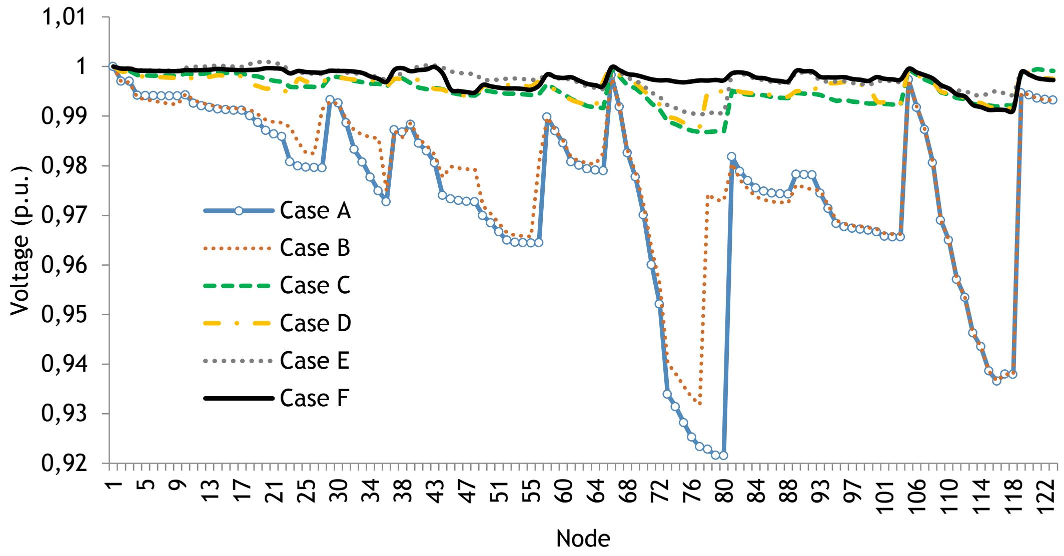

Figure 5.3 - Average voltage profiles in the system for different cases.

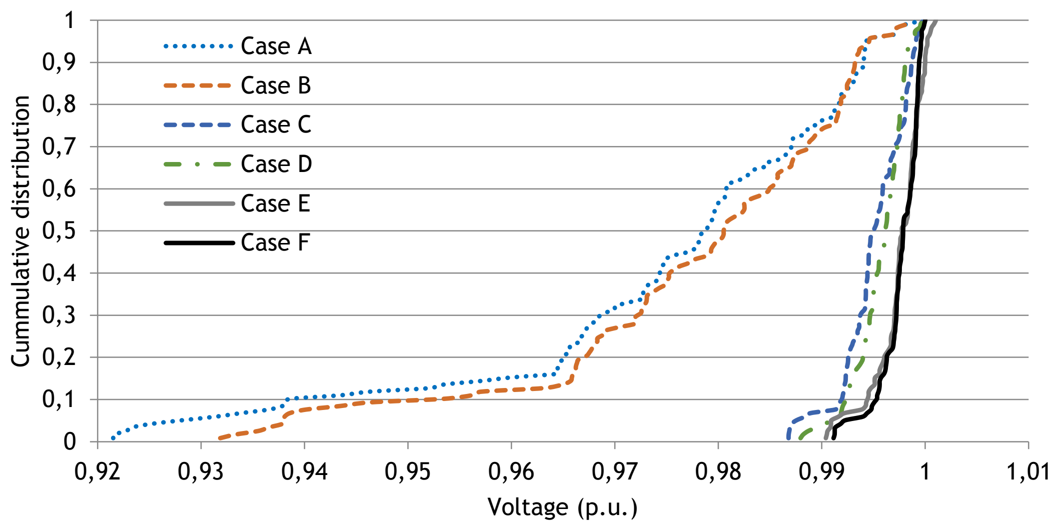

Figure 5.4 - Cumulative distribution function of average voltages in the system for different cases.

Table 5.5 compares the optimal network topologies (i.e. the switches to be opened) corresponding to the different cases with that of the base case topology. The benefit of joint DG and ESS investments along with network reconfiguration in terms of losses reduction (over 89% on average) can be seen in Figure 5.5. The spikes observed in cases D and F are because of the variability in the RES power injected into the system.

Table 5.5 - Optimal reconfiguration outcome for different cases (List of switches to be opened)

Year	Case A	Case B	Case D	Case F
1	(8,24); (9,42); (17,27); (25,36); (38,65); (48,27); (56,45); (61,100); (65,56); (76,95); (91,78); (103,80); (113,86); (110,89); (115,123)	(23,24); (26,27); (35,36); (41,42); (44,45); (48,27); (54,56); (61,100); (64,65); (76,95); (77,78); (103,80); (110,89); (113,86); (115,123)	(17,27); (23,24); (35,36); (41,42); (48,27); (54,56); (56,45); (61,100); (64,65); (76,95); (77,78); (103,80); (110,89); (113,86); (115,123)	(9,42); (17,27); (23,24); (25,36); (38,65); (48,27); (54,56); (56,45); (61,100); (76,95); (91,78); (103,80); (110,89); (113,86); (115,123)
2	(8,24); (9,42); (17,27); (25,36); (38,65); (48,27); (56,45); (61,100); (65,56); (76,95); (91,78); (103,80); (113,86); (110,89); (115,123)	(9,42); (23,24); (26,27); (35,36); (44,45); (48,27); (54,56); (61,100); (64,65); (76,95); (77,78); (103,80); (110,89); (113,86); (115,123)	(17,27); (23,24); (35,36); (38,65); (41,42); (48,27); (54,56); (56,45); (76,95); (77,78); (95,100); (103,80); (110,89); (113,86); (115,123)	(9,42); (17,27); (23,24); (25,36); (44,45); (48,27); (54,56); (61,100); (64,65); (76,95); (91,78); (103,80); (110,89); (113,86); (115,123)
3	(8,24); (9,42); (17,27); (25,36); (38,65); (48,27); (56,45); (61,100); (65,56); (76,95); (91,78); (103,80); (113,86); (110,89); (115,123)	(9,42); (23,24); (26,27); (35,36); (44,45); (48,27); (54,56); (61,100); (64,65); (76,95); (77,78); (103,80); (110,89); (113,86); (115,123)	(17,27); (23,24); (35,36); (41,42); (48,27); (54,56); (56,45); (64,65); (76,95); (77,78); (95,100); (103,80); (110,89); (113,86); (115,123)	(9,42); (17,27); (23,24); (25,36); (38,65); (44,45); (48,27); (54,56); (61,100); (76,95); (91,78); (103,80); (110,89); (113,86); (115,123)

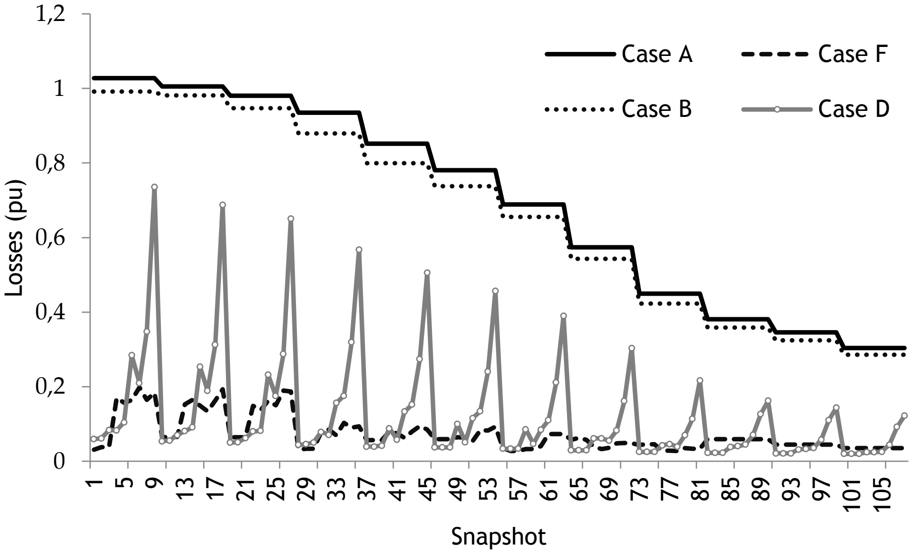

Figure 5.5 - Total system losses profile.

As stated earlier, stability concern is one of the major issues that are associated with high level RES integration in distribution systems. The controllability of voltage and frequency can be dramatically undermined or even sometimes become out of reach. Because of these reasons, the penetration level of DGs (including RESs) in many distribution systems is limited to a value often less than about 25%. However, this contradicts with the ambition to meet other objectives such as reducing the carbon footprint of power production and ensuring energy security among others. The integration of RESs is likely to be supported with enabling technologies that have the capability to effectively address the integration challenges and consequently increase the penetration level. The results in this chapter largely demonstrate the fact that large-scale integration of variable energy sources is possible when such energy sources are optimally deployed with ESSs and a mechanism that improve the flexibility of the network is put in place.

5.4 Chapter Conclusions

There is a wide consensus about integrating more renewable energy sources—RESs to solve a multitude of global concerns such as meeting an increasing demand for electricity, reducing energy security and heavy dependence on fossil fuels for energy production, and reducing the overall carbon footprint of power production. Framed in this context, the coordination of RES integration with ESSs, along with the network's switching capability and/or reinforcement, is expected to significantly improve system flexibility, thereby increasing the capability of the system in accommodating large-scale RES power. Hence, in this chapter a novel mechanism to quantify the impacts of network switching and/or reinforcement as well as deployment of ESSs on the level of renewable power integrated in the system was presented. To carry out this analysis, a dynamic and multi-objective stochastic mixed integer linear programming model was developed, which jointly takes the optimal deployment of RES-based DGs and ESSs into account in coordination with distribution network reinforcement and/or reconfiguration. The IEEE 119-bus test system was used as a case study. The results clearly show the capability of ESS deployment in dramatically increasing the level of renewable DGs integrated in the system. Although case-dependent, the impact of network reconfiguration on RES power integration is not significant.

Chapter 6

New Multi-stage and Stochastic Mathematical Model for Maximizing RES Hosting Capacity

This chapter presents a new coordinated multi-stage and stochastic mathematical model, developed to support the decision-making process of planning distribution network systems (DNSs) for integrating large-scale "clean" energy sources. The model, formulated from the system operator's viewpoint, determines the optimal sizing, timing and placement of distributed energy technologies (particularly, renewables) in coordination with energy storage systems and reactive power sources. The ultimate goal of this optimization work is to maximize the size of renewable power absorbed by the system while maintaining the required/standard levels of power quality and system stability at a minimum possible cost. One of the points that distinguish this chapter from the predecessors is the use of a linearized AC network model, which captures the inherent characteristics of electric networks, and balances well accuracy with computational burden.

6.1 Introduction

Nowadays, the issue of integrating distributed generations (DGs) (renewable DGs, in particular) is globally gaining momentum because of several techno-economic and environmental factors. Since recent years, the size of DGs integrated into distribution systems has been increasing. This trend is more likely to continue in the years to come because it is now widely accepted that DGs bring wide-range benefits to the system. However, given the current set-up of distribution networks (which are generally passive), large-scale DG integration is not technically possible because this brings about tremendous challenges to the system operation, especially in undermining the power system quality and stability.

Such challenges/limitations are expected to be alleviated when distribution networks undergo the anticipated evolutionary process from passive to active networks or smart grids. This transition is expected to result in a system that is adequately equipped with appropriate technologies, state-of-the-art solutions and a new operational philosophy that is totally different from the current 'fit and forget' approach. This is expected to offer sufficient flexibility and control mechanism in the system. Nevertheless, the process is not straightforward as it demands exceptionally huge investments in smart-grid technologies and concepts to fully automate the system, and this should be accompanied by a new operational philosophy. Therefore, the whole transformation process (i.e., the transformation of current distribution systems to full-scale smart-grids) might be very slow, and its realization might take several decades.

However, given the techno-economic factors and global concerns about environmental issues, the integration of renewable energy sources (RESs) cannot be postponed. It is likely that the integration of DGs in distribution systems will go ahead along with smart-grid enabling technologies that have the capability to alleviate the negative consequences of large-scale integration of DGs. In other words, in order to facilitate (speed up) the much-needed transformation of conventional (passive) DNSs and support large-scale RES integration, different smart-grid enabling technologies such as reactive power sources, advanced switching and storage devices are expected to be massively deployed in the near term.

To this end, developing strategies, methods and tools to maximize the penetration level of DGs (particularly, RESs) has become very crucial to guide such a complex decision-making process. In this respect, this chapter focuses on the development of multi-stage mathematical models to determine the optimal sizing, timing and placement of energy storage systems and reactive power sources as well as that of RESs in distribution networks. The ultimate goal of this optimization work is to maximize the RES power absorbed by the system at a minimum cost while maintaining the power quality and stability at the required/standard levels.

The problem is formulated from the system perspective (i.e. in centralized planning framework). In a deregulated environment and from the smart-grid context where the current regulatory and technical challenges are expected to be fully resolved, planning will most likely involve distributed decision-making processes. One may rightfully argue that the investment decisions obtained from a coordinated planning model may not be implemented in reality. This is because distributed decisions often lead to sub-optimal solutions, which may be different from the ones obtained by the centralized planning model. However, this does not mean that the outcomes of the coordinated planning model cannot be used. For instance, these outcomes can be regarded as the best investment targets. Given these targets, distributed decisions (solutions) can be systematically made to approach one or more of these targets (for example, via incentive or market-based mechanisms).

From another perspective, in the absence of "attractive" market environment (seen from the private investors), distribution network systems may not see significant breakthrough when it comes to investments in DGs and energy storage systems (ESSs). In this case, DSOs may, instead, be given additional roles and responsibilities that include investing in DGs and ESSs in coordination with network investments. DSOs may also oversee investments in DGs and ESSs. In addition, DSOs may also be required to manage these assets in a coordinated manner to keep the system integrity, stability and power quality at the required/standard levels. Another issue which explains the versatility of the coordinated approach is related to the realization of smart-grids. Even if there is a general consensus on the smartification of power systems (distribution networks, in particular), and there are signs that some systems are evolving into smart-grids, the whole process is going to probably take very long time. Based on the aforementioned reasons, a centralized (coordinated) approach of the planning problem can provide vital solutions.

Reducing fossil fuel dependence and mitigating climate change have led to an increased pressure to change the current generation paradigm. The compounded effect of increasing demand for electricity, environmental and climate change concerns is triggering a policy shift all over the world, especially when it comes to energy production. Integration of DG, particularly, RESs, in electric distribution network systems is gaining momentum. In particular, the recent developments in a climate change conference held in Paris (COP21) are expected to accelerate renewable integration. It is highly expected that large-scale DG integration will be one of the solutions capable of mitigating the aforementioned problems and overcoming the challenges. Because of this, Governments of various nations have introduced targets to achieve large-scale integration of DGs. In particular, in the European Union, which strongly advocates the importance of integrating renewables, RESs are expected to cover 20% and 50% of the overall energy consumption by 2020 and 2050, respectively.

DGs offer a more environmentally friendly option through great opportunities with renewable-enabling technologies such as wind, photovoltaic, biomass, etc. RESs are abundant in nature, which, under a favorable RES integration policy and incentive mechanism, makes it attractive for the large-scale power generation sector. Nevertheless, there is no rule or partial rule on the DG unit's connection; typically, these are traditionally connected at the end of radial feeder systems or nodes with greater load on the distribution system. This is realized often with several impeding restrictions put in place to alleviate the negative consequences of integrating DGs in the system.

The optimal and dynamic planning of the DG placement and sizing is becoming extremely important for energy producers, consumers and network operators in technical and economic terms. There are many studies in the literature on this topic, yet most of them only consider the optimal location of a single DG unit or do not consider simultaneously positioning and sizing RES units, mainly due to their high dispatch unpredictability. The increase in DG penetration increases the uncertainty and the fluctuations of power production. If the placement and proper sizing is not taken into account, the benefits of DG integration can be lost, leading to inefficient operation and increasing the electricity cost and energy losses. Another major concern with the wide DG penetration is system reliability. The penetration of distributed systems can result in the degradation of power quality, particularly in cases of slightly meshed networks [119] or microgrids. In this paradigm, the use of ESS has been seen as one of the viable options to mitigate the aforementioned concerns.

The DG allocation and sizing subject have attracted special interest from researchers in recent years. An excellent review of previous works related to this subject area, published prior to the year 2013, is presented in [120]. In [120] and [121], an analysis of several techniques used on the DG impact assessment in the electrical system is presented. Most of these techniques analyze the distribution system to determine rules that can be used for DG integration [122]-[126]. Important issues related to the connection of DG units are the network topology, DG capacity and suitable location; because, each bus in the system has an optimal level of DG integration. If the value surpasses this level, system losses can increase [127], [128].

Recently, several methods have been proposed for planning and operation or in some cases for both location and sizing of DGs in the distribution system. In general, these methods can be classified as heuristic [129]-[144], numerical [145]-[152] and analytical [153], [154] based methods. Heuristic based methods apply advanced artificial intelligence algorithms, such as genetic algorithms (GA) [129]-[132], particle swarm optimization (PSO) [133]-[137], harmony search (HS) [138], [139] and big bang crunch (BBC) [140]-[142].

Numerical methods are algorithms that seek numerical results for different problems in particular to the problem in question. Some of the most recently works use nonlinear mixed integer programming (MINLP) [145]-[147], mixed integer linear programming (MILP) [148], [149], quadratic programming (QP) [150] and AC optimal power flow (OPF)-based [151]. The exhaustive search methods seek the optimal DG location for a given DG size under different load models. Therefore, these methods fail to represent accurately the behavior of the DG optimization problem involving two discrete variables, both for optimum DG size and optimal DG location. In [153], authors present a technique with a probabilistic basis for determining the capacity and optimal placement of wind DG units to minimize energy loss in the distribution system. A sensitivity analysis is presented in [154] for DG placement and sizing in the network.

Despite many studies in the literature on areas related to DG placement and sizing problem, most of them only consider the optimal location of a single DG unit, mostly of conventional DGs. The simultaneous consideration of placement, timing and sizing of DG units (especially RESs), along with the placement, timing and sizing of smart-grid enabling technologies, seems to be far from being addressed in the literature. The increase in RES-based DG penetration increases the uncertainty and the fluctuations of the system production. If the placement and proper sizing is not taken into account, the benefits of DG integration may not be exploited; instead, this may result in the degradation of system efficiency, increased cost of electricity and energy losses. Another major concern with the wide-range DG penetration is system reliability. However, the simultaneous investment planning of DGs, ESSs and reactive power sources is expected to significantly alleviate these challenges and increase the penetration level of RES-based DGs.

A new multi-stage and stochastic mathematical model is developed in this chapter to support the decision-making process of planning distribution network systems (DNSs) for integrating large-scale “clean” energy sources. The proposed model, formulated from the system operator’s viewpoint, determines the optimal sizing, timing and placement of distributed energy technologies (particularly, renewables) in coordination with energy storage systems and reactive power sources. The ultimate goal is to maximize the size of renewable power absorbed by the system while maintaining the required/standard levels of power quality and system stability at a minimum possible cost. From the methodological perspective, the entire problem is formulated as a mixed integer linear programming optimization, allowing one to obtain an exact solution within a finite simulation time. Moreover, it employs a linearized AC network model which captures the inherent characteristics of electric networks, and balances well accuracy with computational burden.

This chapter is organized as follows: Section 6.2 presents a brief description of the uncertainty and variability pertaining to variable energy sources and electricity demand, and how these issues are handled in the planning process. The mathematical formulation and detailed description of the proposed model are presented in section 6.3. Subsequently, in section 6.4, the results are presented and discussed. Finally, relevant conclusions are drawn in Section 6.5.

6.2 Uncertainty and Variability Management

There are various sources of uncertainty and variability in a distribution systems planning problem, particularly with intermittent renewable sources. These are related to the variability in time and the randomness of operational situations [105]. In addition, there are other uncertainties mostly related to the long-term electricity, carbon and fuel prices, rules, regulations and policies, etc. To account for uncertainty in demand, two demand scenarios are formed by assuming a ±5% prediction error margin from a long real-life demand profile (which is 8760 long). This gives a total of three demand profile scenarios, which are kept the same throughout the planning horizon. Due to the lack of sufficient historical data, first, synthetic hourly wind speed and solar radiation series (20 for each) are generated using the methods in [119] and [120], respectively considering the autocorrelations and diurnal patterns of each parameter. Then, the average wind speed and solar radiation profiles are determined from the generated series. The power outputs corresponding to each wind speed and solar radiation are then determined by plugging in these values in the respective power curves given by equations (6.1) and (6.2). Note that these power output samples (snapshots) cannot be used directly in the planning process because the resulting wind power output profiles may not respect the natural correlations that exist between them and the average electricity demand profile. These samples should be readjusted to reflect the temporal correlations that naturally exist among demand, solar radiation and wind speed series. To this end, the correlation between wind and solar sources is considered to be -0.3 while that of wind and demand is 0.28, which is in line with the results in [155]. A correlation of 0.5 is assumed between solar and demand, according to [156].

Given this desired correlation matrix, the wind and the solar power output profiles can be transformed into new ones, respecting the correlation among them. Such adjustments in the correlation of data series are performed using Cholesky factorization, a method used for generating correlated random variables. The method works as follows. Given a desired correlation matrix R, and uncorrelated data D, a new data Z whose correlation matrix is R can be generated by simply multiplying the Cholesky decomposition of R by D. Then, the hourly wind and solar power output are determined by plugging in these readjusted series into their corresponding power curves given by equations (6.1) and (6.2).

$$P_{wnd,h} = \begin{matrix} 0 & ; 0 \leq v_h \leq v_{ci} \\ P_r(A + Bv_h^3) & ; v_{ci} \leq v_h \leq v_r \\ P_r & ; v_r \leq v_h \leq v_{co} \\ 0 & ; v_h \leq v_{co} \end{matrix} \tag{6.1}$$

In the above equation, A and B are parameters represented by the expressions in [157] and [158]. Similarly, the hourly solar power output $P_{sol,h}$ is determined by plugging in the hourly solar radiation levels in the solar power output expression given in (6.2) [159].

$$P_{sol,h} = \begin{cases} \dfrac{P_r R_h^2}{R_{std} * R_c} & ; 0 \leq R_h \leq R_c \\ \dfrac{P_r R_h}{R_{std}} & ; R_c \leq R_h \leq R_{std} \\ P_r & ; R_h \geq R_{std} \end{cases} \tag{6.2}$$

In the present work, uncertainty in wind speed and solar radiation is assumed to lead to a ±15% deviation on average from the corresponding average power output profiles. This approximately translates to ±5% forecasting error in wind speed or solar radiation. Note that such error or higher is induced even by the most advanced forecasting tools available today. Based on the assumptions, two hourly profiles of wind power output are generated by considering the ±15% margin (one above the average and one below the average profile). In total, this leads to 3 wind power output profiles (including the average profile). These are defined as wind scenarios. Similarly, to account for the uncertainty in solar power outputs, two profiles are generated for each by considering a ±15% uncertainty margin. The two generated solar power output profiles along with the average profile form the set of solar scenarios. An illustration of uncertainty characterization of wind and solar power outputs was shown in Fig. 4.4.

Note that each of these scenarios has 8760 snapshots of demand, wind and solar power outputs. These individual scenarios are combined to form a set of 27 scenarios (3x3x3), which are used in the analysis. These scenarios are assumed to be equally probable; hence, the probability of realization of each scenario ρ_s is given by $1/27$.

To ensure problem tractability, the multi-dimensional input data (27x8760) is clustered into 27x200 groups via a standard clustering technique (k-means algorithm [160], which has been applied in investment planning problems as in [161]). Here, each cluster represents a group of similar operational situations. A representative snapshot, the medoid in this case, is then selected from each cluster. A weight is assigned to each representative snapshot, which is proportional to the number of operational situations in its group. Note that while clustering such a large number of operational situations in this manner is critically important to guarantee problem tractability, the chronological orders (and by implication the autocorrelations) of the considered data (time series) are not unfortunately preserved in the reduced number of operational situations. In other words, such information is lost during the clustering process. In the context of medium- to long-term planning problems, the impact of such information loss on the planning outcome may not be significant. However, if this is a concern, the chronological information can be somehow recovered by methods as in [162] and [163].

6.3 Mathematical Model

6.3.1 Brief Description of the Problem

As mentioned earlier, this chapter develops an integrated optimization model that simultaneously finds the optimal locations and sizes of installed DG power (particularly, focusing on wind and solar), energy storage systems and reactive power sources such as capacitor banks. The optimal deployment of the aforementioned enabling technologies should inherently meet the goal of maximizing the renewable power integrated/absorbed into the system. The entire model is formulated as a stochastic mixed integer linear programming (SMILP) optimization. In addition, instead of the customary direct current (DC) network models, a linearized AC model is used here to better capture the inherent characteristics of the network system. An ideal representation of the network system would be to use the full AC network model. However, embedding this model in planning problems is computationally unaffordable. Because of their appealing computational performances, DC based optimization models are commonly used in distribution systems planning problems. However, the DC network model does not consider reactive power flows, which can have significant impact on planning solutions, such as investment decisions related to capacitor banks. In addition, voltage magnitudes are often considered to be the same throughout the system. Voltage angles are also sometimes neglected in DC models. All these simplifying assumptions may result in sub-optimal solutions (often underinvestment) when embedded in planning models. The linearized AC model on the contrary acknowledges the presence of both active and reactive power flows, voltage magnitude and angle differences among nodes in the system.

The model captures the physical characteristics of the network system in a better way when compared to DC network models, and very close to the ideal AC network model. Computationally speaking, the linearized AC model is more expensive than the DC network model because it involves a more detailed network representation than the DC model. However, embedding the linearized AC model in planning problems yields far better solutions than when using the DC one. Hence, the linearized AC model can be generally regarded as a bridge between the DC and the AC network models. Planning models based on this linearized AC model are tractable enough, and the results are accurate enough.

The schematic representation in Figure 3.2 illustrates the multi-stage and multi-scenario modeling framework and the expansion solution structure (i.e. X_t's, where X_t represents the solution vectors of several investment variables). At each stage of the planning horizon, we obtain a single investment solution which is good enough for all scenarios [89], [92]. Note that while operational variables depend on each scenario and snapshot, the investment decision variables only depend on the time stage index. This means that the investment solution obtained should satisfy all conditions in every scenario, making the solution robust against any realization of the considered scenarios. It should be noted here that the robustness of the solution is directly related with the level of details of uncertainty and variability characterization.

Generally, the higher the numbers of snapshots and scenarios considered are, the more robust the solution is. However, there is always a threshold beyond which adding more snapshots and scenarios does not significantly change the solution but increases unnecessary computational burden. If the scenarios considered in the planning are carefully selected to be representative enough of all possible uncertainty realizations, then, the robustness and reliability of the solution can be more guaranteed.

The length of the planning horizon in the present work is assumed to be three years, which is then divided into yearly decision stages. In each stage, investment decisions related to DGs, ESSs, capacitor banks and lines are made. These decisions can be regarded as here-and-now because such decisions are independent of any scenario or snapshot. However, operation variables (such as actual power productions, storage level, power flows, etc.) depend on scenarios and snapshots, as well as decision stages.

6.3.2 Objective Function

As mentioned earlier, the objective of this chapter is to maximize RES integration in DNS from the system perspective (or, from the Distribution System Operators' point of view) by optimally deploying different smart-grid enabling technologies at a minimum cost. Here, it is assumed that the DSO owns some generation sources and ESSs.

The resulting problem is formulated as a multi-stage stochastic MILP an overall cost minimization as an objective (6.3). The objective function in (6.3) is composed of Net Present Value (NPV) of five cost terms each multiplied by a certain relevance factor $\alpha_j; \forall j \in \{1,2,\ldots,5\}$. Note that, in this chapter, all cost terms are assumed to be equally important; hence, these factors are set equal. However, depending on the relative importance of the considered costs, different coefficients (relevance factors) can be adopted in the objective function. Note that all cost terms have the same units (Euros). In reality, the objective function is one: the total cost in the system which is the sum of various cost components (operation, maintenance, emission, investment, etc.). However, a decision-maker may not be interested in some of these costs, for instance, because their values (and/their expected influences on the solution) are negligible compared with others. Such cost terms would then have their relevance factors set to zero. It is for this sole purpose that the relevance factors (which should not be confused with weights like in the Pareto-type optimization) are included in the formulation.

In the present work, a perpetual planning horizon [93] is assumed when formulating the integrated planning problem, as in [71]. This is purposely done to balance different cost terms within and outside the actual planning horizon. To further clarify this, consider the illustrative example in Figure 3.3 It is understood that investments are made in a specific year within the planning horizon (the second year in this case) and the investment costs are prorated throughout its lifetime i.e. distributed into equal payments among the years within the life span of the asset.

However, the maintenance and operation (O&M) related costs are incurred every year within and after the planning horizon. To balance these cost terms, a perpetual planning horizon, i.e. an endless payment of fixed payments is assumed. Based on the finance theory [93], the present value of perpetuity, which is the sum of the net worth of infinite annual fixed payments, is determined by dividing the fixed payment at a given period by the interest rate r. Based on this, the O&M costs include the associated annual costs within (part I) and outside the planning horizon (part II). The latter (part II) are determined by the perpetuity of the costs in the last planning stage updated by net present value factor in this case $(1+r)^{-3}$. Note that after the lifetime of a given asset elapses, investments will be made in the same asset with the same cost, leading to a seemingly perpetual planning horizon.

The first term in (6.3), $TInvC$, represents the total investment costs under the assumption of perpetual planning horizon [93]. In other words, "the investment cost is amortized in annual installments throughout the lifetime of the installed component", as is done in [71]. Here, the total investment cost is the sum of investment costs of new and existing DGs, feeders, energy storage system and capacitor banks, as in (6.4).

The second term, TMC, in (6.3) denotes the total maintenance costs, which is given by the sum of individual maintenance costs of new and existing DGs as well as that of feeders, energy storage system and capacitor banks in the system at each stage and the corresponding costs incurred after the last planning stage, as in (6.5). Note that the latter costs depend on the maintenance costs of the last planning stage. Here, a perpetual planning horizon is assumed.

The third term TEC in (6.3) refers to the total cost of energy in the system, which is the sum of the cost of power produced by new and existing DGs, purchased from upstream and supplied by energy storage system at each stage as in (6.6). Equation (6.6) also includes the total energy costs incurred after the last planning stage under a perpetual planning horizon. These depend on the energy costs of the last planning stage.

The fourth term $TENSC$ represents the total cost of unserved power in the system and is calculated as in (6.7).

The last term TImiC gathers the total emission costs in the system, given by the sum of emission costs for the existing and new DGs as well that of power purchased from the grid at the substations.

$$Minimize\ TC = \alpha_1 * TInvC + \alpha_2 * TMC + \alpha_3 * TEC + \alpha_4 * TENSC + \alpha_5 * TImiC \tag{6.3}$$

$$TInvC = \underbrace{\sum_{t\epsilon\Omega^t} \frac{(1+r)^{-t}}{r}(InvC_t^{DG} + InvC_t^{LN} + InvC_t^{ES} + InvC_t^{CAP})}_{NPV\ of\ investment\ cost} \tag{6.4}$$

$$TMC = \underbrace{\sum_{t\epsilon\Omega^t}(1+r)^{-t}\left(MntC_t^{DG} + MntC_t^{LN} + MntC_t^{ES} + MntC_t^{Cap}\right)}_{NPV\ of\ maintenance\ costs} + \underbrace{\frac{(1+r)^{-T}}{r}(MntC_T^{DG} + MntC_T^{LN} + MntC_T^{ES} + MntC_T^{Cap})}_{NPV\ maintenance\ costs\ incured\ after\ stage\ T} \tag{6.5}$$

$$TEC = \underbrace{\sum_{t\epsilon\Omega^t}(1+r)^{-t}\ (EC_t^{DG} + EC_t^{ES} + EC_t^{SS})}_{NPV\ of\ operation\ costs} + \underbrace{\frac{(1+r)^{-T}}{r}(EC_T^{DG} + EC_T^{ES} + EC_T^{SS})}_{NPV\ operation\ costs\ incured\ after\ stage\ T} \tag{6.6}$$

$$ENSC = \underbrace{\sum_{t\epsilon\Omega^t}(1+r)^{-t}\ ENSC_t}_{NPV\ of\ reliability\ costs} + \underbrace{\frac{(1+r)^{-T}}{r}ENSC_T}_{NPV\ reliability\ costs\ incured\ after\ stage\ T} \tag{6.7}$$

$$TEmiC = \underbrace{\sum_{t\epsilon\Omega^t}(1+r)^{-t}\ (EmiC_t^{DG} + EmiC_t^{SS})}_{NPV\ emission\ costs} + \underbrace{\frac{(1+r)^{-T}}{r}(EmiC_T^{DG} + EmiC_T^{SS})}_{NPV\ emission\ costs\ incured\ after\ stage\ T} \tag{6.8}$$

The individual cost components in (6.4)—(6.8) are computed by the following expressions. Equations (6.9)—(6.12) represent the investment costs of DGs, feeders, energy storage system and capacitor banks, respectively. Notice that all investment costs are weighted by the capital recovery factor, $\frac{r(1+r)^{LT}}{(1+r)^{LT}-1}$.

The formulations in (6.9)—(6.12) ensure that the investment cost of each asset added to the system is considered only once in the summation. In this regard, there are two issues that need to be taken care of in the formulation. On one hand, it is required that investment decisions already made at a given stage cannot be reversed back (divested) in the subsequent stages. This condition is met by the set of logical constraints described in the following subsection in the model formulation, for example, $x_{g,i,t} \geq x_{g,i,t-1}$.

Such a logical constraint states that the investment decision at a planning stage t should be at least equal to the investment decision in the preceding stage $t-1$. In other words, $x_{g,i,t}$ should be equal to the investments made in the preceding stages plus the additional investment in stage t.

On the other hand, only the investment costs for the marginal (additional) investment made at each stage should be considered in the investment cost summations in (6.9)—(6.12). In the example, the additional (marginal) investments made at each stage are given by: $\left(x_{g,i,t} - x_{g,i,t-1}\right)$. This is why the investment cost function in (6.9) contains this expression.

Now, suppose the decision variable on DG investments $x_{g,i,t}$ is defined as a binary one. This means that only one DG of type g can be installed at node i in either of the planning stages. Suppose it becomes most economical to install it in the second year i.e. $x_{g,i,2} = 0$. The logical constraint in (6.70) leads to $x_{g,i,3} \geq x_{g,i,2}$ i.e. $x_{g,i,3} \geq 1$. For this particular example, the binary variable for each stage i.e. $\{x_{g,i,1}; x_{g,i,2}; x_{g,i,3}\}$ is equal to $\{0; 1; 1\}$, respectively.

Recall that the investment cost of this DG should be considered only once (in the second year) in the summation, and this is taken care of by the expression $(x_{g,i,t} - x_{g,i,t-1})$ in Equation (6.9). All the differences for this particular example are $(x_{g,i,1} - x_{g,i,0}) = 0$, $(x_{g,i,2} - x_{g,i,1}) = 1$, and $(x_{g,i,3} - x_{g,i,2}) = 0$, which indicates that the investment cost is considered only once at the second stage. Instead of defining the variable $\mathrm{x_{g,i,t}}$ as a binary variable, one may allow it to have any integer value as far as it is deemed optimal.

In this case, for the above example, suppose the optimal solution is to install one DG in the second stage and one more DG in the third stage which means $\{x_{g,i,1}; x_{g,i,2}; x_{g,i,3}\}$ is equal to $\{0; 1; 2\}$. Note that $x_{g,i,3}$ should be equal to 2 because the investment decision made in the preceding stages should be also available in the third stage. For this example, $(x_{g,i,1} - x_{g,i,0}) = 0$, $(x_{g,i,2} - x_{g,i,1}) = 1$, and $(x_{g,i,3} - x_{g,i,2}) = 1$, showing that the investment cost each DG is considered only once in the summation.

In general, the formulation remains valid regardless of how the investment variables are defined. Note that investment variables refer to the decision variables corresponding to investments in DGs, energy storage systems, capacitor banks and distribution lines in each of the decision stages along the 3-year planning horizon.

Equation (6.13) stands for the maintenance costs of new and existing DGs at each time stage. The maintenance cost of a new/existing feeder is included only when its corresponding investment/ utilization variable is different from zero. Similarly, the maintenance costs of new and existing feeders at each stage are given by Equation (6.14). Equations (6.15) and (6.16) are related to the maintenance costs at each stage of energy storage and capacitor banks, respectively.

$$InvC_t^{DG} = \sum_{g\epsilon\Omega^g} \sum_{i\epsilon\Omega^i} \frac{r(1+r)^{LT_g}}{(1+r)^{LT_g} - 1} IC_{g,i}(x_{g,i,t} - x_{g,i,t-1}) \; ; where \; x_{g,i,0} = 0 \tag{6.9}$$

$$InvC_t^{LN} = \sum_{k\epsilon\Omega^\ell} \frac{r(1+r)^{LT_k}}{(1+r)^{LT_k} - 1} IC_k(x_{k,t} - x_{k,t-1}) \; ; \; where \; x_{k,0} = 0 \tag{6.10}$$

$$InvC_t^{ES} = \textstyle\sum_{es\epsilon\Omega^{es}} \sum_{i\epsilon\Omega^i} \frac{r(1+r)^{LT_{es}}}{(1+r)^{LT_{es}-1}} IC_{es}(x_{es,i,t} - x_{es,i,t-1}) \; ; \quad where \; x_{es,i,0} = 0 \tag{6.11}$$

$$InvC_t^{CAP} = \sum_{c\epsilon\Omega^c}\sum_{i\epsilon\Omega^i}\frac{r(1+r)^{LT_c}}{(1+r)^{LT_c}-1}IC_c(x_{c,i,t}-x_{c,i,t-1})\ ; where\ x_{c,i,0}=0 \quad (6.12)$$

$$MntC_t^{DG} = \sum_{g\epsilon\Omega^g}\sum_{i\epsilon\Omega^i}MC_g^N\,x_{g,i,t} + \sum_{g\epsilon\Omega^g}\sum_{i\epsilon\Omega^i}MC_g^E\,u_{g,i,t} \quad (6.13)$$

$$MntC_t^{LN} = \sum_{k\epsilon\Omega^{e\ell}}MC_k^E\,u_{k,t} + \sum_{k\epsilon\Omega^{n\ell}}MC_k^N x_{k,t} \quad (6.14)$$

$$MntC_t^{ES} = \sum_{es\epsilon\Omega^{es}}\sum_{i\epsilon\Omega^i}MC_{es}x_{es,i,t} \quad (6.15)$$

$$MntC_t^{Cap} = \sum_{c\epsilon\Omega^c}\sum_{i\epsilon\Omega^i}MC_c x_{c,i,t} \quad (6.16)$$

The total cost of power produced by new and existing DGs is given by Equation (6.17). Note that these costs depend on the amount of power generated at each scenario, snapshot and stage. Therefore, these costs represent the expected costs of operation. Similarly, Equations (5.18) and (6.19) respectively account for the expected costs of energy supplied by the energy storage system, and that purchased from upstream (i.e., transmission grid).

The penalty for the unserved power, given by (6.20), is also dependent on the scenarios, and time stages. Equation (6.20) therefore gives the expected cost of unserved energy in the system.

The expected emission costs of power generated by new and existing DGs are given by (6.21)—(6.23), and that of energy purchased from the grid is calculated using (6.24). Note that, for the sake of simplicity, a linear emission cost function is assumed here. In reality, the emission cost function is highly nonlinear and nonconvex, as in [44].

$$EC_t^{DG} = \sum_{s\epsilon\Omega^s}\rho_s\sum_{w\epsilon\Omega^w}\pi_w\sum_{g\epsilon\Omega^g}\sum_{i\epsilon\Omega^i}(OC_{g,i,s,w,t}^N P_{g,i,s,w,t}^N + OC_{g,i,s,w,t}^E\,P_{g,i,s,w,t}^E) \quad (6.17)$$

$$EC_t^{ES} = \sum_{s\epsilon\Omega^s}\rho_s\sum_{w\epsilon\Omega^w}\pi_w\sum_{c\epsilon\Omega^c}\sum_{i\epsilon\Omega^i}\lambda_{es,i,s,w,t}^{dch}P_{es,i,s,w,t}^{dch} \quad (6.18)$$

$$EC_t^{SS} = \sum_{s\epsilon\Omega^s} \rho_s \sum_{w\epsilon\Omega^w} \pi_w \sum_{\varsigma,\Omega^\varsigma} \lambda_{s,w,t}^{\varsigma} P_{\varsigma,s,w,t}^{SS} \quad (6.19)$$

$$ENSC_t = \sum_{s\epsilon\Omega^s} \rho_s \sum_{w\epsilon\Omega^w} \sum_{i\epsilon\Omega^i} \pi_w \upsilon_{s,w,t} \delta_{i,s,w,t} \quad (6.20)$$

$$EmiC_t^{DG} = EmiC_t^N + EmiC_t^E \quad (6.21)$$

$$EmiC_t^N = \sum_{s\epsilon\Omega^s} \rho_s \sum_{w\epsilon\Omega^w} \pi_w \sum_{g\epsilon\Omega^g} \sum_{i\epsilon\Omega^i} \lambda_{s,w,t}^{CO_2e} ER_g^N P_{g,i,s,w,t}^N \quad (6.22)$$

$$EmiC_t^E = \sum_{s\epsilon\Omega^s} \rho_s \sum_{w\epsilon\Omega^w} \pi_w \sum_{g\epsilon\Omega^g} \sum_{i\epsilon\Omega^i} \lambda_{s,w,t}^{CO_2e} ER_g^E P_{g,i,s,w,t}^E \quad (6.23)$$

$$EmiC_t^E = \sum_{s\epsilon\Omega^s} \rho_s \sum_{w\epsilon\Omega^w} \pi_w \sum_{g\epsilon\Omega^g} \sum_{i\epsilon\Omega^i} \lambda_{s,w,t}^{CO_2e} ER_g^E P_{g,i,s,w,t}^E \quad (6.24)$$

6.3.3 Constraints

6.3.3.1 *Kirchhoff's Voltage Law*

The customary AC power flow equations, given by (6.25) and (6.26), are highly non-linear and non-convex. Understandably, using these flow expressions in power system planning applications is increasingly difficult. Because of this, Equations (6.25) and (6.26) are often linearized by considering two practical assumptions.

The first assumption is concerning the bus voltage magnitudes, which in distribution systems are expected to be close to the nominal value V_{nom}. The second assumption is in relation to the voltage angle difference θ_k across a line which is practically small, leading to the trigonometric approximations $sin\,\theta_k \approx \theta_k$ and $cos\,\theta_k \approx 1$. Note that this assumption is valid in distribution systems, where the active power flow dominates the total apparent power in lines. Furthermore, the voltage magnitude at bus i can be expressed as the sum of the nominal voltage and a small deviation ΔV_i, as in (6.27).

$$P_k = V_i^2 g_k - V_i V_j (g_k \cos\theta_k + b_k \sin\theta_k) \quad (6.25)$$

$$Q_k = -V_i^2 b_k + V_i V_j (b_k \cos\theta_k - g_k \sin\theta_k) \tag{6.26}$$

$$V_i = V_{nom} + \Delta V_i, \qquad where\ \Delta V^{min} \leq \Delta V_i \leq \Delta V^{max} \tag{6.27}$$

Note that the voltage deviations at each node ΔV_i are expected to be very small. Substituting (6.27) in (6.25) and (6.26) and neglecting higher order terms, we get:

$$P_k \approx (V_{nom}^2 + 2V_{nom}\Delta V_i)g_k - (V_{nom}^2 + V_{nom}\Delta V_i + V_{nom}\Delta V_j)(g_k + b_k\theta_k) \tag{6.28}$$

$$Q_k \approx -(V_{nom}^2 + 2V_{nom}\Delta V_i)b_k + (V_{nom}^2 + V_{nom}\Delta V_i + V_{nom}\Delta V_j)(b_k - g_k\theta_k) \tag{6.29}$$

Note that Equations (6.28) and (6.29) still contain nonlinearities because of the products of two continuous variables—voltage deviations and angle differences. However, since these variables (ΔV_i, ΔV_j and θ_k) are very small, their products can be neglected. Hence, the above flow equations become:

$$P_k \approx V_{nom}(\Delta V_i - \Delta V_j)g_k - V_{nom}^2 b_k \theta_k \tag{6.30}$$

$$Q_k \approx -V_{nom}(\Delta V_i - \Delta V_j)b_k - V_{nom}^2 g_k \theta_k \tag{6.31}$$

The linear planning model proposed here is based on the above linearized flow equations. This linearization approach was first introduced in [95] in the context of transmission expansion planning problem. When the investment planning problem includes network switching, reinforcement, replacement and expansion of feeders, Equations (6.30) and (6.31) must be multiplied by the corresponding binary variables as in (6.32) —(6.35). This is to make sure the flow through an existing/a new feeder is zero when its switching/investment variable is zero; otherwise, the flow in that feeder should obey the Kirchhoff's law.

$$P_k \approx u_{k,t}\{V_{nom}(\Delta V_i - \Delta V_j)g_k - V_{nom}^2 b_k \theta_k\} \tag{6.32}$$

$$Q_k \approx u_{k,t}\{-V_{nom}(\Delta V_i - \Delta V_j)b_k - V_{nom}^2 g_k \theta_k\} \tag{6.33}$$

$$P_k \approx x_{k,t}\{V_{nom}(\Delta V_i - \Delta V_j)g_k - V_{nom}^2 b_k \theta_k\} \quad (6.34)$$

$$Q_k \approx x_{k,t}\{-V_{nom}(\Delta V_i - \Delta V_j)b_k - V_{nom}^2 g_k \theta_k\} \quad (6.35)$$

The bilinear products, involving binary with voltage deviation and angle difference variables, introduces undesirable nonlinearity to the problem. This nonlinearity can be avoided using the big-M formulation i.e. by reformulating the above equations into their respective disjunctive equivalents as in (6.36)—(6.39). As a rule-of-thumb, the big-M parameter is often set to the maximum transfer capacity in the system.

$$\left|P_{k,s,w,t} - \{V_{nom}(\Delta V_{i,s,w,t} - \Delta V_{j,s,w,t})g_k - V_{nom}^2 b_k \theta_{k,s,w,t}\ )\}\right| \leq MP_k(1 - u_{k,t}) \quad (6.36)$$

$$\left|Q_{k,s,w,t} - \{-V_{nom}(\Delta V_{i,s,w,t} - \Delta V_{j,s,w,t})b_k - V_{nom}^2 g_k \theta_{k,s,w,t}\}\ \right| \leq MQ_k(1 - u_{k,t}) \quad (6.37)$$

$$\left|P_{k,s,w,t} - \{V_{nom}(\Delta V_{i,s,w,t} - \Delta V_{j,s,w,t})g_k - V_{nom}^2 b_k \theta_{k,s,w,t}\}\right| \leq MP_k(1 - x_{k,t}) \quad (6.38)$$

$$\left|Q_{k,s,w,t} - \{-V_{nom}(\Delta V_{i,s,w,t} - \Delta V_{j,s,w,t})b_k - V_{nom}^2 g_k \theta_{k,s,w,t}\}\right| \leq MQ_k(1 - x_{k,t}) \quad (6.39)$$

6.3.3.2 *Flow Limits*

The apparent power flow through a line $S_k$is given by $\sqrt{P_k^2 + Q_k^2}$ and this has to be less than or equal to the rated value which is denoted as:

$$P_k^2 + Q_k^2 \leq (S_k^{max})^2 \quad (6.40)$$

Considering line switching/investment, Equation (6.40) can be rewritten as:

$$P_{k,s,w,t}^2 + Q_{k,s,w,t}^2 \leq u_{k,t}(S_k^{max})^2 \quad (6.41)$$

$$P_{k,s,w,t}^2 + Q_{k,s,w,t}^2 \leq x_{k,t}(S_k^{max})^2 \quad (6.42)$$

The quadratic expressions of active and reactive power flows in (6.41) through (6.42) can be easily linearized using piecewise linearization, considering a sufficiently large number of linear segments, L.

There are a number of ways of linearizing such functions such as incremental, multiple choice, convex combination and other approaches in the literature [164]. Here, the first approach (which is based on first-order approximation of the nonlinear curve) is used because of its relatively simple formulation. To this end, two non-negative auxiliary variables are introduced for each of the flows P_k and Q_k such that $P_k = P_k^+ - P_k^-$ and $Q_k = Q_k^+ - Q_k^-$.

Note that these auxiliary variables (i.e., P_k^+ , P_k^-, Q_k^+ andQ_k^-) represent the positive and negative flows of P_k and Q_k, respectively. This helps one to consider only the positive quadrant of the nonlinear curve, resulting in a significant reduction in the mathematical complexity, and by implication the computational burden. In this case, the associated linear constraints are:

$$P_{k,s,w,t}^2 \approx \sum_{l=1}^{L} \alpha_{k,l} p_{k,s,w,t,l} \tag{6.43}$$

$$Q_{k,s,w,t}^2 \approx \sum_{l=1}^{L} \beta_{k,l} q_{k,s,w,t,l} \tag{6.44}$$

$$P_{k,s,w,t}^+ + P_{k,s,w,t}^- = \sum_{l=1}^{L} p_{k,s,w,t,l} \tag{6.45}$$

$$Q_{k,s,w,t}^+ + Q_{k,s,w,t}^- = \sum_{l=1}^{L} q_{k,s,w,t,l} \tag{6.46}$$

where $p_{k,s,w,t,l} \leq P_k^{max}/L$ and $q_{k,s,w,t,l} \leq Q_k^{max}/L$.

6.3.3.3 *Line Losses*

The active and reactive power losses in line k can be approximated as follows:

$$PL_k = P_{k,ij} + P_{k,ji} \approx 2V_{nom}^2 g_k(1 - \cos\theta_k) \approx V_{nom}^2 g_k \theta_k^2 \tag{6.47}$$

$$QL_k = Q_{k,ij} + Q_{k,ji} \approx -2V_{nom}^2 b_k(1 - \cos\theta_k) \approx -b_k V_{nom}^2 \theta_k^2 \tag{6.48}$$

Clearly, Equations (6.47) and (6.48) are nonlinear and nonconvex functions, making the problem more complex to solve. This can be overcome by having the quadratic angle differences piecewise-linearized, as it is done for the quadratic flows in the above. However, instead of doing this, the expressions in (6.47) and (6.48) can be expressed in terms of the active and the reactive power flows as in (6.49) and (6.50). Note that Equation (6.49) can be easily obtained by multiplying the squared expressions of both sides of the equations in (6.30) and (6.31) by the resistance of the branch, combining the resulting equations, neglecting higher order terms and reordering both sides of the resulting equation. Equation (6.50) is also obtained in a similar fashion but by multiplying the squared expressions by reactance. For the sake of completeness, details concerning the derivations (6.49) and (6.50) are presented in Appendix D.

$$PL_{k,s,w,t} = r_k\{P_{k,s,w,t}^2 + Q_{k,s,w,t}^2\}/V_{nom}^2 \tag{6.49}$$

$$QL_{k,s,w,t} = x_k\{P_{k,s,w,t}^2 + Q_{k,s,w,t}^2\}/V_{nom}^2 \tag{6.50}$$

Note that expressing the losses as a function of flows has two advantages. First, doing so reduces the number of nonlinear terms that has to be linearized, which in turn results in a model with a reduced number of equations and variables. For example, if Equations (6.47) and (6.48) are used instead, in addition to the quadratic power flow terms P_k^2 and Q_k^2, the quadratic angle differences θ_k^2 should also be linearized to make the problem linear and convex. On the contrary, when Eqs. (6.49) and (6.50) are used, one is only required to linearize P_k^2 and Q_k^2. Second, it avoids unnecessary constraints on the angle differences when a line between two nodes is not connected or remains not selected for investment. This is often avoided by introducing binary variables and using a so-called big-M formulation [95]. However, this adds extra complexity to the problem.

5.3.3.4 *Kirchhoff's Current Law (Active and Reactive Load Balances)*

All the time, load balance should be respected at each node i.e. the sum of all injections should be equal to the sum of all withdrawals at each node. This is enforced by adding the following two constraints:

$$\sum_{g\epsilon\Omega^{DG}}\left(P^{E}_{g,i,s,w,t}+P^{N}_{g,i,s,w,t}\right)+\sum_{es\epsilon\Omega^{es}}\left(P^{dch}_{es,i,s,w,t}-P^{ch}_{es,i,s,w,t}\right)+P^{SS}_{\varsigma,s,w,t}+\sum_{in,k\epsilon i}P_{k,s,w,t} - \sum_{out,k\epsilon i}P_{k,s,w,t}+\ \delta_{i,s,w,t}=D^{i}_{s,w,t}+PL_{\varsigma,s,w,t}+\sum_{k\epsilon i}\tfrac{1}{2}PL_{k,s,w,t}\ \ ;\ \forall\varsigma,\forall\varsigma\epsilon i \tag{6.51}$$

$$\sum_{g\epsilon\Omega^{DG}}(Q^{E}_{g,i,s,w,t}+Q^{N}_{g,i,s,w,t})+\sum_{c\epsilon\Omega^{c}}Q^{c}_{i,s,w,t}+Q^{SS}_{\varsigma,s,w,t}+\sum_{in,k\epsilon i}Q_{k,s,w,t}-\sum_{out,k\epsilon i}Q_{k,s,w,t} =Q^{i}_{s,w,t}+QL_{\varsigma,s,w,t}+\sum_{in,k\epsilon i}\tfrac{1}{2}QL_{k,s,w,t}+\sum_{out,k\epsilon i}\tfrac{1}{2}QL_{k,s,w,t}\ \ ;\ \forall\varsigma,\forall\varsigma\epsilon i \tag{6.52}$$

Equations (6.51) and (6.52) stand for the active and the reactive power balances at each node, respectively.

6.3.3.5 *Bulk Energy Storage Model Constraints*

The generic bulk ESS is modeled by constraints (6.53) −(6.59).

$$0\le P^{ch}_{es,i,s,w,t}\le I^{ch}_{es,i,s,w,t}x_{es,i,t}P^{ch,max}_{es,i} \tag{6.53}$$

$$0\le P^{dch}_{es,i,s,w,t}\le I^{dch}_{es,i,s,w,t}x_{es,i,t}P^{ch,max}_{es,i} \tag{6.54}$$

$$I^{ch}_{es,i,s,w,t}+I^{dch}_{es,i,s,w,t}\le 1 \tag{6.55}$$

$$E_{es,i,s,w,t}=E_{es,i,s,w-1,t}+\eta^{ch}_{es}P^{ch}_{es,i,s,w,t}-\beta^{dch}_{es}P^{dch}_{es,i,s,w,t}\,;where\ \beta^{dch}_{es}=1/\eta^{dch}_{es} \tag{6.56}$$

$$E^{min}_{es,i}x_{es,i,t}\le E_{es,i,s,w,t}\le x_{es,i,t}E^{max}_{es,i} \tag{6.57}$$

$$E_{es,i,s,w_0,T1}=\mu_{es}x_{es,i,T1}E^{max}_{es,i} \tag{6.58}$$

$$E_{es,i,s,w_1,t+1}=E_{es,i,s,W,t};\ E_{es,i,s,W,T}=E_{es,i,s,w_0,T1} \tag{6.59}$$

The limits on the capacity of ESS while being charged and discharged are considered in Inequalities (6.53) and (6.54), respectively. Inequality (6.55) prevents simultaneous charging and discharging operation of ESS at the same operational time w. The amount of stored energy within the reservoir of bulk ESS at the operational time w as a function of energy stored until $w-1$ is given by (6.56). The maximum and minimum levels of storages in operational time w are also considered through inequality (6.57). Equation (6.58) shows the initial level of stored energy in the bulk ESS as a function of its maximum reservoir capacity. In a multi-stage planning approach, Equation (5.59) ensures that the initial level of energy in the bulk ESS at a given year is equal to the final level of energy in the ESS in the preceding year and the reservoir level at the end of the planning horizon should be equal to the initial level. The latter constraint guarantees that the optimal solution returned by the solution algorithm is not because of the initial reservoir level. For the sake of simplicity, η_{es}^{dch} is assumed to be equal to η_{es}^{ch}, as in [165], [166]. Both the charging η_{es}^{ch} and discharging η_{es}^{dch} efficiencies are expressed in terms of the energy at the nodes where the storage system is connected to. Because of this, a certain percentage of the energy fed to the storage system will be stored while the remaining will be lost in the form of losses (electrical, chemical, heat, etc.). This is related to the charging efficiency, which should then be less than 1. On the other hand, in order to withdraw a given amount of energy from the storage system, more energy is needed to cover the discharging losses. This is why we have $1/\eta_{es}^{dch}$ in Equation (6.56) associated with the energy at the output side of the energy storage system.

Notice that inequalities (6.53) and (6.54) involve products of charging/discharging binary variables and investment variable. In order to linearize these, new continuous positive variables $z_{es,i,s,w,t}^{ch}$, and $z_{es,i,s,w,t}^{dch}$, which replaces the bilinear products in each constraint, is introduced such that the set of linear constraints in (6.60) and (6.61) hold. For instance, the product $I_{es,i,s,w,t}^{dch}x_{es,i,t}$ is replaced by the positive variable $z_{es,i,s,w,t}^{dch}$. Then, the bilinear product is decoupled by introducing the set of constraints in (6.60) [115].

$$z_{es,i,s,w,t}^{dch} \leq x_{es}^{max} I_{es,i,s,w,t}^{dch} \; ; \; z_{es,i,s,w,t}^{dch} \leq x_{es,i,t} \; ; z_{es,i,s,w,t}^{dch} \geq x_{es,i,t} - \left(1 - I_{es,i,s,w,t}^{dch}\right) x_{es}^{max} \tag{6.60}$$

Similarly, the product $I_{es,i,s,w,t}^{ch}x_{es,i,t}$ is decoupled by including the following set of constraints:

$$z_{es,i,s,w,t}^{ch} \leq x_{es}^{max} I_{es,i,s,w,t}^{ch} \; ; \; z_{es,i,s,w,t}^{ch} \leq x_{es,i,t} \; ; z_{es,i,s,w,t}^{ch} \geq x_{es,i,t} - \left(1 - I_{es,i,s,w,t}^{ch}\right) x_{es}^{max} \tag{6.61}$$

The large number of discrete variables in the storage model presented above can render significant computational burden. To overcome this, a relaxed ESS model can be formed without the charging and discharging indicator variables as:

$$0 \leq P_{es,i,s,w,t}^{ch} \leq x_{es,i,t} P_{es,i}^{ch,max} \tag{6.53'}$$

$$0 \leq P^{dch}_{es,i,s,w,t} \leq x_{es,i,t} P^{ch,max}_{es,i} \quad (6.54')$$

$$E_{es,i,s,w,t} = E_{es,i,s,w-1,t} + \eta^{ch}_{es} P^{ch}_{es,i,s,w,t} - \beta^{dch}_{es} P^{dch}_{es,i,s,w,t} \text{ ; } where \ \beta^{dch}_{es} = 1/\eta^{dch}_{es} \quad (6.56')$$

Under normal conditions, the ESS model in (6.53'), (6.54') and (6.56') is exact because by the principle of optimality, at most one of the variables $P^{ch}_{es,i,s,w,t}$ and $P^{dch}_{es,i,s,w,t}$ can be greater than zero. In other words, it does not economic sense to have both variables to be greater than zero at the same time.

6.3.3.6 *Active and Reactive Power Limits of DGs*

The active and reactive power limits of existing generators are given by (6.62) and (6.63), respectively. In the case of new (candidate) generators, the corresponding constraints are (6.64) and (6.65). Note that the binary variables multiply the minimum and the maximum generation limits to make sure that the power generation variable is zero when the generator remains either unutilized or unselected for investment.

$$P^{E,min}_{g,i,s,w,t} u_{g,i,t} \leq P^{E}_{g,i,s,w,t} \leq P^{E,max}_{g,i,s,w,t} u_{g,i,t} \quad (6.62)$$

$$Q^{E,min}_{g,i,s,w,t} u_{g,i,t} \leq Q^{E}_{g,i,s,w,t} \leq Q^{E,max}_{g,i,s,w,t} u_{g,i,t} \quad (6.63)$$

$$P^{N,min}_{g,i,s,w,t} x_{g,i,t} \leq P^{N}_{g,i,s,w,t} \leq P^{N,max}_{g,i,s,w,t} x_{g,i,t} \quad (6.64)$$

$$Q^{N,min}_{g,i,s,w,t} x_{g,i,t} \leq Q^{N}_{g,i,s,w,t} \leq Q^{N,max}_{g,i,s,w,t} x_{g,i,t} \quad (6.65)$$

It should be noted that these constraints are applicable only for conventional DGs which have reactive power support capabilities. In the case of variable generation sources, slight modifications are required. For instance, for wind and solar PV generators, the upper bound $P^{max}_{g,i,s,w,t}$ should be equal to the actual production level at a specific hour, which in turn depends on the level of primary energy source (wind speed and solar radiation). The lower bound $P^{min}_{g,i,s,w,t}$ in this case is simply set to zero.

In addition, conventional wind and solar PV sources do not often have the capability to provide reactive power support; hence, they are operated at a constant and lagging or unity power factor. Under such an operation, the following constraints should be used:

$$Q^{E}_{g,i,s,w,t} = \tan(\cos^{-1}(pf_g)) * P^{E}_{g,i,s,w,t} \tag{6.63'}$$

$$Q^{N}_{g,i,s,w,t} = \tan(\cos^{-1}(pf_g)) * P^{N}_{g,i,s,w,t} \tag{6.65'}$$

where pf_g is the power factor of the wind or solar type generator g. Under normal cases, $P^{E}_{g,i,s,w,t} = P^{E,\ max}_{g,i,s,w,t}$ and $P^{N}_{g,i,s,w,t} = P^{N,\ max}_{g,i,s,w,t}$.

On the other hand, for wind and solar PV type DGs with reactive power support capabilities such as doubly fed induction generator (DFIG) based wind turbine and voltage source inverter (VSI) based PV, the following constraints are used:

$$-\tan\left(\cos^{-1}(pf_g)\right) * P^{E}_{g,i,s,w,t} \leq Q^{E}_{g,i,s,w,t} \leq \tan(\cos^{-1}(pf_g)) * P^{E}_{g,i,s,w,t} \tag{6.63''}$$

$$-\tan\left(\cos^{-1}(pf_g)\right) * P^{N}_{g,i,s,w,t} \leq Q^{N}_{g,i,s,w,t} \leq \tan(\cos^{-1}(pf_g)) * P^{N}_{g,i,s,w,t} \tag{6.65''}$$

The above two inequalities show that the wind and solar type DGs are capable of operating between pf_g leading power factor (capacitive) and pf_g lagging power factor (reactive). This means such DGs are capable of “producing” and “consuming” reactive power depending on operational situations in the system.

6.3.3.7 *Reactive Power Limit of Capacitor Bank*

Inequality (6.66) ensures that the reactive power produced by the reactive power sources (capacitor banks) is bounded between zero and the maximum possible capacity.

$$0 \leq Q^{c}_{i,s,w,t} \leq x_{c,i,t} Q^{0}_{c} \tag{6.66}$$

6.3.3.8 *Active and Reactive Power Limits of Power Purchased*

For technical reasons, the power that can be purchased from the transmission grid could have minimum and maximum limits, which is enforced by (6.67) and (6.68). However, it is understood that, in reality, setting such limits is difficult. They are included here only for the sake of completeness.

$$P^{SS,min}_{\varsigma,s,w,t} \leq P^{SS}_{\varsigma,s,w,t} \leq P^{SS,max}_{\varsigma,s,w,t} \tag{6.67}$$

$$Q_{\varsigma,s,w,t}^{SS,min} \leq Q_{\varsigma,s,w,t}^{SS} \leq Q_{\varsigma,s,w,t}^{SS,max} \tag{6.68}$$

For the analysis, the active power production limits are simply set to 1.5 times the minimum and the maximum levels of total load in the system.

Note that the multiplier is higher than one in the system because of the losses, which needs to be covered by generating extra power. The reactive power limits are determined by the power factor of the substation as: $Q_{\varsigma,s,w,t}^{SS,min} = -tan(cos^{-1}(pf_{ss})) * P_{\varsigma,s,w,t}^{SS}$ and $Q_{\varsigma,s,w,t}^{SS,max} = tan(cos^{-1}(pf_{ss})) * P_{\varsigma,s,w,t}^{SS}$, where pf_{ss} is a given power factor at the substation, which is assumed to be 0.9 throughout the analysis in this chapter.

6.3.3.9 *Logical Constraints*

The following logical constraints ensure that an investment decision cannot be reversed i.e. an investment already made cannot be divested.

$$x_{k,t} \geq x_{k,t-1} \tag{6.69}$$

$$x_{g,i,t} \geq x_{g,i,t-1} \tag{6.70}$$

$$x_{es,i,t} \geq x_{es,i,t-1} \tag{6.71}$$

$$x_{c,i,t} \geq x_{c,i,t-1} \tag{6.72}$$

6.3.3.10 *Radiality Constraints*

Distribution networks are structurally meshed but predominantly operated in a radial manner because of technical reasons (particularly related to the protection). The presence of DGs and reactive power sources in the system nodes other than substation nodes (which is the subject of the present work) may lead to islanding i.e. some loads may be isolated from the mains (substations) and/or loops, breaking the radiality of the network. This is not desired mainly because of the aforementioned technical reasons.

To ensure radiality, two conditions must be fulfilled. First, the solution must have $N_i - N_\varsigma$ circuits. Second, the final topology should be connected. Equation (6.73) represents the first necessary condition for maintaining the radial topology of DNS.

$$\sum_{k\in\Omega^{ij}} OR(x_{k,t}, u_{k,t}) = N_i - N_\varsigma \quad ;\forall t \tag{6.73}$$

Note that the above equation assumes line investment is possible in all corridors. Hence, in a given corridor, we can have either an existing branch, a new one, or both connected in parallel, depending on the economic benefits of the final setup (solution) brings about to the system. The radiality constraint in (6.73) then has to accommodate this condition. One way to do this is using the Boolean logic operation, as in (6.73). Unfortunately, this introduces nonlinearity.

We show how this logic can be linearized using an additional auxiliary variable $\mathrm{z}_{\mathrm{k,t}}$ and the binary variables associated to existing and new branches (i.e., $u_{k,t}$ and $x_{k,t}$), respectively. Given $z_{k,t} := OR(x_{k,t}\ ,\ u_{k,t})$, this Boolean operation can be expressed using the following set of linear constraints:

$$\sum_{k\in\Omega^{ij}} OR(x_{k,t}, u_{k,t}) = N_i - N_\varsigma \quad ;\forall t \tag{6.74}$$

Note that the auxiliary variable $z_{k,t}$ is automatically constrained to be binary. Hence, it is not necessary to explicitly define $z_{k,t}$ as a binary variable; instead, defining it as a continuous positive variable is sufficient.

Alternatively, if $z_{k,t}$ is defined to be binary variable from the outset, then, Equation (6.73) can be converted into a single range constraint as:

$$0 \leq 2z_{k,t} - x_{k,t} - u_{k,t} \leq 1 \quad ;\forall t \tag{6.75}$$

Then, the radiality constraints in (6.73) can be reformulated using the $z_{k,t}$ variables as:

$$\sum_{k\in\Omega^{ij}} z_{k,t} = N_i - N_\varsigma \quad ;\forall t \tag{6.76}$$

When all loads in the DNS are only fed by power from substations, the final solution obtained automatically satisfies the two aforementioned conditions; hence, no additional constraints are required i.e. (6.74) or (6.75) along with (6.76) are sufficient to guarantee radiality.

However, it should be noted that in the presence of DGs and reactive power sources, these constraints alone may not ensure the radiality of the distribution network, as pointed out in [106] and further discussed in [97], [167]-[168]. This is however out of the scope of this chapter. If this is a critical issue, additional constraints need to be added to guarantee that all buses are linked, as proposed in [71], [53]-[55].

The optimization problem, developed here, encompasses Equations (6.3)—(6.24) and constraints (6.36)—(6.39), (6.41)—(6.46), (6.49)—(6.61), (6.62), (6.63), (6.64), (6.65), (6.66)—(6.72), (6.74) or (6.75) and (6.76) when all considered DGs are conventional generators with reactive power support capabilities. Otherwise, constraints (6.63') and (6.65') need to be added in case RES-based DGs which do not have such capabilities are present in the system or included in the planning. In addition, if there are RES-based DGs which are instead capable of operating as "generators" or "consumers" of reactive power depending on system operational situations, constraints (6.63'') and (6.65'') should be included and applied. In addition, if a relaxed ESS model is sought, constraints (6.53)—(6.61) can be replaced with the constraints in (6.53'), (6.54') and (6.56').

6.4 Case Studies

6.4.1 System Data and Assumptions

The radial DNS, shown in Figure 6.1, is used to test the proposed planning model. The total active and reactive loads of the system are 4.635 MW and 3.25 MVAr, respectively. The nominal voltage of the system is 12.66 kV. Information regarding network and demand data is provided in [169] and the data it is also available in the Appendix D. This system is selected for our case study because it is highly lossy and not properly compensated. The voltage profile in the base case, obtained from power flow analysis, can be found in [170]. For the sake of clarity, these nodal voltages are also reproduced in Figure 6.2 in the form of cumulative distribution function. Note that these results correspond to a substation power factor of 0.894 and with no lower voltage limit restrictions imposed on the system. As it can observed in Figure 6.2, more than 70% of the nodal voltages are below 0.95 per unit. However, this contradicts with the minimum voltage set in distribution systems (often above this limit) for stability reasons. Running power flows by imposing minimum voltage limits while keeping the substation power factor at 0.894 leads to infeasibility.

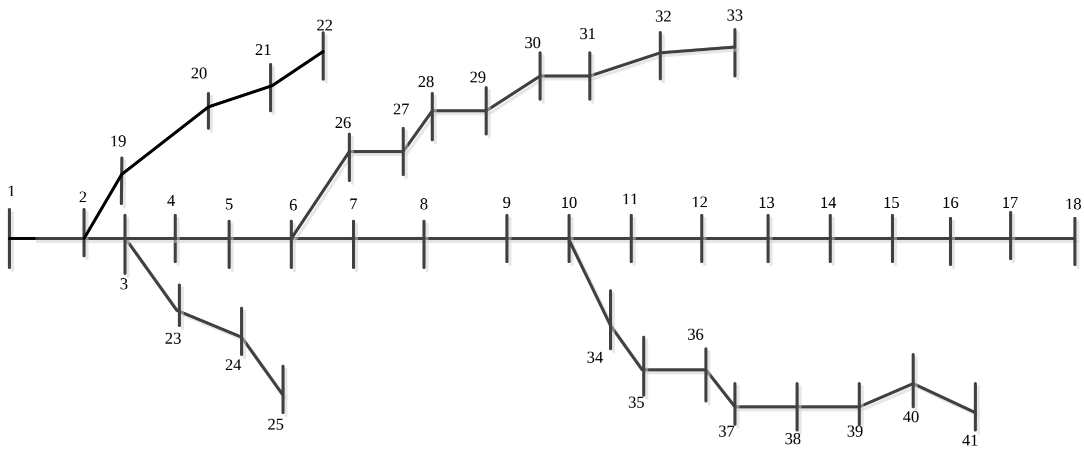

Figure 6.1 - Single-line diagram of the IEEE 41-bus distribution network system.

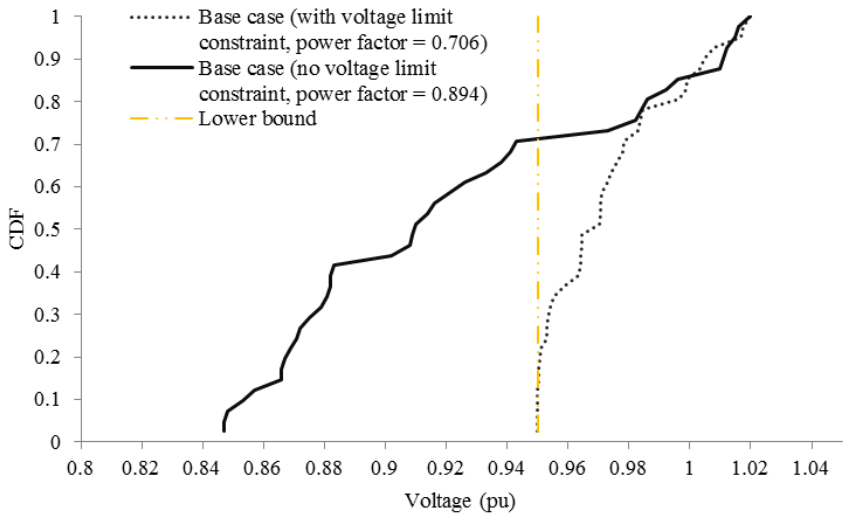

Figure 6.2 - Cumulative distribution function (CDF) of voltages in the base case.

This may be because of the high reactive power requirement in the system, which has to be provided by the substation given the fact that there the system is not well-compensated. Reducing the power factor of the substation to 0.706 results in a feasible solution but around 40% of the voltages are yet very close to the minimum value.

The following assumptions are made when carrying out the simulations:

- A 3-year planning horizon is considered, which is divided into yearly decision stages.
- The interest rate is set to 7%.
- Electricity price at the substation follows the same trend as the demand i.e. electricity price and demand profile are 100% correlated.
- For the sake of simplicity, maintenance costs are taken to be 2% of the corresponding investment costs.
- The expected lifetime of capacitor banks and energy storage systems is assumed to be 15 years [171], [172], while that of DGs and feeders is 25 years [71].
- A 5% voltage deviation is considered to be the maximum allowable deviation from the nominal value that one can have in the system nodes i.e. $-0.95V_{nom} \leq V_i \leq 1.05V_{nom}$.
- The power transfer capacity of all feeders is assumed to be 6.986 MVA.
- All big-M parameters in the model formulation are set to 10, which is sufficiently higher than the power transfer capacity of all feeders.
- When linearizing quadratic terms in the developed planning model, the number of partitions is set equal to 5. This balances well accuracy with computation burden, as concluded in [94].
- The efficiency of the bulk ES is assumed to be 90%.
- The unit cost of capacitor banks is assumed to be €25/kVAr.
- The size of the minimum deployable capacitor bank is considered to be 0.1 MVAr.
- The investment cost of a 1.0 MW bulk ES, whose energy reservoir is 5 MWh, is considered to be 1.0 M€.

- The emission rate of power purchased is arbitrarily set equal to 0.4 tCO_2e/MWh.
- The investment cost of a given feeder is assumed to be directly proportional to its impedance i.e. $C_{ij} = \alpha * Z_{ij}$ where the proportionality constant α is 10,000 €/Ω.
- Wind and solar type DGs, each with a 1 MW installed capacity, are considered as potential candidates to be deployed in the system. The investment costs of these generators are assumed to be 2.64 M€ and 3.00 M€, respectively.
- Electricity demand in the first, the second and the third planning stages is assumed to be 5%, 10% and 15% higher than the demand in the base-case, respectively.
- The emission prices in the first, second and third stages are set to 25, 45 and 60 €/tCO_2e, respectively.
- Variable power generation sources (wind and solar, in particular) are assumed to be available in every node. This assumption emanates from the fact that distribution networks span over a small geographical area. Hence, the distribution of resources in this area can be considered to be the same.
- The substation node (node 1) is considered as a reference; hence, its voltage magnitude and angle are set to $1.02 * V_{nom}$and 0, respectively.
- The cost of unserved energy is set to 3000 €/MWh.

6.4.2 A Strategy for Reducing Combinatorial Solution Search Space

In the case study presented above, all nodes in the system are assumed to be candidates for the placement of DGs, ESS and capacitor banks. However, this is not possible when the planning work is carried out on large-scale DNSs because the size of the problem becomes huge as a result of combinatorial explosion, rendering difficulty in solving the problem.

Owing to this fact, the potential candidate nodes are often predetermined either arbitrarily or using some criteria for the selection such as the level of load, availability of resources, etc. For example, the possible connection points of RES-based DGs are often known a priori based on the availability of primary energy sources (such as wind speed and solar radiation). However, the variation in the availability of wind speed and solar radiation among the connection points in the DNS is not expected to be significant because it normally spans over a geographically small area, where the weather situation is more or less the same.

Here, we show how the combinatorial solution search space can be substantially reduced using a simple heuristic method [89]. The method is based on solving a relaxed version of the original problem. This is done by treating all (normally integer) investment variables as continuous ones, with the exception of the line reinforcement variables. This effectively means fractional investment decisions are allowed.

The method here works by first establishing a threshold for each fractional investment solution (i.e., corresponding to DGs, ESS and capacitor banks).

Then, those nodes whose corresponding values of investment solutions are lower than the preset thresholds are neglected. For instance, consider the investment solution of the relaxed problem corresponding to ESS at each node, as shown in Figure 6.3 In this case, the threshold is arbitrarily set to 0.15. As we can see, for most of the nodes, the investment values corresponding to ESS fall below this threshold. Only those values at the following nodes are significant: $\{14, 18, 29, 30, 31, 32, 37, 38, 39, 40\}$. This set of nodes is hence considered as the most likely locations in the system for ESS placements in the full stochastic mixed integer linear programming (S-MILP) model. It should be noted that such a reduction in possible connection points (from 41 to 10) substantially speeds up the solution process as a result of the combinatorial solution search space. Similarly, the reduced set of nodes for possible capacitor and DG connections are obtained by arbitrarily considering 1.0 and 0.2 as the respective thresholds, as shown in Figures 6.4 and 6.5.

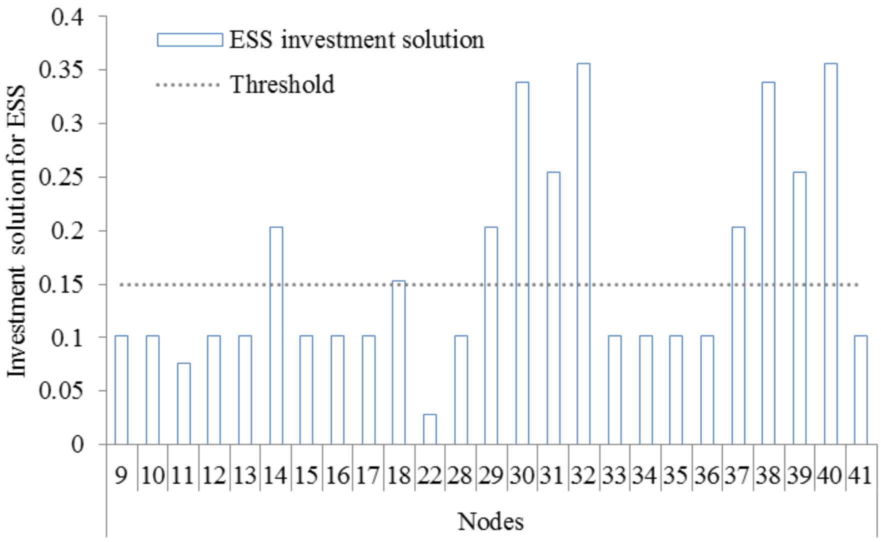

Figure 6.3 - Decision variable for ESS at each node (last stage).

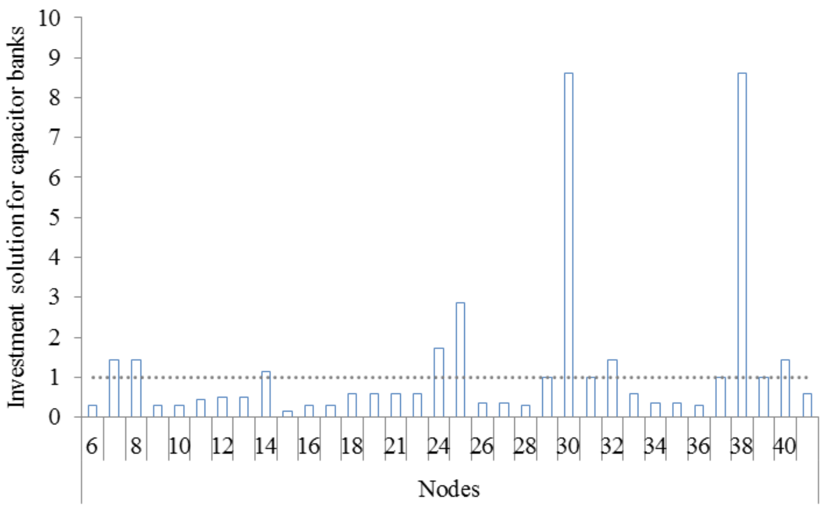

Figure 6.4 - Investment solution for capacitor banks at each node (last stage).

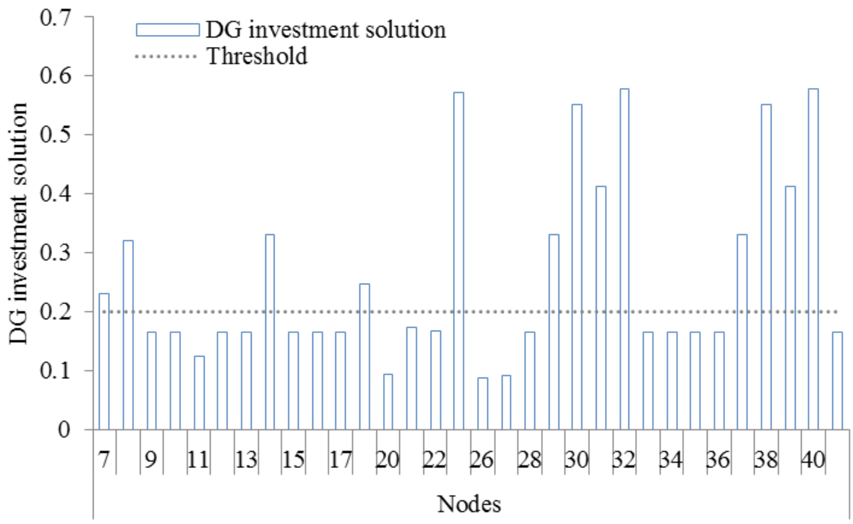

Figure 6.5 - Investment solution for DGs at each node (last stage).

In this case, $\{7, 8, 14, 24, 25, 29, 30, 31, 32, 37, 38, 39, 40\}$ is the reduced set of nodes for capacitor bank connections, while that of DGs is $\{7, 8, 14, 18, 25, 29, 30, 31, 32, 37, 38, 39, 40\}$. Note that the procedure/criterion for setting the threshold in each case is an open question. It may also depend on the nature and the size of the system under consideration. In general, each threshold should be carefully set to a sufficiently low value so that relevant information is not lost (i.e. potential candidate nodes are not excluded). The thresholds in this chapter are set based on the intuition that those nodes, whose investment values are zero or close to zero, are less likely to appear in the final set of solutions.

A deterministic planning model (i.e. considering a single scenario corresponding to the average demand, wind and solar PV power output profiles) is used to evaluate the performance of the heuristic approach proposed here. The results of the deterministic model obtained by applying the heuristic method are compared with that of the "brute force" model i.e. without reducing the set of candidate nodes for DG, ESS and capacitor placements. The investment decisions obtained are the same in both cases but the computational requirements substantially differ from one another. The proposed method helps to significantly reduce the combinatorial solution search space, and thus the computational effort by more than sevenfold. In general, for distribution networks of this size, the proposed heuristic approach may not be needed or a short-list of candidate nodes for DG, ESS and capacitor placement may be made available based on expert knowledge. The problem is tractable without the need of reducing the solution search space as shown in Table 6.1. However, one cannot rely on expert knowledge when the planning involves large-scale distribution network systems. In such problems, and when there is a lack of adequate computing machine, it is critical to employ mechanisms that reduce the combinatorial solution search space. In our case, this relates to reducing the number of candidate nodes for allocating DGs, ESSs and capacitor banks.

Table 6.1 – Computational size of the optimization problem

	Brute-force	Reduced
Number of equations	11,032,828	9,039,895
Number of variables	9,315,028	8,100,028
Discrete variables	720	387
Simulation time (hours)	26.2	3.7

For the case study considered in this chapter, the results obtained by applying the heuristic approach are the same as those obtained with the "brute-force" model which treats every node as a candidate for placement of DGs, ESSs and capacitor banks. However, it should be noted that since the proposed method is heuristic, its performance can be different for different systems. The approach contributes a lot to the solution process; yet, the conclusions drawn from the test results in this chapter cannot be generalized. The authors acknowledge that vital information could be excluded when setting the threshold to reduce the number of candidate nodes. For instance, even if the investment solution at a certain node in the relaxed problem is close to zero, the node could still be feasible for DG, ESS and/or capacitor placement in the full-scale stochastic model. As a final remark, careful analysis of the system under consideration is required when applying the reduction method proposed in this chapter. Table 6.1 compares the size of the problem before and after applying the heuristic combinatorial solution search space reduction method. We can see that the combinatorial solution search space is reduced from 2^{720} to 2^{387}, and this also helps to reduce the number of equations and continuous variables by more than 18% and 13%, respectively.

6.4.3 Results and Discussion

Intermittent power generation sources such as wind and solar PV type DGs normally operate with a fixed lagging power factor [173]. In other words, such generators "consume" reactive power, instead of "producing" and contributing to the voltage regulation in the system (also known as reactive power support). For instance, wind turbines installed in power systems throughout the world are predominantly based on asynchronous generators (also known as induction generators). As mentioned above, one of the typical characteristics of such machines is that they always "consume" reactive power. Because of this, such wind turbines are often operated at a constant power factor. It is well-known that, in power systems, voltage regulation has been traditionally supported by conventional (synchronous) generators. However, this is likely to change in the near future given the upward trend of integrating such resources in power systems. Variable power generators, equipped with reactive power support devices predominantly based on power electronics, are expected to be deployed to enhance their capability to provide reactive power when it is needed in the system. We have carried out the system expansion for two cases: DGs without and with reactive power support capabilities.

The first case assumes that all wind and solar PV generators always "consume" reactive power, and they are operated at a fixed lagging power factor pf_g. The reactive power Q_g, in this case, is given by the product of the actual production of the DG and the tangent of the phase angle between voltage and current i.e. $Q_g = P_g * tan\big(cos^{-1}(pf_g)\big)$. In other words, the ratio between active and apparent power is kept constant. For instance, asynchronous (induction) generators used in conventional wind turbines have such characteristics. Most solar PVs also "consume" reactive power because of the power electronics involved. The second case assumes that all wind and solar PV generators have the capability to "produce" or "consume" reactive power depending on the operational situations, in a "similar" way as conventional power generators. For instance, a variable generation source g in this category is capable of operating between pf_g lagging power factor (reactive) to pf_g leading power factor (capacitive) depending on system requirements i.e. $-P_g * tan\big(cos^{-1}(pf_g)\big) \leq Q_g \leq P_g * tan\big(cos^{-1}(pf_g)\big)$ where P_g is the actual power output of the generator at a particular time and Q_g is the reactive power "produced" or "consumed". The results corresponding for each case are discussed as follows.

6.4.3.1 *Considering DGs Without Reactive Power Support*

The power factor of wind and solar PV type DGs is varied from 0.8 lagging power factor (reactive) to unity power factor [173]. This means such DGs consume reactive power all the time. The system is expanded considering this case, and the expansion results are discussed below.

The optimal solution for capacitor banks, DGs and bulk ES in the system are shown in Tables 6.2 through 6.4, respectively. In general, majority of the investments are made in the first stage. This is because the NPV of operation and emission costs are higher in the first stage than those in any of the subsequent stages. This makes it attractive to invest more in renewables in the first stage than in the other stages so that these costs are drastically reduced.

Table 6.2 – Optimal investment solution of capacitor banks at the end of the planning horizon.

Location	Power factor				
	1.0	0.95	0.9	0.85	0.8
7	6	9	13	3	7
8	1	0	0	5	11
14	3	13	16	20	20
24	0	1	2	2	10
25	3	3	3	9	10
29	0	3	1	12	20
30	8	10	13	9	10
31	1	2	1	7	1
32	2	5	7	2	2
37	1	1	1	8	4
38	9	20	13	8	20
39	1	1	10	7	8
40	2	6	2	2	2
Total MVAr	3.7	7.4	8.2	9.4	12.5

Table 6.3 – Optimal investment solution of DGs at the end of the planning horizon

DG type	Location	Power factor				
		1.0	0.95	0.9	0.85	0.8
PV	29	0	0	0	1	0
PV	32	0	1	0	0	0
PV	38	1	1	0	0	1
PV	39	0	0	1	0	0
Wind	7	0	1	1	0	1
Wind	14	3	3	3	3	3
Wind	25	0	0	0	1	1
Wind	29	0	1	0	1	3
Wind	30	2	0	1	0	0
Wind	31	0	0	0	1	0
Wind	32	1	1	1	0	0
Wind	37	0	0	0	1	0
Wind	38	2	1	1	0	1
Wind	39	0	1	1	1	1
Total (MW)		9	10	9	9	11

Table 6.4 – Optimal investment solution of ESS at the end of the planning horizon

Location	Power factor				
	1.00	0.95	0.90	0.85	0.80
14	2	2	2	2	2
30	0	1	2	0	0
31	0	0	0	1	0
32	2	1	1	0	2
38	2	0	0	2	0
40	0	1	1	1	1
Total (MW)	6	5	6	6	5

As we can see in Table 6.2, the optimal location of capacitor banks mostly coincides with high load connection points (nodes) as well as with those closer to the end nodes. This is expected from the system operation point of view because capacitor banks are required at such nodes to meet the reactive power requirements and thus keep the corresponding voltages within allowable operational limits. Otherwise, the voltages are expected to drop at these nodes without a reactive power compensation mechanism put in place. As shown in Table 6.2, the total size of investment in capacitor banks required throughout the planning horizon varies from 3.7 MVAr at unity power factor to 12.5 MVAr at 0.8 lagging power factor, most of which are installed in the first stage of the planning horizon.

As shown in Table 6.4, more investments are made in wind than in solar PV type DGs. This is because of the higher capacity factor of potential wind power generators compared to solar PV ones. In general, the total MW of DG power installed at each node throughout the planning horizon is shown in Table 6.4.

Here, it can be observed that the overall optimal size of DGs integrated into the system remains more or less the same regardless of the power factor setting. However, the optimal placements of the installed DGs are in some cases different for different power factor settings. It is worth mentioning here that majority of these investments are made in the first stage of the planning horizon. This may be due to the absence of investment constraints or because the NPV cost of operation and emissions is higher in the foremost stages than in the following ones. The results in Tables 6.2 through 6.4 show the strong relationships among the optimal investment solutions. For instance, Table 6.2 indicates that the lower the power factor is, the higher the investment requirement in capacitor banks is. This is due to the increasing reactive power consumption by the DGs. Unlike in capacitor banks, the total amount of DGs and ESSs installed in the system (see Tables 6.3 and 6.4) do not show significant variations with the reactive power settings. This is an indication that capacitor banks play a vital role in maintaining system integrity and stability as well as ensuring essentially the same level of DG integration regardless of the power factor setting. The results in Tables 6.3 and 6.4 also reveal that, the bulk ESSs and DGs in particular are optimally located close to one another. This is mainly because placing the ESSs close to the RES-based DG connection points ensures optimal utilization and integration of such DGs in the system.

It is well known that bulk ESS can bring significant benefits such as load following, power stability improvements, and enhancing the dispatchability of RESs from the system operator’s point of view according to their operation modes. Likewise, the optimal deployment of capacitor banks also brings substantial benefits to the system. The combination of all these entirely helps one to dramatically increase the size of RES-based DGs (up to 11 MW) that can be integrated into the system without violating system constraints. The optimal size of DGs would, otherwise, be limited to less than 3 MW [174]. It is interesting to see here that the integration of ESSs and capacitor banks has such a dramatic impact on the level of DG integration. This is due to the fact that ESSs and capacitor banks bring about significant flexibility and control mechanism to the system. Substantial improvements in voltage controllability are also clearly visible in Figures. 6.6 and 6.7 corresponding to a power factor setting of 0.95. These figures show the voltage deviation profiles at each node with the selected operational situations (which can alternatively be understood as “long hours”) without and with system expansion, respectively. In the base case (shown in Figure 6.6), one can see that some of the node voltage deviations (especially those at the extreme nodes) tend to be very close to the minimum allowable limit. On the contrary, all node voltages largely stay very close to the nominal one (with an average deviation of approximately 1.5 %), leaving significant margins to the operational limits. Alternatively, Figure 6.8 conveniently shows the variance of the voltage deviations at each node. It is also evident to see here that the variance of most of the deviations is very low. The highest variances at nodes 20 to 22 are due to high impedance of the feeder connected between nodes 19 and 20. The same reasoning explains the relatively high variances in the voltage deviations between nodes 13 and 18. However, these variances are negligible when put in perspective with the square of maximum deviation, i.e. $(2 * \Delta V^{max}/V_{nom})^2$, which in this case is approximately $(2 * 0.05)^2 \approx 1.0\ \%$. In general, such a substantial improvement in voltage controllability has come from the combined effect of expansion decisions in DGs, ESSs and capacitor banks.

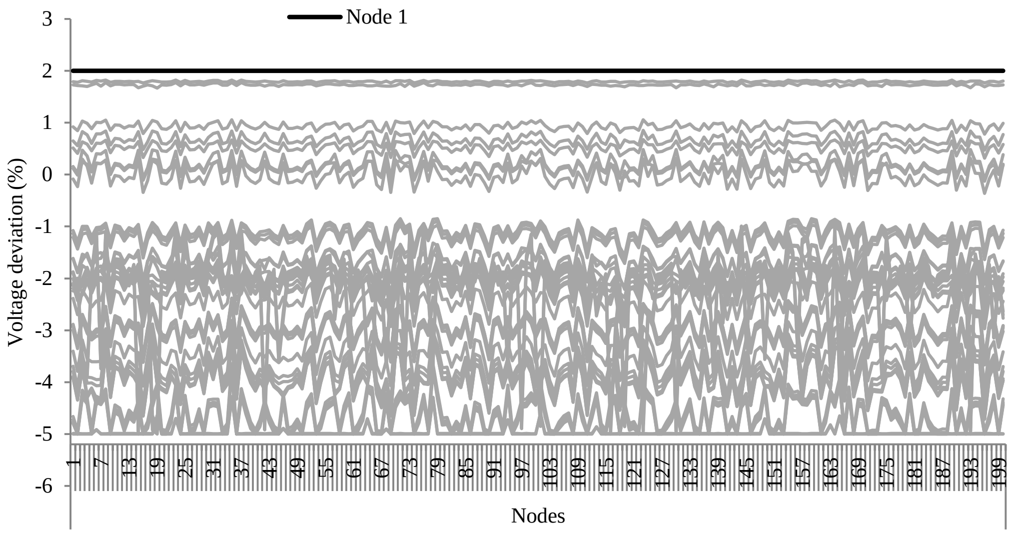

Figure 6.6 - Profiles of voltage deviations without system expansion in the first stage.

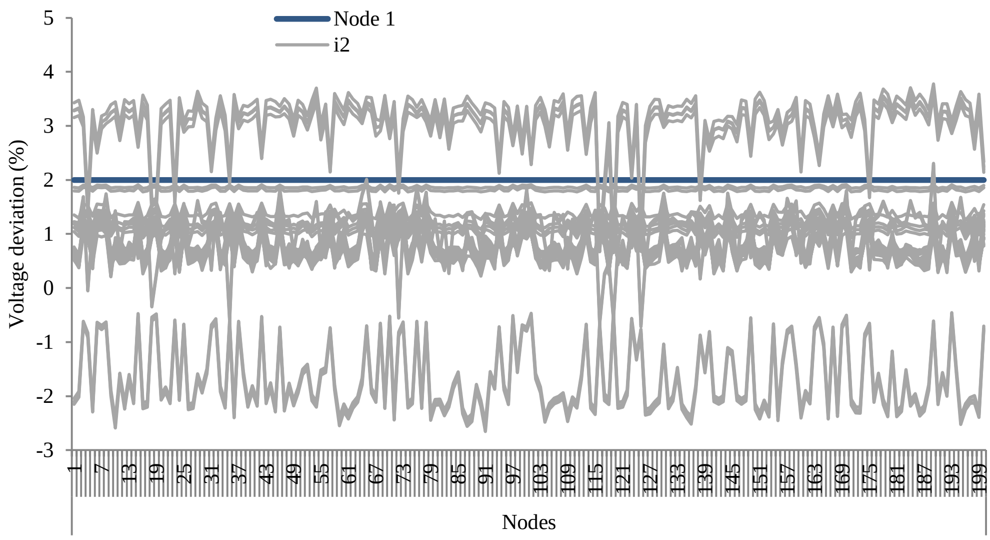

Figure 6.7 - Profiles of voltage deviations at each node after expansion in the first stage.

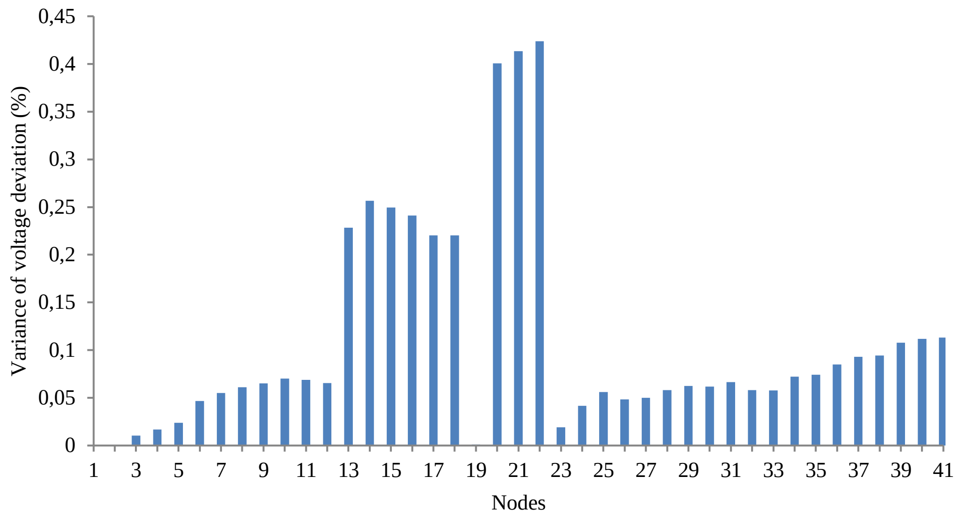

Figure 6.8 - Variance of voltage deviations at each node as a result of variations in system operational states.

Other important aspects in this expansion analysis are related to the impact of system expansion on the network losses and investments. Figure 6.9 shows a comparison of the network losses in the base case and with expansion for every operational state. We can see a significant reduction in network losses in the system (by nearly 50% on average) after the expansion planning is carried out. This is one of the major benefits of integrating DGs in the system. Concerning investments in lines, in this particular case study, not a single feeder is selected for reinforcements. This clearly indicates that a properly designed integration of DGs leads to substantial network reinforcement/investment deferrals.

Table 6.5 summarizes the analysis results, showing the variations of different system variables for different values of power factors.

Figure 6.10 also conveniently plots the trend of wind as well as combined solar and wind energy production shares for different power factor values. The results in this figure show that the wind energy production share increases when the power factor is further reduced. This may be because of the inherent characteristics of wind power production. In most cases, the availability and strength of wind speed is higher during low demand consumption hours (during night and early morning hours for instance) and lower during peak hours. This is directly related to the power production. During valley hours, the wind turbines act as reactive power sinks.

In relation to this, it can generally be observed that the lower the power factor is, the higher the reactive power consumed by the wind turbines. This may improve system efficiency and pave the way to higher wind power production. Hence, this may justify their increasing share of power production with decreasing power factor.

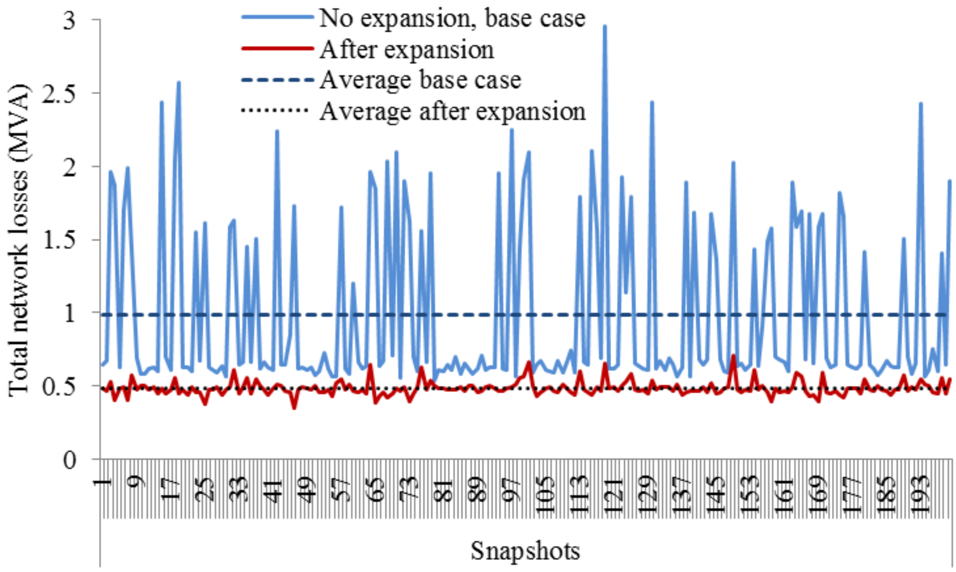

Figure 6.9 - Network losses with and without system expansion (first stage).

Table 6.5 - Values of system variables with varying power factor of RES-based DGs

	Power factor	1.0	0.95	0.9	0.85	0.8
Total energy production (MWh)		179329	175545	176024	178848	172037
RES energy production share (%)	Wind	44.00	45.08	45.23	46.31	46.90
	PV	0.71	2.02	4.31	2.39	1.96
	Wind+PV	44.71	47.10	49.54	48.69	48.86
Cost terms (M€)	Investment cost	33.94	35.88	34.35	35.69	38.91
	Maintenance Cost	9.47	9.47	9.53	9.43	10.10
	Emission Cost	9.44	8.10	8.08	8.12	6.76
	Energy Cost	29.31	27.10	27.65	27.20	25.22
Total cost (M€)		82.16	80.55	79.61	80.44	80.99
Investment decisions	Storage (MW)	6	5	6	6	5
	Capacitor (MVAr)	3.7	7.4	8.2	9.4	12.5
	DG (MW)	9	10	9	9	11
	Line reinforcements	1	3	1	1	2
Average active power losses in stage 1 (MW)		0.448	0.440	0.430	0.441	0.448
Average reactive power losses in stage 1 (MVAr)		0.339	0.745	0.983	1.098	1.602

Contrary to the case with wind type DGs, the peak power production of solar PV based DGs occur around the peak hours of consumption. This means that, unlike the wind type DGs, their contribution to the system as reactive power sinks during valley hours is limited.

Hence, as can be seen in Figure 6.11, the optimal power factor setting for such DGs seems to be 0.9. In general, this also seems to be the optimal power factor setting for the system because this results in the highest share of combined wind and solar PV energy production (see Figure 6.10). Besides, as can be seen in Table 6.5, the lowest overall cost (79.61 M€) as well as the lowest active power losses (0.430 MW) are achieved when the power factor is set to 0.9.

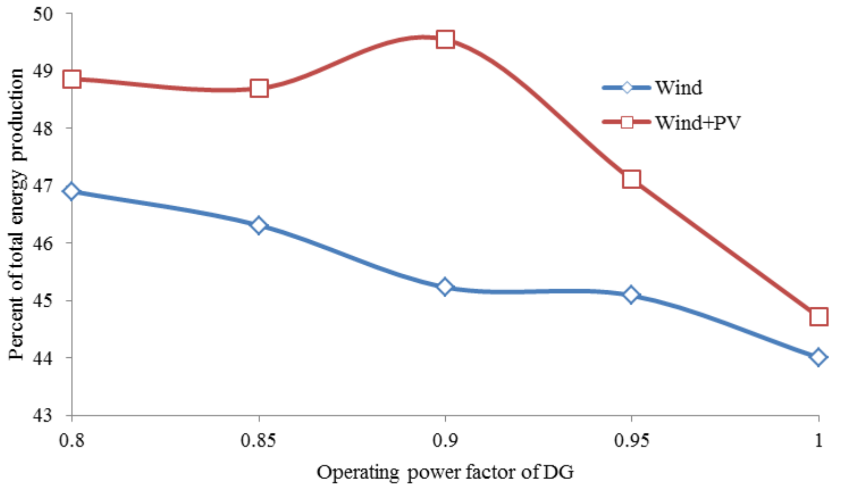

Figure 6.10 - Evolution of solar and wind energy production share with varying power factor.

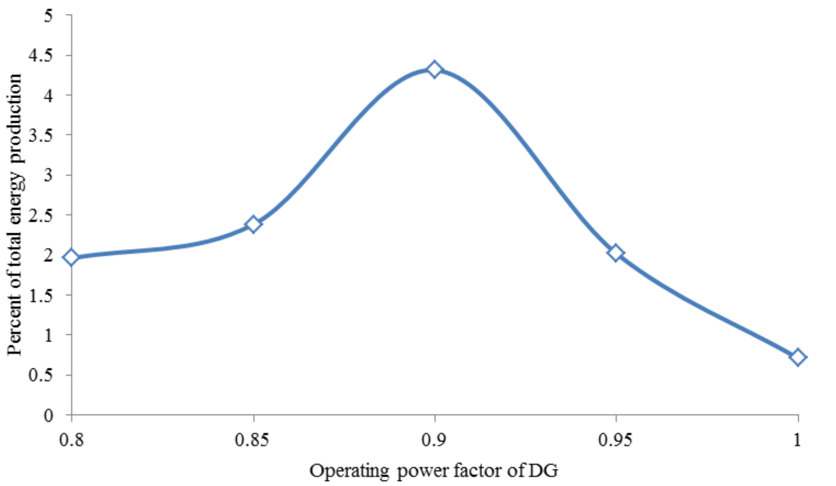

Figure 6.11 - Evolution of solar PV energy production share with varying power factor.

As shown in Table 6.5, the amount of installed reactive power sources (capacitor banks, in this case) as well as the reactive power losses in the system increase with decreasing power factor. This is expected because the lower the power factor is, the higher the reactive power requirement of the DGs is. Transporting the reactive power generated by such reactive power sources increases the reactive power losses in the system.

The impact of varying power factor on the voltage profile in the system is also investigated. Figures 6.12 and 6.13 illustrate the changes in the voltage profiles as a result of changing the power factor during peak and valley hours, respectively. In both cases, there are no significantly visible variations in voltage profiles regardless of the power factor settings, except for some nodes as in Figure 6.13.

The average voltage deviations at each node for different power factor settings are also shown in Figure 6.14. In general, based on the results in Figures 6.13 and 6.14, there is no clear indication to say that one power factor setting is better than the other; it can be observed that what is deemed good for one node may be “bad” for another one. However, it is worth mentioning here that the voltage profiles are significantly improved as a result of simultaneously integrating DG, ESS and capacitor banks. The voltage deviations for those nodes, where DGs and capacitor banks are connected to, seem to be higher in absolute terms; yet, they remain within the permissible range.

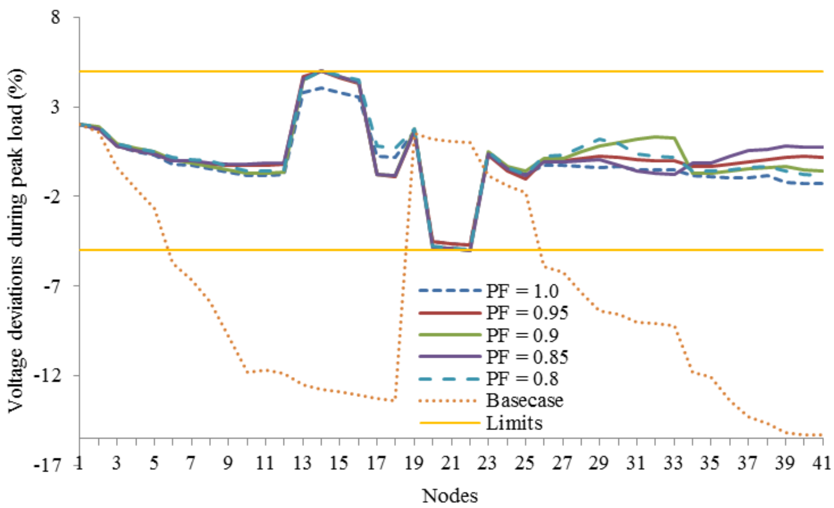

Figure 6.12 - Voltage deviation at each node during peak demand hour for different power factor values.

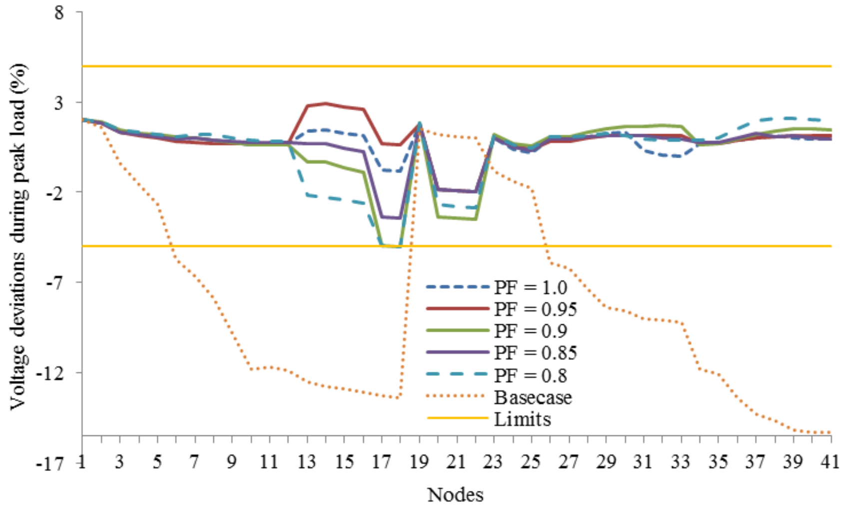

Figure 6.13 - Voltage deviation at each node during valley hour for different power factor values.

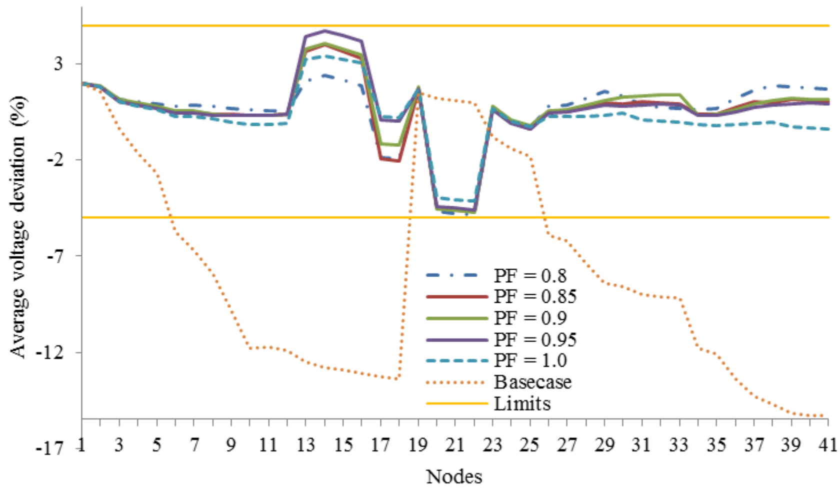

Figure 6.14 - Average voltage deviations at each node for different power factor values.

6.4.3.2 *Considering DGs With Reactive Power Support*

Nowadays, RES-based DGs (wind and solar types) are required to adhere to certain grid codes such as reactive power support, voltage ride through, etc. to alleviate the negative impacts of integrating such DGs in the system. Examples in this case are doubly fed induction generator (DFIG) based wind turbines and voltage-source inverter (VSI) based PV generators. In some systems, the grid codes are already being enforced, and consequently wind/solar PV farms are required to operate from 0.95 lagging to 0.95 leading power factor [175].

For the analysis in this section, wind and solar PV type DGs with reactive power support capability are considered in the simulations. The power factor is varied to investigate its effects on selected system variables, and the results are summarized in Table 6.6. The results here show that the optimal power factor setting for the wind type DGs seems to be 0.95 because this leads to the highest wind energy production level (47.13%) compared to any other setting. This is also clearly shown in Figure 6.15. The combined share of wind and solar PV energy production also peaks when the power factor is set to 0.95, as depicted in Figure 6.15.

From Table 6.6 and Figure 6.16, one can see that the overall cost (which is the sum of investment, maintenance, emission and energy costs) is the lowest at the same power factor (79.40 M€). The lowest active power losses seem to however occur at a power factor of 0.9.

The profiles of average voltage deviations at each node corresponding to different power factor settings are shown in Figure 6.17. Figure 6.18 also depicts the voltage deviations at each node corresponding to the valley hour of electricity consumption. One can see that there are no significant differences in these profiles, except for nodes where the distributed energy resources (DG, ESS and reactive sources) are connected to. The voltage variations at these nodes with the changes in power factor settings can be explained by the fact that the amount of each distributed energy resource installed at these nodes is different for different power factor values (see Table 6.6).

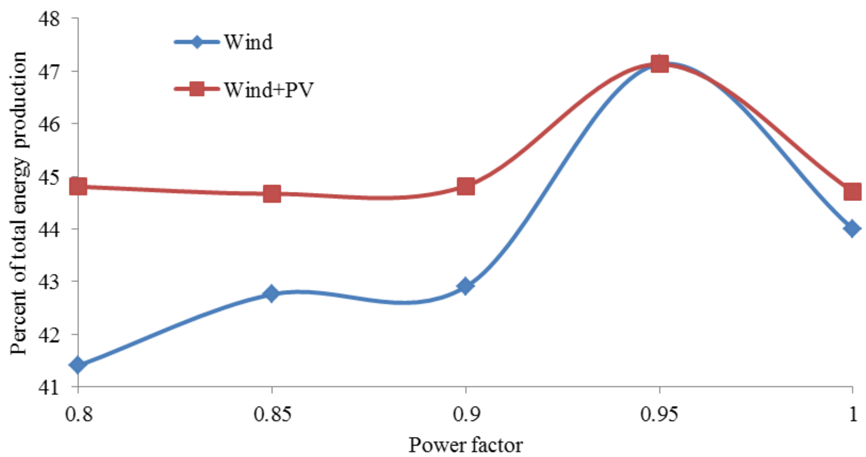

Figure 6.15 - Evolution of wind and solar PV energy production share with varying power factor.

Table 6.6 – Values of system variables with varying power factor of RES-based DGs

	Power factor	1.00	0.95	0.9	0.85	0.80
Total energy (MWh)		179329	179329	179851	175527	176027
RES energy production share (%)	Wind	44.00	47.13	42.90	42.76	41.41
	PV	0.71	0.00	1.91	1.91	3.40
	Wind+PV	44.71	47.13	44.82	44.67	44.81
Cost terms (M€)	Investment cost	33.94	33.18	33.09	31.68	32.56
	Maintenance Cost	9.47	9.98	8.92	9.00	8.48
	Emission Cost	9.44	8.07	9.38	9.44	9.40
	Energy Cost	29.31	28.17	29.04	29.49	28.76
Total cost (M€)		82.16	79.40	80.43	79.61	79.20
Investment decisions	Storage (MW)	6	8	5	6	4
	Capacitor (MVAr)	3.7	3.4	3.3	7.9	5
	RES (MW)	9	8	9	8	9
	Line reinforcements	1	1	8	0	7
Average active power losses in stage 1 (MW)		0.448	0.437	0.425	0.427	0.448
Average reactive power losses in stage 1 (MVAr)		0.339	0.629	0.797	0.904	1.06

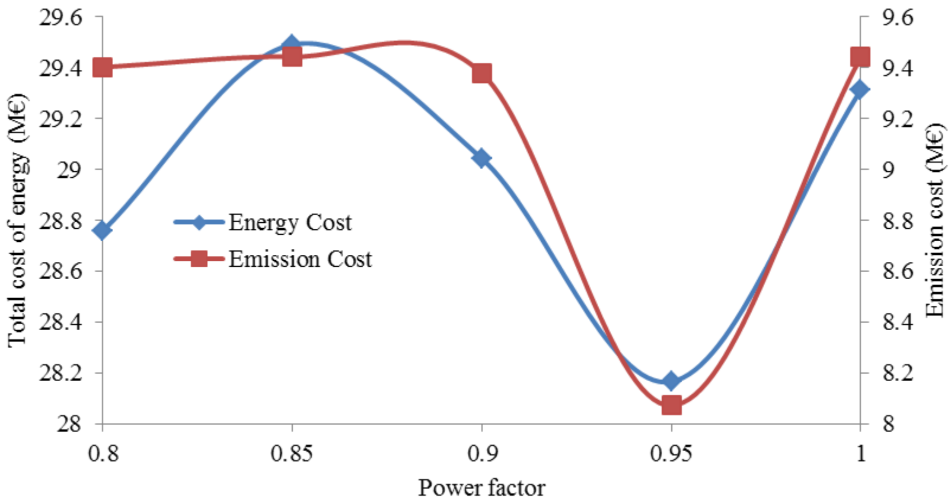

Figure 6.16 - Evolution of total energy and emission costs with varying power factor.

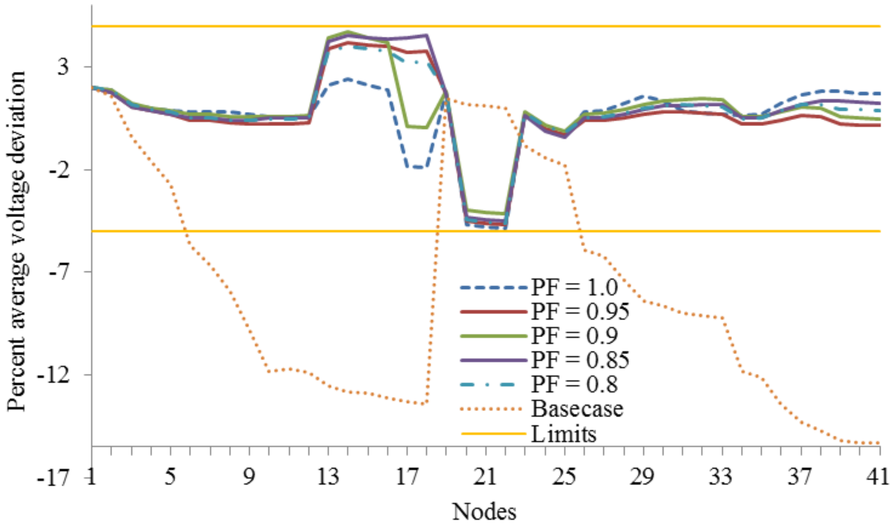

Figure 6.17 - Average voltage deviations at each node for different power factor values.

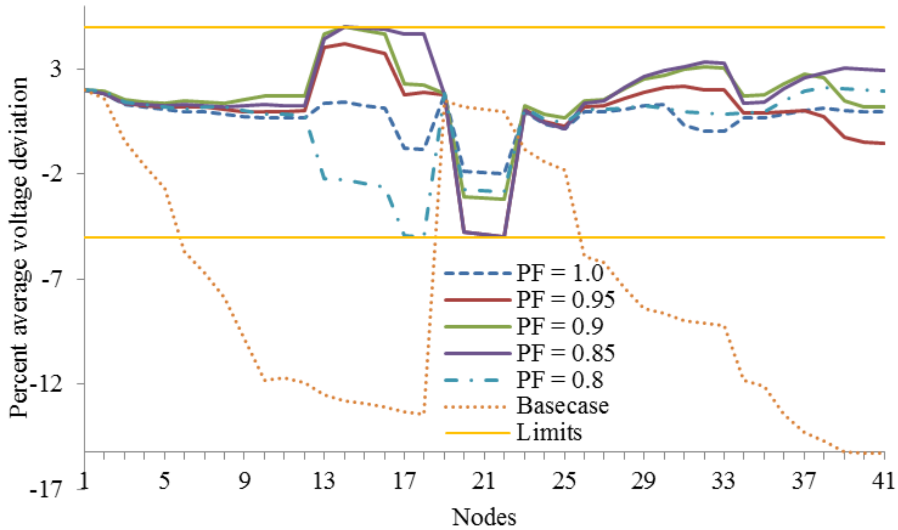

Figure 6.18 - Voltage deviations at each node during valley hour for different power factor values.

Comparing the results in Tables 6.5 and 6.6, one can observe that the consideration of reactive power support capability in the planning process results in a slight reduction in the objective function value (overall cost) and about 5% increase in the wind energy production share. In addition, as illustrated in Tables 6.5 and 6.6, when DGs with reactive power support capability are considered, losses in the system are lower than when DGs without such capability are instead installed.

6.4.3.3 *Impact of Wind Turbine and Solar PV Selections on the Results*

To carry out this analysis, the wind and solar PV DGs are assumed to operate from 0.95 lagging to 0.95 leading. Two wind turbine sizes, with 1.0 MW and 2 MW capacities respectively, are considered for the analysis here. Similarly, solar PV units with 1.0 and 1.5 MW installed capacities are used here as candidates for investment. Note that the results in the previous subsection correspond to wind and solar PV type DGs both with a 1.0 MW capacity. The results corresponding to the second case, presented here, are compared with those corresponding to the 0.95 power factor setting in Table 6.6, also reproduced in Table 6.7.

The differences in the results of both cases are visible. For instance, the total MW RES installed in the system increased from 8 MW in the previous case to 13.5 MW when wind turbines of 2.0 MW are used. As a result, the share of combined wind and solar PV energy production throughout the planning horizon is nearly 30% higher when DGs with higher capacity are installed. In addition, all cost terms and active power losses are lowered as a result of investing in DGs with higher installed capacities.

Table 6.7 – Values of system variables with different sizes of RES-based DGs

	Wind/ solar PV size(MW)	1.0/1.0	2.0/1.5
Total energy (MWh)		179329	167330
RES energy production share (%)	Wind	47.13	59.05
	PV	0.00	1.44
	Wind+PV	47.13	60.49
Cost terms (M€)	Investment cost	33.18	37.57
	Maintenance Cost	9.98	9.85
	Emission Cost	8.07	6.67
	Energy Cost	28.17	24.36
Total cost (M€)		79.40	78.45
Investment decisions	Storage (MW)	8	5.0
	Capacitor (MVAr)	3.4	3.3
	RES (MW)	8	13.5
	Line reinforcements	1	1
Average active power losses in stage 1 (MW)		0.437	0.408
Average reactive power losses in stage 1 (MVAr)		0.629	0.742

Surprisingly, the storage requirement (5 MW) is significantly lower when wind turbines with higher installed capacity are used than in the other case (8 MW) as shown in Table 6.7, while the reactive power requirement is almost the same for both cases. The average voltage profiles of both cases in the system are also very similar (as shown in Figure 6.19).

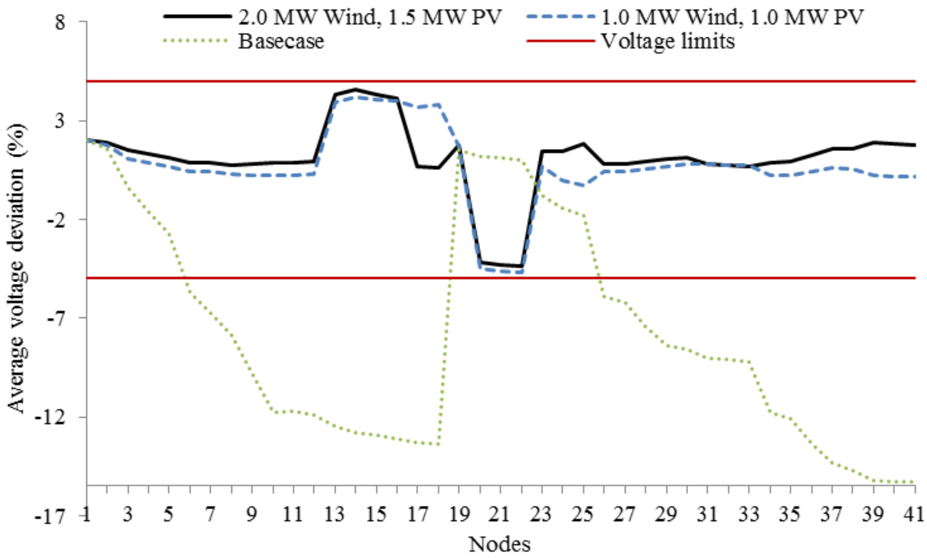

Figure 6.19 - Average voltage deviations at each node for different DG sizes.

6.5 Chapter Conclusions

A new dynamic and stochastic mathematical model of an integrated distribution system planning problem was proposed in this chapter. The results showed that the simultaneous integration of ESSs and reactive power sources largely enabled a substantially increased penetration of variable generation (wind and solar) in the system, and consequently reduced system costs and network losses as well as deferred network expansion or reinforcement needs, which is of crucial importance. For the case study, up to 13.5 MW installed capacity of wind and solar power has been added to the system within a three-years planning horizon. One can put this into perspective with the base-case peak load of 4.635 MW in the system. This means it has been possible to integrate RES power more than twice the peak demand in the base case. Generally, it has been unequivocally demonstrated that the joint planning of DGs, reactive power sources and ESS, proposed in this chapter, brings about significant improvements to the system, such as reduction of losses, electricity cost and emissions. Besides, the proposed modeling framework considerably contributes to improved voltage profile in the system. This in turn leads to an increased voltage stability margin in the system, which is essential for a normal/secure operation of the system as a whole. Overall, the novel planning model proposed here can be considered as a major leap forward towards developing controllable grids, supporting large-scale integration of RESs.

Chapter 7

Conclusions, Directions for Future Work and Contributions

In this chapter, the main conclusions of the thesis are highlighted on the basis of answering the research questions that constituted the main motivation of this research. The limitations of the work in this thesis, and some directions of future work are also discussed. Finally, the contributions of this work are highlighted by presenting the set of publications, in journals with high impact factor (first quartile), as book chapters or in conference proceedings of high standard (IEEE), leading to this thesis work.

7.1 Main Conclusions

The main conclusions drawn from the thesis work, pertaining to the research questions presented in Section 1.6, are summarized as follows. For the sake of clarity the research questions are reproduced here.

- ***What is the current status of RES penetration across the world (with a special focus at distribution levels)? What are the main impeding factors for RES integration? How can the potential benefits of RESs be reaped without significant negative consequences?***

  An increase in an overall world trend in the awareness of climate change and the need for mitigation efforts is bringing forth huge increase in the deployment of renewable energy in comparison to fossil fuel energy sources. The landmark that signals the dawning of this “renewables age” goes hand in hand with the degree of advancement in technologies and a higher level of RES penetration, which is being achieved around the world. Furthermore, there are several driving factors for these remarkable growths, among which are favorable government support policies and increasing competitiveness in costs. After several decades of efforts in research and continuous development in RESs, the yearly growth in the capacity of these plants is becoming greater than the total investment capacity added in power plants based on coal, natural gas and oil, all combined together. Nowadays, RESs have reached a significant level of share in energy supply options, becoming one of the prominent global alternative power supply sources. This trend will continue to increase at faster rates as long as the world’s desire for industrial-scale clean energy sources is on the higher side.

Thus, there is a global consensus on climate change mitigation and curbing GHG emissions which along with energy dependence, security and other structural issues are forcing states to create new market policies and the introduction of new energy policies (in particular, policies related to RESs that support the development and effective utilization of RESs). The integration of RESs in the electrical systems (particularly at distribution levels) is expected to accelerate in the years to come as a result of the recent agreement among several countries to limit GHG emissions and mitigate climate change. The level of DG integrated in distribution systems follows an upward trend, and there is a general consensus that DGs will contribute immensely to the effort of solving a multitude of global and local concerns, including the realization of RES integration goals set forth by different entities.

The latest global trends in RES investment status reports indicate that renewables represented a 58.5% of net additions to global power capacity in 2014, with significant growth in all regions, which represents an estimated 27.7% of the world's power generating capacity, enough to supply an estimated 22.8% of global electricity demand. Wind, solar and biomass power generations reached an estimated 9.1% of the world's electricity in 2014, up from 8.5% in 2013. According to a renewables status report, the overall cost-cutting achieved to date helped to ensure such a strong momentum in 2014, reaching an investment boom up to 29% in solar, and 11% in wind technologies, and geothermal managing to raise 23%. Among the several renewable energy types, large-scale hydro was the one that showed the highest growth in terms of new investments. However, excluding this one, wind and solar were the ones that grew the most (62 and 56 GW respectively) in terms of new installed capacity, well above the corresponding values in 2014. For the first time in 2015, the amount of investment in RES generation made in the developing countries worldwide exceeded the investment made in developed economies. However, with the new capacity conventional generation added, the generation from clean energy in the world in 2015 covered only 10% of world's electricity demand. However, this avoided an amount of CO_2 emissions equivalent to 1.5 Gigatons in 2015.

Moreover, despite the robust growth of integration RESs in many power systems, there are still certain challenges and barriers that impede the smooth integration of RESs. These challenges and barriers can be broadly classified into two categories: technical and non-technical. The non-technical category includes challenges and barriers related to capital costs, market and economic issues, information and public awareness, socio-cultural matters, the conflict between stakeholders, regulation and policy. Most of the challenges and barriers explained before have proven solutions that happen to be overlooked in many systems; therefore, they are preventing the spread of RES development across the world.

In general, arising from the comprehensive overview of RES carried out in **Chapter 2**, these are summarized as follows:

1. Market and economic barriers can be fixed by streamlining appropriate market and economic signals related to carbon taxes, emission trading schemes, finances and incentive mechanisms, as well as enhancing public support for R&D and creating a conducive environment for RES development. All this can have a considerable positive impact on the level of RES integration.
2. Setting energy standards, continuous information campaigns and technical training about RESs and their benefits can enhance public knowledge and awareness, which can in the end have supportive roles in RES development.
3. Creating an enabling environment for R&D, improving technical regulations, scaling up international support for technology transfer, liberalizing energy industries, providing incentive packages to RES developers, designing appropriate policies of RESs and conventional energy sources to minimize the regulatory and policy barriers to developing RESs.
4. Coordinating investments of RESs based on variable generation resources such as wind and solar power with large-scale energy storage systems, demand side management participation and grid expansion can significantly increase the level of RES integration.
5. Enhancing operation and the flexibility of conventional power generation sources can also be very useful to scale up RES integration.
6. Designing an efficient wholesale market such as dynamic retail pricing and developing coordinated operation and planning tools (such as joint network and generation investment planning models) can have a positive role in RES integration.
7. For full utilization of RESs, the coordination between distribution system operators (DSOs) and transmission system operators (TSOs) is also vital.
8. It is also important to improve prediction tools, monitoring and control protocols that can help efficient utilization of the RESs.
9. Ensuring regional interconnections via regional cooperation and increasing the level of participation of all stakeholders (including RES generators) in voltage control, provision of reserves, reactive power support, etc., are significantly helpful for the stated purpose.
10. Using smart-grid technologies and concepts are also expected to facilitate a smooth integration of large-scale RESs because these are equipped with advanced control and management tools to counterbalance the intermittent nature of most RES energy productions.

- ***What are the parameters of uncertainty and/or variability that most influence the decision-making process in terms of investment solutions in DGs (especially, renewables)?***

  The various sources of uncertainties and/or variability in DG investment planning are related to the variability and randomness of operational situations. Therefore, the combined effect of the variability and uncertainty is of utmost importance so that an economic integration of DGs can be carried out in distribution network systems. Accordingly, in **Chapter 3**, a comprehensive sensitivity analysis was carried out to identify the uncertain parameters which significantly influence the decision-making process in DG investments and quantify their degree of influence. To perform the analysis, a DG investment planning model was formulated as a novel multi-stage and multi-scenario optimization problem. Based on the numerical studies, the following conclusions can be drawn:

  1. The results of the numerical analyses generally show that both uncertainty and variability have a meaningful influence on DG investment decisions. In fact, the degree of influence varies from one parameter to another.
  2. The results from the particular case study show that generator outages have little or no impact on the RES-based DG investments; whereas, uncertainty in CO_2 and fuel prices, interest rate and RES power outputs significantly influence investment decisions, especially in variable energy sources. In particular, it has been found out that uncertainty in CO_2 and fuel prices as well as in the interest rate seem to dramatically condition decisions compared to the uncertainty in demand growth and RES power outputs.
  3. In general, the results revealed that ignoring or inadequately considering uncertainty and variability in model parameters has a quantifiable cost.
  4. Based on the extensive analysis, a stochastic modeling of uncertainty related to emission and fuel prices, interest rate, RES power outputs and demand growth is very critical for obtaining robust investment decisions.

- ***How should different sources of uncertainty be modeled in the complex decision-making problem concerning DG investment planning?***

  The advent of emerging solutions such as active management of distribution networks or fully automated and intelligent networks — the so-called smart grids — is expected to keep on facilitating smooth integration of DGs by alleviating existing technical limitations. However, several DG sources are intermittent in nature, making the operation and planning of distribution networks very challenging. This is because such sources introduce significant operational variability and uncertainty to the system.

Hence, in **Chapter 4**, a novel multi-stage stochastic MILP model has been developed to guide the complex decision-making process of DG investment planning in distribution systems in the face of uncertainty. Chapter 4 used the outputs of Chapter 3 to improve the developed model, and make it more robust. The established model features a number of important aspects that should be considered in the decision-making process of a DG investment planning problem:

1. It has an objective function which jointly minimizes cost of emission, operation, maintenance and energy not served;
2. It accounts for the operational variability due to intermittent power sources and electricity demand via probabilistic methods.
3. Uncertainty related to emission price, demand growth and the unpredictability of intermittent generation sources is handled via a stochastic approach.
4. It is based on a dynamic decision framework, i.e., involving a multi-year decision structure.
5. It is anchored on a two-period planning framework, involving short-term and medium/long-term planning windows. This allows obtaining robust short-term decisions in the face of uncertainty along with strategic (or flexible) decisions in the medium to long-term planning horizon.

- ***From a quantitative and qualitative point of view, what are the impacts of network switching and/or reinforcement, as well as deployment of ESSs on the level of renewable power integrated in the system?***

There is a global consensus for the integration of DG sources, especially RESs, as a way to meet the growing demand for electric energy and to reduce the carbon footprint of energy production. Nevertheless, the realization of this considerable objective faces two big challenges. The first challenge is related to the variability and uncertainty introduced on the system by RESs. The second one is related to the stability of the system and quality of energy supplied. To overcome these challenges, it is necessary to integrate a set of enabling technologies, as well as to design an effective coordination mechanism among different technologies in distribution systems.

Hence, in **Chapter 5**, a stochastic MILP optimization model has been developed to investigate the impacts of installing ESSs as well as network switching on the level of renewable power integration in a distribution network system. The resulting model is equipped with the necessary tools to jointly optimize the placement, timing and sizing of RES-based DGs and ESSs in coordination with optimal network reconfiguration, while respecting a number of technical, economic and environmental constraints.

The results have showed that:

1. The capability of ESS integration dramatically increased the level and the optimal exploitation of renewable DGs. According to the results obtained, the simultaneous integration of DGs and ESSs resulted in an overall cost and average losses reduction of 60% and 90%, respectively, which is significant.
2. Moreover, as high as 90% RES penetration level seems to be largely possible provided that this is supported by ESS deployments, again noteworthy.
3. The contributions of DG and ESS installations to voltage profile improvement and overall system stability is substantial. The coordinated integration of DGs and ESSs along with reconfiguration leads to the best voltage profile, which is almost flat throughout the system.
4. It was largely demonstrated the fact that large-scale integration of variable energy sources is possible when such energy sources are optimally deployed with ESSs and a mechanism that improve the flexibility of the network is put in place.
5. Therefore, the optimal network reconfiguration, DG and ESS installations (jointly or separately) substantially contributed to voltage stability. In this particular case study, the impact of network switching on RES power integration has not been significant. However, it should be noted that this can be case-dependent; a more frequent switching operation can substantially influence the level of renewable integration.

- ***How can the penetration of renewable energy sources in the power distribution system be maximized with currently available technologies?***

Given the techno-economic factors and global concerns about environmental issues, the integration of renewable energy sources (RESs) cannot be postponed. It is likely that the integration of DGs in distribution systems will go ahead along with smart-grid enabling technologies that have the capability to alleviate the negative consequences of large-scale integration of DGs. In other words, in order to facilitate (speed up) the much-needed transformation of conventional (passive) DNSs and support large-scale RES integration, different smart-grid enabling technologies such as reactive power sources, advanced switching and storage devices are expected to be massively deployed in the near term. To this end, developing strategies, methods and tools to maximize the penetration level of DGs (particularly, RESs) has become very crucial to guide such a complex decision-making process.

Therefore, in **Chapter 6**, a new multi-stage and stochastic model for jointly optimizing the integration of smart-grid enabling technologies such as ESS, reactive power sources, and network switching, reinforcement and/or expansion has been developed to support large-scale renewable integration.

Due the complexity of the issue, this one was analyzed according the several problem aspects, giving rise to the following sub-questions:

- *What is the effect of reactive power support capability on the RES-based DG integration level?*

  Intermittent power generation sources such as wind and solar PV type DGs normally operate with a fixed lagging power factor. In other words, such generators "consume" reactive power, instead of "producing" and contributing to the voltage regulation in the system (also known as reactive power support). For instance, wind turbines installed in power systems throughout the world are predominantly based on asynchronous generators (also known as induction generators). As mentioned above, one of the typical characteristics of such machines is that they always "consume" reactive power. Because of this, such wind turbines are often operated at a constant power factor. It is well-known that, in power systems, voltage regulation has been traditionally supported by conventional (synchronous) generators.

  The results of considering DGs without reactive power support show a strong relationship among the optimal investments. That is, the lower the power factor is the higher the investment requirement in capacitor banks is. This is due to the increasing reactive power consumption by DGs. Unlike in capacitor banks, the total amount of DGs and ESSs installed in the system do not significantly vary with the reactive power settings. This is an indication that capacitor banks play a vital role in maintaining systems integrity and stability as well as ensuring essentially the same level of DG integration regardless of the power factor setting. The results of considering DGs with reactive power support show that the optimal power factor for wind type DG seems to be 0.95 because this leads to the highest wind energy production level compared to any other setting. The combined share of wind and solar PV energy production also peaks when the power factor is set to 0.95. In general, it is demonstrated that the simultaneous integration of ESSs and reactive power sources largely enables a substantially increased penetration of variable generation (wind and solar) in the system.

- *What are the implications of integrating smart-grid enabling technologies in the distribution systems with respect to maximizing RES integration, reducing energy losses, costs and improving voltage profiles?*

  The results showed a substantial improvement in voltage controllability due to the combined effect of expansion decisions in DGs, ESSs and capacitor banks. Such an investment also leads to a significant reduction in network losses in the system (by nearly 50%, on average).

Generally, it has been unequivocally demonstrated that the joint planning of DGs, reactive power sources and ESS, proposed in this thesis, brings about significant improvements to the system, such as reduction of losses, electricity cost and emissions. Besides, the proposed modeling framework considerably contributes to an improved voltage profile in the system. This in turn leads to an increased voltage stability margin in the system, which is essential for a normal/secure operation of the system as a whole.

Comparing the results, it was observed that the consideration of reactive power support capability in the planning process results in a slight reduction in the objective function value (overall cost) and about 5% increase in the wind energy production share. In addition, when DGs with reactive power support capability are considered, losses in the system are lower than when DGs without such capability are instead installed.

7.2 Directions for Future Works

The following points may be further studied in order to broaden the understanding of the topics treated in this thesis:

- With the introduction of enabling technologies, it is necessary to structure the system response in transient state having in view the smart grids implementation.
- Investigate the application of new cluster techniques to improve the performance of the developed algorithms.
- Stochastic models may bear a significant computational burden that may hamper their applicability. Several measures can be applied in order to reduce the computational time required to solve such models. First, modern computing techniques such as grid and cloud computing may be used. Since there are already companies that provide computational power at affordable prices, this proposal promises tractability even for large-scale mathematical programming problems.

7.3 Contributions of the Thesis

7.3.1 Book Chapters

1. **S. F. Santos**, D. Z. Fitiwi, M. Shafie-khah, A. W. Bizuayehu, J. P. S. Catalão, "Optimal sizing and placement of smart grid enabling technologies for maximizing renewable integration", in: *Smart Energy Grid Engineering*, UK: ACADEMIC Press (**ELSEVIER**), ISBN: 978-0-12-805343-0, pp. 47-81, 2017. http://dx.doi.org/10.1016/B978-0-12-805343-0.00003-6

2. **S. F. Santos**, D. Z. Fitiwi, M. Shafie-khah, A. W. Bizuayehu, J. P. S. Catalão, "Introduction to renewable energy systems", in: *Optimization in Renewable Energy Systems*, London, UK: ACADEMIC Press (**ELSEVIER**), 2016 (aceite). http://dx.doi.org/TBD

3. **S. F. Santos**, N. Paterakis, J. P. S. Catalão, "New multi-objective decision support methodology to solve problems of reconfiguration in the electric distribution systems", in: *Technological Innovation for Cloud-based Engineering Systems*, Germany: **SPRINGER**, ISBN: 978-3-319-16765-7, pp. 395-404, April 2015. http://dx.doi.org/10.1007/978-3-319-16766-4_42

7.3.2 Publications in Peer-Reviewed Journals

1. **S. F. Santos**, D. Z. Fitiwi, M. R. M. Cruz, C. M. P. Cabrita, J. P. S. Catalão, "Impacts of Optimal Energy Storage Deployment and Network Reconfiguration on Renewable Integration Level in Distribution Systems", ***Applied Energy*** (**ELSEVIER**), Vol. 185, pp. 44-55, January 2017.
   http://dx.doi.org/10.1016/j.apenergy.2016.10.053
   Impact factor: 5.746; Q1 (First Quartile) journal in ISI Web of Science and Scopus

2. **S. F. Santos**, D. Z. Fitiwi, A. W. Bizuayehu, M. Shafie-khah, M. Asensio, J. Contreras, C. M. P. Cabrita, J. P. S. Catalão, "Impacts of Operational Variability and Uncertainty on Distributed Generation Investment Planning: A Comprehensive Sensitivity Analysis", ***IEEE Transactions on Sustainable Energy***, 2016 (aceite).
   http://dx.doi.org/10.1109/TSTE.2016.2624506
   Impact factor: 3.727; Q1 (First Quartile) journal in ISI Web of Science and Scopus

3. **S. F. Santos**, D. Z. Fitiwi, A.W. Bizuayehu, M. Shafie-khah, M. Asensio, J. Contreras, C.M.P. Cabrita, J.P.S. Catalão, "Novel Multi-Stage Stochastic DG Investment Planning with Recourse", ***IEEE Transactions on Sustainable Energy***, 2016 (aceite).
   http://dx.doi.org/10.1109/TSTE.2016.2590460
   Impact factor: 3.727; Q1 (First Quartile) journal in ISI Web of Science and Scopus

4. **S. F. Santos**, D. Z. Fitiwi, M. Shafie-khah, A. W. Bizuayehu, C. M. P. Cabrita, J. P. S. Catalão, "New Multi-Stage and Stochastic Mathematical Model for Maximizing RES Hosting Capacity—Part II: Numerical Results", ***IEEE Transactions on Sustainable Energy***, 2016 (aceite).
   http://dx.doi.org/10.1109/TSTE.2016.2584122
   Impact factor: 3.727; Q1 (First Quartile) journal in ISI Web of Science and Scopus

5. **S. F. Santos**, D. Z. Fitiwi, M. Shafie-khah, A. W. Bizuayehu, C. M. P. Cabrita, J. P. S. Catalão, "New Multi-Stage and Stochastic Mathematical Model for Maximizing RES Hosting Capacity—Part I: Problem Formulation", ***IEEE Transactions on Sustainable Energy***, 2016 (aceite).
   http://dx.doi.org/10.1109/TSTE.2016.2598400
   Impact factor: 3.727; Q1 (First Quartile) journal in ISI Web of Science and Scopus

6. N. G. Paterakis, A. Mazza, **S. F. Santos**, O. Erdinc, G. Chicco, A. G. Bakirtzis, J. P. S. Catalão, "Multi-Objective Reconfiguration of Radial Distribution Systems using Reliability Indices", ***IEEE Transactions on Power Systems***, Vol. 31, No. 2, pp. 1048-1062, March 2016.
   http://dx.doi.org/10.1109/TPWRS.2015.2425801
   Impact factor: 3.342; Q1 (First Quartile) journal in ISI Web of Science and Scopus

7.3.3 Publications in International Conference Proceedings

1. **S. F. Santos**, D. Z. Fitiwi, A. W. Bizuayehu, J. P. S. Catalão, M. Shafie-khah, "Optimal Integration of RES-based DGs with Reactive Power Support Capabilities in Distribution Network Systems", in *Proceedings of the 13th International Conference on the European Energy Market — EEM 2016 (technically co-sponsored by **IEEE**)*, Porto, Portugal, USB flash drive, 6-9 June, 2016.
   http://dx.doi.org/10.1109/EEM.2016.7521317

2. D. Z. Fitiwi, **S. F. Santos**, A. W. Bizuayehu, M. Shafie-khah, J.P.S. Catalão, "A New Dynamic and Stochastic Distributed Generation Investment Planning Model with Recourse", in: *Proceedings of the 2016 **IEEE** Power & Energy Society General Meeting — PESGM 2016*, Boston, Massachusetts, USA, USB flash drive, July 17-21, 2016.
   http://dx.doi.org/10.1109/PESGM.2016.7741093

3. M. R. M. Cruz, D. Z. Fitiwi, **S. F. Santos**, J. P. S. Catalão, "Influence of Distributed Storage Systems and Network Switching/Reinforcement on RES-based DG Integration Level", in *Proceedings of the 13th International Conference on the European Energy Market — EEM 2016 (technically co-sponsored by **IEEE**)*, Porto, Portugal, USB flash drive, 6-9 June, 2016.
   http://dx.doi.org/10.1109/EEM.2016.7521337

4. D. Z. Fitiwi, **S. F. Santos**, A. W. Bizuayehu, M. Shafie-khah, J. P. S. Catalão, M. Asensio, J. Contreras, "DG Investment Planning Analysis with Renewable Integration and Considering Emission Costs", in: *Proceedings of the* ***IEEE*** *Region 8 International Conference on Computer as a Tool — EUROCON 2015*, Salamanca, Spain, USB flash drive, 8-11 September, 2015.
http://dx.doi.org/10.1109/EUROCON.2015.7313735

5. N. G. Paterakis, **S. F. Santos**, J. P. S. Catalão, A. Mazza, G. Chicco, O. Erdinc, A. G. Bakirtzis, "Multi-Objective Distribution System Reconfiguration for Reliability Enhancement and Loss Reduction", in: *Proceedings of the 2015* ***IEEE*** *Power & Energy Society General Meeting — PESGM 2015*, Denver, Colorado, USA, USB flash drive, July 26-30, 2015.
http://dx.doi.org/10.1109/PESGM.2015.7286524

Appendices

Appendix A

Piecewise Linearization

Notice that equations (3.1.10) and (4.12) contains a quadratic flow term in Chapters 3 and 4, respectively. For the sake of simplicity, the indices are dropped here. This quadratic term is linearized using a first-order approximation as:

$$f_{nm}^2 = \sum_{l=1}^{L}(2l-1)\frac{f_{nm}^{max}}{L}\Delta f_{nm,l} \qquad \text{(A.1)}$$

$$f_{nm} = f_{nm}^{+} - f_{nm}^{-} \qquad \text{(A.2)}$$

$$f_{nm}^{+} \geq 0; f_{nm}^{-} \geq 0 \qquad \text{(A.3)}$$

$$f_{nm}^{+} + f_{nm}^{-} = \sum_{l=1}^{L}\Delta f_{nm,l} \qquad \text{(A.4)}$$

$$\Delta f_{nm,l} \geq \Delta f_{nm,l+1}\ ;\ \forall l < L \qquad \text{(A.5)}$$

where (A.1) represents the piecewise approximation of the quadratic flow variable by considering L segments. In order to use only the first quadrant of the quadratic curve (which is advantageous in terms of reducing problem complexity [94]), the flow variable is decomposed into its forward (positive) and reverse (negative) auxiliary flow variables as in (A.2). Note that both of these variables cannot be nonzero at the same time and are non-negative as enforced by (A.3). Eq. (A.4) ensures that the sum of the step-size flow variables $\Delta f_{nm,l}$ is equal to the flow. Eq. (A.5) guarantees a successive filling of the partitions.

Appendix B

Deterministic Investment Solution

A deterministic DGIP model can be formed by allowing the DG investment variables (in the presented model) to be scenario-dependent, i.e. by assuming a given scenario happens with certainty. The investment solution of each scenario is presented in Table B.1. As it can be seen, the DG investments are particularly sensitive to the variation of CO_2 price. Note that, in Table B.1, T_i (where $i \epsilon \{1,2,3\}$) denotes the time stage in which the corresponding DG is installed.

B.1 DG investment decisions for each scenario and stage.

Scenarios		DGs								
Demand growth	CO_2 price	PV4	P32V5	PV6	PV7	PV8	WD1	WD2	WD3	WD4
Low	Low	0	0	0	0	T1	T1	T1	T1	T1
Moderate	Low	0	0	0	0	T1	T1	T1	T1	T1
High	Low	0	0	0	0	T1	T1	T1	T1	T1
Low	Moderate	0	0	0	T3	T1	T1	T1	T1	T1
Moderate	Moderate	0	0	0	T2	T1	T1	T1	T1	T1
High	Moderate	0	0	T3	T2	T1	T1	T1	T1	T1
Low	High	0	0	T2	T1	T1	T1	T1	T1	T1
Moderate	High	T3	T3	T2	T1	T1	T1	T1	T1	T1
High	High	T3	T2	T2	T1	T1	T1	T1	T1	T1

Appendix C

SOS2-Based Generation Cost Linearization

As mentioned in Chapter 4, generation costs are assumed to be quadratic functions of the generated power. Such nonlinear cost functions are linearly represented by making use of SOS2 variables [176]. This linearization technique leads to a set of convex combinations of piecewise linear segments of each quadratic generation cost curve. The set of constraints required in the linear cost model include the "function rows" related to existing DGs (C.1), and new DGs (C.2) and (C.3) corresponding to the first and the second periods. And, the respective "reference rows" are given by (C.4)—(C.6). Eqs. (C.7)—(C.9) ensure that the sum of all SOS2 variables used to linearize a particular generation cost curve is equal to 1. Such constraints are also referred to as "convexity rows". Finally, Eq. (C.10) guarantees that no more than two adjacent SOS2 variables can have non-zero values.

$$OC^{E}_{p,k,n,s,w,t} = \sum_{l \in \Omega^l} \lambda^{E}_{p,k,n,s,w,t,l} * GC^{E}_{p,k,s,n,w,t,l} \; ; \quad \forall n \in \Omega^n; \; \forall t \in \Omega^t; \; \forall s \in \Omega^s; \; \forall w \in \Omega^w; \; \forall k \in \Omega^k; \forall p \in \Omega^p \tag{C.1}$$

$$OC^{N1}_{p,k,n,s,w,t} = \sum_{l \in \Omega^l} \lambda^{N1}_{p,k,n,s,w,t,l} * GC^{N1}_{p,k,n,s,w,t,l} \; ; \quad \forall n \in \Omega^n; \; \forall t \in \Omega^t; \; \forall s \in \Omega^s; \; \forall w \in \Omega^w \; ; \; \forall k \in \Omega^k; \forall p \in \Omega^p \tag{C.2}$$

$$OC^{N2}_{p,k,n,s,w,\zeta} = \sum_{l \in \Omega^l} \lambda^{N2}_{p,k,n,s,w,\zeta,l} * GC^{N2}_{p,k,n,s,w,\zeta,l} \; ; \quad \forall n \in \Omega^n; \; \forall \zeta \in \Omega^{P2}; \; \forall s \in \Omega^s; \; \forall w \in \Omega^w; \; \forall k \in \Omega^k; \; \forall p \in \Omega^p \tag{C.3}$$

$$g^{E}_{p,k,n,s,w,t} = \sum_{l \in \Omega^l} \lambda^{E}_{p,k,n,s,w,t,l} * (l * Gmax^{E}_{p,k,s,w} / L) \; ; \quad \forall n \in \Omega^n; \; \forall t \in \Omega^t; \; \forall s \in \Omega^s; \; \forall w \in \Omega^w; \; \forall k \in \Omega^k; \; \forall p \in \Omega^p \tag{C.4}$$

$$g^{N1}_{p,k,n,s,w,t} = \sum_{l \in \Omega^l} \lambda^{N1}_{p,k,n,s,w,t,l} * \left(l * \frac{Gmax^{N1}_{p,k,s,w}}{L} \right) ; \quad \forall n \in \Omega^n; \; \forall t \in \Omega^t; \; \forall s \in \Omega^s; \; \forall w \in \Omega^w; \; \forall k \in \Omega^k; \; \forall p \in \Omega^p \tag{C.5}$$

$$g^{N2}_{p,k,n,s,w,\zeta} = \sum_{l \in \Omega^l} \lambda^{N2}_{p,k,n,s,w,\zeta,l} * (l * Gmax^{N2}_{p,k,s,w} / L) \; ; \quad \forall n \in \Omega^n; \; \forall \zeta \in \Omega^{P2}; \; \forall s \in \Omega^s; \; \forall w \in \Omega^w; \; \forall k \in \Omega^k; \; \forall p \in \Omega^p \tag{C.6}$$

$$\sum_{l\in\Omega^l} \lambda^{E}_{p,k,n,s,w,t,l} = 1 \quad ; \tag{C.7}$$

$$\forall n \in \Omega^n ;\forall t \in \Omega^t;\ \forall s \in \Omega^s;\ \forall w \in \Omega^w;\ \forall k \in \Omega^k;\ \forall p \in \Omega^p$$

$$\sum_{l\in\Omega^l} \lambda^{N1}_{p,k,n,s,w,t,l} = 1 \quad ; \tag{C.8}$$

$$\forall n \in \Omega^n;\ \forall t \in \Omega^t;\ \forall s \in \Omega^s;\ \forall w \in \Omega^w;\ \forall k \in \Omega^k;\ \forall p \in \Omega^p$$

$$\sum_{l\in\Omega^l} \lambda^{N2}_{p,k,n,s,w,\zeta,l} = 1 \ ; \tag{C.9}$$

$$\forall n \in \Omega^n;\ \forall \zeta \in \Omega^{P2} ;\forall s \in \Omega^s;\ \forall w \in \Omega^w;\ \forall k \in \Omega^k;\ \forall p \in \Omega^p$$

$\lambda^{E}_{p,k,n,s,w,t,l}, \lambda^{N1}_{p,k,n,s,w,t,l}, \lambda^{N2}_{p,k,n,s,w,\zeta,l}$ are SOS2 variables; (C.10)

$$\forall n \in \Omega^n;\ \forall t \in \Omega^t;\ \forall \zeta \in \Omega^{P2};\ \forall s \in \Omega^s;\ \forall w \in \Omega^w;\ \forall k \in \Omega^k;\ \forall p \in \Omega^p$$

where $GC^{E}_{p,k,n,s,w,t,l} = A^{E}_{p,k} + (B^{E}_{p,k} * l * Gmax^{E}_{p,k,s,w}/L) + C^{E}_{p,k} * (l * Gmax^{E}_{p,k,s,w}/L)^2$

$GC^{N1}_{p,k,s,n,w,t,l} = A^{N1}_{p,k} + (B^{N1}_{p,k} * l * Gmax^{N1}_{p,k,s,w}/L) + C^{N1}_{p,k} * (l * Gmax^{N1}_{p,k,s,w}/L)^2$

and $GC^{N2}_{p,k,n,s,w,\zeta,l} = A^{N2}_{p,k} + (B^{N2}_{p,k} * l * Gmax^{N2}_{p,k,s,w}/L) + C^{N2}_{p,k} * (l * Gmax^{N2}_{p,k,s,w}/L)^2$.,

Appendix D

The derivations related to the losses equations in (6.49) and (6.50) are provided here. Squaring both sides of the flow equations in (6.49) and (6.50) and dividing each by V_{nom}^2, we get:

$$\frac{(P_k)^2}{V_{nom}^2} \approx \underbrace{\left[(\Delta V_i - \Delta V_j)g_k\right]^2}_{I} - \underbrace{2 * g_k V_{nom} b_k \theta_k * (\Delta V_i - \Delta V_j)}_{II} + (V_{nom} b_k \theta_k)^2 \tag{D.1}$$

$$\frac{(Q_k)^2}{V_{nom}^2} \approx \underbrace{\left[(\Delta V_i - \Delta V_j)b_k\right]^2}_{I} + \underbrace{2 * b_k V_{nom} g_k \theta_k * (\Delta V_i - \Delta V_j)}_{II} + (V_{nom} g_k \theta_k)^2 \tag{D.2}$$

Since the variables θ_k, ΔV_i and ΔV_j are very small, the second order terms (i.e. products of these variables) are close to zero. Hence, the first and the second terms in (D.1) and (D.2) can be neglected, leading to the following expressions, respectively.

$$\frac{(P_k)^2}{V_{nom}^2} \approx (V_{nom} b_k \theta_k)^2 \tag{D.3}$$

$$\frac{(Q_k)^2}{V_{nom}^2} \approx (V_{nom} g_k \theta_k)^2 \tag{D.4}$$

Multiplying both sides of (D.3) and (D.4) by r_k and summing gives:

$$r_k \left(\frac{P_k}{V_{nom}}\right)^2 + r_k \left(\frac{Q_k}{V_{nom}}\right)^2 \approx r_k (V_{nom} b_k \theta_k)^2 + r_k (V_{nom} g_k \theta_k)^2 \tag{D.5}$$

After rearranging Eq. (D.5), we get:

$$r_k (P_k^2 + Q_k^2)/V_{nom}^2 \approx g_k (V_{nom} \theta_k)^2 r_k \left(\frac{(b_k)^2}{g_k} + g_k\right) \tag{D.6}$$

One can easily verify that $r_k \left(\frac{(b_k)^2}{g_k} + g_k\right) = 1$, reducing Eq. (D.5) to:

$$r_k (P_k^2 + Q_k^2)/V_{nom}^2 \approx g_k (V_{nom} \theta_k)^2 \tag{D.7}$$

Recall that the right hand side of (D.7) corresponds to the active power losses expression in (6.49), which proves the derivation. The flow-based reactive power losses in (6.50) are derived in a similar way. Multiplying both sides of (D.3) and (D.4) by $\mathrm{x_k}$ instead of $\mathrm{r_k}$, adding both and rearranging the resulting equation leads to:

$$r_k\left(P_k^2 + Q_k^2\right)/V_{nom}^2 \approx -b_k V_{nom}^2 \theta_k^2 x_k[-b_k + (g_k)^2/(-b_k)] \tag{D.8}$$

Note that, in Eq. (D.8), $\mathrm{x_k[-b_k + (g_k)^2/(-b_k)] = 1}$. Hence, the equation reduces to:

$$r_k\left(P_k^2 + Q_k^2\right)/V_{nom}^2 \approx -b_k V_{nom}^2 \theta_k^2 \tag{D.9}$$

Notice that the right hand side of Eq. (D.8) is equal to the reactive losses expression in (6.50).

Appendix E

Test Systems

IEEE 119 BUS DISTRIBUTION SYSTEM

Line Index	From Bus Index	To Bus Index	Line Resistance R [Ω]	Line Reactance X [Ω]	From bus Load Active Power P [kW]	From bus Load Active Power Q [kvar]
1	1	2	0.036	0.01296	0	0
2	2	3	0.033	0.01188	133.84	101.14
3	2	4	0.045	0.0162	1	11.292
4	4	5	0.015	0.054	34.315	21.845
5	5	6	0.015	0.054	73.016	63.602
6	6	7	0.015	0.0125	144.2	68.604
7	7	8	0.018	0.014	104.47	61.725
8	8	9	0.021	0.063	28.547	11.503
9	2	10	0.166	0.01344	87.56	51.073
10	10	11	0.112	0.0789	198.2	106.77
11	11	12	0.187	0.313	146.8	75.995
12	12	13	0.142	0.1512	26.04	18.687
13	13	14	0.18	0.118	52.1	23.22
14	14	15	0.15	0.045	141.9	117.5
15	15	16	0.16	0.18	21.87	28.79
16	16	17	0.157	0.171	33.37	26.45
17	11	18	0.218	0.285	32.43	25.23
18	18	19	0.118	0.185	20.234	11.906
19	19	20	0.16	0.196	156.94	78.523
20	20	21	0.12	0.189	546.29	351.4
21	21	22	0.12	0.0789	93.167	54.594
22	22	23	1.41	0.723	85.18	39.65
23	23	24	0.293	0.1348	168.1	95.178
24	24	25	0.133	0.104	125.11	150.22
25	25	26	0.178	0.134	16.03	24.62
26	26	27	0.178	0.134	26.03	24.62
27	4	28	0.015	0.0296	594.56	522.62
28	28	29	0.012	0.0276	120.62	59.117
29	29	30	0.12	0.2766	102.38	99.554
30	30	31	0.21	0.243	513.4	318.5
31	31	32	0.12	0.054	475.25	456.14
32	32	33	0.178	0.234	151.43	136.79
33	33	34	0.178	0.234	205.38	83.302
34	34	35	0.154	0.162	131.6	93.082
35	30	36	0.187	0.261	448.4	369.79
36	36	37	0.133	0.099	440.52	321.64
37	29	38	0.33	0.194	112.54	55.134
38	38	39	0.31	0.194	53.963	38.998
39	39	40	0.13	0.194	26.04	18.687

(Continuation of the previous table)

Line Index	From Bus Index	To Bus Index	Line Resistance R [Ω]	Line Reactance X [Ω]	From bus Load Active Power P [kW]	From bus Load Active Power Q [kvar]
40	40	41	0.28	0.15	393.05	342.6
41	41	42	1.18	0.85	326.74	278.56
42	42	43	0.42	0.2436	536.26	240.24
43	43	44	0.27	0.0972	76.247	66.562
44	44	45	0.339	0.1221	53.52	39.76
45	45	46	0.27	0.1779	40.328	31.964
46	35	47	0.21	0.1383	39.653	20.758
47	47	48	0.12	0.0789	66.195	42.361
48	48	49	0.15	0.0987	73.904	51.653
49	49	50	0.15	0.0987	114.77	57.965
50	50	51	0.24	0.1581	918.37	1205.1
51	51	52	0.12	0.0789	210.3	146.66
52	52	53	0.405	0.1458	66.68	56.608
53	53	54	0.405	0.1458	42.207	40.184
54	29	55	0.391	0.141	433.74	283.41
55	55	56	0.406	0.1461	62.1	26.86
56	56	57	0.406	0.1461	92.46	88.38
57	57	58	0.706	0.5461	85.188	55.436
58	58	59	0.338	0.1218	345.3	332.4
59	59	60	0.338	0.1218	22.5	16.83
60	60	61	0.207	0.0747	467.5	395.14
61	61	62	0.247	0.8922	95.86	90.758
62	1	63	0.028	0.0418	62.92	47.7
63	63	64	0.117	0.2016	478.8	463.74
64	64	65	0.255	0.0918	120.94	52.006
65	65	66	0.21	0.0759	139.11	100.34
66	66	67	0.383	0.138	391.78	193.5
67	67	68	0.504	0.3303	27.741	26.713
68	68	69	0.406	0.1461	52.814	25.257
69	69	70	0.962	0.761	66.89	38.713
70	70	71	0.165	0.06	467.5	395.14
71	71	72	0.303	0.1092	594.85	239.74
72	72	73	0.303	0.1092	132.5	84.363
73	73	74	0.206	0.144	52.699	22.482
74	74	75	0.233	0.084	869.79	614.775
75	75	76	0.591	0.1773	31.349	29.817
76	76	77	0.126	0.0453	192.39	122.43
77	64	78	0.559	0.3687	65.75	45.37
78	78	79	0.186	0.1227	238.15	223.22
79	79	80	0.186	0.1227	294.55	162.47

(Continuation of the previous table)

Line Index	From Bus Index	To Bus Index	Line Resistance R [Ω]	Line Reactance X [Ω]	From bus Load Active Power P [kW]	From bus Load Active Power Q [kvar]
80	80	81	0.26	0.139	485.57	437.92
81	81	82	0.154	0.148	243.53	183.03
82	82	83	0.23	0.128	243.53	183.03
83	83	84	0.252	0.106	134.25	119.29
84	84	85	0.18	0.148	22.71	27.96
85	79	86	0.16	0.182	49.513	26.515
86	86	87	0.2	0.23	383.78	257.16
87	87	88	0.16	0.393	49.64	20.6
88	65	89	0.669	0.2412	22.473	11.806
89	89	90	0.266	0.1227	62.93	42.96
90	90	91	0.266	0.1227	30.67	34.93
91	91	92	0.266	0.1227	62.53	66.79
92	92	93	0.226	0.1227	114.57	81.748
93	93	94	0.233	0.115	81.292	66.526
94	94	95	0.496	0.138	31.733	15.96
95	91	96	0.196	0.18	33.32	60.48
96	96	97	0.196	0.18	531.28	224.85
97	97	98	0.1866	0.122	507.03	367.42
98	98	99	0.0746	0.318	26.39	11.7
99	1	100	0.0625	0.0265	96.793	83.647
100	100	101	0.1501	0.234	100.66	47.572
101	101	102	0.1347	0.0888	456.48	350.3
102	102	103	0.2307	0.1203	522.56	449.29
103	103	104	0.447	0.1608	408.43	168.46
104	104	105	0.1632	0.0588	141.48	134.25
105	105	106	0.33	0.099	104.43	66.024
106	106	107	0.156	0.0561	96.793	83.647
107	107	108	0.3819	0.1374	493.92	419.34
108	108	109	0.1626	0.0585	225.38	135.88
109	109	110	0.3819	0.1374	509.21	387.21
110	110	111	0.2445	0.0879	188.5	173.46
111	109	112	0.2088	0.0753	918.03	898.55
112	112	113	0.2301	0.0828	305.08	215.37
113	100	114	0.6102	0.2196	54.38	40.97
114	114	115	0.1866	0.127	211.14	192.9
115	115	116	0.3732	0.246	67.009	53.336
116	116	117	0.405	0.367	162.07	90.321
117	117	118	0.489	0.438	48.785	29.156
		118			33.9	18.98

IEEE 41 BUS DISTRIBUTION SYSTEM

Line Index	To Bus Index	From Bus Index	Line Resistance R [Ω]	Line Reactance X [Ω]	From bus Load Active Power P [kW]	From bus Load Active Power Q [kvar]
1	1	2	0.0992	0.0470	100	60
2	2	3	0.4930	0.2511	90	40
3	3	4	0.3660	0.1864	120	80
4	4	5	0.3811	1.1941	60	30
5	5	6	0.8190	0.7070	60	20
6	6	7	0.1872	0.6188	200	100
7	7	8	0.7114	0.2351	200	100
8	8	9	1.0300	0.7400	60	20
9	9	10	1.0440	0.7400	60	20
10	10	11	0.1966	0.0650	45	30
11	11	12	0.3744	0.1238	60	35
12	12	13	1.4680	1.1550	60	35
13	13	14	0.5416	0.7129	120	80
14	14	15	0.5910	0.5260	60	10
15	15	16	0.7463	0.5450	60	20
16	16	17	1.2890	1.7210	60	20
17	17	18	0.7320	0.5470	90	40
18	2	19	0.1640	0.1565	90	40
19	19	20	1.5042	1.3554	90	40
20	20	21	0.4095	0.4784	90	40
21	21	22	0.7089	0.9373	90	40
22	3	23	0.4512	0.3083	90	50
23	23	24	0.8980	0.7091	420	200
24	24	25	0.8960	0.7011	420	200
25	6	26	0.2030	0.1034	60	25
26	26	27	0.2842	0.1447	60	25
27	27	28	1.0590	0.9337	60	20
28	28	29	0.8042	0.7006	120	70
29	29	30	0.5075	0.2585	200	600
30	30	31	0.9744	0.9630	150	70
31	31	32	0.3105	0.3619	210	100
32	32	33	0.3410	0.5302	60	40
33	10	34	0.2030	0.1034	60	25
34	34	35	0.2842	0.1447	60	25
35	35	36	1.0590	0.9337	60	20
36	36	37	0.8042	0.7006	120	70
37	37	38	0.5075	0.2585	200	600
38	38	39	0.9744	0.9630	150	70
39	39	40	0.3105	0.3619	210	100
40	40	41	0.3410	0.5302	60	40

Bibliography

[1] A. McCrone, U. Moslener, and F. Grüning, “Global Trends in Renewable Energy Investment 2016l,” Frankfurt School-UNEP Collaborating Centre for Climate, Frankfurt, Germany, Mar. 2016.

[2] “Energy Climate and Change - World Energy Outlook Special Briefing for COP21,” International Energy Agency (IEA), 2015.

[3] *World Energy Outlook 2015 - Special Reporton*. Paris, France: International Enjergy Agency.

[4] V. C. Nelson and K. L. Starcher, *Introduction to Renewable Energy*. New Mexico, USA: CRC Press, 2011.

[5] “Renewables 20116 - Global Status Report,” Renewable Energy Policy Network for 21st Century, Paris, France, 20016.

[6] S. F. Santos, D. Z. Fitiwi, M. Shafie-khah, A. W. Bizuayehu, and J. P. S. Catalão, “Introduction to renewable energy systems,” in *Optimization in Renewable Energy Systems*, London, UK: ACADEMIC Press (ELSEVIER), 2016 (aceite).

[7] S. F. Santos, D. Z. Fitiwi, A. W. Bizuayehu, M. Shafie-khah, M. Asensio, J. Contreras, C. M. P. Cabrita, J. P. S. Catalão, “Impacts of Operational Variability and Uncertainty on Distributed Generation Investment Planning: A Comprehensive Sensitivity Analysis,” *IEEE Trans. Sustain. Energy*, 2016 (aceite), DOI:10.1109/TSTE.2016.2624506.

[8] S. F. Santos, D. Z. Fitiwi, A. W. Bizuayehu, M. Shafie-khah, M. Asensio, J. Contreras, C. M. P. Cabrita, J. P. S. Catalão, “Novel Multi-Stage Stochastic DG Investment Planning with Recourse,” *IEEE Trans. Sustain. Energy*, 2016 (aceite), DOI: 10.1109/TSTE.2016.2590460.

[9] S. F. Santos, D. Z. Fitiwi, M. R. M. Cruz, C. M. P. Cabrita, and J. P. S. Catalão, “Impacts of Optimal Energy Storage Deployment and Network Reconfiguration on Renewable Integration Level in Distribution Systems,” *Appl. Energy*, Vol. 185, pp. 44-55, January 2017, DOI: 10.1016/j.apenergy.2016.10.053.

[10] S. F. Santos, D. Z. Fitiwi, M. Shafie-khah, A. W. Bizuayehu, C. M. P. Cabrita, and J. P. S. Catalao, “New Multi-Stage and Stochastic Mathematical Model for Maximizing RES Hosting Capacity—Part I: Problem Formulation,” *IEEE Trans. Sustain. Energy*, 2016 (aceite), DOI: 10.1109/TSTE.2016.2598400.

[11] S. F. Santos, D. Z. Fitiwi, M. Shafie-khah, A. W. Bizuayehu, C. M. P. Cabrita, and J. P. S. Catalao, “New Multi-Stage and Stochastic Mathematical Model for Maximizing RES Hosting Capacity—Part II: Numerical Results,” *IEEE Trans. Sustain. Energy*, 2016 (aceite), DOI: 10.1109/TSTE.2016.2584122.

[12] C. J. Cleveland, R. Costanza, C. A. S. Hall, and R. K. Kaufmann, “Energy and the U:S: Economy: A Biophysical Prespective,” *Science*, vol. 225, pp. 890–897.

[13] L. Brookes, “Energy efficiency fallacies revisited,” *Energy Policy*, vol. 28, no. 6, pp. 355–366, 2000.

[14] R. K. Kaufmann, “The mechanisms for autonomous energy efficiency increases: A cointegration analysis of the US energy/GDP ratio,” *Energy J.*, pp. 63–86, 2004.

[15] J. Khan and M. H. Arsalan, “Solar power technologies for sustainable electricity generation – A review,” *Renew. Sustain. Energy Rev.*, vol. 55, pp. 414–425, Mar. 2016.

[16] S. Comello and S. Reichelstein, “The U.S. investment tax credit for solar energy: Alternatives to the anticipated 2017 step-down,” *Renew. Sustain. Energy Rev.*, vol. 55, pp. 591–602, Mar. 2016.

[17] R. Bertani, “Geothermal power generation in the world 2010–2014 update report,” *Geothermics*, vol. 60, pp. 31–43, Mar. 2016.

[18] R. K. Pachauri and Intergovernmental Panel on Climate Change, Eds., *Climate change 2007:: contribution of ... to the fourth assessment report of the Intergovernmental Panel on Climate Change. 4: Synthesis report: [a report of the Intergovernmental Panel on Climate Change]*. Geneva: IPCC, 2008.

[19] P. Del Duca *et al.*, “MEXICO UPDATE,” 2011.

[20] *Renewables 2014 - Global Status Report*. Renewable Energy Policy Network for the 21st Century.

[21] European Commission, “Paris climate change conference (COP21/CMP11).” [Online]. Available: http://ec.europa.eu/clima/events/articles/0107_en.htm. [Accessed: 29-Jan-2016].

[22] *Climate Change 2014: Synthesis Report*. Geneva, Switzerland: Intergovernmental Panel on Climate Change -IPCC.

[23] *Renewables 2015 - Global Status Report*, Renewable Energy Policy Network for the 21st Century. .

[24] *Renewable Power Generation Costs in 2014*. International Renewable Energy Agency.

[25] S. Tegen, E. Lantz, M. Hand, B. Maples, A. Smith, and P. Schwabe, “2011 Cost of Wind Energy Review.” National Renewable Energy Laboratory, 2011.

[26] N. Gupta, “A review on the inclusion of wind generation in power system studies,” *Renew. Sustain. Energy Rev.*, vol. 59, pp. 530–543, Jun. 2016.

[27] M. Finster, C. Clark, J. Schroeder, and L. Martino, “Geothermal produced fluids: Characteristics, treatment technologies, and management options,” *Renew. Sustain. Energy Rev.*, vol. 50, pp. 952–966, Oct. 2015.

[28] B. Sung, “Public policy supports and export performance of bioenergy technologies: A dynamic panel approach,” *Renew. Sustain. Energy Rev.*, vol. 42, pp. 477–495, Feb. 2015.

[29] G. Fiorese, M. Catenacci, V. Bosetti, and E. Verdolini, “The power of biomass: Experts disclose the potential for success of bioenergy technologies,” *Energy Policy*, vol. 65, pp. 94–114, 2014.

[30] European Biomass and Association (AEBIOM), “AEBIOM-Statistical-Report-2015: European Bioenergy Outlook,” European Biomass Association, Brussels.

[31] A. F. de O. Falcão, “Wave energy utilization: A review of the technologies,” *Renew. Sustain. Energy Rev.*, vol. 14, no. 3, pp. 899–918, Apr. 2010.

[32] European Commission, “Harnessing the power of the sea: The future of ocean energy.” European Commission, 2014.

[33] Wissenschaftlicher Beirat Globale Umweltveränderungen, Ed., *Welt im Wandel - Sicherheitsrisiko Klimawandel*. Berlin: Springer, 2008.

[34] Müller, Brown, and S. Ölz, “Renew_Policies -Policy considerations for deploying renewables,” International Energy Agency, Paris, 2011.

[35] J. Lilliestam and S. Ellenbeck, “Energy security and renewable electricity trade—Will Desertec make Europe vulnerable to the ‘energy weapon’?,” *Energy Policy*, vol. 39, no. 6, pp. 3380–3391, Jun. 2011.

[36] “The oil age poster,” *The oil age poster*. [Online]. Available: http://www.oilposter.org. [Accessed: 25-Jan-2016].

[37] F. Hedenus, C. Azar, and D. J. A. Johansson, “Energy security policies in EU-25—The expected cost of oil supply disruptions,” *Energy Policy*, vol. 38, no. 3, pp. 1241–1250, Mar. 2010.

[38] European Comission, “Impact Assessment, Accompanying the document to Energy Roadmap 2050,” European Comission, Brussels, 2011.

[39] W. Lacher and D. Kumetat, “The security of energy infrastructure and supply in North Africa: Hydrocarbons and renewable energies in comparative perspective,” *Energy Policy*, vol. 39, no. 8, pp. 4466–4478, Aug. 2011.

[40] M. Mobjörk, M. Eriksson, and H. Carlsen, “On connecting climate change with security and armed conflict,” *Investig. Knowl. Sci. Community FOI Stockh.*, 2010.

[41] M. Z. Jacobson and M. A. Delucchi, “Providing all global energy with wind, water, and solar power, Part I: Technologies, energy resources, quantities and areas of infrastructure, and materials,” *Energy Policy*, vol. 39, no. 3, pp. 1154–1169, Mar. 2011.

[42] M. A. Delucchi and M. Z. Jacobson, “Providing all global energy with wind, water, and solar power, Part II: Reliability, system and transmission costs, and policies,” *Energy Policy*, vol. 39, no. 3, pp. 1170–1190, Mar. 2011.

[43] D. S. Parakh and M. M. D. Ross, “Clean Energy Management Software,” Canada.

[44] A. L. R. Jackson, “Renewable energy vs. biodiversity: Policy conflicts and the future of nature conservation,” *Glob. Environ. Change*, vol. 21, no. 4, pp. 1195–1208, Oct. 2011.

[45] Lazard, “Levelized Cost of Energy -Vergion 2.0,” Jun-2008.

[46] J. Glassmire, P. Komor, and P. Lilienthal, “Electricity demand savings from distributed solar photovoltaics,” *Energy Policy*, vol. 51, pp. 323–331, Dec. 2012.

[47] H. Lund and B. V. Mathiesen, “Energy system analysis of 100% renewable energy systems—The case of Denmark in years 2030 and 2050,” *Energy*, vol. 34, no. 5, pp. 524–531, May 2009.

[48] R. Bove, M. Bucher, and F. Ferretti, “Integrating large shares of wind energy in macro-economical cost-effective way,” *Energy*, vol. 43, no. 1, pp. 438–447, Jul. 2012.

[49] H. Auer and B. Burgholzer, “D2. 1 Opportunities, Challenges and Risks for RES-E Deployment in a fully Integrated European Electricity Market,” 2015.

[50] E. B. Zane, R. Brückmann, and D. Bauknecht, “Integration of electricity from renewables to the electricity grid and to the electricity market - RES - Integration,” Berlin, Final Report, 2012.

[51] International, Electrotechnical, and International Electrotechnical Commission, “Grid integration of large-capacity Renewable Energy sources and use of large-capacity Electrical Energy Storage.” .

[52] GEA, *Global Energy Assessment - Toward a Sustainable Future*. Cambridge University Press, Cambridge, UK and New York, NY, USA and the International Institute for Applied Systems Analysis, Laxenburg, Austria, 2012.

[53] M. Stappel and A. Energiewende, “The European power system in 2030: flexibility challenges and integration benefits: an analysis with a focus on the pentalateral energy forum region.”

[54] A. Ulbig and others, “Analyzing operational flexibility of power systems,” *ArXiv Prepr. ArXiv13127618*, 2013.

[55] R. Poudineh and T. Jamasb, “Distributed generation, storage, demand response and energy efficiency as alternatives to grid capacity enhancement,” *Energy Policy*, vol. 67, pp. 222–231, Apr. 2014.

[56] C. L. T. Borges and V. F. Martins, “Multistage expansion planning for active distribution networks under demand and Distributed Generation uncertainties,” *Int. J. Electr. Power Energy Syst.*, vol. 36, no. 1, pp. 107–116, Mar. 2012.

[57] J. A. P. Lopes, N. Hatziargyriou, J. Mutale, P. Djapic, and N. Jenkins, “Integrating distributed generation into electric power systems: A review of drivers, challenges and opportunities,” *Electr. Power Syst. Res.*, vol. 77, no. 9, pp. 1189–1203, Jul. 2007.

[58] M. O. W. Grond, J. Morren, and J. G. Slootweg, “Integrating smart grid solutions into distribution network planning,” in *PowerTech (POWERTECH), 2013 IEEE Grenoble*, 2013, pp. 1–6.

[59] A. Yadav and L. Srivastava, “Optimal placement of distributed generation: An overview and key issues,” in *2014 International Conference on Power Signals Control and Computations (EPSCICON)*, 2014, pp. 1–6.

[60] M. E. Samper and A. Vargas, “Investment Decisions in Distribution Networks Under Uncertainty With Distributed Generation - Part I: Model Formulation,” *IEEE Trans. Power Syst.*, vol. 28, no. 3, pp. 2331–2340, Aug. 2013.

[61] M. E. Samper and A. Vargas, “Investment Decisions in Distribution Networks Under Uncertainty With Distributed Generation - Part II: Implementation and Results,” *IEEE Trans. Power Syst.*, vol. 28, no. 3, pp. 2341–2351, Aug. 2013.

[62] A. Piccolo and P. Siano, “Evaluating the Impact of Network Investment Deferral on Distributed Generation Expansion,” *IEEE Trans. Power Syst.*, vol. 24, no. 3, pp. 1559-1567, Aug. 2009.

[63] T. Niknam, S. I. Taheri, J. Aghaei, S. Tabatabaei, and M. Nayeripour, “A modified honey bee mating optimization algorithm for multiobjective placement of renewable energy resources,” *Appl. Energy*, vol. 88, no. 12, pp. 4817–4830, Dec. 2011.

[64] H. Hedayati, S. A. Nabaviniaki, and A. Akbarimajd, “A Method for Placement of DG Units in Distribution Networks,” *IEEE Trans. Power Deliv.*, vol. 23, no. 3, pp. 1620–1628, Jul. 2008.

[65] C. L. T. Borges and D. M. Falcão, “Optimal distributed generation allocation for reliability, losses, and voltage improvement,” *Int. J. Electr. Power Energy Syst.*, vol. 28, no. 6, pp. 413–420, Jul. 2006.

[66] M. A. Abdullah, A. P. Agalgaonkar, and K. M. Muttaqi, “Assessment of energy supply and continuity of service in distribution network with renewable distributed generation,” *Appl. Energy*, vol. 113, pp. 1015–1026, Jan. 2014.

[67] J. Liu, W. Zhang, R. Zhou, and J. Zhong, “Impacts of distributed renewable energy generations on smart grid operation and dispatch,” in *2012 IEEE Power and Energy Society General Meeting*, 2012, pp. 1–5.

[68] F. Katiraei and J. R. Agüero, “Solar PV Integration Challenges,” *IEEE Power Energy Mag.*, vol. 9, no. 3, pp. 62–71, May 2011.

[69] S. Eftekharnejad, V. Vittal, G. T. Heydt, B. Keel, and J. Loehr, “Impact of increased penetration of photovoltaic generation on power systems,” *IEEE Trans. Power Syst.*, vol. 28, no. 2, pp. 893–901, May 2013.

[70] M. Shivaie, M. T. Ameli, M. S. Sepasian, P. D. Weinsier, and V. Vahidinasab, “A multistage framework for reliability-based distribution expansion planning considering distributed generations by A self-adaptive global-based harmony search algorithm,” *Reliab. Eng. Syst. Saf.*, Mar. 2015.

[71] G. Munoz-Delgado, J. Contreras, and J. M. Arroyo, “Joint Expansion Planning of Distributed Generation and Distribution Networks,” *IEEE Trans. Power Syst.*, vol. 30, no. 5, pp. 2579–2590, Sep. 2015.

[72] Ž. N. Popović, V. D. Kerleta, and D. S. Popović, “Hybrid simulated annealing and mixed integer linear programming algorithm for optimal planning of radial distribution networks with distributed generation,” *Electr. Power Syst. Res.*, vol. 108, pp. 211–222, Mar. 2014.

[73] M.-C. Alvarez-Herault, N. N’Doye, C. Gandioli, N. Hadjsaid, and P. Tixador, “Meshed distribution network vs reinforcement to increase the distributed generation connection,” *Sustain. Energy Grids Netw.*, vol. 1, pp. 20–27, Mar. 2015.

[74] M. Jalali, K. Zare, and M. T. Hagh, “A multi-stage MINLP-based model for sub-transmission system expansion planning considering the placement of DG units,” *Int. J. Electr. Power Energy Syst.*, vol. 63, pp. 8–16, Dec. 2014.

[75] H. Shayeghi and A. Bagheri, “Dynamic sub-transmission system expansion planning incorporating distributed generation using hybrid DCGA and LP technique,” *Int. J. Electr. Power Energy Syst.*, vol. 48, pp. 111–122, Jun. 2013.

[76] M. Sedghi, M. Aliakbar-Golkar, and M.-R. Haghifam, “Distribution network expansion considering distributed generation and storage units using modified PSO algorithm,” *Int. J. Electr. Power Energy Syst.*, vol. 52, pp. 221–230, Nov. 2013.

[77] M. Sadeghi and M. Kalantar, “Multi types DG expansion dynamic planning in distribution system under stochastic conditions using Covariance Matrix Adaptation Evolutionary Strategy and Monte-Carlo simulation,” *Energy Convers. Manag.*, vol. 87, pp. 455–471, Nov. 2014.

[78] M. Ahmadigorji and N. Amjady, “A new evolutionary solution method for dynamic expansion planning of DG-integrated primary distribution networks,” *Energy Convers. Manag.*, vol. 82, pp. 61–70, Jun. 2014.

[79] M. Arriaga, C. A. Canizares, and M. Kazerani, “Long-Term Renewable Energy Planning Model for Remote Communities,” *IEEE Trans. Sustain. Energy*, vol. 7, no. 1, pp. 221–231, Jan. 2016.

[80] M. V. Kirthiga, S. A. Daniel, and S. Gurunathan, “A Methodology for Transforming an Existing Distribution Network Into a Sustainable Autonomous Micro-Grid,” *IEEE Trans. Sustain. Energy*, vol. 4, no. 1, pp. 31–41, Jan. 2013.

[81] G. Liu, Y. Xu, and K. Tomsovic, “Bidding Strategy for Microgrid in Day-Ahead Market Based on Hybrid Stochastic/Robust Optimization,” *IEEE Trans. Smart Grid*, vol. 7, no. 1, pp. 227–237, Jan. 2016.

[82] G. Martinez, N. Gatsis, and G. Giannakis, “Stochastic programming for energy planning in microgrids with renewables,” in *2013 IEEE 5th International Workshop on Computational Advances in Multi-Sensor Adaptive Processing (CAMSAP)*, 2013, pp. 472–475.

[83] A. T. Al-Awami and E. Sortomme, “Coordinating Vehicle-to-Grid Services With Energy Trading,” *IEEE Trans. Smart Grid*, vol. 3, no. 1, pp. 453–462, Mar. 2012.

[84] S. Montoya-Bueno, J. I. Munoz, and J. Contreras, “A Stochastic Investment Model for Renewable Generation in Distribution Systems,” *IEEE Trans. Sustain. Energy*, vol. 6, no. 4, pp. 1466–1474, Oct. 2015.

[85] H. Moghimi, A. Ahmadi, J. Aghaei, and A. Rabiee, “Stochastic techno-economic operation of power systems in the presence of distributed energy resources,” *Int. J. Electr. Power Energy Syst.*, vol. 45, no. 1, pp. 477–488, Feb. 2013.

[86] S. Ganguly and D. Samajpati, “Distributed Generation Allocation on Radial Distribution Networks Under Uncertainties of Load and Generation Using Genetic Algorithm,” *IEEE Trans. Sustain. Energy*, vol. 6, no. 3, pp. 688–697, Jul. 2015.

[87] M. Ahmadigorji and N. Amjady, “A multiyear DG-incorporated framework for expansion planning of distribution networks using binary chaotic shark smell optimization algorithm,” *Energy*, vol. 102, pp. 199–215, May 2016.

[88] D. Q. Hung, N. Mithulananthan, and R. C. Bansal, “An optimal investment planning framework for multiple distributed generation units in industrial distribution systems,” *Appl. Energy*, vol. 124, pp. 62–72, Jul. 2014.

[89] D. Z. Fitiwi, “Strategy, Methods and Tools for Solving Long-term Transmission Expansion Planning in Large-scale Power Systems,” Comillas Pontifical University, 2016.

[90] Gerald van Belle, *Statistical Rules of Thumb*, 2nd ed. Wiley, 2008.

[91] M. O. Buygi, G. Balzer, H. M. Shanechi, and M. Shahidehpour, “Market-Based Transmission Expansion Planning,” *IEEE Trans. Power Syst.*, vol. 19, no. 4, pp. 2060–2067, Nov. 2004.

[92] F. Desta Zahlay, F. de Cuadra, L. Olmos, M. Rivier, and I. J. Perez-Arriaga, “A formulation for large-scale transmission expansion planning problem and a solution strategy,” in *10th International Conference on the European Energy Market (EEM)*, 2013, pp. 1–8.

[93] L. Blank and A. Tarquin, *Engineering Economy*, 7th ed. New York: McGraw-Hill Science/Engineering/Math, 2011.

[94] D. Z. Fitiwi, L. Olmos, M. Rivier, F. de Cuadra, and I. J. Pérez-Arriaga, "Finding a representative network losses model for large-scale transmission expansion planning with renewable energy sources," *Energy*, vol. 101, pp. 343–358, Apr. 2016.

[95] H. Zhang, G. T. Heydt, V. Vittal, and J. Quintero, "An Improved Network Model for Transmission Expansion Planning Considering Reactive Power and Network Losses," *IEEE Trans. Power Syst.*, vol. 28, no. 3, pp. 3471–3479, Aug. 2013.

[96] S. F. Santos, D. Z. Fitiwi, M. Shafie-khah, A. W. Bizuayehu, and J. P. S. Catalão, "Optimal Sizing and Placement of Smart Grid Enabling Technologies for Maximizing Renewable Integration," in *Smart Energy Grid Engineering*, In press., 2015.

[97] M. Lavorato, J. F. Franco, M. J. Rider, and R. Romero, "Imposing Radiality Constraints in Distribution System Optimization Problems," *IEEE Trans. Power Syst.*, vol. 27, no. 1, pp. 172–180, Feb. 2012.

[98] R. Viral and D. K. Khatod, "Optimal planning of distributed generation systems in distribution system: A review," *Renew. Sustain. Energy Rev.*, vol. 16, no. 7, pp. 5146–5165, Sep. 2012.

[99] M. Bazilian *et al.*, "Re-considering the economics of photovoltaic power," *Renew. Energy*, vol. 53, pp. 329–338, May 2013.

[100] J. Sweeting, *Project Cost Estimating: Principles and Practice*. IChemE, 1997.

[101] The World Data Center for Remote Sensing of the Atmosphere, "SOLEMI database for long-term global and direct irradiance at WDC-RSAT." [Online]. Available: https://wdc.dlr.de/data_products/SERVICES/SOLARENERGY/description.php. [Accessed: 02-Nov-2015].

[102] The SoDa Service, "Solar Radiation Data." [Online]. Available: http://www.soda-is.com/eng/index.html. [Accessed: 02-Nov-2015].

[103] Gregorio Muñoz-Delgado, Sergio Montoya-Bueno, Miguel Asensio, Javier Contreras, JoséI Muñoz, and JoséM Arroyo, "Renewable Generation and Distribution Grid Expansion Planning," in *Smart and Sustainable Power Systems*, 0 vols., CRC Press, 2015, pp. 345–404.

[104] J. Momoh, *Smart Grid: Fundamentals of Design and Analysis*. John Wiley & Sons, 2012.

[105] P. S. Georgilakis and N. D. Hatziargyriou, "A review of power distribution planning in the modern power systems era: Models, methods and future research," *Electr. Power Syst. Res.*, vol. 121, pp. 89–100, Apr. 2015.

[106] E. Romero-Ramos, J. Riquelme-Santos, and J. Reyes, “A simpler and exact mathematical model for the computation of the minimal power losses tree,” *Electr. Power Syst. Res.*, vol. 80, no. 5, pp. 562–571, May 2010.

[107] A. Chauhan and R. P. Saini, “A review on Integrated Renewable Energy System based power generation for stand-alone applications: Configurations, storage options, sizing methodologies and control,” *Renew. Sustain. Energy Rev.*, vol. 38, pp. 99–120, Oct. 2014.

[108] M. Aneke and M. Wang, “Energy storage technologies and real life applications – A state of the art review,” *Appl. Energy*, vol. 179, pp. 350–377, Oct. 2016.

[109] A. Chauhan and R. P. Saini, “A review on Integrated Renewable Energy System based power generation for stand-alone applications: Configurations, storage options, sizing methodologies and control,” *Renew. Sustain. Energy Rev.*, vol. 38, pp. 99–120, Oct. 2014.

[110] D. Q. Hung and N. Mithulananthan, “Loss reduction and loadability enhancement with DG: A dual-index analytical approach,” *Appl. Energy*, vol. 115, pp. 233–241, Feb. 2014.

[111] M. R. Dorostkar-Ghamsari, M. Fotuhi-Firuzabad, M. Lehtonen, and A. Safdarian, “Value of Distribution Network Reconfiguration in Presence of Renewable Energy Resources,” *IEEE Trans. Power Syst.*, vol. 31, no. 3, pp. 1879–1888, May 2016.

[112] I.-K. Song, W.-W. Jung, J.-Y. Kim, S.-Y. Yun, J.-H. Choi, and S.-J. Ahn, “Operation Schemes of Smart Distribution Networks With Distributed Energy Resources for Loss Reduction and Service Restoration,” *IEEE Trans. Smart Grid*, vol. 4, no. 1, pp. 367–374, Mar. 2013.

[113] D. Q. Hung, N. Mithulananthan, and R. C. Bansal, “A combined practical approach for distribution system loss reduction,” *Int. J. Ambient Energy*, vol. 36, no. 3, pp. 123–131, May 2015.

[114] G. Munoz-Delgado, J. Contreras, and J. M. Arroyo, “Joint Expansion Planning of Distributed Generation and Distribution Networks,” *IEEE Trans. Power Syst.*, vol. 30, no. 5, pp. 2579–2590, Sep. 2015.

[115] H. P. Williams, *Model Building in Mathematical Programming*, 4th ed. Wiley, 1999.

[116] D. Zhang, Z. Fu, and L. Zhang, “An improved TS algorithm for loss-minimum reconfiguration in large-scale distribution systems,” *Electr. Power Syst. Res.*, vol. 77, no. 5–6, pp. 685–694, Apr. 2007.

[117] R. S. Rao, S. V. L. Narasimham, M. R. Raju, and A. S. Rao, “Optimal Network Reconfiguration of Large-Scale Distribution System Using Harmony Search Algorithm,” *IEEE Trans. Power Syst.*, vol. 26, no. 3, pp. 1080–1088, Aug. 2011.

[118] D. Z. Fitiwi, A. W. Bizuayehu, M. Shafie-khah, J. P. S. Catalão, M. Asenso, and J. Contreras, “DG Investment Planning Analysis with Renewable Integration and Considering Emission Costs,” in *the 16th Int. Conf. on Computer as a Tool, EuroCon2015*, Salamanca, 2015.

[119] P. K. Ray, S. R. Mohanty, and N. Kishor, “Classification of Power Quality Disturbances Due to Environmental Characteristics in Distributed Generation System,” *IEEE Trans. Sustain. Energy*, vol. 4, no. 2, pp. 302–313, Apr. 2013.

[120] P. S. Georgilakis and N. D. Hatziargyriou, “Optimal Distributed Generation Placement in Power Distribution Networks: Models, Methods, and Future Research,” *IEEE Trans. Power Syst.*, vol. 28, no. 3, pp. 3420–3428, Aug. 2013.

[121] P. Paliwal, N. P. Patidar, and R. K. Nema, “Planning of grid integrated distributed generators: A review of technology, objectives and techniques,” *Renew. Sustain. Energy Rev.*, vol. 40, pp. 557–570, Dec. 2014.

[122] D. Q. Hung, N. Mithulananthan, and R. C. Bansal, “An optimal investment planning framework for multiple distributed generation units in industrial distribution systems,” *Appl. Energy*, vol. 124, pp. 62–72, Jul. 2014.

[123] F. S. Abu-Mouti and M. E. El-Hawary, “Heuristic curve-fitted technique for distributed generation optimisation in radial distribution feeder systems,” *IET Gener. Transm. Distrib.*, vol. 5, no. 2, p. 172, 2011.

[124] B. C. Pal and R. A. Jabr, “Ordinal optimisation approach for locating and sizing of distributed generation,” *IET Gener. Transm. Distrib.*, vol. 3, no. 8, pp. 713–723, Aug. 2009.

[125] R. S. Maciel, M. Rosa, V. Miranda, and A. Padilha-Feltrin, “Multi-objective evolutionary particle swarm optimization in the assessment of the impact of distributed generation,” *Electr. Power Syst. Res.*, vol. 89, pp. 100–108, Aug. 2012.

[126] K. Vinothkumar and M. P. Selvan, “Fuzzy Embedded Genetic Algorithm Method for Distributed Generation Planning,” *Electr. Power Compon. Syst.*, vol. 39, no. 4, pp. 346–366, Feb. 2011.

[127] F. Ugranlı and E. Karatepe, “Convergence of rule-of-thumb sizing and allocating rules of distributed generation in meshed power networks,” *Renew. Sustain. Energy Rev.*, vol. 16, no. 1, pp. 582–590, Jan. 2012.

[128] V. V. S. N. Murty and A. Kumar, “Optimal placement of DG in radial distribution systems based on new voltage stability index under load growth,” *Int. J. Electr. Power Energy Syst.*, vol. 69, pp. 246–256, Jul. 2015.

[129] A. Bagheri, H. Monsef, and H. Lesani, “Integrated distribution network expansion planning incorporating distributed generation considering uncertainties, reliability, and operational conditions,” *Int. J. Electr. Power Energy Syst.*, vol. 73, pp. 56–70, Dec. 2015.

[130] W. Sheng, K. Liu, Y. Liu, X. Meng, and Y. Li, “Optimal Placement and Sizing of Distributed Generation via an Improved Nondominated Sorting Genetic Algorithm II,” *IEEE Trans. Power Deliv.*, vol. 30, no. 2, pp. 569–578, Apr. 2015.

[131] R. Mena, M. Hennebel, Y.-F. Li, C. Ruiz, and E. Zio, “A risk-based simulation and multi-objective optimization framework for the integration of distributed renewable generation and storage,” *Renew. Sustain. Energy Rev.*, vol. 37, pp. 778–793, Sep. 2014.

[132] J. D. Foster, A. M. Berry, N. Boland, and H. Waterer, “Comparison of Mixed-Integer Programming and Genetic Algorithm Methods for Distributed Generation Planning,” *IEEE Trans. Power Syst.*, vol. 29, no. 2, pp. 833–843, Mar. 2014.

[133] A. Ameli, S. Bahrami, F. Khazaeli, and M.-R. Haghifam, “A Multiobjective Particle Swarm Optimization for Sizing and Placement of DGs from DG Owner’s and Distribution Company’s Viewpoints,” *IEEE Trans. Power Deliv.*, vol. 29, no. 4, pp. 1831–1840, Aug. 2014.

[134] S. Wen, H. Lan, Q. Fu, D. C. Yu, and L. Zhang, “Economic Allocation for Energy Storage System Considering Wind Power Distribution,” *IEEE Trans. Power Syst.*, vol. 30, no. 2, pp. 644–652, Mar. 2015.

[135] M. Sedghi, M. Aliakbar-Golkar, and M.-R. Haghifam, “Distribution network expansion considering distributed generation and storage units using modified PSO algorithm,” *Int. J. Electr. Power Energy Syst.*, vol. 52, pp. 221–230, Nov. 2013.

[136] H. Saboori, R. Hemmati, and V. Abbasi, “Multistage distribution network expansion planning considering the emerging energy storage systems,” *Energy Convers. Manag.*, vol. 105, pp. 938–945, Nov. 2015.

[137] M. M. Aman, G. B. Jasmon, A. H. A. Bakar, and H. Mokhlis, “A new approach for optimum simultaneous multi-DG distributed generation Units placement and sizing based on maximization of system loadability using HPSO (hybrid particle swarm optimization) algorithm,” *Energy*, vol. 66, pp. 202–215, Mar. 2014.

[138] R. S. Rao, K. Ravindra, K. Satish, and S. V. L. Narasimham, “Power Loss Minimization in Distribution System Using Network Reconfiguration in the Presence of Distributed Generation,” *IEEE Trans. Power Syst.*, vol. 28, no. 1, pp. 317–325, Feb. 2013.

[139] K. Nekooei, M. M. Farsangi, H. Nezamabadi-Pour, and K. Y. Lee, “An Improved Multi-Objective Harmony Search for Optimal Placement of DGs in Distribution Systems,” *IEEE Trans. Smart Grid*, vol. 4, no. 1, pp. 557–567, Mar. 2013.

[140] M. Sedighizadeh, M. Esmaili, and M. Esmaeili, “Application of the hybrid Big Bang-Big Crunch algorithm to optimal reconfiguration and distributed generation power allocation in distribution systems,” *Energy*, vol. 76, pp. 920–930, Nov. 2014.

[141] A. Y. Abdelaziz, Y. G. Hegazy, W. El-Khattam, and M. M. Othman, “Optimal allocation of stochastically dependent renewable energy based distributed generators in unbalanced distribution networks,” *Electr. Power Syst. Res.*, vol. 119, pp. 34–44, Feb. 2015.

[142] M. M. Othman, W. El-Khattam, Y. G. Hegazy, and A. Y. Abdelaziz, “Optimal Placement and Sizing of Distributed Generators in Unbalanced Distribution Systems Using Supervised Big Bang-Big Crunch Method,” *IEEE Trans. Power Syst.*, vol. 30, no. 2, pp. 911–919, Mar. 2015.

[143] D. Rama Prabha, T. Jayabarathi, R. Umamageswari, and S. Saranya, “Optimal location and sizing of distributed generation unit using intelligent water drop algorithm,” *Sustain. Energy Technol. Assess.*, vol. 11, pp. 106–113, Sep. 2015.

[144] A. Mohamed Imran, M. Kowsalya, and D. P. Kothari, “A novel integration technique for optimal network reconfiguration and distributed generation placement in power distribution networks,” *Int. J. Electr. Power Energy Syst.*, vol. 63, pp. 461–472, Dec. 2014.

[145] A. K. Singh and S. K. Parida, “Allocation of distributed generation using proposed DMSP approach based on utility and customers aspects under deregulated environment,” *Int. J. Electr. Power Energy Syst.*, vol. 68, pp. 159–169, Jun. 2015.

[146] R. S. Al Abri, E. F. El-Saadany, and Y. M. Atwa, “Optimal Placement and Sizing Method to Improve the Voltage Stability Margin in a Distribution System Using Distributed Generation,” *IEEE Trans. Power Syst.*, vol. 28, no. 1, pp. 326–334, Feb. 2013.

[147] Y. M. Atwa, E. F. El-Saadany, M. M. A. Salama, and R. Seethapathy, “Optimal Renewable Resources Mix for Distribution System Energy Loss Minimization,” *IEEE Trans. Power Syst.*, vol. 25, no. 1, pp. 360–370, Feb. 2010.

[148] Y. Yang, S. Zhang, and Y. Xiao, “An MILP (mixed integer linear programming) model for optimal design of district-scale distributed energy resource systems,” *Energy*, Jul. 2015.

[149] S. Montoya-Bueno, J. I. Munoz, and J. Contreras, “A Stochastic Investment Model for Renewable Generation in Distribution Systems,” *IEEE Trans. Sustain. Energy*, vol. 6, no. 4, pp. 1466–1474, Oct. 2015.

[150] E. E. Sfikas, Y. A. Katsigiannis, and P. S. Georgilakis, “Simultaneous capacity optimization of distributed generation and storage in medium voltage microgrids,” *Int. J. Electr. Power Energy Syst.*, vol. 67, pp. 101–113, May 2015.

[151] K. Mahmoud, N. Yorino, and A. Ahmed, “Optimal Distributed Generation Allocation in Distribution Systems for Loss Minimization,” *IEEE Trans. Power Syst.*, pp. 1–10, 2015.

[152] K. Vinothkumar and M. P. Selvan, “Hierarchical Agglomerative Clustering Algorithm method for distributed generation planning,” *Int. J. Electr. Power Energy Syst.*, vol. 56, pp. 259–269, Mar. 2014.

[153] Y. M. Atwa and E. F. El-Saadany, “Probabilistic approach for optimal allocation of wind-based distributed generation in distribution systems,” *IET Renew. Power Gener.*, vol. 5, no. 1, p. 79, 2011.

[154] V. V. S. . Murty and A. Kumar, “Mesh distribution system analysis in presence of distributed generation with time varying load model,” *Int. J. Electr. Power Energy Syst.*, vol. 62, pp. 836–854, Nov. 2014.

[155] G. Sinden, “Characteristics of the UK wind resource: Long-term patterns and relationship to electricity demand,” *Energy Policy*, vol. 35, no. 1, pp. 112–127, Jan. 2007.

[156] S. Subhadarshi, “Minding the P’s and Q’s: Real and reactive power assessment of hybrid energy conversion systems with wind and solar resources,” Iowa State University, 2013.

[157] Y. Z. Li, Q. H. Wu, M. S. Li, and J. P. Zhan, “Mean-variance model for power system economic dispatch with wind power integrated,” *Energy*, vol. 72, pp. 510–520, Aug. 2014.

[158] M. Zhao, Z. Chen, and F. Blaabjerg, “Probabilistic capacity of a grid connected wind farm based on optimization method,” *Renew. Energy*, vol. 31, no. 13, pp. 2171–2187, Oct. 2006.

[159] M. Aien, M. Rashidinejad, and M. Fotuhi-Firuzabad, “On possibilistic and probabilistic uncertainty assessment of power flow problem: A review and a new approach,” *Renew. Sustain. Energy Rev.*, vol. 37, pp. 883–895, Sep. 2014.

[160] J. Hartigan and M. Wong, “Algorithm AS 136: A k-means clustering algorithm,” *Appl. Stat.*, vol. 28, no. 1, pp. 100–108, 1979.

[161] L. Baringo and A. J. Conejo, “Correlated wind-power production and electric load scenarios for investment decisions,” *Appl. Energy*, vol. 101, pp. 475–482, Jan. 2013.

[162] S. Wogrin, P. Duenas, A. Delgadillo, and J. Reneses, “A New Approach to Model Load Levels in Electric Power Systems With High Renewable Penetration,” *IEEE Trans. Power Syst.*, vol. 29, no. 5, pp. 2210–2218, Sep. 2014.

[163] P. Phonrattanasak, “Optimal placement of DG using multiobjective particle swarm optimization,” in *2010 2nd International Conference on Mechanical and Electrical Technology (ICMET)*, 2010, pp. 342–346.

[164] J. P. Vielma, S. Ahmed, and G. Nemhauser, “Mixed-Integer Models for Nonseparable Piecewise-Linear Optimization: Unifying Framework and Extensions,” *Oper. Res.*, vol. 58, no. 2, pp. 303–315, Oct. 2009.

[165] C. Abbey and G. Joos, “A Stochastic Optimization Approach to Rating of Energy Storage Systems in Wind-Diesel Isolated Grids,” *IEEE Trans. Power Syst.*, vol. 24, no. 1, pp. 418–426, Feb. 2009.

[166] D. Pozo, J. Contreras, and E. E. Sauma, “Unit Commitment With Ideal and Generic Energy Storage Units,” *IEEE Trans. Power Syst.*, vol. 29, no. 6, pp. 2974–2984, Nov. 2014.

[167] J. Zhang, X. Yuan, and Y. Yuan, “A novel genetic algorithm based on all spanning trees of undirected graph for distribution network reconfiguration,” *J. Mod. Power Syst. Clean Energy*, vol. 2, no. 2, pp. 143–149, Jun. 2014.

[168] H. Ahmadi and J. R. Martí, “Mathematical representation of radiality constraint in distribution system reconfiguration problem,” *Int. J. Electr. Power Energy Syst.*, vol. 64, pp. 293–299, Jan. 2015.

[169] M. Wang and J. Zhong, “Islanding of systems of distributed generation using optimization methodology,” in *2012 IEEE Power and Energy Society General Meeting*, 2012, pp. 1–7.

[170] M. E. Baran and F. F. Wu, “Network reconfiguration in distribution systems for loss reduction and load balancing,” *Power Deliv. IEEE Trans. On*, vol. 4, no. 2, pp. 1401–1407, 1989.

[171] F. Díaz-González, A. Sumper, O. Gomis-Bellmunt, and R. Villafáfila-Robles, “A review of energy storage technologies for wind power applications,” *Renew. Sustain. Energy Rev.*, vol. 16, no. 4, pp. 2154–2171, May 2012.

[172] B. Zakeri and S. Syri, “Electrical energy storage systems: A comparative life cycle cost analysis,” *Renew. Sustain. Energy Rev.*, vol. 42, pp. 569–596, Feb. 2015.

[173] A. Ellis *et al.*, “Reactive power performance requirements for wind and solar plants,” in *2012 IEEE Power and Energy Society General Meeting*, 2012, pp. 1–8.

[174] A. Sadighmanesh, K. Zare, and M. Sabahi, “Distributed Generation unit and Capacitor Placement for Loss, Voltage profile and ATC Optimization,” *Int. J. Electr. Comput. Eng. IJECE*, vol. 2, no. 6, pp. 774–780, Dec. 2012.

[175] Jenkins *et al.*, *Wind Power Integration: Connection and system operational aspects*. Institution of Engineering and Technology, 2007.

[176] D. Z. Fitiwi, L. Olmos, M. Rivier, F. de Cuadra, and I. J. Pérez-Arriaga, “Finding a representative network losses model for large-scale transmission expansion planning with renewable energy sources,” *Energy*, vol. 101, pp. 343–358, Apr. 2016.